CRANFIELD INSTITUTE OF TECHNOLOGY

SCHOOL OF MECHANICAL ENGINEERING

Ph.D. THESIS

Academic Year 1980-1981

S. EL-SHAMARKA

An investigation of methanol and inorganic bromides for thermally operated heat pumps

Supervisor: Prof. I.E. SMITH

October 1981

ABSTRACT

Working fluids for thermal heat pump cycles have been studied. Methanol in conjunction with a mixture of inorganic bromides has been identified as being suitable for transforming heat from temperatures below zero centigrade.

A computer programme was written in order to calculate the performance of such a combination, and its accuracy was verified by comparing its predictions with the actual performance of existing (commercial) heat pumps and chillers using combinations other than the above.

Transport and other properties of the mixture have been measured, including vapour pressure, specific heat, viscosity, relative density, solubility, thermal conductivity, surface tension, heat of absorption, absorption coefficient, and hence mass diffusivity.

An intermittent absorption heat pump was constructed and its performance measured. The tests demonstrated that it was capable of pumping heat from -10 ^{o}C up to 74 ^{o}C.

Acknowledgements

The author would like to express his sincere and profound gratitude to his supervisor, Prof. I.E. Smith, in the School of Mechanical Engineering, for his valuable help, guidance and advice. Being deeply involved in every problem during this work, made it easier for me to accomplish it. His moral encouragements were as helpful as his technical discussions and help from which I learnt so much.

Thanks are also due to Mr. B. Moffitt and Mr. J. Dawe, the instrumentation engineers, for their great help, particularly during thermal conductivity measurements. Mr. M.A. Bell should be thanked for measuring the specific heat of two samples of the solution using differential scanning calorimeter. Mr. C. Chapman the academic support officer of the Applied Energy Group and Mr. T.A. Carberry the academic support officer of the Applied Mechanics Group for the continuous help during different stages of the work. Also Mr. N. Butcher and the rest of the workshop staff for the response and help in the test facility preparation.

I would also like to thank all fellow Ph.D. students in the Applied Energy Group for the useful and helpful discussions.

CONTENTS

FIGURES

TABLES

NOTATION

a	area of absorption per unit volume of the absorber m^{-1}
a_e	effective area of absorption per unit volume of the absorber m^{-1}
a_t	dry area of packings per unit volume m^{-1}
a_w	wetted area of packings per unit volume m^{-1}
C	the heat equivalent of the calorimeter used in specific heat measurements $J/^oC$ methanol concentration in solutions kg/m^3
C_{pL}	specific heat of lithium bromide salt kJ/kg ^oK
C_{pm}	specific heat of liquid methanol kJ/kg ^oC
C_{ps}	specific heat of methanol solutions kJ/kg ^oC
C_{pZ}	specific heat of zinc bromide salt kJ/kg ^oK
D	diffusion coefficient of heat or mass m^2/sec
9_{ES}	rate of absorbed methanol per unit effective area of the absorber kg/m^2sec
H	heat of vaporisation of pure methanol kJ/kg
H^1	heat of vaporisation of methanol from the solutions kJ/kg

I	current passing in the circuit used for thermal conductivity measurements
k	thermal conductivity watt/m ^{o}C
k_1	mass transfer coefficient (film coefficient) m/sec or kg/m^2% sec
M	molecular weight
N	electric power input
P_C	condensation pressure
P_E	evaporation pressure
Q_A	heat output from the absorber per unit mass absorbed refrigerant
Q_C	heat output from the condenser per unit mass of condensed refrigerant
Q_E	heat input into the evaporator per unit mass of evaporated refrigerant
Q_G	heat input into the generator per unit mass of evaporated refrigerant
Q_{ex}	heat exchanged within the solution heat exchanger per unit mass of refrigerant circulated in the cycle
R	the gas constant kJ/kg ^{o}K
	rate of absorption of methanol vapour per unit volume of the absorber kg/m^3sec

r	radius in cylindrical coordinates the hot wire radius
R_o	resistance of the platinum wire at 0 ^oC
R_t	total resistance of one branch of the bridge used in thermal conductivity measurements
R_w	resistance of the platinum wire at any temperature t ^oC
T_A	absorber temperature
T_C	condenser temperature
T_E	evaporator temperature
T_G	generator temperature
t	temperature ^oC
ΔT	temperature approach in the low temperature side of the solution heat exchanger
W	rate of circulation of rich solution per unit mass refrigerant circulated in the cycle
X, x	methanol concentration in the solutions by weight ratio or percentage
X_9	concentration of rich solution leaving the absorber
X_{10}	concentration of lean solution leaving the generator

ΔX	concentration difference
Y	mass of saturated liquid methanol evaporated in the throttle valve
Z	vertical distance in cylindrical coordinates
α	the platinum wire temperature coefficient
θ	angle in the cylindrical coordinates
ρ	relative density kg/m^3
μ	viscosity CP
ν	kinamatic viscosity CS
σ	surface tension N/M
ε	heat ratio at evaporator conditions
Fe	Froude number
Gr	Grashoff number
Re	Reynold number
Sc	Smitch number
We	Weber number
Nu	Nusselt number

CHAPTER 1

INTRODUCTION

1.1 Historical background

There is no doubt that man, in the beginning of life was interested in cold as much as he was interested in heat. Although fossil fuels and wood were always available, to burn for heating, in most cases natural snow was not. For this reason, he became more interested in the artificial production of cold.

It is well known in history that the ancient Egyptians used diffusion processes (absorption, mass transfer) to produce cold, using water as the refrigerant and air as the absorbent. They used vaporization of water through vases of porous pottery. An egyptian frieze of the IIIrd millennium shows a slave waving a fan in front of earthenware Jars (Ref 1).

The earliest vapour absorption machine known to history was invented in 1755 by William Cullen (Ref 2). It was introduced as an ice maker. The absorption process was performed mechanically by using a high vacuum maintained by an air pump. Owing, however to the low vapour pressure of water, a very good vacuum was necessary to secure a sufficiently intense refrigeration. These mechanical difficulties led to the introduction of the first absorption machine using an absorbing agent.

In 1810 sulphuric acid was used as absorbent for pure water vapour. Cullen's machine, modified, was probably the basis of Vallance's sulphuric acid machine invented in 1824, and of which Edmund Carre's machine, invented in 1850, was an improvement. Carre's machine consisted of a glass vessel containing water which, under the influence of vacuum and in conjunction of a supply of sulphuric acid, froze rapidly. The machine cooled the water vessel and heated the acid. A few years later Edmund Carre's brother, Fredinand, invented an ammonia absorption machine, which was the forerunner of the absorption machines of the present time. Fredinand Carre's first machine was exceedingly crude, and consisted only of two vessels. One vessel was used as generator and absorber, the other

one as condenser and evaporator. The first vessel contained the solution of ammonia and water, the second contained pure ammonia (refrigerant). When the solution in the generator was heated the ammonia was driven off and liquified in the second vessel using an external water supply. On becoming sufficiently lean, the solution was then cooled by water. The pure condensed ammonia in the other vessel began to evaporate at once and to be reabsorbed by the cold lean solution.

The machine was afterwards greately improved by inventors in France and Germany, by Reece and Stanley in England, and by Mort and Nicolle in Australia. Reece in 1867, introduced the rectifier and seperated the generator from the absorber. In 1870 Mort introduced the solution heat exchanger (named the economizer), designed to transfer heat from the lean solution leaving the generator to the rich solution entering from the absorber. Later on Stanley introduced steam coils into the generator. Several improvements were applied afterwards until finally Pontifex and Wood succeeded in bringing the absorption machine to a high state of perfection and a considerable state of efficiency.

It was as early as 1852, when Lord Kelvin remarked that a "reverse heat engine" could be used not only for cooling but also for heating. However it was not until three quarters of a century later that the first application was made by T.G.N. Haldane (Ref 3) in 1927-28, to heat his London office and his Scottish home. Around 1930, Altenkirch and Maiuri, proposed using an absorption refrigeration machine to air-condition and to heat water. From that time the interest in heat pumps gradually increased. The number of heat pumps installed up to 1938 was only of the order of a few dozen, but it rapidly increased reaching 1.6 M in 1976 in U.S.A. alone.

The Germans, notably K. Nesselmann and W. Niebergall, were interested in absorption refrigerating machines working as heat pumps. There were some installed from 1947 onwards in several countries and breweries to heat liquids, and as well as for air conditioning.

The 1973 energy crisis gave special importance to this system of heating, and research into absorption machines increased.

1.2 The Virtue of heat pumps

The wasteful way in which we use energy have resulted from the availability of cheap sources of fossil fuels. But now, the prices of fuels are increasing and we should not expect them to be again (relatively) as cheap as once they were.

The energy used in buildings and dwellings accounts for approximately one-third of the world's annual energy consumption with space heating representing large percentage of this energy (Ref 4). In the USA, residential and commercial buildings account for approximately one-third of the total energy consumption and over 70% of this energy goes to space heating and hot water for domestic use (Ref 5). In the U.K. the energy consumption for space heating of buildings and hot water for domestic use represents 30% of the gross national energy consumption of which domestic accounts for slightly higher than the half (Ref 6 & 7). This energy increased by 7% from 1978 to 1979, and indeed future increases may be anticipated unless primary fuels are used more efficiently. The importance of the heat pump lies in its greater primary fuel utilisation than convential boilers.

The term "heat pump" was found in the british literature around 1895 (Ref. 1). It is defined as the machine which can elevate heat up a temperature gradient. Heat pumps are two types, mechanical and thermal. A mechanical heat pump is driven by compressor while a thermal heat pump is driven by a source of heat. In both types the energy that is pumped is obtained from environmental sources. The output energy can be used for space and water heating or low temperature process heat.

Although the mechanical heat pump is capable of pumping $2\frac{1}{2}$ - 3 times the heat as power it consumes, the arguments against this system as an energy saver are by now well known. If the compressor is electrically driven, with electricity generated at an efficiency of about 27% in terms of primary fuels, the overall efficiency of the heating process is little better than if the equivalent amount of primary fuel were consumed locally in a conventional boiler. An improvement in primary fuel utilization can be achieved by using a direct drive to the compressor, (e.g. a diesel engine), specially if

the waste heat from the drive unit is recovered. However the high capital cost coupled with the necessity of skilled maintenance militates against its adoption in small buildings.

A thermal heat pump, on the other hand, can usefully pump heat utilizing a reasonably low temperature heat source but, with the limitations imposed by the second law of thermodynamics, its performance expressed as the quantity of heat delivered to the quantity of heat supplied is far less glamourous than the mechanical heat pump. However, the thermal heat pumps is capable of rejecting 1.3 - 1.7 times the quantity of heat it consumes, at useful temperatures for space and water heating. A realistic figure of 1.5 is considered a good objective target. It thus offers a potential energy saving of about 30% in terms of primary energy.

Principles of operation

The second law of thermodynamics states that if heat is transferred reversibly, then the change in entropy will be zero. Furthermore if heat can be transferred reversibly down a temperature gradient then by implication, it must also be possible to transfer it up a temperature gradient. Evaporation followed by condensation is fully reversible process, although pure substances evaporate and condense at the same temperature. However, by providing an absorping material, in the physico-chemical sense, a substance may be caused to evaporate at a higher temperature than that at which it condenses, as a result of the lowering of the vapour pressure by the absorbent. Thus the heat necessary for evaporation will have to be supplied at a higher temperature than is librated during condensation. Having achieved this, the cycle may then be reversed, and the heat necessary for evaporation of the pure substance may be taken in at a lower temperature than that at which it is released when condensation takes place in the absorbing medium. Such is the principle of the absorption heat pump, and a schematic diagram of such a cycle is shown in Fig. (1.1). The four major steps, (latent-heat processes), involving the transfer of the pure substance between the liquid and vapour states take place in four main components forming the cycle, the generator, condenser, evaporator and absorber.

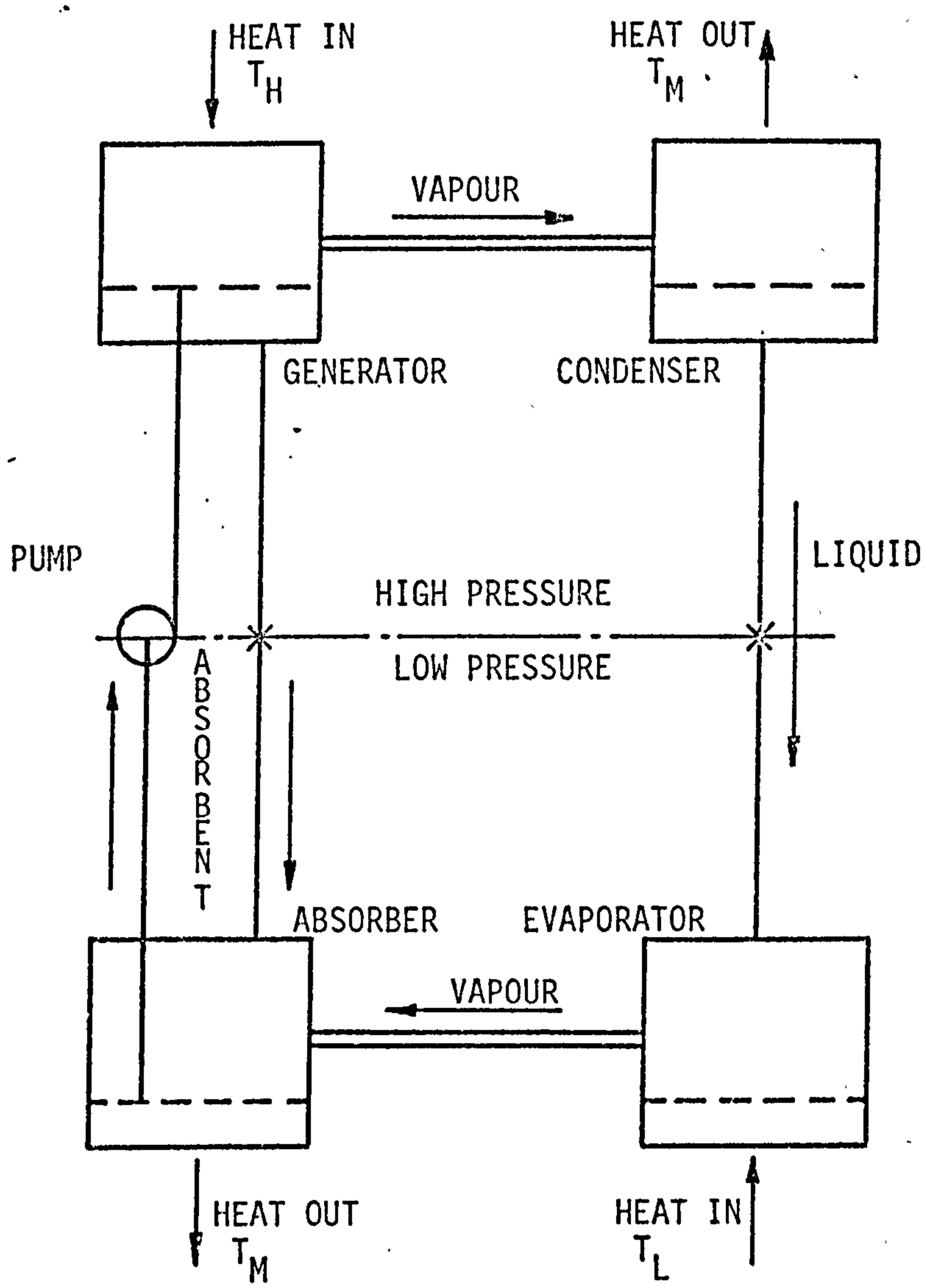

Figure 1.1 Thermal Heat Pump

In order to examine the cycle in detail it is necessary to refer to the vapour pressure-temperature diagram for the pure working fluid and mixtures with the absorbent as is shown schematically in Fig. (1.2). Methanol evaporated at temperature T_E and pressure P_E will be in equilibrium with concentration X_1 solution at T_A. If the solution temperature is lower than this, say T_A, methanol will be absorbed by the solution until it reaches a concentration of X_2, when again equilibrium will exist. The solution is now raised in pressure to P_C and heated to T_G when the absorbed methanol is driven off as superheated vapour and may be condensed at T_C. The condensation and absorption temperatures (T_C & T_A) may or may not be identical, but will be temperatures at which the heat is "useful". T_E will be a temperature at which "non-useful" heat is available, typically the external environmental temperature, or perhaps a little below it.

For a continuous cycle evaporation will take place continuously both in the generator and evaporator and there will be a continuous circulation of methanol rich solution from the absorber to the generator and of lean solution back again.

1.3 Research and development (R & D) of heat pump

The science and technology necessary for the development of the absorption cycle heat pump falls into three broad areas: the operating cycle of the machine, the refrigerant/absorbent pairs that may be used, and the thermal and mechanical design of the components of the machine.

Reviewing the literature and through personal communication it has been possible to carry out a survey in the field of R & D concerning the above mentioned areas.

In 1962, Howatt (Ref 8) compared the performance of gas-fired absorption system with a vapour-compression heat pump for heating and cooling of identical classrooms in a school, and concluded that the operating costs per year of the 3.5 tons (13 kW) absorption unit indicated a saving of 36% with respect to the 3 ton Mechanical heat pump unit used.

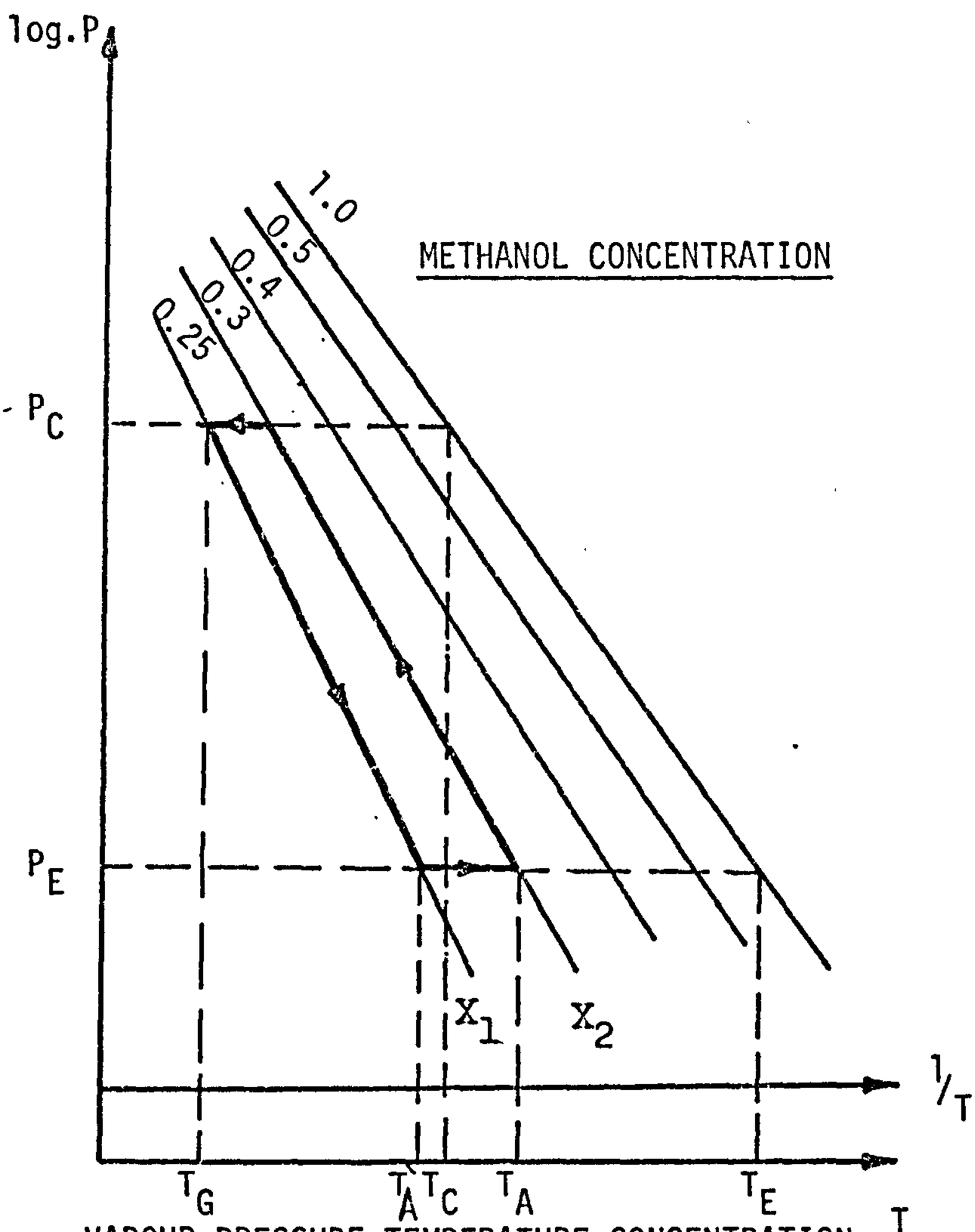

VAPOUR PRESSURE-TEMPERATURE-CONCENTRATION RELATIONSHIPS

Figure 1.2

In 1973 R. H. Merrick et. al (Ref 9) published a theoretical report related to the modification of a domestic 3 ton absorption cycle utilizing solar energy for heating and cooling. However the temperatures obtained when heating were too low to have any practical applications.

In 1974, Williams and Tiedermann (Ref 10) conducted a theoretical study concerning the use of a 3 stages aqua-ammonia absorption system operating between sea water and cold air, to heat a dwelling at higher temperature. The performance was poor and the cycle was too complicated to adapt to domestic use.

In 1976, Best (Ref 11) investigated the overall coefficient of performance (COP) of heat pump using a new candidate (methanol and mixed bromides) and claimed attractive COP values (1.8).

Gallagher-Daggitt et al (Ref 12) constructed a heat pump of 5 kW output power using sulphuric acid/water combinations. The machine was tested achieving a temperature lift of about 52°C and technical limitations to the performance were identified. They recommended more investigation of heat transfer in the evaporator for boiling at low pressures.

Qasrawi (Ref 13) developed an ammonia/water heat pump of 10 kW nominal output power and claimed the following conclusions:

- A rectifying column and a partial condenser are necessary parts of the generator system in an absorption device using an ammonia/water system.

- The dribble wetted-wall absorber in which heat and mass transfer occur simultanously is adequate for an efficient absorption process with an ammonia/water working fluid.

- The existence of a detailed and realistic computer model for the prediction and optimization of cycle performance is an essential requirement and is dependent on the availability of accurate thermodynamic data for the working fluids involved.

The cycle was modelled with a computer programe able to

predict the steady state behaviour. A solution circulation pump has been specified and a prototype is in the design stage. Values of COP are around 1.45 were anticipated at evaporation temperature around $0^{o}C$. The search is a continuous one for the acquisition of physico-chemical data for alternative working fluids to facilitate the further implementation of mathematical modelling techniques.

Iedema (Ref 14) has been collecting data from experiments on the absorption process of methanol and mixed bromides for a low temperature ($35 - 45^{o}C$) heat pump. A calculated mass transfer coefficient is given (7×10^{-6} m/sec) but a comprehensive set of results is not yet available.

Oelert (Ref 15) developed a primary energy driven absorption heat pump for domestic heating. Working conditions were specified as follows:

- Temperature lift = $55-(-2) = 57^{o}C$

- power output = 12 kW

Among the investigated combinations R22/E181 (tetraethylene glycol dimethylether) was selected to meet the specifications. A prototype was produced using a jet pump between the evaporator and the absorber, activated by desuperheated R22 vapour from the condenser to boost the absorber performance at low heat source temperature. The absorber was operated adiabatically and the lean mixture was cooled by a water heat exchanger up-stream of the absorber. A 35% fuel saving is expected, but the work is still in progress and results have not yet been published.

Muller (Ref 16), constructed a research in the application of absorption heat pump for drying process. A device was constructed using lithium chloride and substantial savings were achieved as 1 kWh replaces 7 kWh, which saves a total of 1250 toe per year.

Hour and Bugarel (Ref 17) studied the control of absorption heat pump under part load in 3 different ways, viz control of the power input to the generator, control of the solution circulation flow rate, or control of both. They showed that the operating conditions

and the COP of the pump hardly vary regardless of the load. However, they showed that the first two types of control limit the modulation to not more than 60% of the maximum load, while the last type of control allows a much greater modulation range.

An interesting research has been conducted by Malewski (Ref 18) which led to the development of a district heating absorption plant of an output of 3.5 MW for a domestic space heating. The plant has been in operation since Autumn, 1980. The COP obtained is 1.458 at an evaporation temperature of 15 - 20^{o}C. A heating temperature of 90^{o}C is achieved with a generator temperature 180^{o}C. However, pressures of up to 40 bars are reached in the equipment (ammonia/water).

The effect of components design on the performance of the absorption heat pump and the investigation of new technologies to improve the performance of the machine is being studied, in the Katholieke University in Heverlec, Belgium.

It has been realised that very few investigations are concerned with the thermodynamic and physico-chemical properties of new fluids for the absorption heat pump. Most of the previous works were concentrated in adopting the well known pairs (ammonia/water and water/lithium bromide) typically used for refrigeration. Even those who considered other pairs restricted their investigations to the determination of vapour pressure equilibrium data. Investigations concerning other required data of new refrigerant/absorbent combinations have not been published. However, it was not possible to find some work - apart from (Ref 14) - dealing with the physco-chemical properties of new combinations for heat pump applications.

The technology of absorption cycle design and construction gained by the experience from conventional absorption refrigeration machines falls far short of the requirements of the absorption heat pump particularly in respect of the temperature range over which the materials have to operate.

In this work a preliminary computer program was written to study the effect of working conditions on the overall COP of an absorption heat pump utilizing methanol/2 LiBr - $ZnBr_2$ as working fluids. The program, based on estimated data of solution properties, is capable of

calculating the effect of uncertainties in the properties on the COP of the cycle. The fluid was identified for heat pump application by the determination of thermodynamic, transport, and physico-chemical properties. The enthalpy of vaporisation was determined for a range of temperature and pressure suitable for heat pump operational conditions. The program was modified in later stages of the work utilising the measured properties and the enthalpy of vaporisation to study some design parameters of major components in the cycle.

An intermittently operating absorption device of 1 kW output power was designed and built and the performance of the low pressure side was measured at realistic working conditions.

CHAPTER 2

PRELIMINARY CALCULATIONS OF THE HEAT PUMP CYCLE AND ESTIMATION OF ITS PERFORMANCE

An engineering study of absorption heat pump should embrace the following aspects; the investigation of the thermophysical properties of different absorbent-refrigerant combinations, their thermodynamics, and the study of the cycle including the estimation of the equipment performance as well as the effect of operating conditions.

Hainsworth (Ref 19) pointed out that, the study of refrigerants and absorbents constitutes a specialised part of the search. However it is apparent that a study of refrigerants and absorbents cannot be isolated from considerations of the cycle and equipment.

The purpose of this chapter can be stated as a review of an important combination in the literature (methanol-salt solutions) and estimating the performance of a heat pump cycle utilising them. This was done firstly by examining the properties of an ideal working fluid. Then, in conjunction with the requirements of the proposed cycle, the fluids employed in the existing absorption machines were discussed.

2.1 Review of working substance

2.1.1 Desirable properties of combinations

It was not until 1944, that Hainsworth (Ref 19, 20) made a theoretical survey of a large number of combinations that might be employed in an absorption cycle. As a conclusion of his work it was clear that careful study should be made of different combinations before selecting the best. Buffington (Ref 21), followed Hainsworth's work with more details about the effect of the combination properties in the real cycle performance. A study

of the theory and principles of absorption cycle in connection with combination properties and cycle economy at different working conditions as compared with vapour compression cycle have been given in Ref 22.

The most significant feature of the absorption cycle is the mass and heat transfer process which takes place in the absorber. Accordingly care should be given to the combination of properties affecting the efficiency of this process. The properties of the binary system are divided into two groups:

(a) Properties which affect the common processes of heat transfer and phase-change as well as fluid flow along the cycle (relative density, viscosity, thermal conductivity and specific heat).

(b) Properties of significant importance as to the absorption cycle in particular, (solubility deviation from Raoult's law, chemical stability and diffusion coefficients).

The required properties are:

(1) High solubility and negative deviation from Raoult's law. If P is the vapour pressure of the pure refrigerant at the evaporator temperature (the low side pressure) and P_o is the vapour pressure of the pure refrigerant at the absorber temperature. If the condensation temperature is equal to the absorber temperature (a typical case), then P/P_o corresponds roughly to the reciprocal of the compression ratio of an equivalent vapour compression cycle. Accordingly the higher the negative deviation from Raoult's law, the higher the possible achieved temperature differences between the evaporator and the condenser. Jacob et al (Ref 23) showed that high negative deviations account for high heat of mixing and lower coefficient of performance (COP). However employing an ideal solution of Raoult's solubility in an absorption machine might give low weight fraction of the refrigerant in the rich liquid corresponding to certain absorber conditions. Thus it would be necessary to circulate high rate of solution to deliver one unit of mass of the refrigerant to the condenser and the evaporator. This would increase the sensible heat

load on the generator and lower COP again. For the same reason an excessively large equipment would be necessary.

Although it is always referred to the behaviour of the mixture at absorber conditions, Olama (Ref 24) showed that ideal behaviour of the solution at generator conditions is more desirable so that lower generation temperatures can maximise the performance of the cycle specially at high temperature lifts.

It must be remembered that Raoult's law refers to molar concentrations, so low molecular weight is an important criterion in selecting absorbents and can sometimes outweight the benefits of larger deviations from Raoult's law. Low molecular weights unfortunately in general imply low boiling points and high vapour pressures which are a serious disadvantage in absorbents. Solubility of absorbents is effective in the way that the rate of circulation of solution relative to the flow rate of pure refrigerant through the condenser and the evaporator will also depend upon the concentration change that takes place in the solution during the cycle. This change in concentration is dependent on the degree of salt richness that can be obtained in the solution, which is fixed by the salt solubility limits. That is why a wide range of weight fractions of the solution without separation of constitutents is of great significance specially for solid absorbents. This will keep the solution circulation rate minimum which will increase the temperature lift and reduce the heat load on the generator, thus accounting for high COP.

(2) Vapour pressure

Moderate vapour pressure of the refrigerant over the employed temperature range between the evaporator and the condenser is highly recommended. High vapour pressures at the condenser temperature will necessitate the adoption of an expensive high pressure system, particularly in respect of the solution pump. On the other hand very low vapour pressure at the evaporator temperature will dictate a vacuum technology in the production of the equipment

to avoid leaks to the system. Such technologies will complicate the maintenance routines and increase the cost. Furthermore low pressures lead to very large specific volumes of refrigerant vapour, and tend to increase pressure losses.

Solutions exhibiting high negative deviations from Raoult's law at absorber conditions require a high generator temperature and this leads to higher heat losses, more super heat irreversibilities, and increase the risks of corrosion and decomposition. Also, the pressure difference between the evaporator and the condenser is of recognisable importance as it might be possible to avoid pumping and utilise a thermosyphon arrangement to transport the absorbent from the absorber to the generator. This would be of great advantage in terms of the reduction of cost, complex and reliability.

(3) Volatility ratio

Buffington (Ref 21) draws attention to the fact that although the normal boiling points in ammonia/water combination systems differ by more than 110 ^{o}C, fractional distillation is required which accounts for more equipment and less efficient thermal processes. The absorbent should ideally be non-volatile, or at least very much less volatile than the refrigerant. In this respect salt absorbents predominate.

(4) Mass transfer

In order to keep the circulation rate of the solution to a minimum the concentration change taking place in both the absorber and the generator should be as large as possible. To achieve this in the absorber the absorption process should be rapid and the actual concentraction of rich liquid should approach the equilibrium value. Higher diffusion coefficients will accelerate the process whatever mass transfer mechanism is utilised. Also a lower rate of change of vapour pressure relative to concentration change at absorber condition will improve the absorber performance. It is fortunate that the primary reaction at the absorbing surface is

practically always extremely rapid, the question is whether the secondary processes of diffusion mixing and heat transfer to the external cooling medium are fast enough. These processes are aided also by the solution physical and thermal properties such as viscosity, thermal conductivity and surface tension.

(5) Freezing point

It is meaningful to have low freezing point refrigerant particularly for heat pumps, as heat extraction from ambient at subzero temperatures would be possible. The absorbent/refrigerant combinations should have low freezing point too to avoid freezing of the fluids in the machine during shut down, especially under winter conditions. It should be noted that low freezing point of the solution requires an absorbent of considerably lower freezing point which contradicts with that of having a high boiling point absorbent. Although some techniques of using anti-freeze fluids or even azeotropes may be explored in the future the complication in using them is appreciated. Solar assisted evaporators provide a solution against refrigerant freezing and frost but, necessarily, they are more expensive.

As a rough rule, the freezing point of fluids of all compositions which may occur during operation should be lower than the lowest temperature to which they may be subjected.

(6) Stability

Working fluids in absorption machines undergo repetitive changes of state and temperature over long periods, thus one must seek materials which are stable over the working range of temperatures and pressures. Combinations differ from one another and one which may be stable at the working conditions of an air conditioner where low temperatures are employed may not be stable over a relatively high temperature range utilised in heat pumps. On the other hand a combination for a heat up-grading machine for industrial processes will certainly need severe requirements on stability. Decomposition, formation of solids or unwanted reaction products are serious

disadvantages of a combination and certainly will eliminate it from being employed. Corrosive combinations militate against the production of reasonably cheap heat pump machines, as expensive metals or other materials may have to be used. The corrosion may also cause the evolution of gaseous contaminants. Because absorption machines conventionally employ, as the materials of choice, copper tubing for the heat transfer functions and steel for mechanical enclosures several works have been published in the investigation of corrosion inhibitors in limiting the effect of the more common working substances on such materials (Refs 25, 26, 27).

(6) Safety

Refrigerants, absorbents and their combinations should be non-toxic and non-flammable. For domestic use, with refrigerant solution being heated by gas flame for instance, non-flammability is particularly important. It is also desirable to have non-toxic products when heated in a flame. Toxicity is, in fact, more serious than inflammability, however, various system design can to some extent reduce the risk. Using central heating systems for example with a secondary cooling fluid circulated in the radiators with the machine itself as retrofit to the conventional boiler will certainly limit the danger of toxicity.

(7) Viscosity

Low viscosity is an important feature in selecting absorbents. The effect of operating temperature level is of significance since viscous solutions which may not be used in cooling devices may however be used in heat pumps where temperatures are higher. The role played by viscosity affects one of the most technologically difficult aspects of absorption, namely the wetting efficiency of the absorber surface. In addition, a lower viscosity increases the heat transfer coefficient, hence reduces the size of the heat transfer equipment and also the power losses in circulating the solution.

(8) Thermal conductivity and specific heat of the solutions

Such thermal properties are generally required for all working substances that are involved in thermal processes in different cycles. Their effect within the absorption heat pump cycle is unique. With the solution heat exchanger duty found to be several times as high as the total output of the machine itself (Ref 36), as is shown in Fig.2.1, a low specific heat and a high thermal conductivity of the mixture will obviously be beneficial.

The main source of irreversibility in the system is that taking place in the circulation of cool rich solution to the generator and the hot lean solution back to the absorber. The lower the specific heat of the solution the lower is this irreversibility, hence higher COP and vice-versa. For that reason refrigerants of high latent heat to specific heat ratio and absorbents of low specific heat are strongly recommended. Specific heat affects the absorber performance too. The lower the specific heat the higher the temperature increase of the solution due to absorption and therefore the slower the process. This will limit the concentration change, particularly in adiabatic absorbers.

2.1.2 Existing Cycles

The main widely used absorption cycles for refrigeration and air conditioning are those employing ammonia/water and water/lithium bromide systems. Many researches have been carried out in order to employ them for heating, too, as was shown in Chapter 1.

(i) Ammonia/water cycle

Ammonia as refrigerant is second only to water in terms of latent heat, but it is very toxic and has a very high vapour pressure. Water, as the classic absorbent to ammonia, is of low molecular weight but it also has a relatively high vapour pressure and a high specific heat.

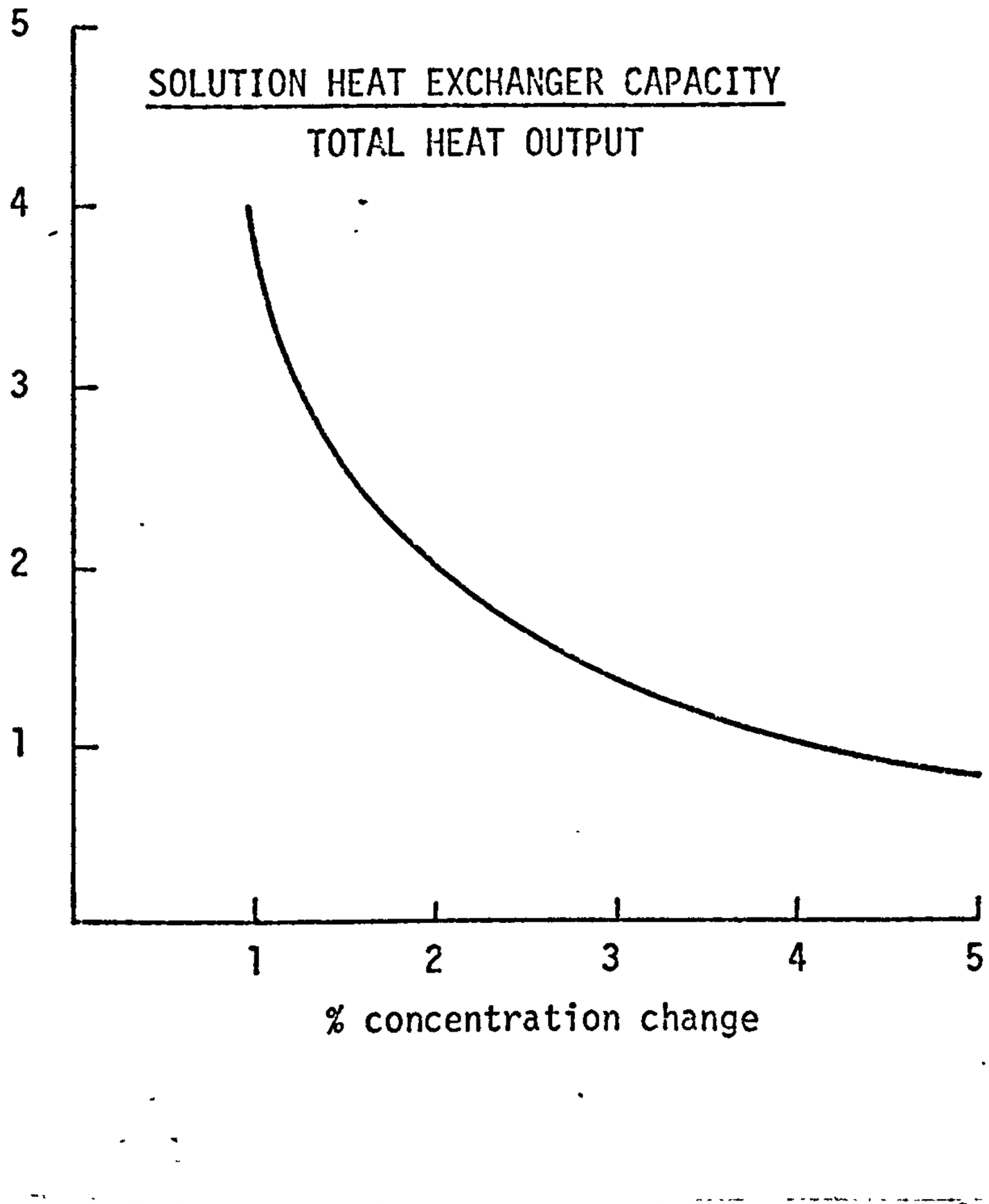

Figure 2.1 Solution heat exchanger capacity in the methanol thermal heat pump

The combination is good in having a large range of solubilities and exhibiting high negative deviations from Raoult's law. However, low volatility ratio dictates the use of additional equipment (a rectifier) and the high pressure of the system necessitates pressure equipment and, even more, a high solution pumping requirement. Because ammonia is toxic, the machines are recommended for installation outside residential dwellings. The mixture is stable but corrodes copper, tin and zinc, but iron and steel have considerable corrosion resistance. The absorbability of ammonia by water is known to be high having a diffusion coefficient of $2 \times 10^{-9} m^2/sec$. There exists an experience of long standing with ammonia-water mixtures in refrigeration and this would certainly help in adoption for heat pumps.

(ii) Water/lithium bromide

While water is considered as a reasonable absorbent for ammonia, it is the best refrigerant in terms of its high ratio of latent heat to specific heat. On the other hand its low vapour pressure leads to high specific volumes at evaporator conditions and it freezes at $0\ ^{o}C$ which prevent its exploitation as a fluid at sub-zero temperature.

Lithium bromide is a salt absorbent of negligible vapour pressure but having a high molecular weight.

The material is attractive in its low vapour pressure characteristics and high deviation from Raoult's law, however, salt solubility is limited by temperature.

The mixture is corrosive but a few inhibitors are known and mild steel can be used. The system, used as a heat pump, would not achieve high temperature lifts, although solar assisted evaporators could be employed. The solution is rather viscous but has a reasonably high thermal conductivity. Stability presents no problem as well as safety. The system is widely used in various areas of cooling, heating and air conditioning.

(iii) Other combinations

Several refrigerant/absorbent combinations are under development. None of them is as widely used as the two just discussed. Different salts are used with wide range of refrigerants. Water/ sulphuric acid has certain attractive properties. Methanol and some salts were studied and reported to have promising characteristics. Fluorocarbon refrigerants are under investigation but it should be kept in mind, as it was mentioned before, that none of the combinations is ideal for all applications and careful choice should be made and certain disadvantages must be accepted.

2.1.3 Methanol salt solutions and the proposed cycle

In seeking an absorption heat pump that will transfer heat from ambient temperatures to meet the requirements of a living environment it is apparent that it should be capable of absorbing heat at, say, -10 ^{o}C with delivery at a temperature of perhaps 50 - 70 ^{o}C. The higher figure is dictated by the design of current "wet" space heating systems (although it may alter in the future), and also by domestic hot water requirements. The latter should not be underestimated for as insulation levels are increased and other thermal losses from buildings reduced, the hot water load may be expected to constitute an increasing fraction of the total. Clearly the water/LiBr combination already referred to is incapable of operating at temperatures below 0 ^{o}C whilst the ammonia/water system will develop a pressure over 30 bar if condensation takes place at 70 ^{o}C with the associated difficulties mentioned above.

Following a thorough search of the literature for more suitable working fluid/absorbent combinations, methanols was identified as being the next most suitable working fluid in respect of its vapour pressure and latent heat/specific heat ratio, with a mixture of lithium bromide and zinc bromide in 2:1 molar ratio as the absorbing medium. Methanol salt solutions were first proposed to the absorption machines in 1965 by Aker et al (Ref 28). They investigated methanol as a

refrigerant with various salt absorbent and found that all solutions with the exception of those containing zinc bromide, exhibited high negative deviation from Raoult's law over the entire concentration range and that solutions containing zinc bromide exhibited a positive deviation at low salt concentration. But they warned that salting out might possibly occur under some circumstances in the absorption units because of incomplete miscibility. However, they concluded that salt solutions with methanol based on thermodynamic and solubility considerations may find application in absorption machines for different purposes, with special recommendation of systems containing methanol plus mixtures of about 2 moles of lithium bromide and 1 mole of zinc bromide, not only because they can possess higher concentration change but also for relatively low viscosity.

Aker's work was followed by few investigations aiming in addition to more measurements of solubility, to find other properties of the solutions.

Uemura and Hasaba (Ref 29, 30) published a comprehensive set of data for the methanol-salt solutions (vapour pressure, viscosity, relative density, specific heat, salt solubility, heat of mixing and enthalpy diagram) and predicted the overall performance of a refrigeration unit at different working conditions. Grossman et al (Ref 31, 32, 33) published similar work to that of Uemura in the U.S.S.R about the same time (1965-1970) but only for methanol/lithium bromide and recommended their use for absorption refrigeration and heat pumps. The only practical absorption equipment which employs methanol is that of Olama (Ref 24) modified by Alloush (Ref 34). Olama investigated the thermodynamic properties of a few methanol/salt solutions and constructed an absorption cooler employing methanol/2LiBr-$ZnBr_2$ as working fluids. The COP was estimated and then the performance of a chiller was measured yielding a value of 0.2 at an evaporation temperature of -11 ^{o}C and absorber-condenser temperature of 35 ^{o}C. Olama concluded that by using this mixture the generator temperature would be lower than for ammonia/water and water/LiBr if other

temperature conditions were kept the same.

Renz et al (Ref 35) again measured the vapour pressure, solubility, viscosity and relative density of methanol/LiBr over a wider temperature range applicable to the absorption pump and made some useful comparisons with other investigations of various pairs.

For the thermally driven heat pump with the previously mentioned working conditions, the choice of working substance was limited to the methanol based salt solutions. Figure 2.2 shows the vapour pressure of possible compositions of four different methanol solutions reported by Aker (Ref 28) at a temperature of 54.5 ^{o}C. It was clear from the figure that although solution (1) exhibited the highest negative deviation from Raoult's law it has limited salt solubilities, and while solution rates of circulation in a practical machine using this substance would seem to be low, the concentration change will be restricted by possible crystallisation and so the circulation rates will be high. In addition to that the evaporator temperature such as was proposed for the cycle will not be possible.

Solution (4) (pure zinc bromide) in the same figure showed higher salt solubilities but vapour pressure was not at any fraction as low as 15 mm Hg (methanol vapour pressure at about -10 ^{o}C) and the solution was excluded. Salt solubilities of solution (3) are higher and pressure is lower than solution (4) but again concentration change is restricted by solubility limits. Solution (2) showed the optimum characteristics. Reasonable negative deviations from Raoult's law were observed, on the other hand salt solubilities are so high that at an evaporator temperature of -10 ^{o}C about 5 - 7% concentration changes may be possible. Salt solubilities of that solution over a temperature range from 0 to 70 ^{o}C were reported by Uemura and Hasaba (Ref 30). Their results are shown in Fig.2.3.

Such results show that the solubility of the mixed bromides

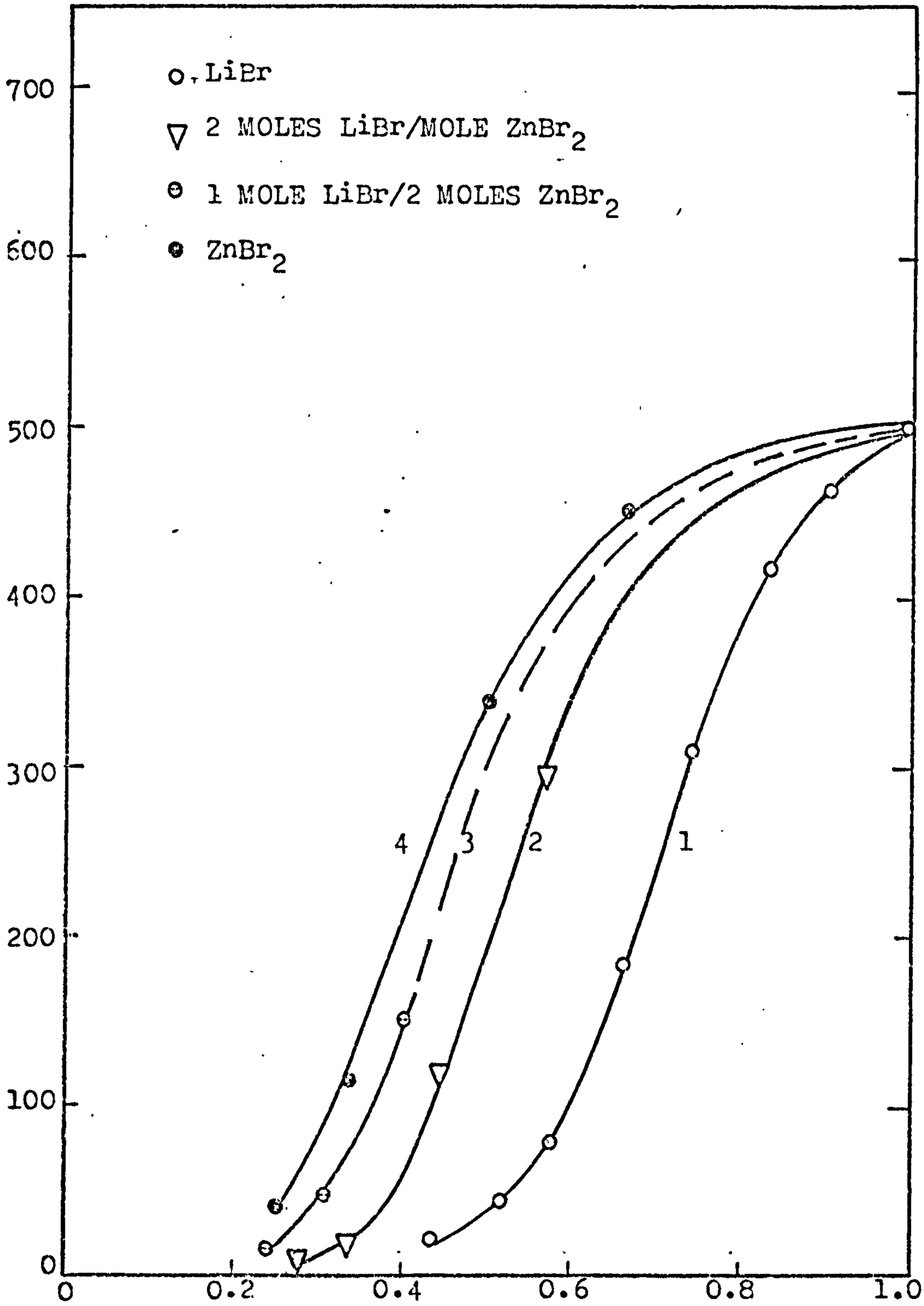

Figure 2.2 Vapour pressure of Methanol-Salt solutions at 54.5°C

(reproduced from Ref 28)

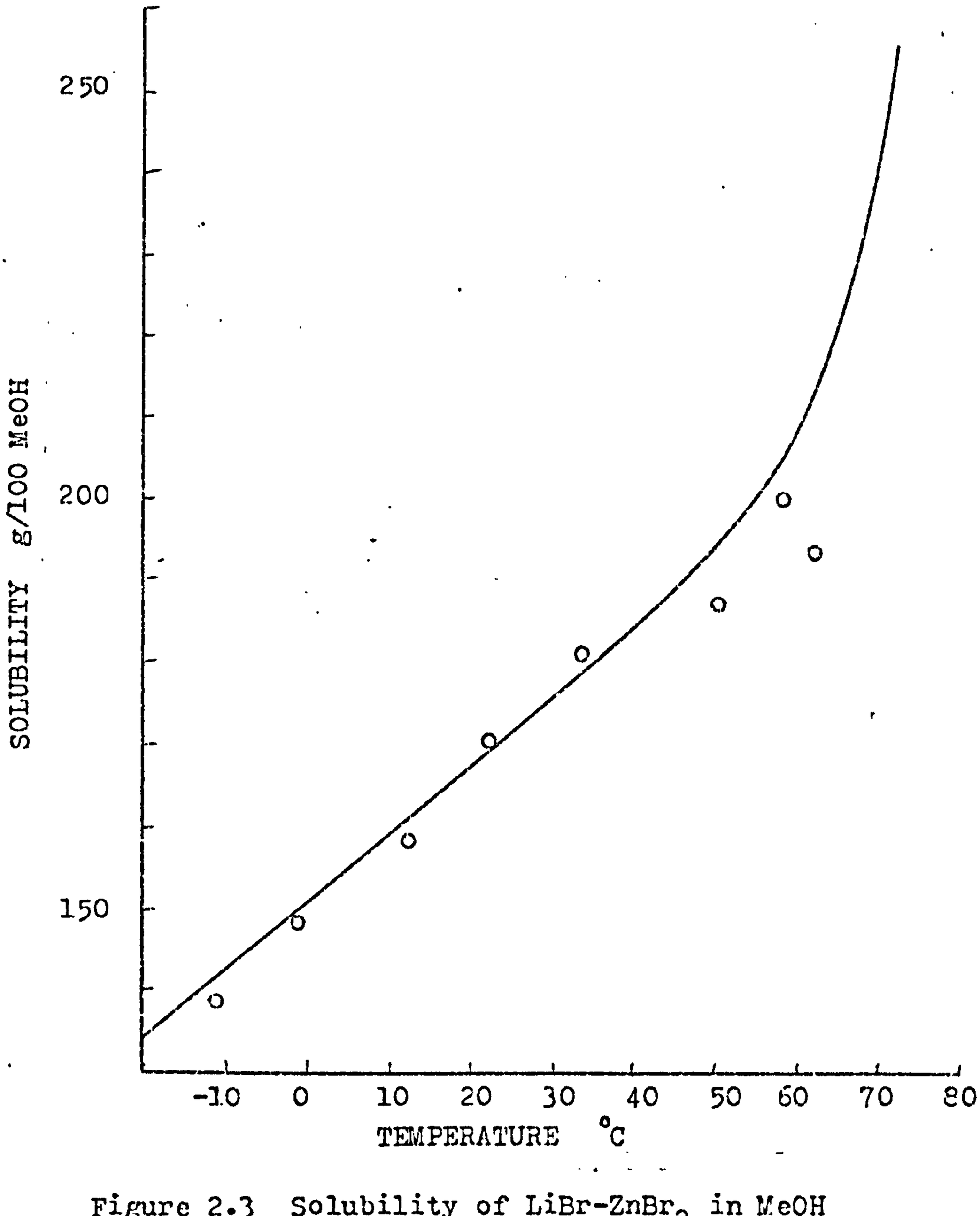

Figure 2.3 Solubility of $LiBr-ZnBr_2$ in MeOH
(reproduced from Ref 30)

in methanol varied only from 1.5 - 2 kg/kg solvent giving a low temperature coefficient of solubility which reduces the risk of solidification of the absorbent due to crystallisation during shut-down periods. The role of zinc bromide in conjunction with the principle absorbent, lithium bromide merits comment. The viscosity of the absorbing solution was drastically reduced hence reducing the pumping power necessary through the solution heat exchanger. Comparison of viscosity of different pairs is shown in (Fig.2.4) from which the effect of zinc bromide towards the reduction of viscosity is seen.

Toxicity and inflammability of methanol are the main drawbacks of the system. However, 200 ppm are allowed in comparison to 50 ppm only for ammonia which is already in wide applications (Ref 37).

Corrosion ; Kruegan (Ref 27) reported on the corrosion inhibitor tests to such solutions and showed that by adding a synergistic combination of arsenic trioxide and the sodium salt of ethylene-diaminetetracetic acid in 2% concentration to the solutions the loss for mild steel 1018 was reduced to 20% of the uninhibited system. They found that such corrosion rate is only 3.5 MPY (mils per year) at a temperature of 171 ^{o}C and concluded that the mixture mentioned above works as corrosion inhibitor to the methanol/LiBr-$ZnBr_2$ system.

The relative density of the system is higher than relative density of the water/LiBr system and the thermal conductivity (measured later in this work) is lower, however specific heat, surface tension and viscosity are higher. When employing methanol systems the safety precautions are of great importance and the central heating systems with secondary heating fluids are an ideal solution to that problem. Due to the fact that salts are of high boiling point, no rectifier is necessary on the other hand the problem of salt separation is less severe than lithium bromide in water.

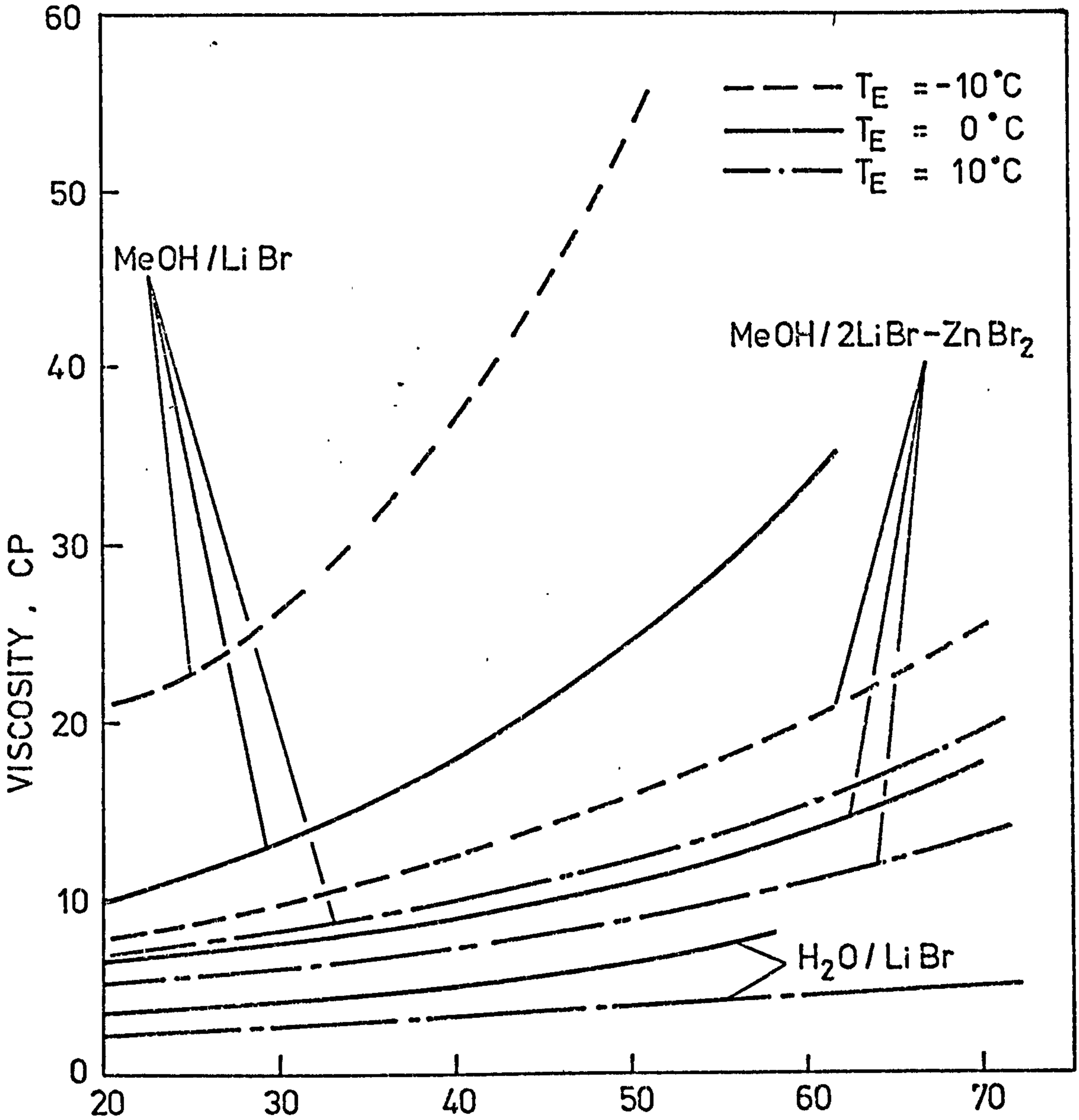

Figure 2.4 Viscosity in relation to absorber temperature -

2.2 Estimation of the properties of 2LiBr-$ZnBr_2$/Methanol solutions

2.2.1 Vapour pressure of the solutions

From the available data on vapour pressure of the mixtures (Ref 28, 29 and 30) it was possible to find the temperature of saturated states of methanol and solutions of different concentrations at equal pressures. These results were correlated using Duhring's rule and correlating relationships were deduced to determine the equilibrium concentrations at absorber and generator conditions. These formulae are

$$X_9 = 1.502 \frac{T_E}{T_A} - 0.873 \qquad (2.1)$$

$$X_{10} = 1.473 \frac{T_c}{T_G} - 0.873 \qquad (2.2)$$

where X_9, X_{10} are equilibrium mass fraction of methanol at absorber and generator conditions respectively

T_E is evaporator temperature

T_A is absorber temperature

T_c is condenser temperature

T_G is generator temperature

2.2.2 Specific heat of solutions

In the estimation of the specific heat of the solutions, it was assumed to depend linearly on the ratio of the constituents

$$C_{ps} = xC_{pm} + (1 - x)(0.436\ C_{pL} + 0.564\ C_{pZ})$$

where C_{ps} solution specific heat

C_{pm} specific heat of methanol

x weight fraction methanol

C_{pL} specific heat of lithium bromide

C_{pZ} specific heat of zinc bromide

The specific heat of lithium bromide was taken from Ref 38 and the specific heat of zinc bromide from Ref 39.

$$C_{pL} = 11.5 + 0.00302\ T \qquad \text{k cal/kg mol } ^{o}K$$

$$C_{pZ} = 12.6 + 0.0104\ T \qquad \text{k cal/kg mol } ^{o}K$$

The specific heat of methanol was taken from Ref 40, as

$$C_{pm} = 2.3529 + 0.5166\ \left(\frac{t}{100}\right) + .003011\ \left(\frac{t}{100}\right)^{2} \qquad J/gm\ ^{o}C$$

This equation gives results to within 2% of those experiments reported in the literature.

For the solution

$$C_{ps} = x * (((3.0 * 10^{-5} * (T-273) + 5.2 * 10^{-3}) * (T-273)) + 2.35) + (1 - x) * (0.373 + 2.5 * 10^{-4} * T) \qquad kJ/kg\ ^{o}K \qquad (2.3)$$

This equation was compared with the data of Uemura and Hassaba (Ref 30) when it showed about 8% higher specific heat than their smoothed data.

2.2.3 Heat of vaporisation of the solutions

The dependance of the vapour pressure of a sbstance on its temperature is described by the Clausuis-Clapeyron equation

$$d \ln P = \frac{H}{R}\ d\left(\frac{1}{T}\right) \qquad (2.4)$$

where P is vapour pressure in any units
T is absolute temperature of the substance
R is the gas constant
H is the heat of vaporisation of that substance

Two assumptions have been made to deduce this equation, the pressure is so low that the specific volume of the liquid phase is negligibly small relative to the specific volume of the vapour phase, and the vapour of the substance obeys the ideal gas law. In practice however it is well known that most of pure substances as well as solutions obey this equation reasonably well, up to within 0.8 of the critical temperature (absolute).

The latent heat of vaporisation of pure methanol was calculated employing the previous equation and the experimental results of vapour pressure found in literatures. The calculated values agreed within 1% with published data of latent heat over a temperature range up to 130 ^{o}C and within 8% up to 200 ^{o}C.

Because the solutions exhibit a lower vapour pressure than methanol at the same temperature, equation (2.4) would be applicable even at higher temperatures. The expected inaccuracy due to that when solutions of less than 0.35 methanol fraction at lower temperatures than 200 is not greater than 2%. The new notation, $\hat{H}$, is the enthalpy of vaporisation from the solution.

The ratio of $\hat{H}/H$ may be obtained by comparison of the slope of the vapour pressure lines $\ln p \times \frac{1}{T}$ for pure refrigerant and different compositions Fig.3.11. This comparison may be carried out at equal temperatures (Othmer's rule) or at equal pressures (Dhüring's rule). Because Clausius-Clapeyron is more reliable at low pressure conditions it was decided to use Dhüring's rule to calculate H' in terms of H. Data for these calculations was found in Best (Ref 41), derived from vapour pressure results published

by Aker (Ref 28). A relation of H'/H as a funtion of methanol fraction was deduced.

$$\frac{H'}{H} = 1.689 - 1.942\,x + 1.397\,x^2 \qquad (2.5)$$

where x is weight fraction of methanol

The formula for heat of vaporisation of pure methanol was taken from Ref 41.

$$H = 2.62.79\left(\frac{513 - T}{175.3}\right) \text{ k cal/kg} \qquad (2.6)$$

Results of this formula were confirmed over the range of temperature from 0 to 240 ^{o}C and were found within a maximum error of less than 2% from experimental data in Refs 38 and 42.

Other correlations found in References (40) and (43) showed more deviations from experimental results. It was not possible to confirm results at sub-zero temperatures because of lack of information.

2.3 Evaluation of the performance of the methanol heat pump cycle

2.3.1 Basic calculations

The typical absorption cycle, already referred to in Chapter 1 consists of two main flow streams, the pure refrigerant flowing between the generator and the absorber under-going change of phase processes in the condenser and the evaporator and the solution stream circulating between the generator and the absorber. The basic calculations include the determination of the state properties of these two streams at any point of the cycle.

In order to carry out a more detailed analysis of the absorption heat pump further to the general previous description (Chapter 1), the proposed methanol heat pump cycle is shown in Fig.2.5.

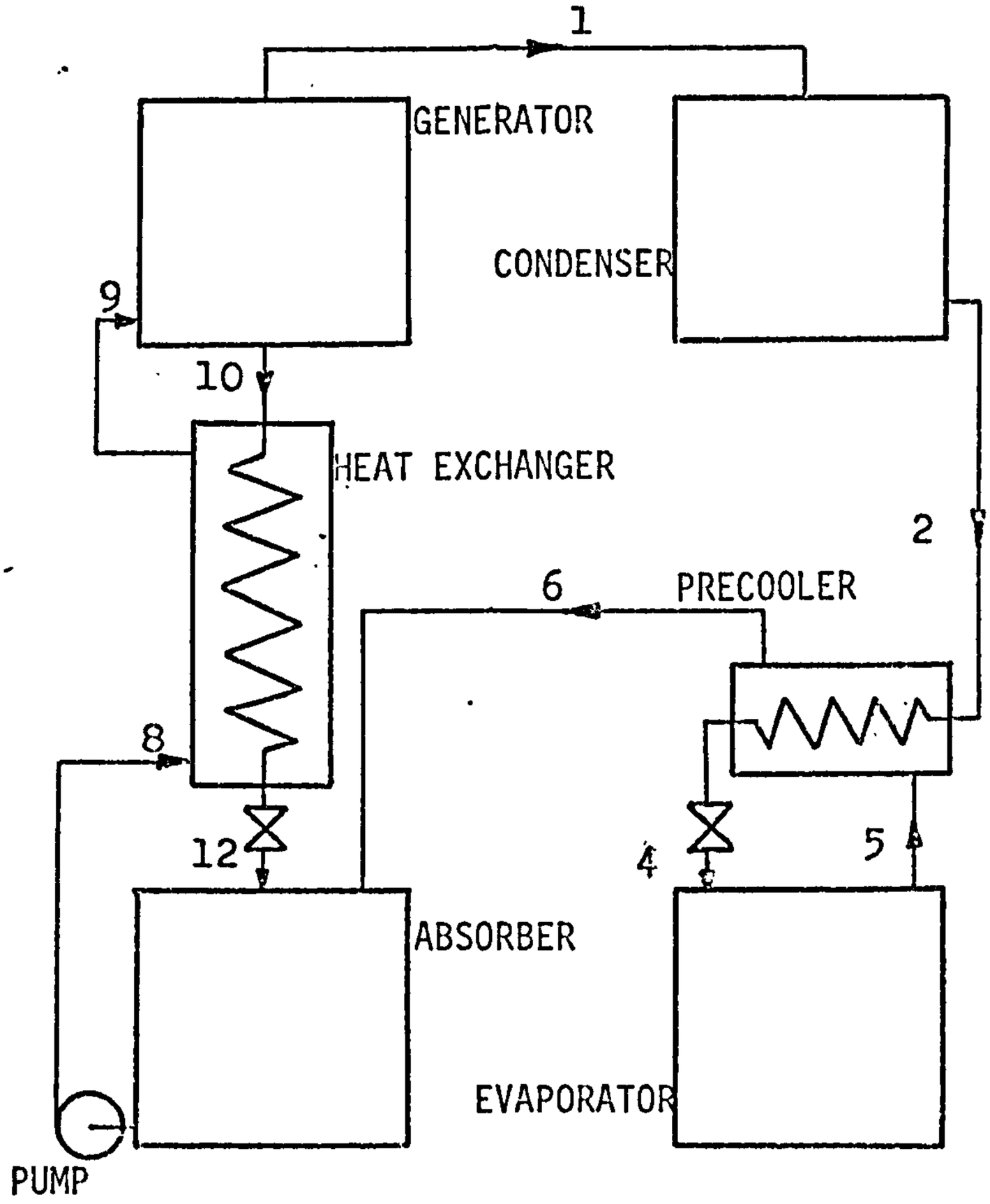

Figure 2.5 Thermal Heat Pump Cycle

A liquid heat exchanger is included to recover heat contained in the hot lean solution leaving the generator and a pre-cooler is employed to heat methanol vapour leaving the evaporator utilising the sensible heat of liquid refrigerant leaving the condenser. No provisions are provided in the cycle for the separate recovery of the super-heat in the refrigerant leaving the generator. Because the solvents are non-volatile no rectification was necessary. The states of the two streams (refrigerant and solution) are indicated in the figure and the following ideal conditions were assumed applicable:

(1) Equilibrium conditions occured between the refrigerant gas state (1) and the solution state (10) leaving the generator at its temperature and pressure T_G and P_C respectively.

(2) The work required to pump the strong solution to the high pressure side of the cycle was assumed to be negligible.

(3) No heat losses or pressure drops (other than that between the high and low pressure sides) occured in the overall process.

(4) The states 2 and 5 are saturated states of the refrigerant corresponding to condenser and evaporator conditions respectively.

The following analysis is made on the basis of a heat and mass balance within the cycle. Figure 2.6 shows the energy flow within the absorption cycle in which

Q_E is heat absorbed in the evaporator at an absolute temperature T_E and pressure P_E

Q_C is heat removed from the condenser at T_C and P_C

Q_A is heat removed from the absorbent T_A and P_E

Q_G is heat supplied to the generator at T_G and P_C

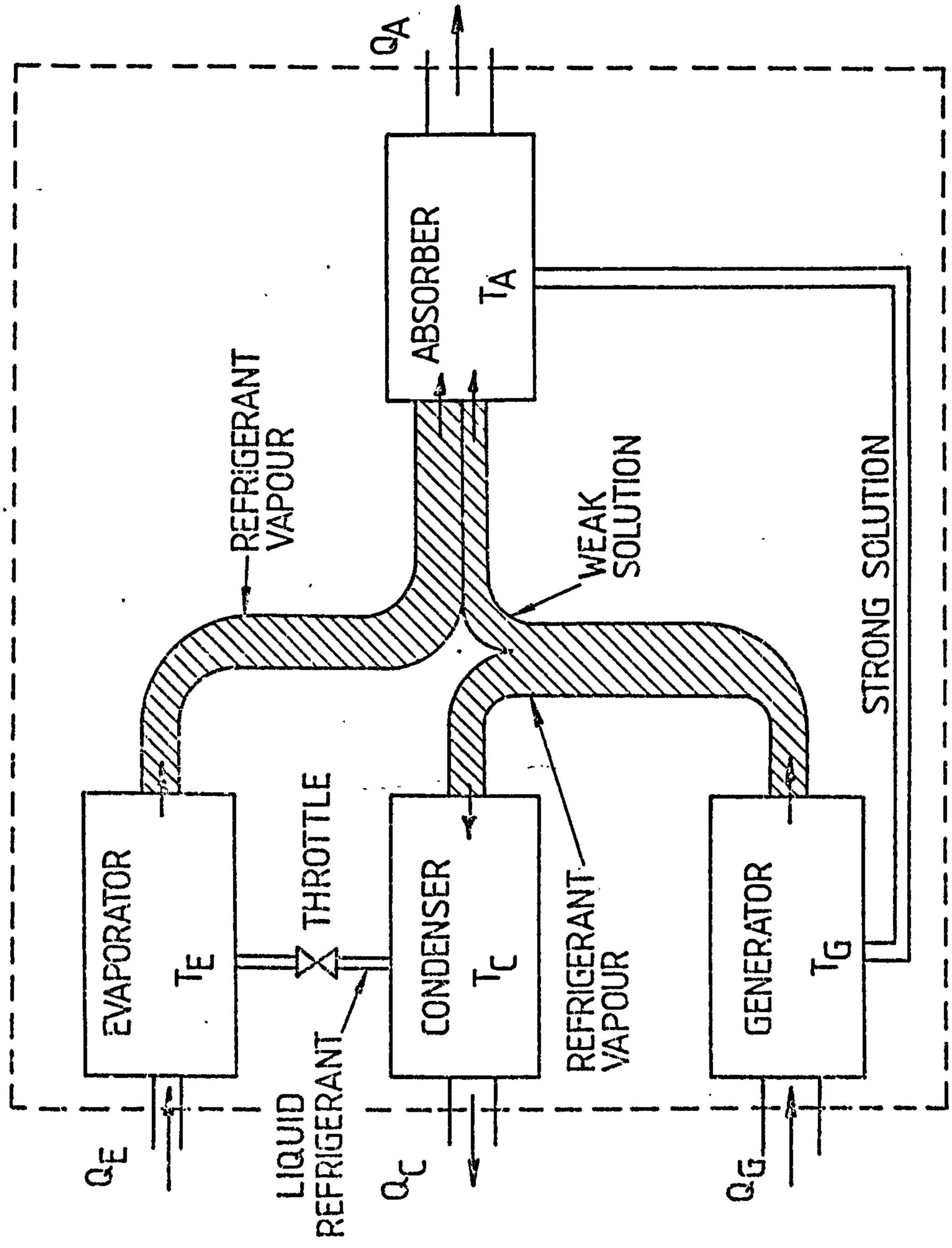

Figure 2.6 Energy chart in thermal heat pump

It is convenient to relate all quantities to unit mass of refrigerant (kg) circulated in the cycle; on that basis the conditions throughout the cycle may be given in terms of generally specified temperatures, pressures and concentrations, as shown in Fig.2.7. The heat input to the generator is equal to the sensible heat to bring the rich solution from heat exchanger outlet temperature T_9 to the saturation temperature of the solution corresponding to the condenser pressure P_C (T_{9E}) and also through the change of phase up to the generator temperature T_G plus the heat of vaporisation of 1kg of methanol from the solution during the concentration change from x_9 to x_{10} at a pressure P_C $(H')_{P_C}$ (assuming small difference of T_G from T_{9E}).

$$Q_G = WC_{ps9} (T_G - T_9) + (H')_{P_C} \Big|_{x_9}^{x_{10}} \qquad (2.7)$$

where w is the weight of the solution leaving the absorber per one kg of refrigerant

C_{ps9} is the specific heat of solution at state 9

The heat removed from the condenser is equal to the heat released when cooling the refrigerant vapour from T_G to the condenser temperature T_C (the super heat) plus the latent heat of condensation of 1kg of pure methanol at P_C.

$$Q_C = C_{pv} (T_G - T_C) + (H)_{P_C} \qquad (2.8)$$

where C_{pv} specific heat of methanol vapour

The throttling process by which the liquefied refrigerant is passed from the condenser at P_C, to the evaporator at P_E, is carried out with essentially no heat exchange with the surroundings and, therefore, at constant enthalpy. During the throttling part of the liquid refrigerant will flash into vapour and absorb heat from the remaining liquid and cool it to the evaporator temperature T_E. The fraction of liquid changed to vapour (Y) is given by the heat and material balance of that component $h_2 = (1 - Y) h_4 + Y h_4$

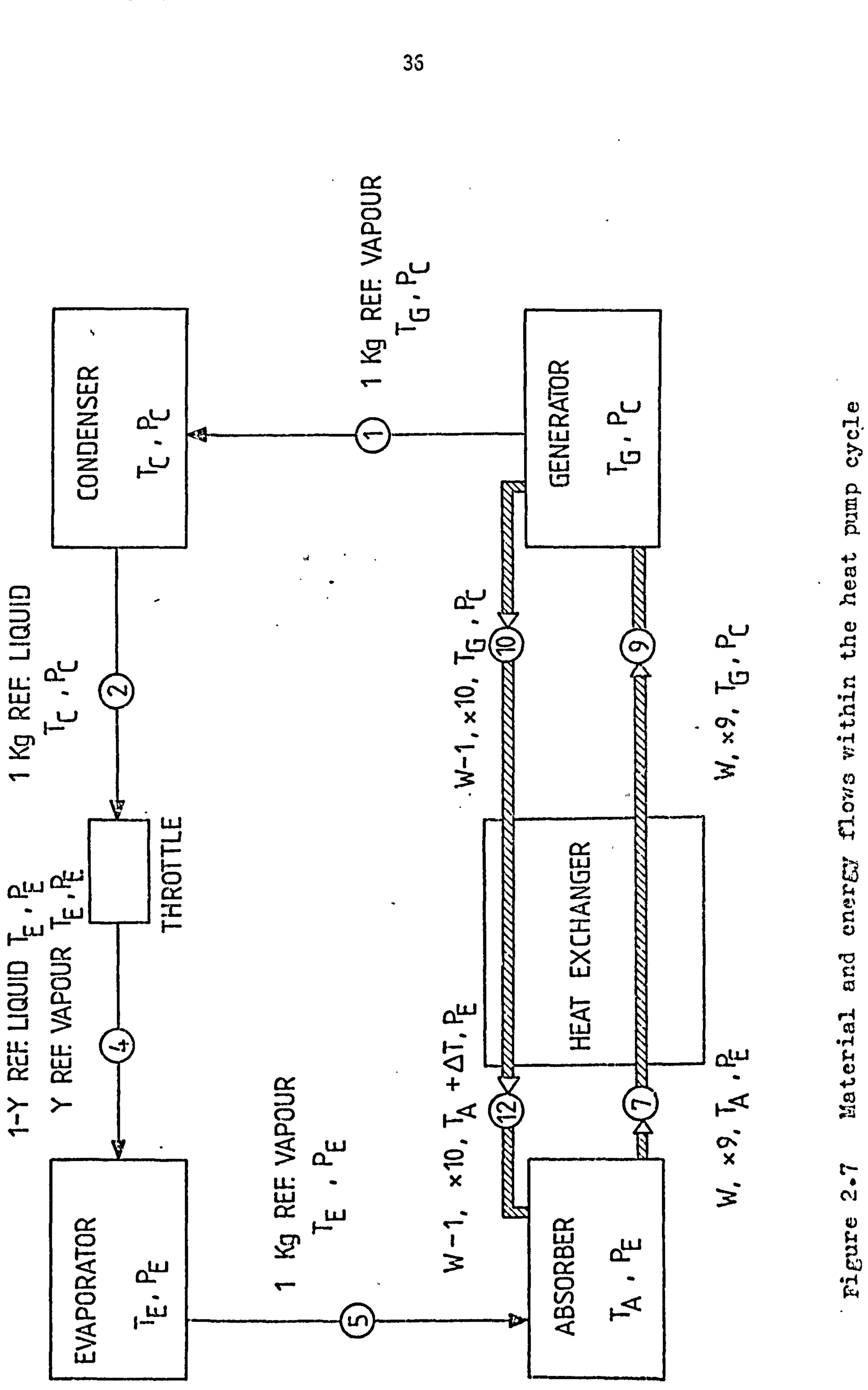

Figure 2.7 Material and energy flows within the heat pump cycle

$$C_{pm}\,(T_C - T_E) = Y\,(H)_{P_E}$$

$$Y = \frac{C_{pm}\,(T_C - T_E)}{(H)_{P_E}} \qquad (2.9)$$

where C_{pm} is the specific heat of the liquid refrigerant at the throttle value conditions

$(H)_{P_E}$ is latent heat of the vaporisation of methanol at P_E

The pre-cooler (shown in Fig.2.5) is included in actual cycles to minimise Y by exchanging the superheat of the refrigerant condensate with the vapour refrigerant before being delivered to the absorber.

The heat absorbed in the evaporator will simply be the latent heat of evaporation of (1 - Y) kg of methanol at P_E.

$$Q_E = (1 - Y)\,(H)_{P_E} \qquad (2.10)$$

In the absorber, the lean solution inlet is cooled from temperature $T_A + \Delta T$ to T_A, ΔT being the temperature approach at the low temperature side of the solution heat exchanger. Methanol vapour is heated from T_E to T_A and is absorbed by the lean solution giving a total heat of solution equal to H' at P_E through concentration change from x_{10} to x_9

$$Q_A = (w - 1)\,c_{ps12}\,(\Delta T) - C_{pm}(T_A - T_E) + (H')_{P_E}\Big|_{x_{10}}^{x_9} \qquad (2.11)$$

where C_{ps12} specific heat of the solution at state 12

C_{pm} specific heat of liquid methanol

The heat exchanged within the liquid heat exchanger is

$$Q_{ex} = W\text{-}1\, C_{ps10}\, (T_G - T_A - \Delta T)$$

$$= W\, C_{ps9}\, (T_9 - T_A) \qquad (2.12)$$

Setting ΔT by design conditions T_9 can be calculated and the area of the heat exchanger can be determined, and hence its cost. Calculation of this area may have to be made a number of times to determine the proper economic balance between heat exchanger cost, and addition to operating costs represented by the changes in Q_G and Q_A.

2.3.2. Computation of the coefficient of performance of the cycle and effects of various factors

Following the energy chart in Fig.2.6, and applying the first law of thermodynamics to the heat exchange of the system with the surroundings then

$$Q_G + Q_E = Q_A + Q_C \qquad (2.13)$$

In ideal cycles where Carnot processes are assumed the second law of thermodynamics would be applicable and

$$\frac{Q_G}{T_G} + \frac{Q_E}{T_E} = \frac{Q_A}{T_A} + \frac{Q_C}{T_C} \qquad (2.14)$$

The coefficient of performance of an absorption heat pump is defined as the total heat output per unit heat input to the generator

$$COP = \frac{Q_A + Q_C}{Q_G} = \frac{Q_{total}}{Q_G} \qquad (2.15)$$

assuming $T_A = T_C$, then from (2.14)

$$\frac{Q_G}{T_G} + \frac{Q_E}{T_E} = \frac{Q_A}{T_A} + \frac{Q_C}{T_A} = \frac{Q_{total}}{T_A}$$

$$\frac{Q_G}{T_G} - \frac{Q_G - Q_{total}}{T_E} = \frac{Q_{total}}{T_A}$$

$$\frac{Q_G}{T_G} - \frac{Q_G}{T_E} = \frac{Q_{total}}{T_A} - \frac{Q_{total}}{T_E}$$

$$Q_G \left(\frac{1}{T_G} - \frac{1}{T_E} \right) = Q_{total} \left(\frac{1}{T_A} - \frac{1}{T_E} \right)$$

thus $$\frac{Q_{total}}{Q_G} = \frac{T_G - T_E}{T_A - T_E} \cdot \frac{T_A}{T_G}$$

hence the COP for an ideal heat pump cycle is

$$COP = \frac{T_G - T_E}{T_A - T_E} \cdot \frac{T_A}{T_G} \qquad (2.16)$$

In most cases, the analysis of an ideal cycle helps to establish the effect of operating conditions on the performance of such cycle. However, as it was pointed out by Smith and El-Shamarka (Ref 36), the overall performance of the absorption cycle is determined both by thermodynamic factors associated with the working fluids and the design considerations associated with irreversible heat flows along the actual cycle components. The principle thermodynamic factor is the ratio of the total heat of solution of vapour into absorbent to the latent heat of vaporisation of the refrigerant (methanol) at condenser and evaporator pressures. These may be evaluated from the slope of the vapour pressure

temperature lines for the pure vapour and the various solution concentrations by the use of the Callusuis-Clapeyron relationship that have already been referred to (equation 2.4). At the low pressures of the methanol system this relationship, which assumes a negligible liquid/vapour volume, is sufficiently accurate for practical purposes. It was applied in the advanced stages of COP computation to calculate the total heat of vaporisation of the methanol solutions directly from vapour pressure measurements over useful ranges of temperatures and methanol fractions, calculations are presented in Appendix (A). A computer program was written and tested based on the estimation of physical and thermodynamic properties from section 2.2 (an example is shown in Fig.2.8) From this program an estimation of the effect of undertainties of the estimated properties (specific heat and heat of vaporisation) was computed and shown in Figs.(2.9, 2.10). The program has been written to predict the COP of the absorption heat pump by making an energy balance around the entire apparatus for a given set of operating conditions. The limitations imposed by components like the solution heat exchanger and the refrigerant throttle valve were included. By means of this the four temperatures, evaporator, condenser, absorber and generator can be inserted and the coefficient of performance calculated. Based on the experimental data determined in Chapter 3, new equal pressure relation of temperatures of saturated states of pure methanol and its solutions was deduced (Appendix A). Such a relation in addition to experimental results of specific heat and the calculated heat of vaporisation of the solutions replaced the estimated properties in the program. Thus the performance of the methanol heat pump cycle was determined.

The effect of operating conditions was studied by changing the set of temperatures fed to the program. The quantity of heat transfer within the solution heat exchanger was calculated and was taken as an indication to its size and the influence of its effectiveness was also studied. The crystallisation limits were applied and the region of the crystallisation is marked with dashed lines on the diagram showing the performance.

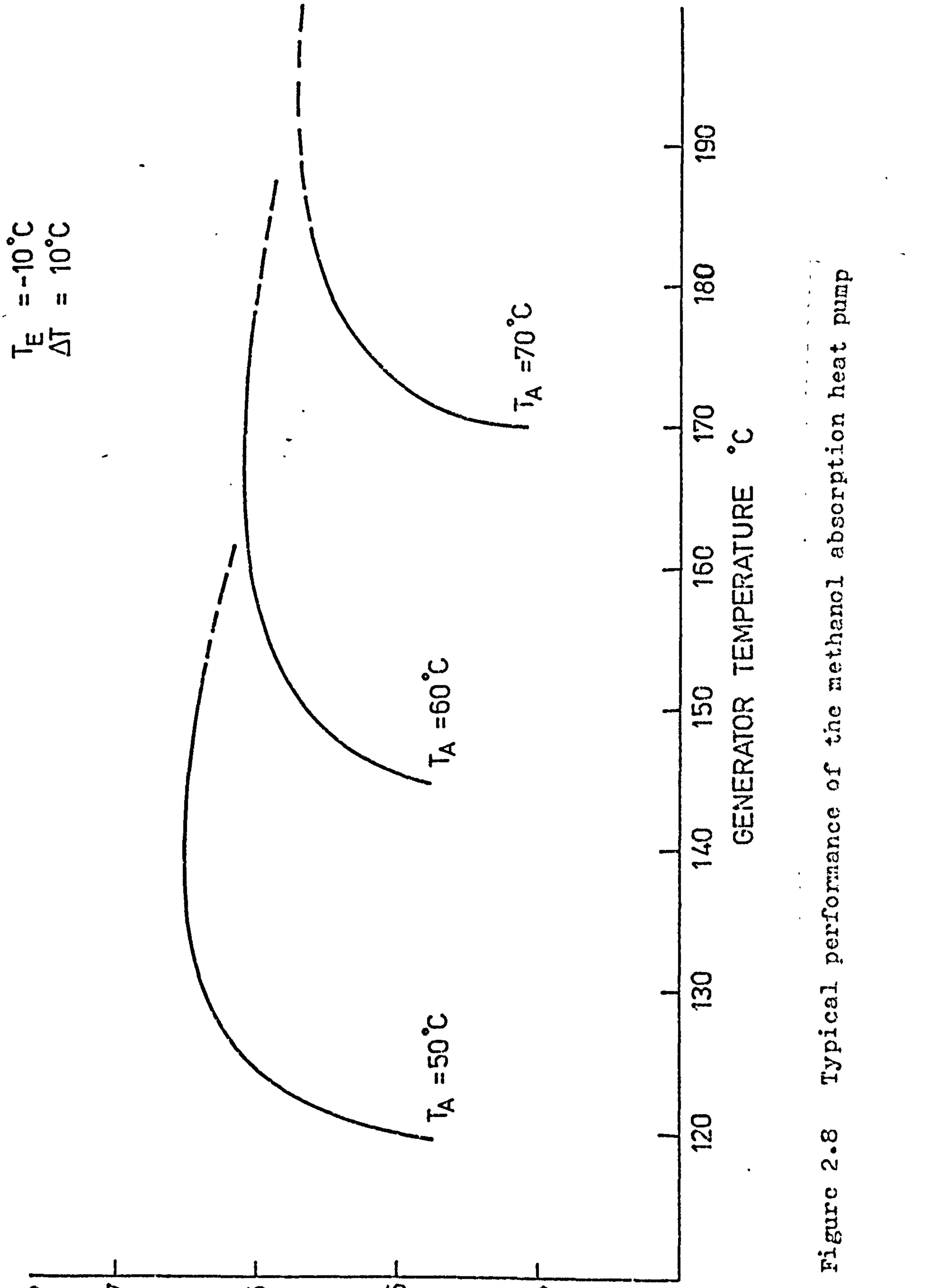

Figure 2.8 Typical performance of the methanol absorption heat pump

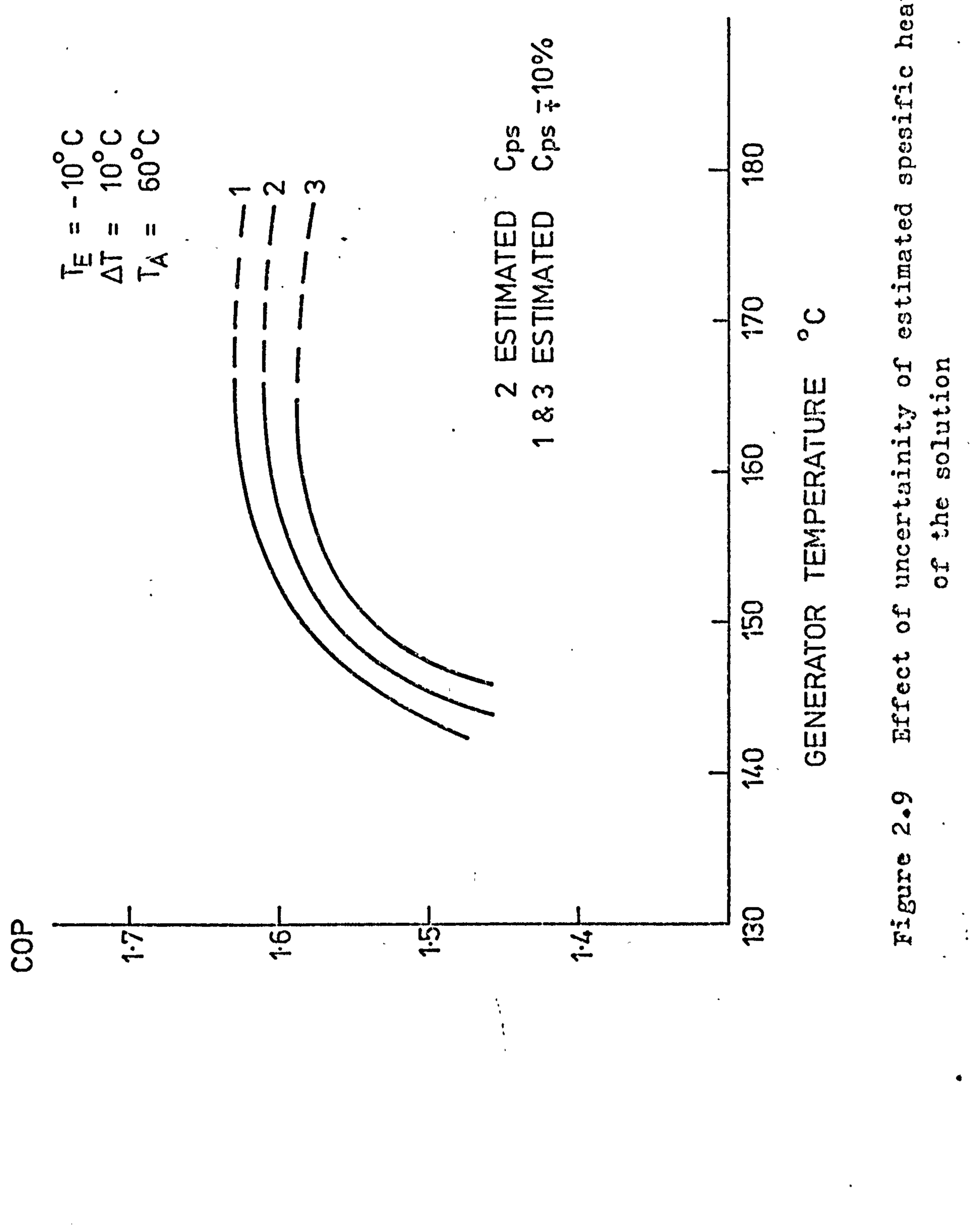

Figure 2.9 Effect of uncertainity of estimated spesific heat of the solution

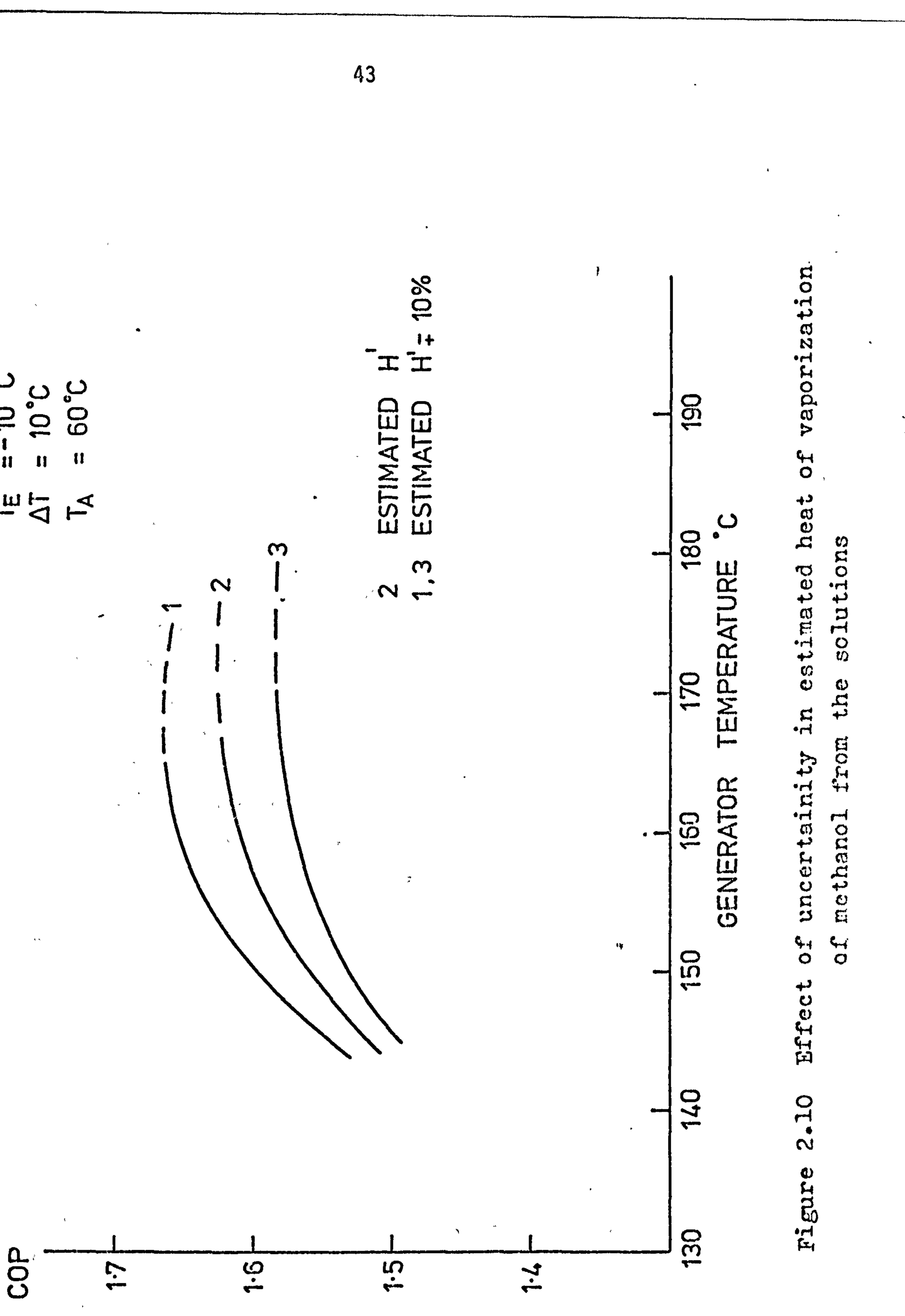

Figure 2.10 Effect of uncertainity in estimated heat of vaporization of methanol from the solutions

2.3.3 Results

The performance of the cycle was determined and the effect of working conditions and design parameters were studied. The results are shown in Figs. 2.11, 2.12, 2.13. It is clear from these figures that the generator temperature has an optimum value to which corresponds the maximum COP at certain evaporator and condenser/absorber temperature. Since for these conditions the rich composition is fixed the generator temperature however defines the lean composition, so the higher this temperature is, the higher the concentration difference and the lower is the solution circulation rate thus COP increases. Lower COP at very high T_G are caused by excessive methanol vapour super heat. Such effects of T_G were described in References 23, 44 and 45 for the refrigeration cycle. The effect of super heat was shown by Ref 44 but no calculations were done in this investigation to confirm it. Better illustration of the machine performance is shown in Fig.2.14 where the COP is determined with respect to solution concentration change, with 10 ^{o}C temperature approach in the solution heat exchanger. The absorber/condenser temperature (assumed to be equal); generator and evaporator temperatures are indicated on the figure. Maximum absorber temperatures are indicated along the curve, representing the onset of crystallisation.

The effect of the evaporator temperature is recognised by the comparison of the COP values obtained in Figs. 2.11, 2.12, 2.13 where higher values are achieved with higher T_E. It is also found that maximum COP value corresponding to fixed condenser temperature is obtained at lower T_G when T_E increases.

Unlike T_E, the condenser temperature has an adverse effect on COP values. COP are lower for higher T_C and optimum generator temperature is also higher. The effect of both T_E and T_C are summarised in Fig.2.15 where maximum values of COP is depicted versus the temperature lift (T_C - T_E) with conditions the same as those noted in Fig.2.14. The weak dependance of COP on temperature lift is immediately apparent, in strong contrast to the vapour compression

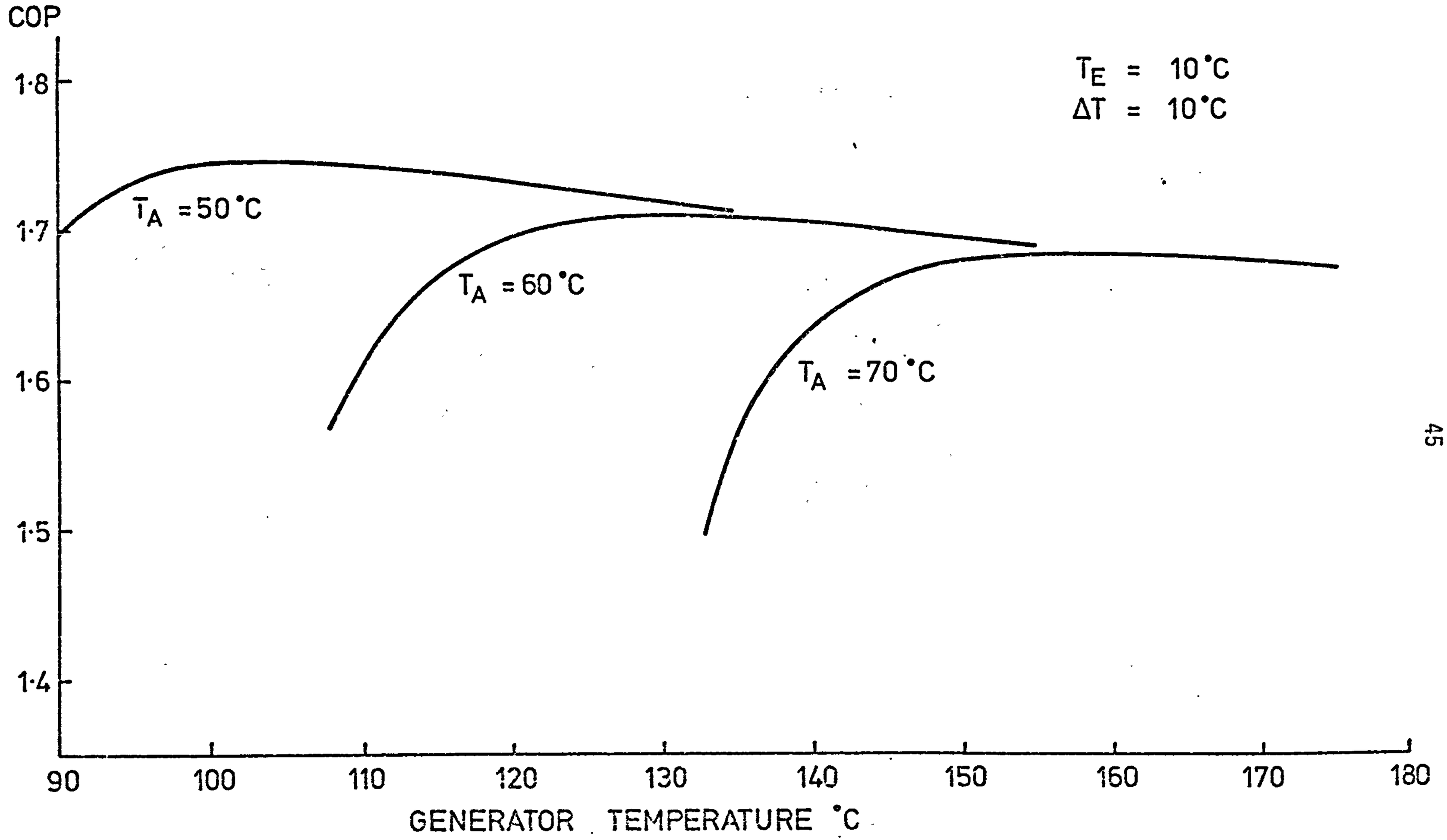

Figure 2.11 Performance of the thermal heat pump cycle at T_E= 10 °C

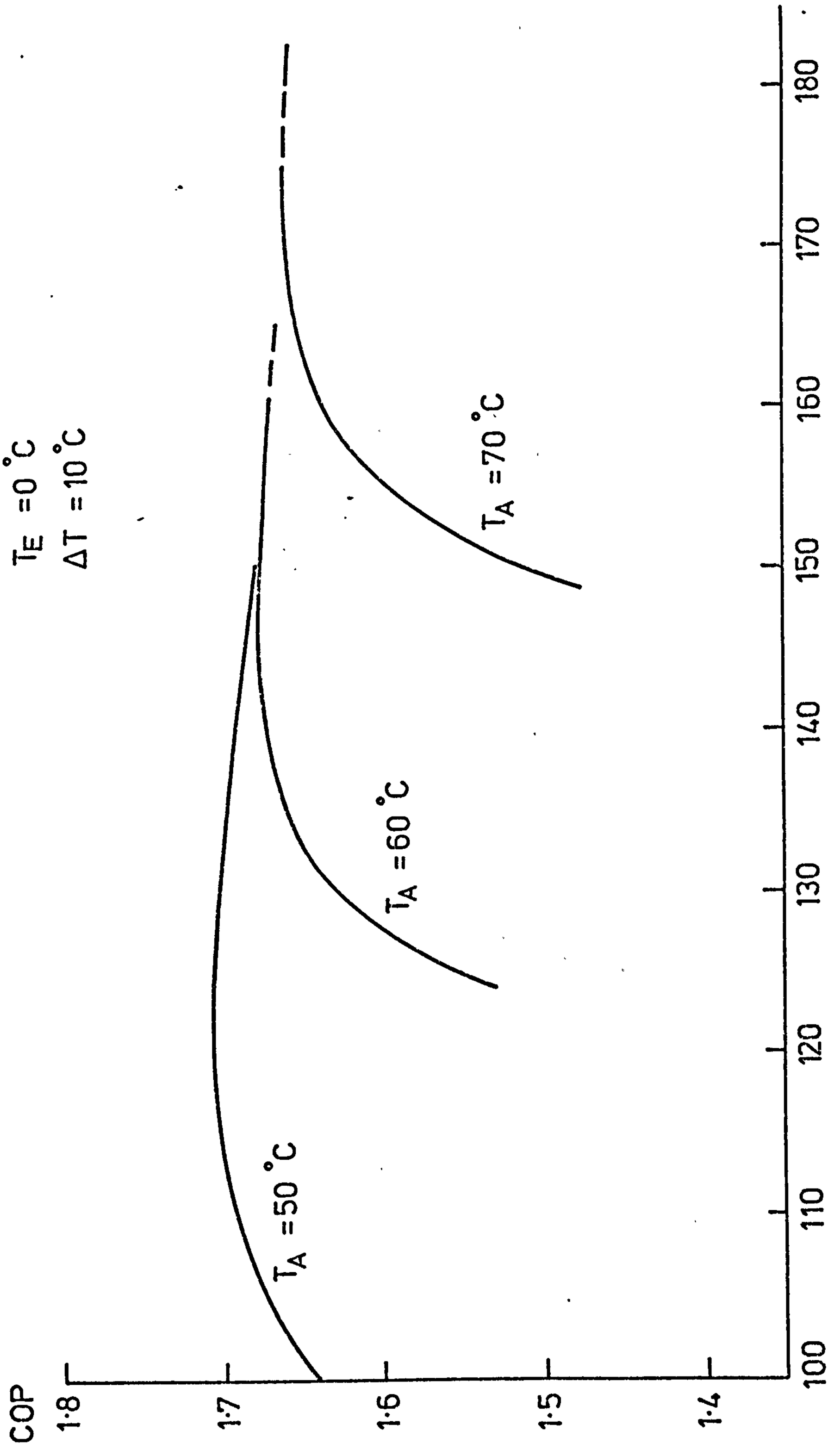

Figure 2.12 performance of the heat pump cycle at T_E= 0 °C

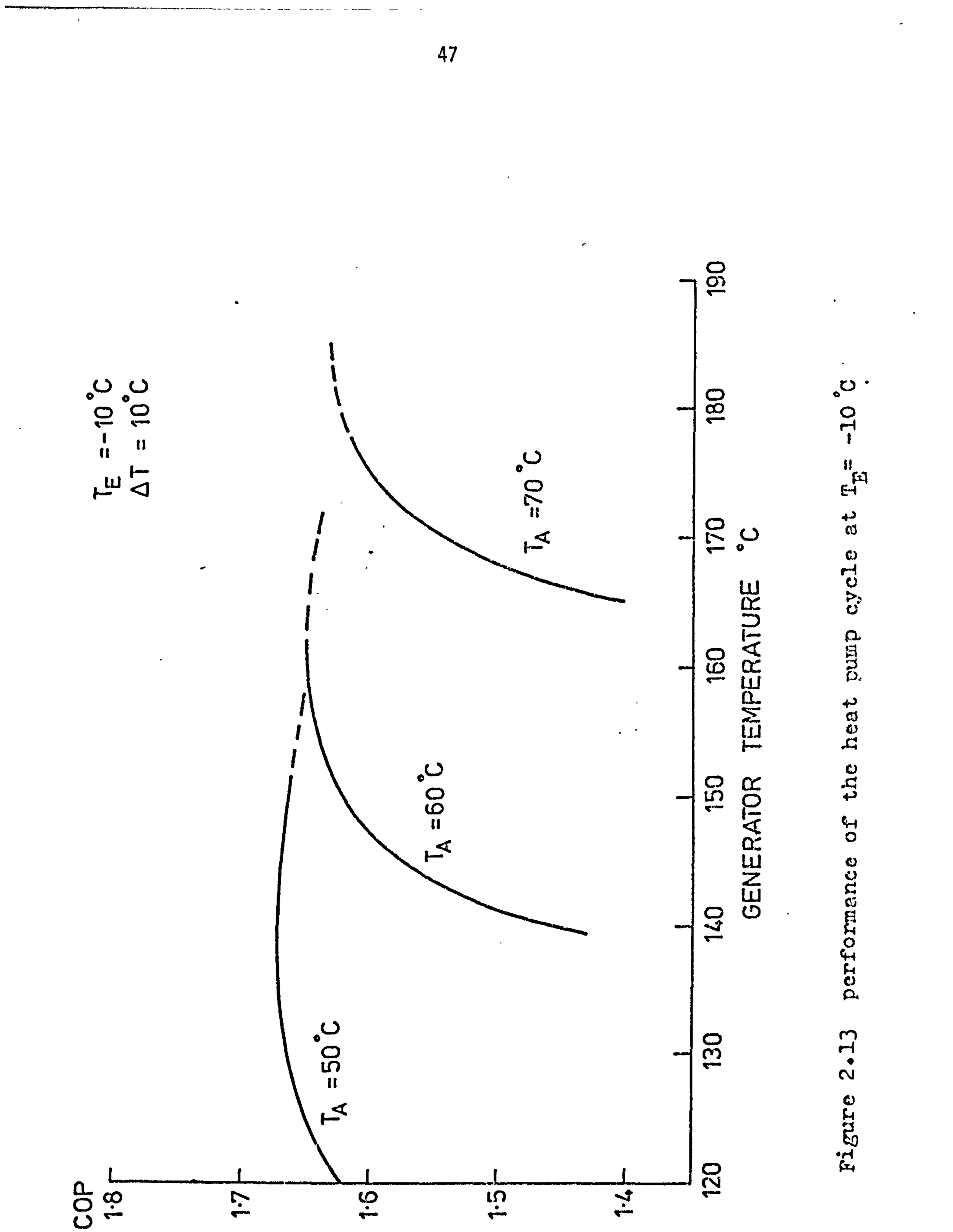

Figure 2.13 performance of the heat pump cycle at T_E = -10°C

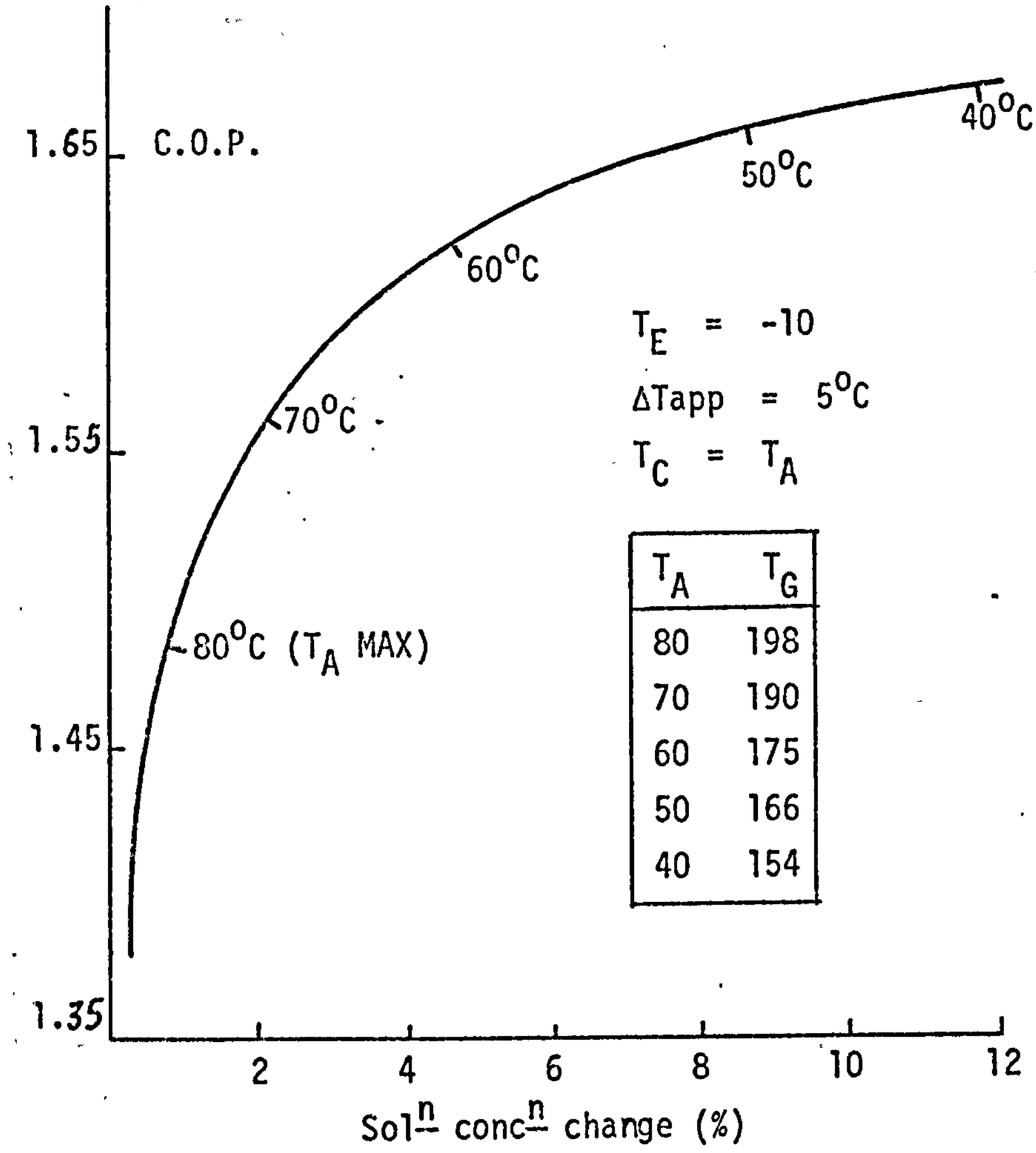

Figure 2.14 Overall performance against concentration difference

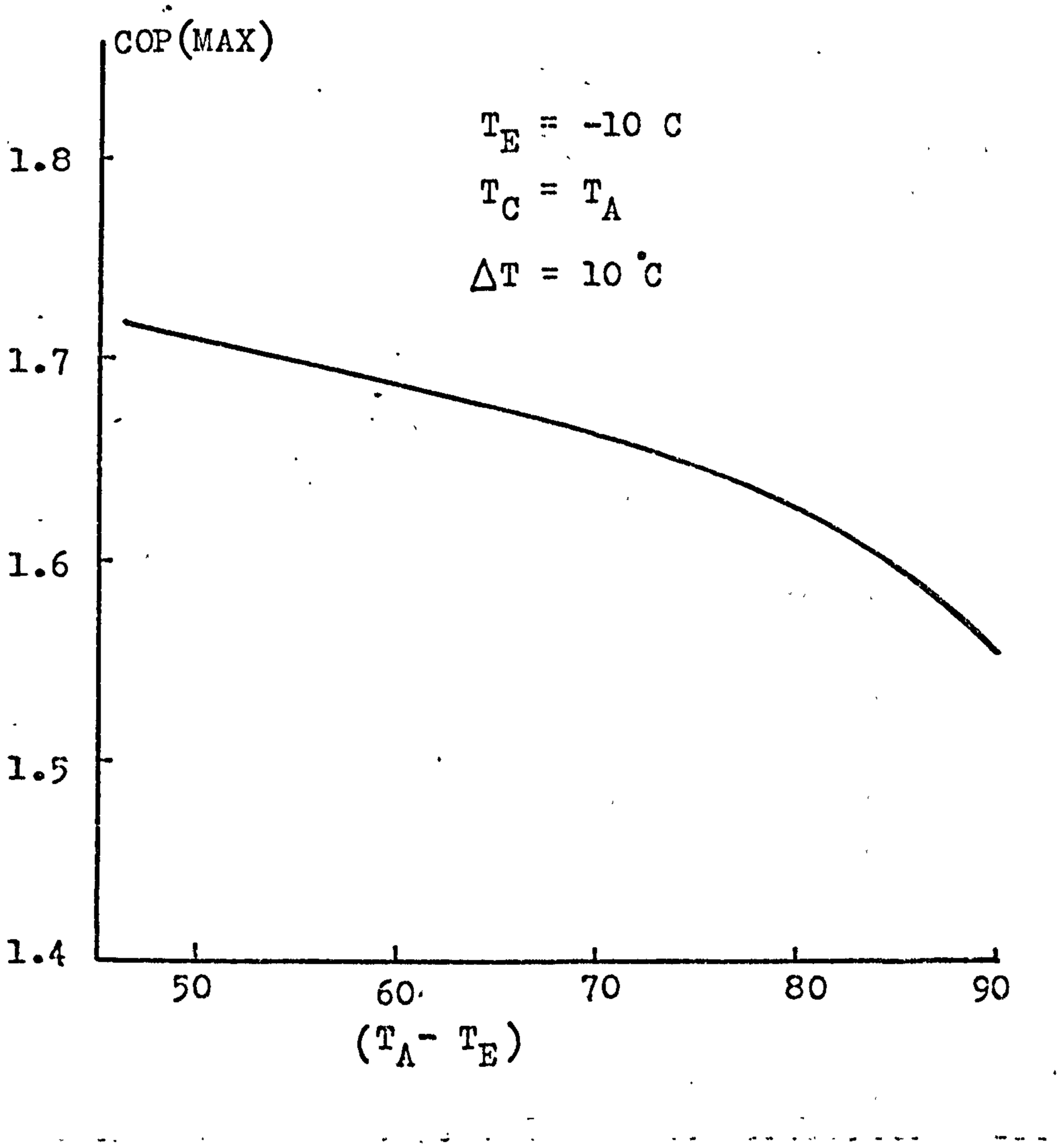

Figure 2.15 Dependance of COP on temperature lift

heat pump, but it must not be forgotten that the greater the lift, the higher must be the generator temperature, i.e. the lower the entropy of the source heat.

Only the effect of the heat exchanger, from the irreversibility sources, is studied by arbitary choice of the approach temperature (ΔT) of the low temperature side of the component. ΔT = o means a 100% heat exchanger effectiveness and $\Delta T = (T_G - T_C)$ means no heat exchanger at all. The dependance of the COP on the temperature approach ΔT (Fig.2.16) is determined and optimum design can be obtained by few trials including economical considerations. The results showed that the optimum generator temperature is lower when an effective exchanger is installed because the super-heat has higher influence when Q_G is reduced. Recently the performance of the only experimental cooling cycle utilising MeoH/2LiBr-$ZnBr_2$ (Ref 24) was measured and a COP of 0.65 was claimed at generator temperature of 95^oC, absorber/condenser temperature of 20^oC and evaporator temperature of 0^oC (Ref 46). The cycle does not include a solution heat exchanger and the hot lean solution is cooled with an external source of water. When this set of operating conditions were fed into the programme, the corresponding COP was (0.675), i.e. 4% higher than the measured COP.

The prediction published by best (Ref 11) were higher than the results of this investigation. With the help of Fig.2.10 it is believed that because Best used equal temperature relation to calculate the heat of vaporisation over higher temperature range than 130 ^oC was the reason (it was shown previously that Clausius-Clapeyron equation is not accurate enough over such range).

The same calculation procedure was used to write similar programs for water-LiBr and ammonia-water employing the available data of these systems in the literature. The results agreed with the claimed performance of practical machines.

A listing of the program together with a print out at similar working conditions of (Ref 46) are given in Appendix(F).

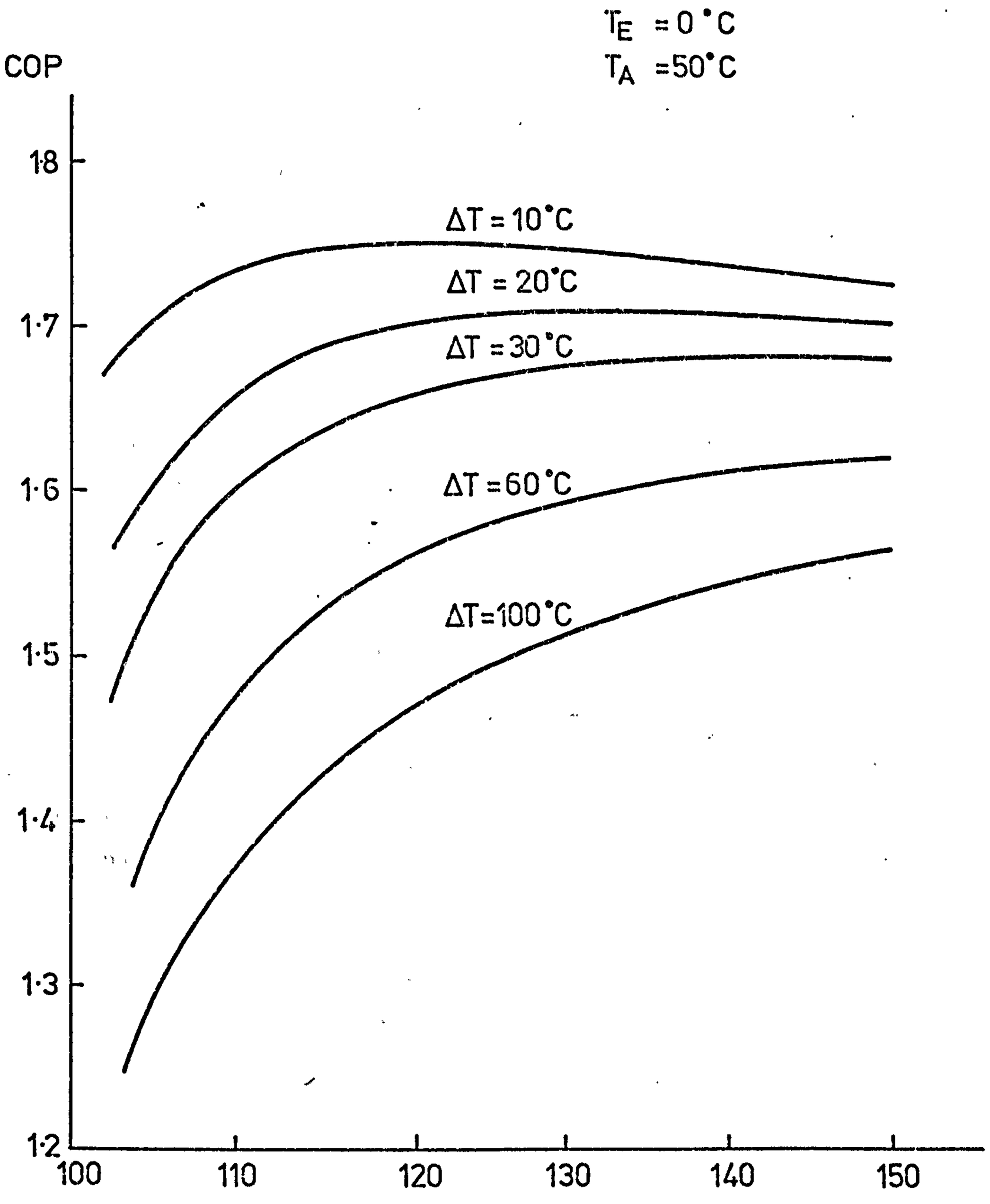

Figure 2.16 Effect of the temperature approach in the heat exchanger

CHAPTER 3

THERMODYNAMIC PROPERTIES OF THE SOLUTIONS

3.1 Vapour Pressure

Determination of vapour pressure data has been always the first step towards the investigation of new fluids for the absorption refrigeration (or heat pump) cycle. A complete experimental set of results of vapour-liquid equilibrium data gives much information about solubility and deviations from Raoult's law, which are significant properties when evaluating a working subsistance. Although the cycle itself can be represented either on enthalpy/concentration diagram or vapour pressure/temperature, a particular cycle is better presented on the latter as the driving potentials are then directly shown in terms of pressure differences.

The vapour pressure of methanol-salt solutions were first published by Aker (Ref 28). Since then more data have been published by other investigators (Ref 24, 30, 35 and 47). However none of these investigators carried out their measurements to temperatures useful for heat pumps working at a moderate heating temperature (60 - 80 ^{o}C). A brief review of the techniques employed for vapour pressure measurement, and an assessment of their likely accuracy are given below followed by a more detailed description of the method employed in this work.

3.1.1 Methods Previously Employed

(i) Pennington's apparatus (Ref 48)

The need for accurate vapour pressure data on water-LiBr solutions is important, since this combination is remarkably widely employed in air conditioning machines. Pennington reported on the measurement and correlation of vapour pressure property of these solutions to a considerable accuracy (the average deviations of his correlations is 2%). The early apparatus Fig.(3.1) consisted of an ebuilliometer with connected mercury (sometimes Merian No.3

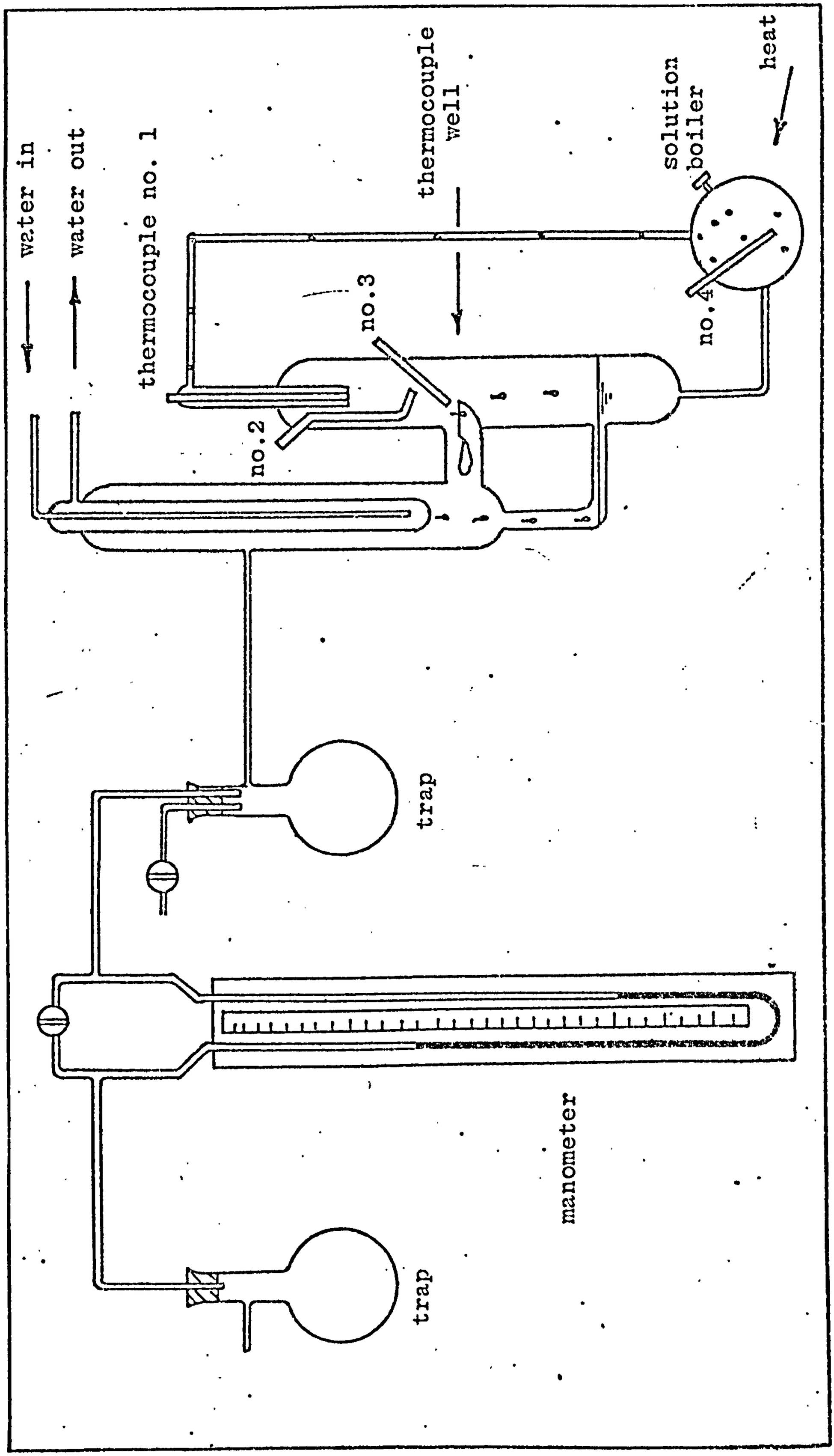

Fig. 3.1 Schematic diagram of the vapour pressure ebulliometer of Pennington (Reproduced from Clema)

manometer fluid) manometer. The temperature was measured by means of four thermocouples. The apparatus succeeded in measuring the vapour pressure property of a single component substance (water) but failed to work for the solutions, simply because the four thermocouples gave different temperature readings. Pennington used another systematic technique for the determination of vapour pressure curves of the solutions water-LiBr. Measuring the boiling point of solutions of 40-50% concentrations at room pressure, together with the vapour pressure at single temperature (30.4 ^{o}C) and the heat of dilution at another temperature (25 ^{o}C) he was able to deduce reasonably accurate correlations. However he concluded that the previous ebulliometer may be used provided that the reading of thermocouple (1) only is taken and the super heat in the boiling flask is taken into consideration.

(ii) The apparatus of Aker (Ref 49)

The apparatus used by Aker is shown in Fig.(3.2). It consisted of 300 ml pyrex glass bulb as the equilibrium cell to which was attached two capillary tubes; one of which was used to evacuate the system and the other to admit the sample. Both lines were provided with high vacuum stopcocks. The cell is connected to a mercury manometer specially designed to allow a reference point at the left leg, then the height of the mercury column in the right leg is measured to 0.1 mm by means of cathetometer.

The cell was placed in an oil bath which temperature is controlled automatically to within 0.1 ^{o}C and measured to within 0.1 ^{o}C when lower than 100 ^{o}C and to 0.5 ^{o}C when higher. Parts of the system outside the bath and containing refrigerant vapour were warmed by nichrome wire heater to prevent condensation.

The salts were dried under vacuum at 250 ^{o}C in a heat resistant loading cell. Solutions were prepared by admitting a sample of liquid methanol into the loading cell.

Aker investigated salt solutions of lithium and zinc

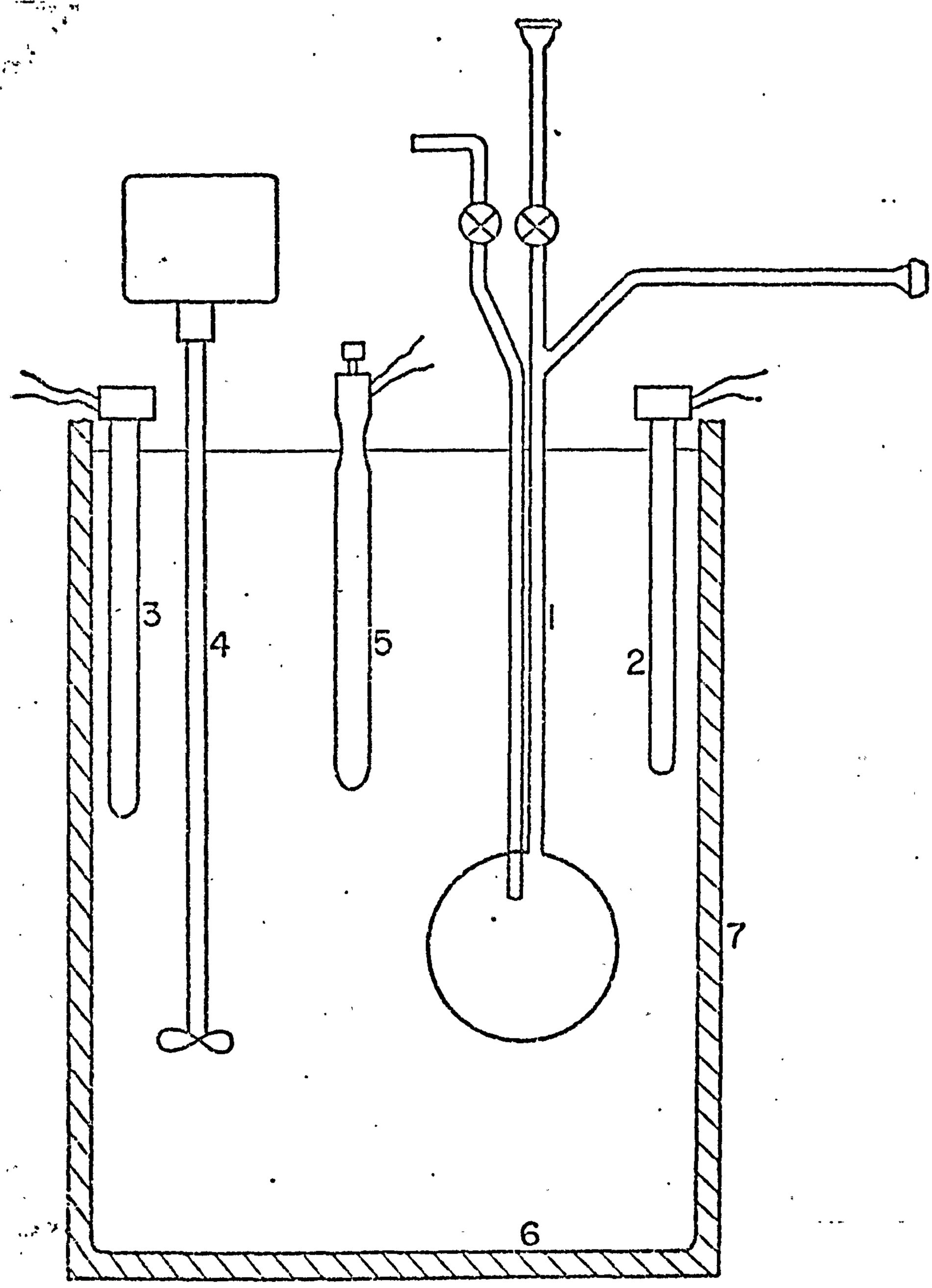

1 EQUILIBRIUM CELL
2 AUXILIARY HEATER
3 CONTROL HEATER
4 STIRRER
5 MERCURY THERMOSTAT
6 STAINLESS STEEL BEAKER
7 INSULATION

Figure 3.2 Aker's apparatus (reproduced from Ref 28)

bromides and chlorides as well as mixtures of these salts in methanol and ethanol. An error of less than 2.5% was reported when published data of water, methanol, ethanol and LiBr/water solutions were checked by the apparatus. The vapour pressure of the solution was determined to within 0.3 mm Hg. The results were obtained at subatmospheric pressure at temperatures from about 29 to 135 ^{o}C. This apparatus is believed to be simple and accurate.

(iii) The Apparatus of Olama (Ref 24)

Olama used the apparatus shown in Fig.(3.3) to measure the vapour pressure of solutions of three different salts and their mixtures in methanol. It consisted of a heat resistant glass cell connected through valves and tubing to a mercury manometer, the other side of which was connected to a vacuum system. The equilibrium pressure in the cell was read directly on the manometer which was immersed in a circulated oil bath. The oil in the bath was circulated by means of two pumps and the bath temperature was manually controlled to 0.1 ^{o}C, as measured by four calibrated thermometers. Salts were dried under vacuum at about a 100 ^{o}C lower than their melting point in the same cell, then the solution was mixed by introducing liquid methanol into the cell after it had cooled. Measurements were carried out at subatmospheric pressures and over a temperature range of 27 to 120 ^{o}C. The accuracy of the apparatus was checked using pure substances such as water and methanol and the accuracy was claimed as 2.5%. The measurements were carried out primarily to confirm those of Aker.

(iv) The Apparatus of Albright

The solubility of refrigerants R11, 21 and 22 in some organic solvents were measured by Albright (Ref 50) in the apparatus shown in Fig.(3.4). It consisted of static equilibrium cell with internal volume of (50 - 100 ml). For pressures lower than seven bars the cell was aerosol type glass tube attached to metal top. A neoprene gasket and Teflon insert were used to obtain a seal

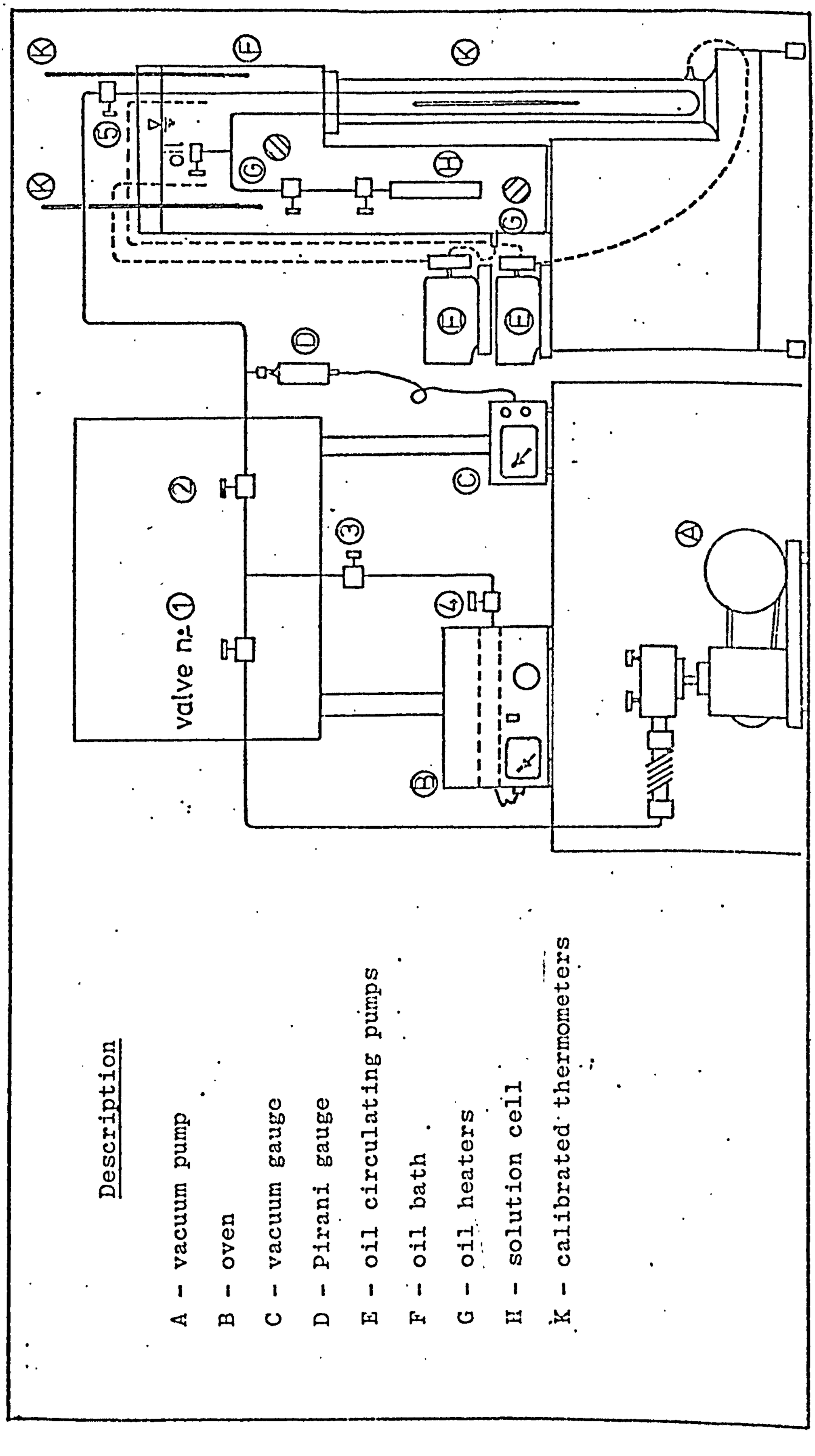

Description

A - vacuum pump
B - oven
C - vacuum gauge
D - Pirani gauge
E - oil circulating pumps
F - oil bath
G - oil heaters
H - solution cell
K - calibrated thermometers

Figure 3.3 Schematic diagram of the experimental vapour pressure apparatus used by Clarke (reproduced from Ref 24)

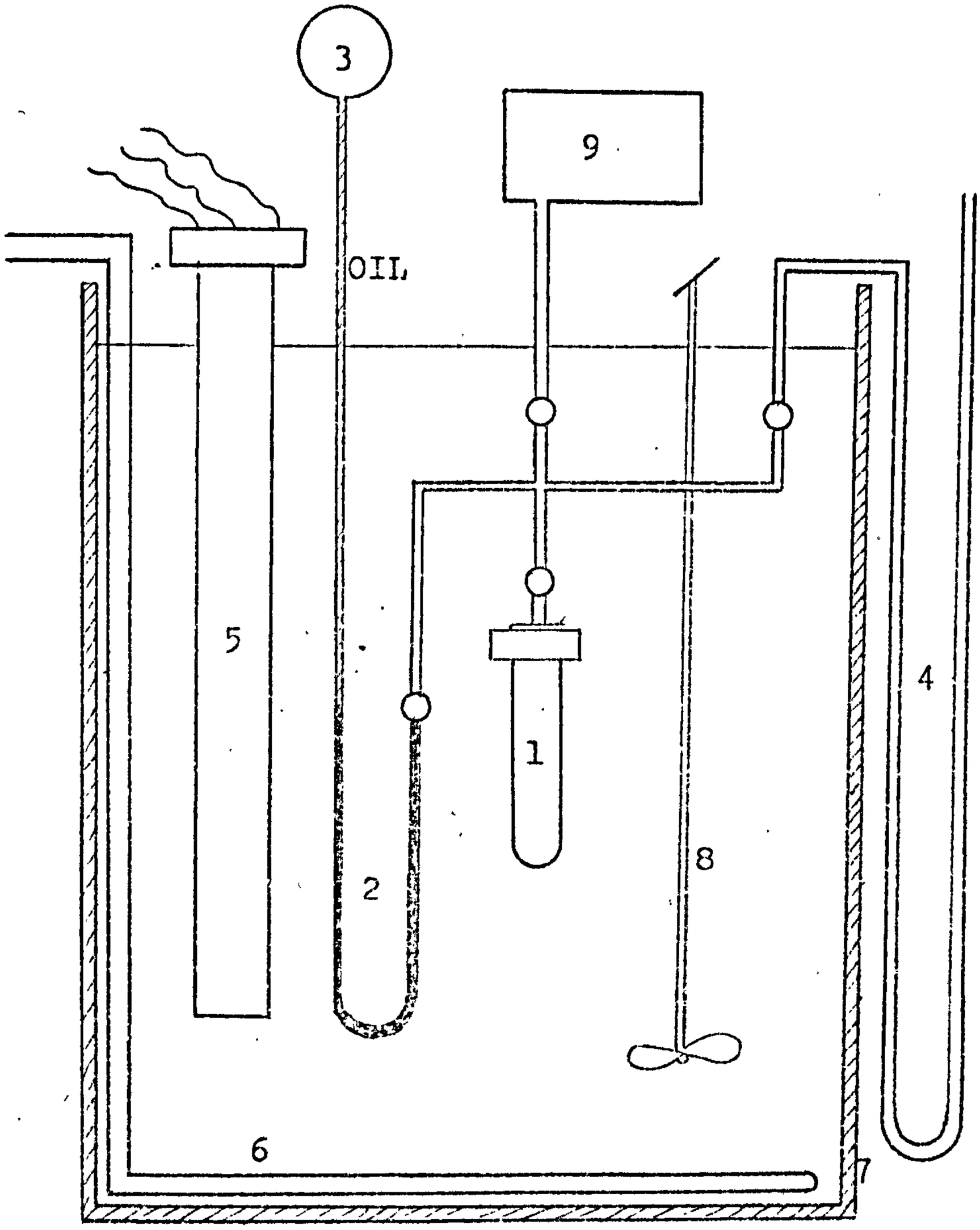

1 EQUILIBRIUM CELL
2 OIL-MERCURY
3 PRESSURE GAUGE
4 MANOMETER
5 ELECTRIC HEATERS
6 HEATING COIL
7 JAR FOR BATH
8 AGITATOR
9 VACUUM PUMP

Figure 3.4 Vapour pressure equipment used by Albright

between the tube and the metal top and flange arrangement. A valve was provided in the opening at the top of the cell. For higher pressure studies, the cell was machined from stainless steel.

The equilibrium cell was connected to an open end manometer, a vacuum pump, and an oil mercury leg on which was mounted a pressure gauge. The leg allowed the pressure in the cell to be transmitted to the gauge, and yet restricted tested fluids to equipment immersed in the oil bath. The oil bath temperature was controlled manually to within 0.05 ^{o}C as measured by calibrated mercury thermometers.

At the beginning, the mixture was prepared in an evacuated cell, then the cell was connected to the apparatus; the lines to the oil-mercury leg were evacauted, and the bath temperature was set-up. The equilibrium pressure at the cell was measured after the pressure readings were constant for at least five minutes.

Although it is simple and compact the apparatus is reasonably accurate (4% inaccuracy) but the function of the open end manometer was not described.

3.1.2 The Experimental Equipment

In the early stages of this work, only the data of Aker (Ref 28) and Uemura (Ref 29) were available for the vapour pressure of 2LiBr-$ZnBr_2$/methanol. Uemura published smoothed data, while those of Aker are experimental. Comparison of results was not possible because concentrations were different. However there was a striking disagreement over certain ranges. The vapour pressure of 60% methanol by weight in Uemura's smoothed results (accuracy of correlations claimed was 0.65%) was considerably lower than the vapour pressure of 53.7% concentration in Aker's results; this is shown in Fig.(3.5). In addition, there was a need for the measurements to be extended to certain concentration ranges suitable for the heat pump cycle proposed in Chapter 2. It was therefore decided to confirm the published data and extend the range of measurements. The equipment used in the first stage of measurements was all made of glass.

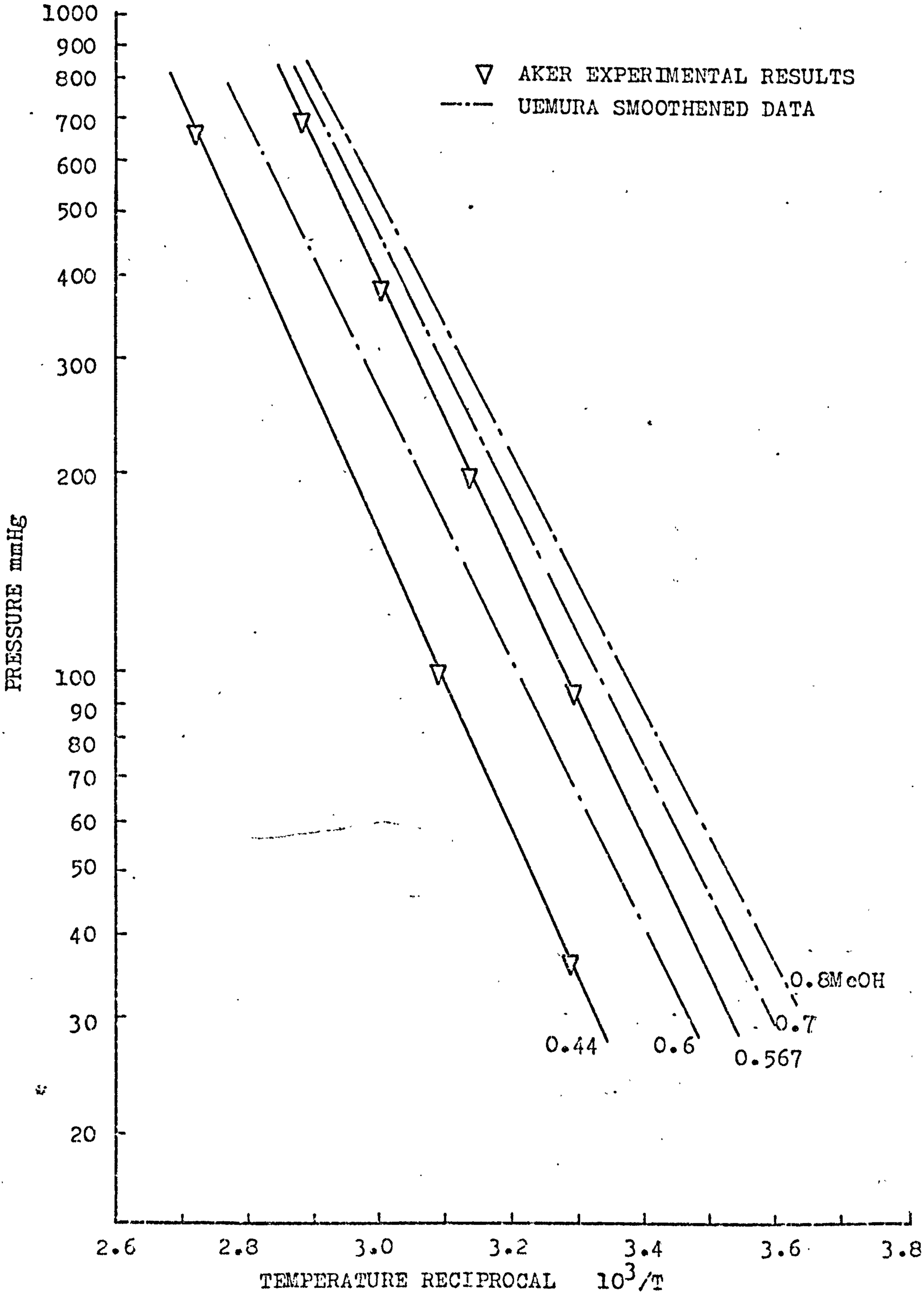

Figure 3.5 Comparison of vapour pressure data of Aker and Uemura

It consisted of a loading cell, an equilibrium cell and a pressure transmitter, connected to a manometer or McLeod vacuum gauge, and the thermally controlled water (or Glycerol) bath. Figure (3.6) shows a schematic diagram of the system.

The loading cell (shown in Plate 3.1)consisted of a 500 ml pyrex round bottom flask with 24/29 ground glass joint on top to which was attached a vacuum stopcock.

The equilibrium cell Fig.(3.7) consisted of a 100 ml round bottom flask with 10/14 ground glass vacuum tight joint to which a glass vacuum stopcock was fitted. The cell with the valve was connected to one leg of the U shape glass capillary tube containing a fluid of very low vapour pressure characteristics (Di-n-butyl phthalate $C_6H_4(COOC_4H_9)_2$. The other leg was connected through glass tube to a McLeod vacuum gauge which reads to 0.1 mm in the range 1-2 mm Hg and to 1 mm in the range 2-10 mm, an open end mercury manometer, and pressure ballasting 2½ litre glass bottle which was connected through a vacuum valve either to the atmosphere or to a vacuum pump when needed.

The cell with the U tube pressure transmitter was placed in the constant temperature bath. The bath consisted of a 5 litre clear pyrex glass beaker, heated with an electric thermostirrer. The bath temperature could be adjusted to within 0.3 ^{o}C and controlled automatically to within 0.1 ^{o}C when lower than 100 ^{o}C and 0.2 ^{o}C when higher. Glycerol was not used below 40 ^{o}C to avoid high temperature gradients in the bath and excessive loading of the stirrer. The temperature of the bath was measured to within 0.1 ^{o}C by means of mercury in glass thermometers and was assumed to be equal to the temperature of the sample after at least 15 minutes of pressure equilibrium. The bath was placed on a hot plate to assist in heating at high temperatures and it was also insulated by means of a fibre glass layer.

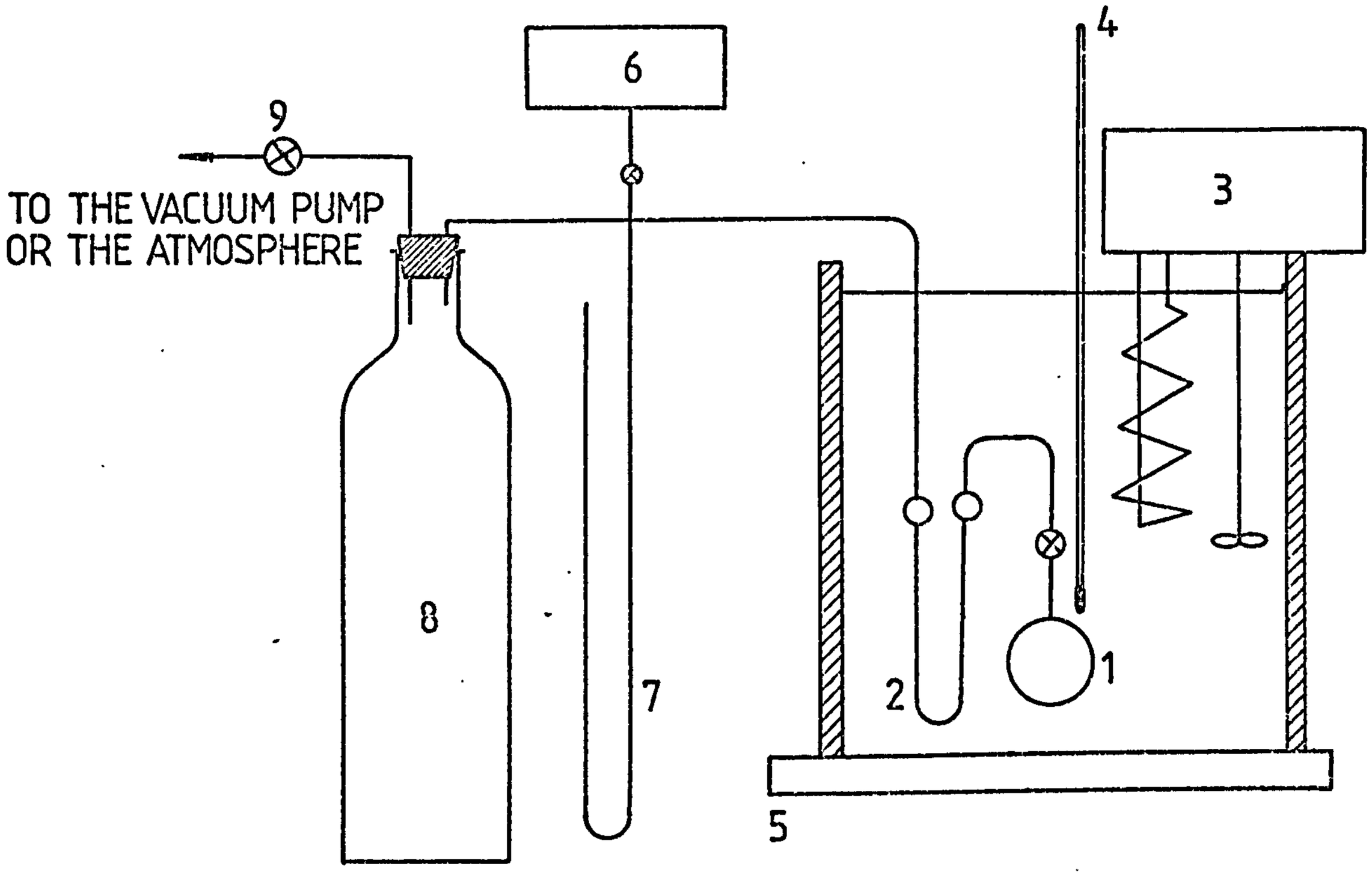

1. EQUILIBRIUM CELL
2. PRESSURE TRANSMITTER
3. THERMO-STIRRER
4. THERMOMETER
5. HOT PLATE HEATER
6. Mc LEOD VACUUM GAUGE
7. MANOMETER
8. GLASS BOTTLE
9. VACUUM VALVE

Figure 3.6 Schematic diagram of the apparatus of the first stage measurements

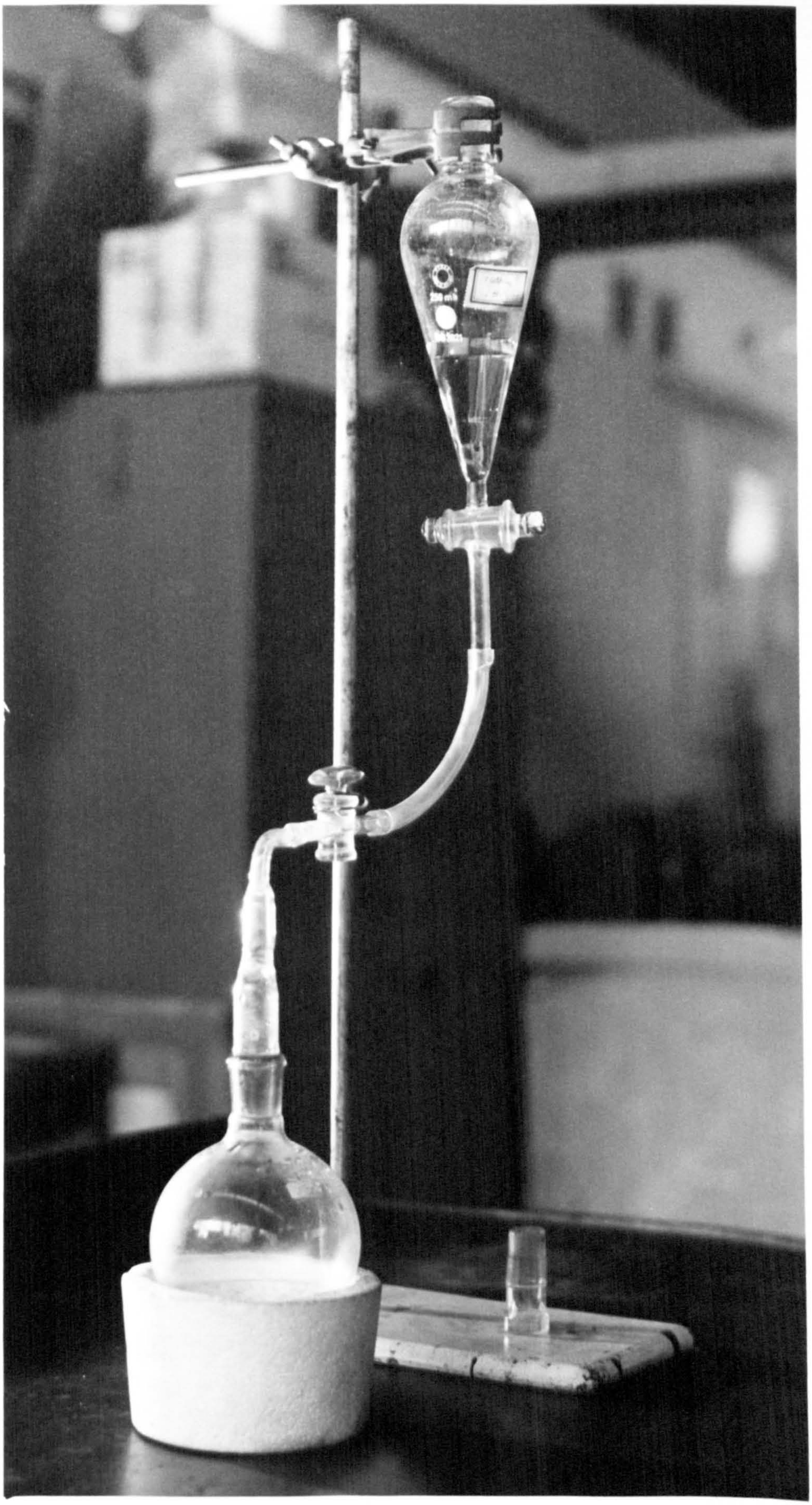

PLATE 3.1

3.1.3 Measurement Procedure

Solutions were prepared from analar methanol and anhydrous salts supplied by the BDH Chemical Company. The specifications of the substances used are given in Appendix (B).

The loading and equilibrium cells were thoroughly cleaned and dried, then evacuated to 0.03 mm Hg and checked for tightness The cells were able to hold vacuum for an extended period of time. Still in vacuum, the loading cell was weighted to 0.01 gm, then the vacuum was released and the valve was disconnected. The $ZnBr_2$ salt was introduced into the cell which was heated under vacuum in an oven to a temperature of 250 ^{o}C to dry the salt. The cell was weighted frequently until the weight remained constant. Then it was left to cool and reweighted to find the weight of $ZnBr_2$. In a similar way LiBr was added in such a quantity to give two moles per one mole of $ZnBr_2$ and was dried. The salts were reasonably dry (1% moisture) and it was possible to estimate the moisture in the weight of LiBr, and make the necessary correction so as to obtain a molar ratio close to the desired value (2:1).

The cell was left to cool and was reweighted for the third time to find the quantity of LiBr, when its vacuum tightness was again checked. To prepare the solution, the cell was connected through a clear plastic pipe to a glass funnel filled with methanol (Plate 3.1). Methanol was admitted to the loading cell drop by drop to prevent pressure build up. Care was taken to prevent air from getting into the cell by keeping a liquid column always above the cell valve. As a safety precaution, the cell was covered with a thick piece of cloth. The cell was shaken until all salts were disolved. If difficulty was experienced in dissolving the salts, more methanol was admitted and the solutions were then boiled at reduced pressures to obtain the desired concentration.

The loading cell was then connected to the equilibrium cell and the vacuum pump through the stopcock. Vacuum was applied

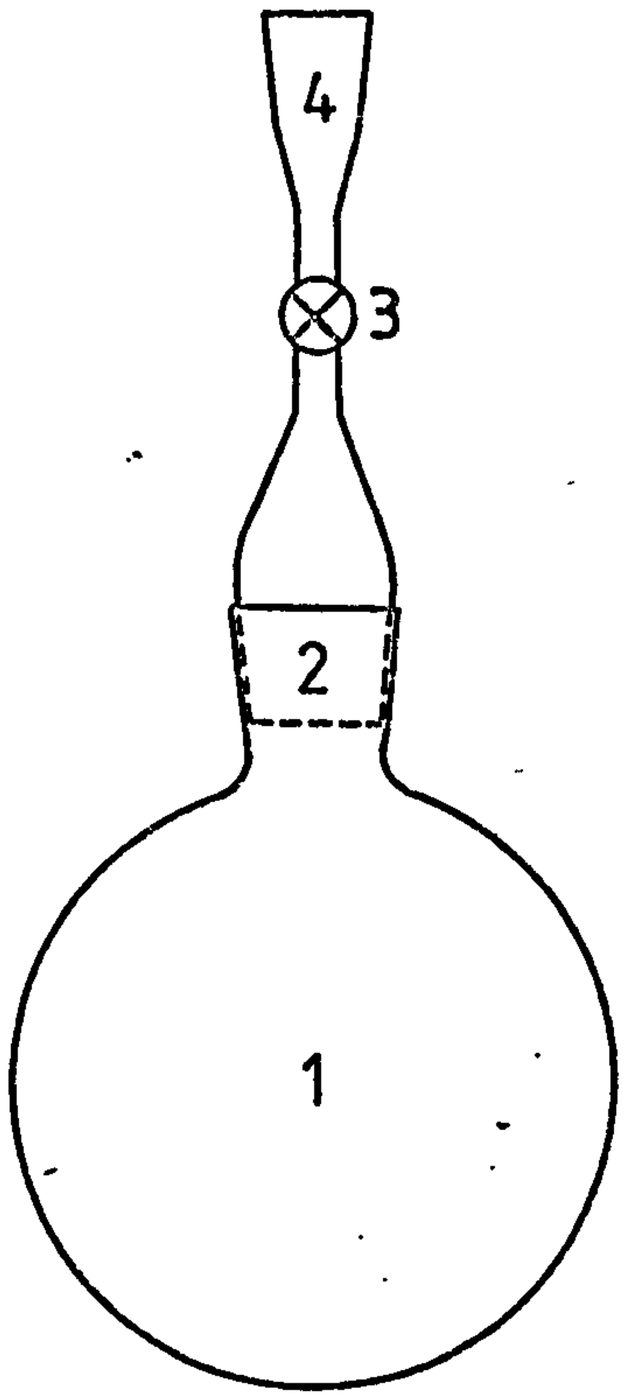

1. 100 ml PYREX FLASK
2. 10-14 GROUND GLASS JOINT
3. VACUUM STOPCOCK
4. 10-14 GROUND GLASS CONE

Figure 3.7 The first stage equilibrium cell

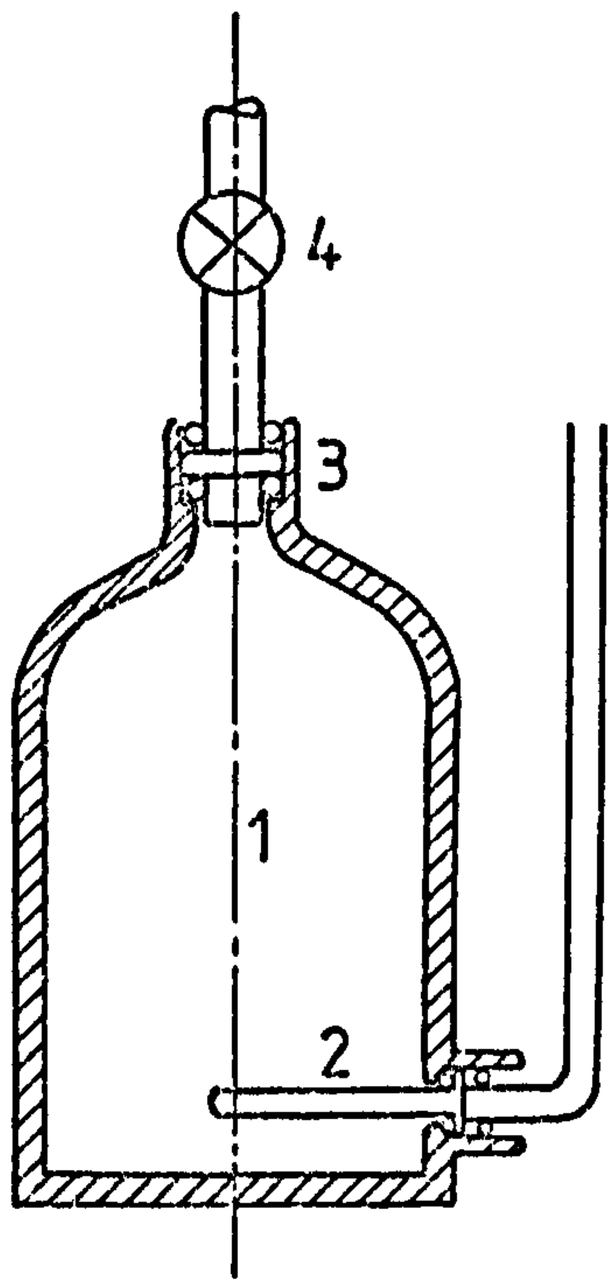

1. 100ml PRESSURE CHAMBER
2. THERMOCOUPLE WELL
3. GLASS VACUUM TIGHT FITTING
4. GLASS VACUUM STOP COCK

Figure 3.8 The second stage equilibrium cell

until a pressure of 0.03 mm Hg was obtained. The line stopcock was closed and the equilibrium cell was charged with about 50 ml of the sample. The valves of both cells were closed, the vacuum was released and the cells were separated. The top end of the equilibrium cell valve was thoroughly cleaned and the cell was connected to the apparatus.

The system was evacuated including the U tube which liquid was bubbling in one of the two bulbs. The tightness of the system was checked, and the vacuum pump was disconnected then both the cell valve and the air admittance valve were opened gradually to equalise the pressure in the two legs of the U tube.

To measure the vapour pressure, the bath temperature was brought up to the required temperature while pressure in the cell was always equalised by admitting or evacuating air through the pressure line. When the pressure was constant for at least fifteen minutes, the temperature and pressure readings were taken. Any leaks during that period would have been detected by the pressure transmitter. The McLeod vacuum gauge was used to measure pressures lower than 10 mm Hg, otherwise the mercury manometer was used. The pressure range from 10 to 20 mm Hg was avoided for fear of inaccuracy due to the manometer readings. A few readings (typically 3-5) were taken to each concentration and the vapour pressure of five different samples (50.9%, 40.3%, 35.6%, 28%, and 24.3%) was measured. Since information on vapour pressure was needed at above atmospheric pressures (ca 2 bars. abs.) and since vapour pressure measurements are fundamental to the physical property determinations it was decided to measure these directly rather than rely on extrapolation from sub-atmospheric measurements. The above equipment was not capable of operation at super-atmospheric pressures, hence a new system was constructed. In principle, the equipment did not change drastically, the loading cell was the same, but the equilibrium cell Fig.(3.8) was made of a 100 ml thick wall brass pressure chamber with a glass to metal vacuum tight joint on the top attached to which was the vacuum stopcock. This was connected to the same

U tube pressure transmitter. The bath was replaced by a thermally controlled oven with glass window to observe the liquid levels in the U tube. The glass bottle in the pressure equalising section was replaced by an air reservoir made of steel so that higher pressures could be realised. The air admittance valve was either connected to the atmosphere, vacuum pump, or to a pressurised air line through a pressure regulating valve and indicator. A schematic diagram of the equipment is shown in Fig.(3.9) and the system is shown in Plate 3.2. The sample temperature was measured by means of a chromel-alumel thermocouple inserted in a thermocouple well as shown in Fig.(3.8). The thermocouple circuit was arranged as shown in Fig.(3.10). The reference junction in this arrangement consisted of an ice bath with the reference junction immersed in a kerosine filled 50 ml test tube. The thermocouple was calibrated and found in good agreement with tables (Ref 51). The oven temperature could be set to within 2 ^{o}C.

The procedure of operation of the apparatus in the second stage of measurements was exactly the same as in the first stage and the vapour pressure of three more solutions (30.1%, 26.2%, and 25%) was measured over a temperature range of 51-192 ^{o}C and at pressures up to 2 bar.

The same apparatus described above was used to measure the vapour pressure of a - saturated solution over a temperature range from 180 ^{o}C to 55 ^{o}C. A solution of about 30% concentration was prepared and boiled at room pressure until salt crystals were seen, then it was charged while boiling into the pre-heated equilibrium cell in the way shown in Plate 3.3 to keep it boiling, thus avoiding the absorption of water vapour from the atmosphere. The cell was closed by a rubber stopper and placed in the oven at a temperature of 180 ^{o}C. The U tube was connected to the pressure equalisation section which was connected to the vacuum pump. The cell was left to cool to the oven temperature while pressure was equalised. Then, again, the reading was taken when the pressure had been constant for at least fifteen minutes. The oven temperature

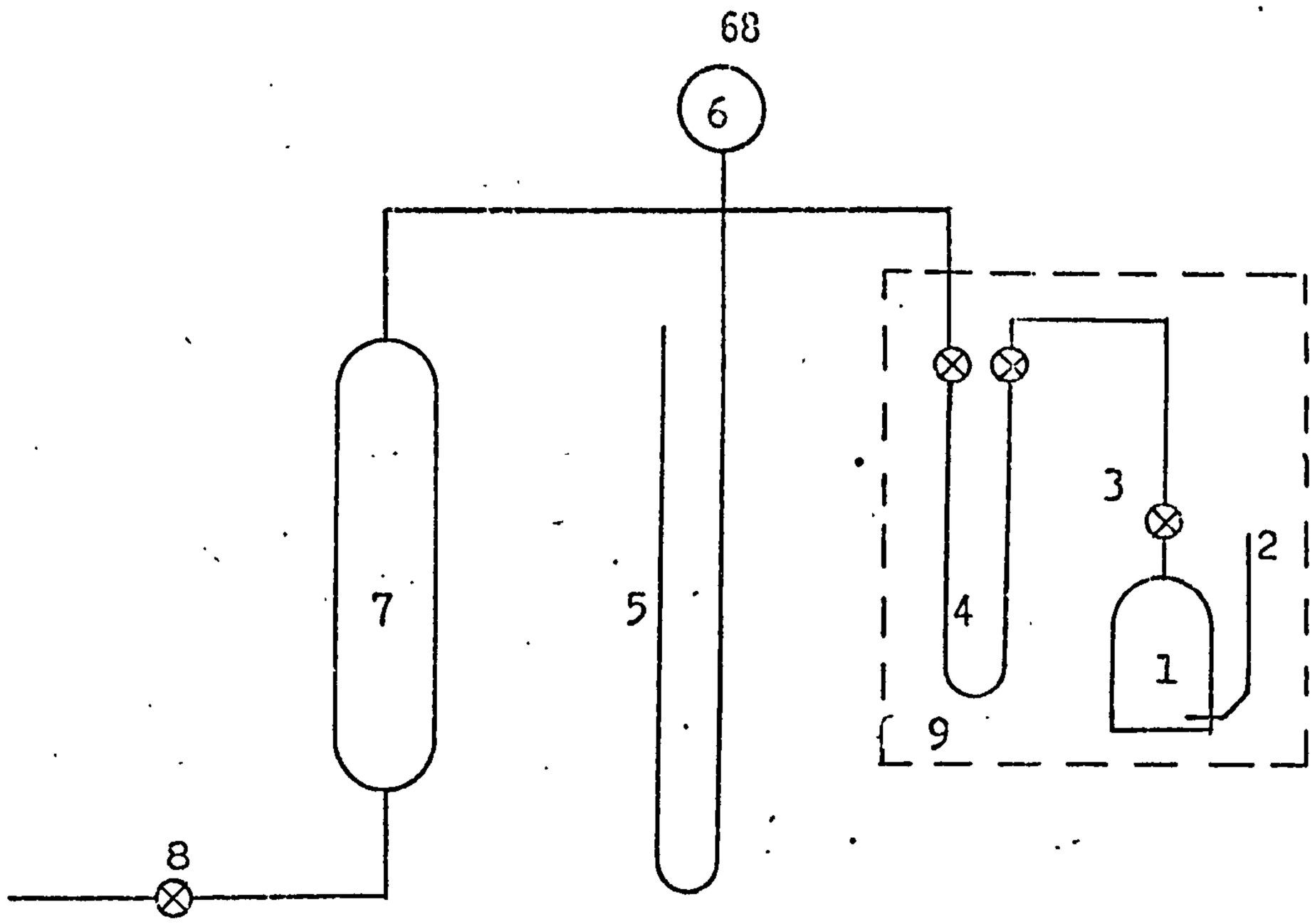

1 PRESSURE CELL
2 THERMOCOUBLE WELL
3 VACUUM STOPCOCK
4 PRESSURE TRANSMITTER
5 MERCURY MANOMETER
6 McLEOD VACUUM GAUGE
7 PRESSURE RESERVOIR
8 AIR ADDMITANCE VALVE

Figure 3.9 Schematic diagram of the experimental vapour pressure apparatus 2nd stage

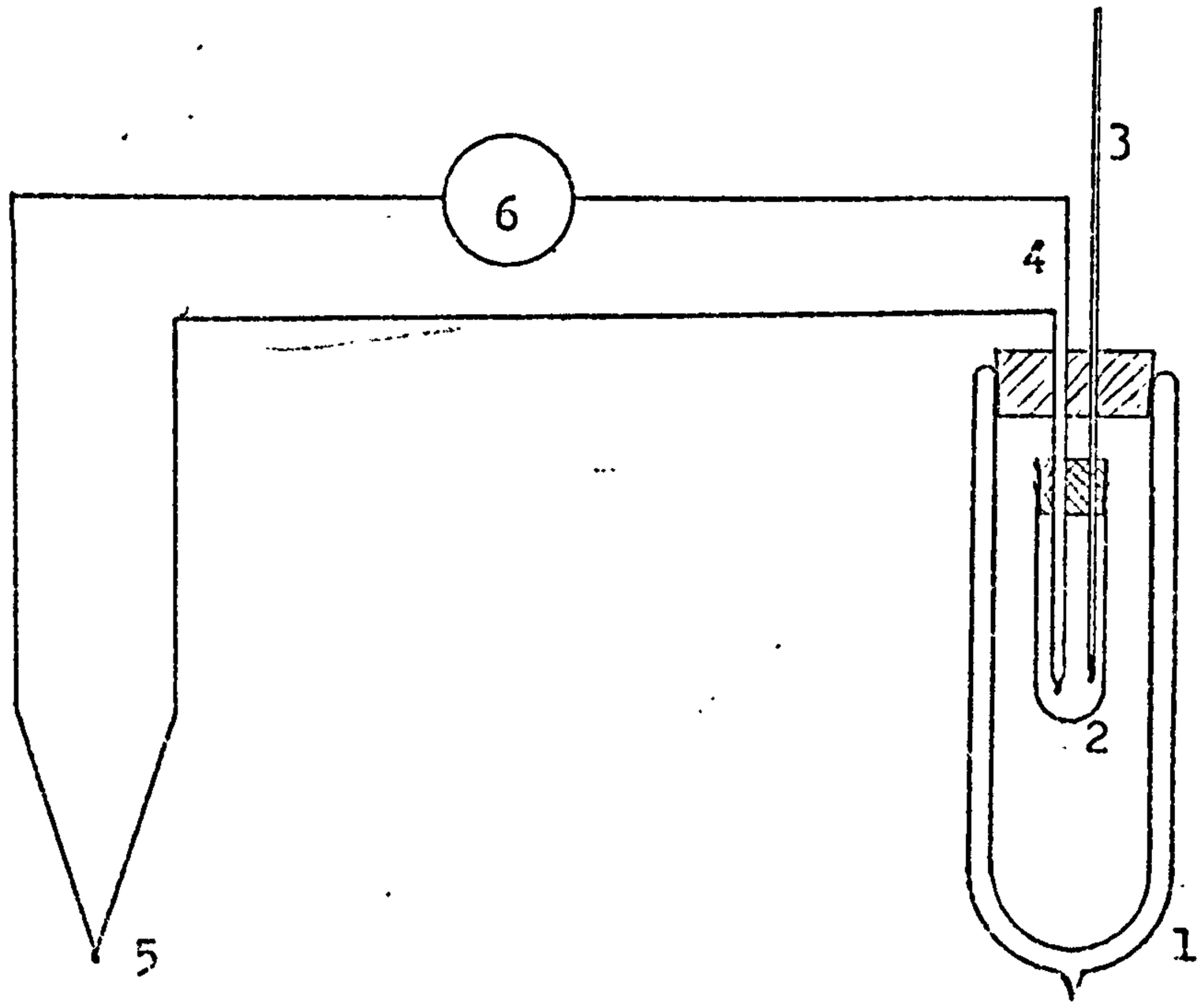

1 ICE BATH
2 TEST TUBE WITH KEROSENE
3 CALIBRATED THERMOMETER
4 REFRENCE POINT
5 HOT POINT
6 DIGITAL VOLTMETER

Figure 3.10 Arrangement for thermocouple calibration

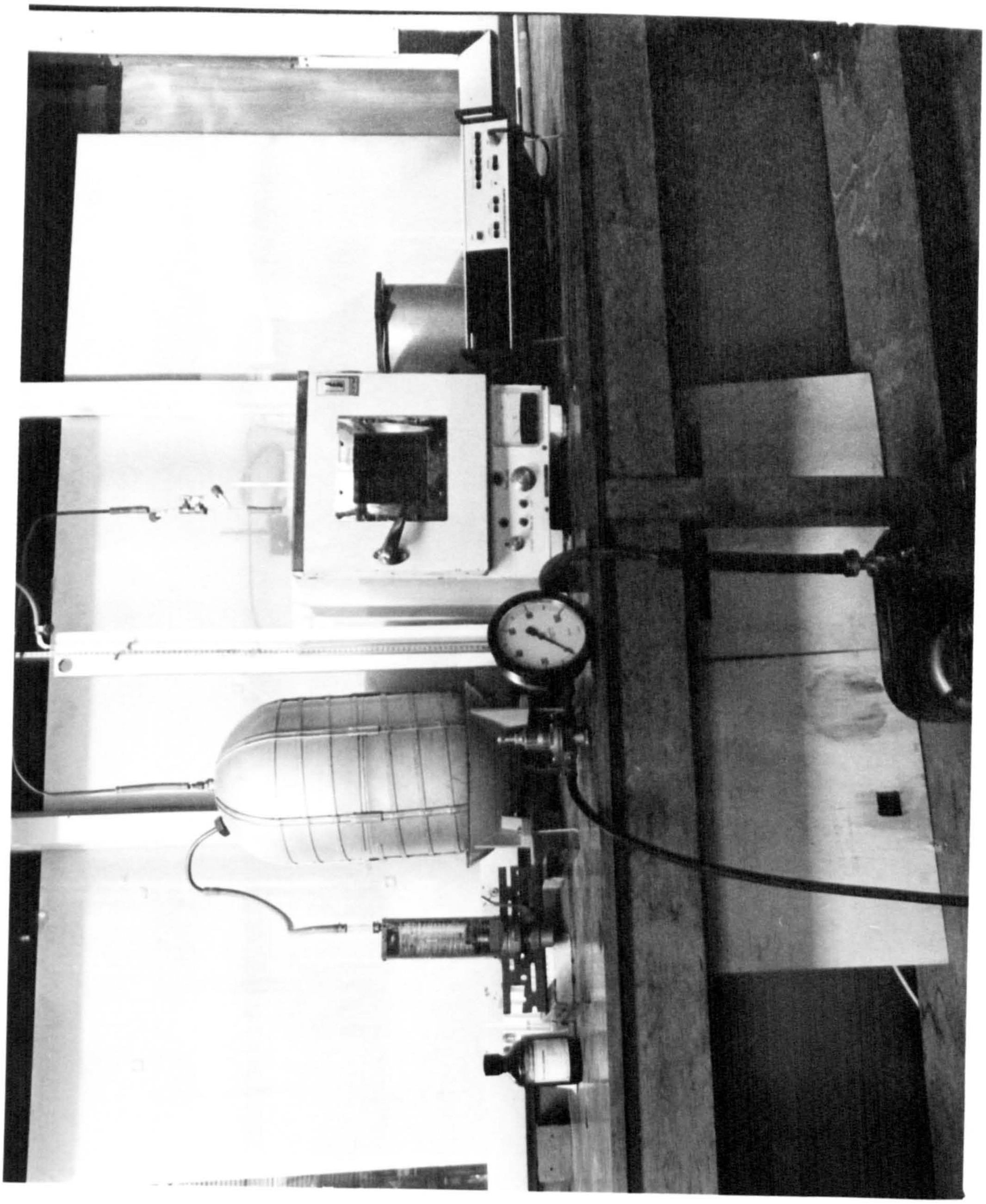

PLATE 3.2

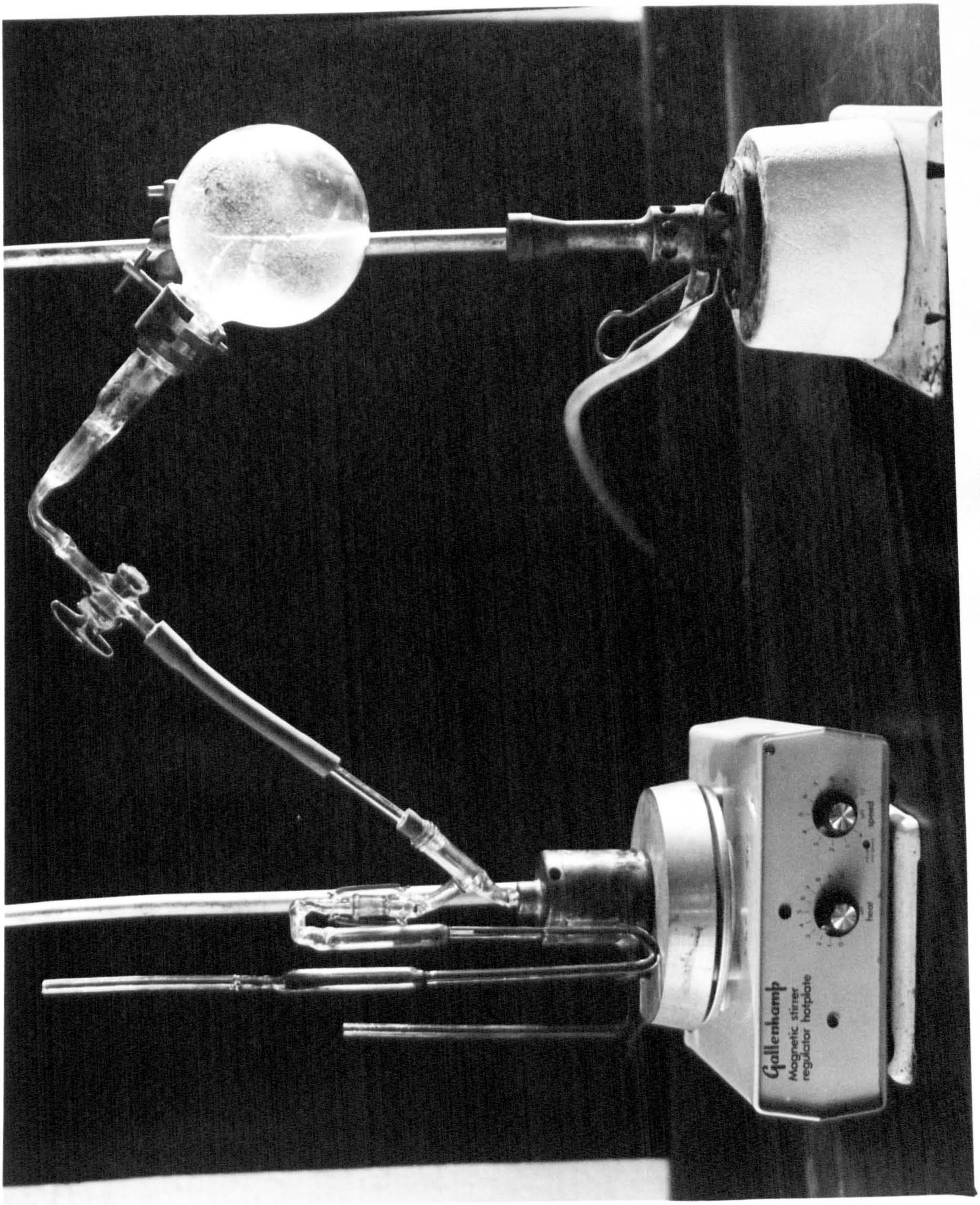
Gallenkamp
Magnetic stirrer
regulator hotplate
speed
heat

PLATE 3.3

was then reduced and left to cool by degrees and vapour pressure points were determined. The experiment was repeated three times and results were plotted on the vapour pressure diagram Fig.(3.11). It should be noted that corrections to the measured pressures at temperatures higher than 140 ^{o}C were necessary owing to the vapour pressure of n-di-butyl phthalate.

3.1.4 Results

The vapour pressure of eight different concentrations of the mixture (Methanol/2LiBr-$ZnBr_2$) were measured. A data sheet of one test (Appendix B) shows data collected of weight, concentration, temperature and pressure. The experimental results are tabulated in table 3.1 for the first stage of measurements and table 3.2 for the second stage.

The vapour pressure data for each concentration was smoothed by plotting vapour pressure as a function of the reciprocal of absolute temperature, as shown in Fig.(3.11). The resulting curves are straight line functions within the experimental accuracy of this investigation. As it is shown in Chapter 2, this linear relationship is predicted by the integrated form of the Clausius-Claperon equation with the assumption of constant latent heat of vaporisation and the validity of the equation of state for ideal gases. The correlations were given in the form

$$\log P = C_i + C_2\left(\frac{10^3}{T} - 2.3\right) \qquad (3.1)$$

where P is in m bars, the constants C_1 and C_2 for the tested compositions are given in table 3.3. The vapour pressure of the saturated solution at different temperatures regardless of the ratio of methanol is given in table 3.4. The experimental points are plotted on Fig.(3.11) to show the crystallisation line. These results should be able to given an answer to the solubility over the temperature range of the test. For example, from Fig.(3.11) the solubility of 310 gms of salts in 100 gms of methanol was found corresponding

% MeOH	Temperature ^{o}C	Pressure mm Hg	Pressure m bar
24.3	96.5	22.0	16.7
	117.5	59.0	44.8
	130.0	95.0	72.2
28.01	77.2	26.0	19.8
	93.3	60.0	45.6
	119.0	170.0	129.2
	141.0	427.5	324.9
35.56	42.0	11.5	8.9
	63.5	37.0	28.1
	89.2	139.0	105.6
40.3	30.8	17.5	13.3
	53.9	67.5	51.3
	80.1	250.0	190.0
	94.5	404.5	307.4
50.9	14.7	37.0	28.1
	30.7	82.0	62.3
	47.0	180.0	136.8
	54.6	274.5	208.6
	62.4	362.4	275.4
	75.2	593.5	451.0

Table (3.1)

Pressure measurements in first stage

% MeOH	Temperature ^{o}C	Pressure mm Hg	Pressure m bar
25.0	72.0	8.4	6.3
	120.0	101.5	77.1
	172.0	793.5	602.9
	192.5	1595.0	1212.0
26.2	68.3	9.9	7.5
	107:6	79.5	60.4
	144.0	374.0	284.2
	160.0	680.5	517.1
	181.3	1415.0	1075.3
30.1	51.0	9.6	7.3
	105.6	172.6	131.2
	138.2	670.0	509.1
	159.1	1440.0	1094.3

Table (3.2)

Pressure measurements in second stage

% MeOH	24.3	25.0	26.2	28.0	30.1	35.6	40.3	50.9
C_1	2.6712	2.8572	2.9758	3.0535	3.3146	3.4604	3.7770	4.0494
$-C_2$	3.0602	3.0344	2.9531	2.7278	2.8197	2.6219	2.4256	2.0194

Table 3.3

Correlation constants of equation (3.1)

Temp. ^{o}C	179.47	160.43	143.56	117.63	88.56	125.4	110.9
Pressure mm Hg	358.0	246.9	137.6	52.0	12.5	81.5	39.5
Pressure m bar	471.11	324.91	181.07	68.43	16.45	107.25	51.98

Temp. ^{o}C	94.57	73.15	55.3	119.0	59.85	37.05
Pressure mm Hg	16.5	5.6	2.7	53.2	3.2	0.98
Pressure m bar	21.71	7.37	3.55	76.59	4.21	1.29

Table 3.4

Pressure measurements of super saturated solution

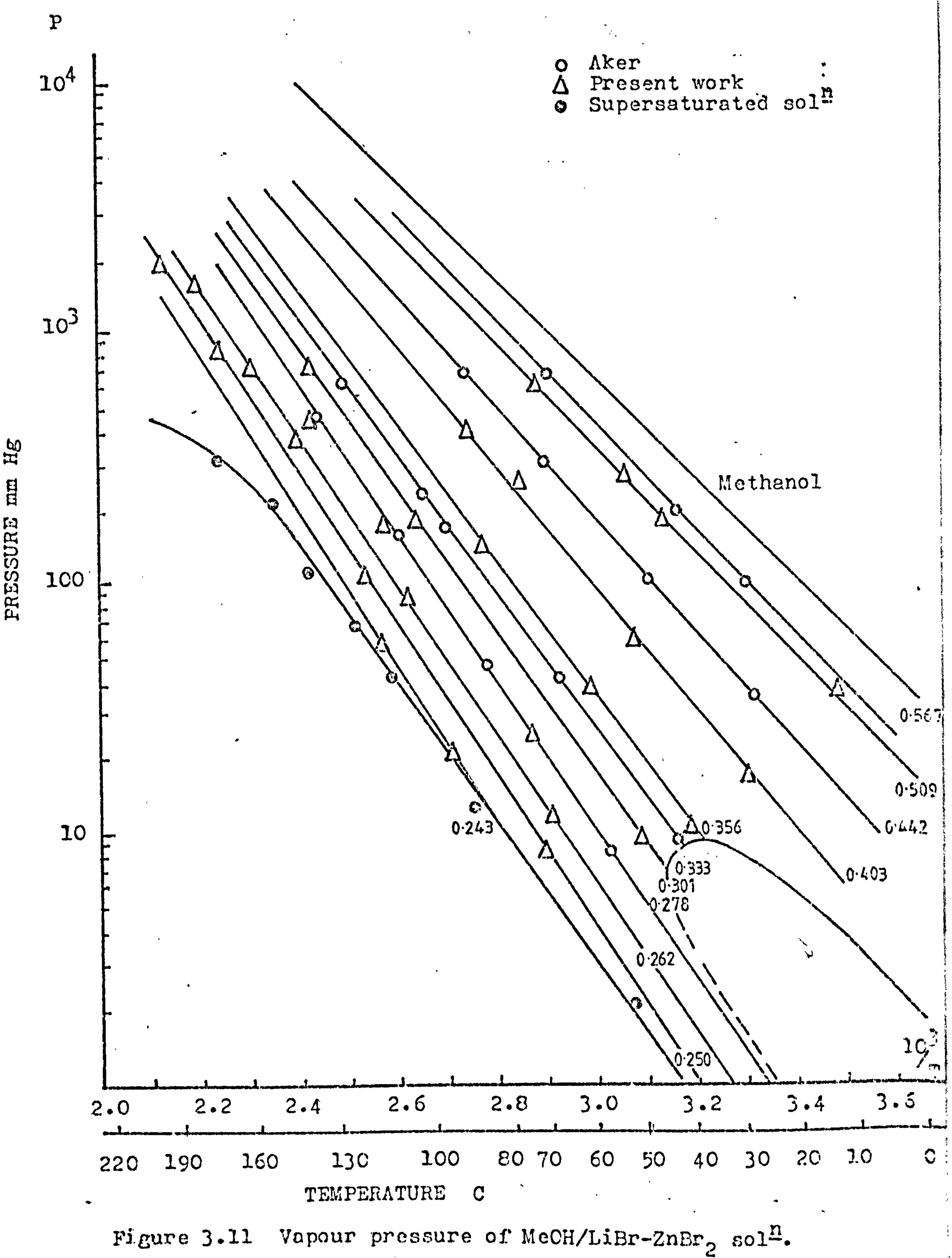

Figure 3.11 Vapour pressure of MeOH/LiBr-$ZnBr_2$ soln.

to a temperature of 88 °C. Such a solubility was obtained at 84 °C when extrapolating the data given by Uemura (Ref 30). Solubility at lower temperatures were not covered by that test; however a concentration of 25% methanol by weight formed crystals at a temperature of +10 to - 10 °C. A solution of 27.3 per cent methanol by weight was also checked for crystallisation and no crystals were seen while cooling the sample to as low as -40 °C in an environmental chamber. The discussion of the solubility of the mixture given in Chapter 2 together with the results shown in this chapter made it possible to believe that the severe problem of crystallisation may not arise in the proposed cycle.

The results of the vapour pressure measurements were evaluated from the accuracy point of view by measuring the vapour pressure of distilled water in each of the apparatuses before carrying out the experiments. Experimental points on vapour pressure of water were compared with those reported in the literatures. An error of less than 1.7% is observed in the first stage results and 2.4% in the second stage results.

The primary source of error in these measurements were due to inaccuracy in weighting, error in temperature readings, inaccuracy in pressure readings and the deviation of smoothed data from experimental points. The components of the mixture in both apparatuses were weighed to within 0.01 grams. An error of this magnitude in the refrigerant weight would represent less than .05% of the total and can be considered negligible. The weight of methanol vapour in the loading cell when it is cool was negligible, but in the equilibrium cell it was calculated at maximum temperature and pressure and was found to be 0.16 grams which represents a maximum error of less than 0.7% in the weight of methanol. The temperature control in the first apparatus held the temperature fluctuation to within 0.2 °C. This error together with a maximum error of 0.1 °C in the thermometer reading account for 0.3 °C error in the temperature measurement. This error would affect the pressure by approximately

1.5%. Whereas the temperature fluctuation of the sample in the second apparatus was only 0.05 ^{o}C due to the high thermal inertia of the brass cell and an error of 0.1 ^{o}C is expected in reading the ice bath temperature, as well as a random error of less than $\pm$ 0.05 ^{o}C found as a deviation from the used emf-temperature tables of the thermocouple. This error in temperature accounts for approximately 1% error in pressure readings.

The pressure measurements were carried out by the same instruments in both apparatuses and the expected error should be similar. When the McLeod vacuum gauge was used below 10 mm Hg, the typical error is expected to be less than 3% and this is believed to be the maximum error in pressure reading. The pressure reading was corrected at higher temperatures than 140 ^{o}C allowing for the vapour pressure of the fluid in the U tube pressure transmitter. At lower temperatures this pressure was neglected.

Although the two apparatuses showed less than 2.4% error from published data of water vapour pressure it is believed that the actual relative error is as high as 4% because low vapour pressure of water (less than 10 mm Hg) was not checked. Comparison of results of this investigation with the results of References 24, 28 and 29 was not possible because weight fractions of methanol were different in each of them than the compositions tested here. For the same reason Olama (Ref 24) was unable to compare his results too.

3.2 Specific Heat of the Solutions

The importance of the specific heat of the mixture was discussed in Chapter 2. It was measured by Uemura (Ref 30) and Olama (Ref 24). Uemura published smooth data covering a range of methanol weight fraction from 0.4 to 1.0. Such range does not include concentrations which may be required in the proposed cycle in Chapter 2. As for Olama, he measured the specific heat of only one fraction 30.7% methanol by weight. This concentration may fall in the range required by the heat pump but more data are

required. It was therefore decided to determine the specific heat of the mixture experimentally.

3.2.1 Principle of Measurements

If a known heat power input is supplied to certain quantity of substance in a calorimeter, the specific heat of that substance can be determined by observing the rate of change of temperature with time. However, it is also necessary to find out the heat losses during the process and allow for them. Because the rate of energy dissipation changes with the temperature difference between the laboratory and the calorimeter, it is preferable to measure the heat input to the solution over a small temperature interval. The specific heat of the solutions may be assumed to be reasonably constant over a temperature interval of 10 ^{o}C (the error resulting from this is only about 0.6%). The following quantities have to be known

- the heat equivalent of the calorimeter
- the weight of the subsistance in the calorimeter
- the heat power input N
- the rate of temperature increase relative to the time during heat $\left(\frac{dt}{d\tau}\right)_1$
- the rate of temperature decrease relative to time caused by heat dissipation $\left(\frac{dt}{d\tau}\right)_2$

The typical behaviour of temperature of a sample heated for time duration and left to cool is shown in Fig.3.12. The specific heat of the sample is given by the equation

$$mC_{ps} + C\left(\left(\frac{dt}{d\tau}\right)_1 + \left(\frac{dt}{d\tau}\right)_2\right) = N \qquad (3.2)$$

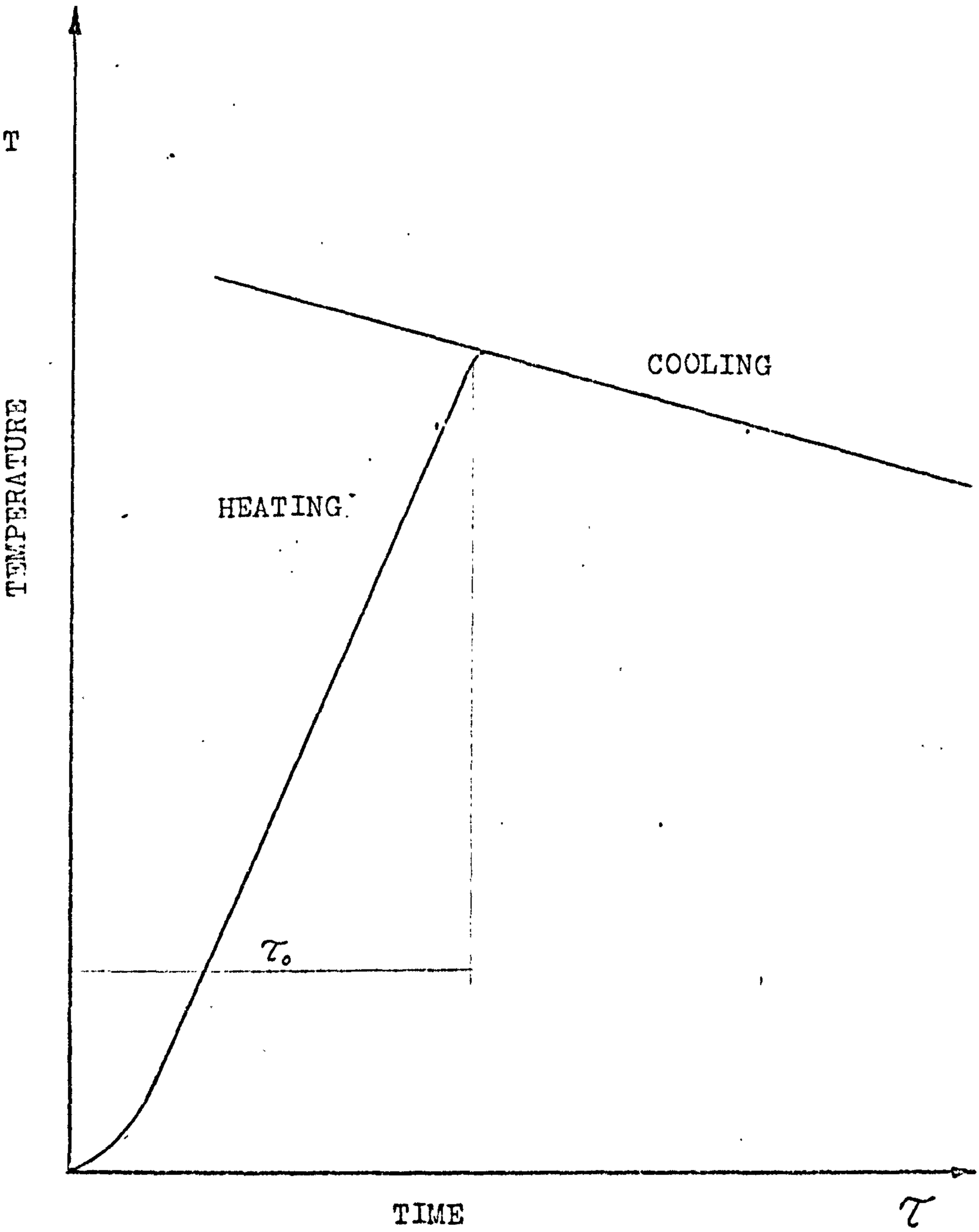

Figure 3.12 Typical temperature-time dependance of the calorimeter

where

m is the mass of the fluid in the calorimeter gms

c_{ps} is the specific heat of the fluid J/gms ^{o}C

C is the heat equivalent of the calorimeter J/^{o}C

$(\frac{dt}{d\tau})_1$ is the rate of temperature increase at the heating process

$(\frac{dt}{d\tau})_2$ rate of temperature decrease at cooling

N Heat input power watts

3.2.2 Equipment

The equipment for specific heat measurements (Plate 3.4) consisted of a one litre vacuum flask calorimeter (Fig. 3.13) inside which an electric oil heater was used to heat the contained liquid. Power was supplied to the heater from a stable DC power supply and the heater itself was made of a nichrome wire coil inside a U shape glass tube filled with oil. The tube was sealed at both ends with rubber stoppers while oil is at about 150 ^{o}C. The oil level in the heater was high enough to cover the coil but lower than the liquid level in the calorimeter. The power input was measured by means of a wattmeter. A stirrer was used to agitate the liquid bulk during measurements as shown in the figure. The temperature of the liquid inside the calorimeter was measured by means of a mercury in glass thermometer which scale read to 0.1 ^{o}C and a stop clock measured the time.

3.2.3 Procedure

It was necessary to determine the calorimeter heat equivalent before carrying out the measurements. High boiling turbine oil No.3 was chosen to calibrate the calorimeter. It was chosen since the oil has about the same viscosity as that of the solutions and this will account for similar hydrodynamic conditions within the cell. The properties of turbine oil No.3 quoted from (Ref 52) is given in table 3.5 and the specific heat at different temperatures (Ref 53) is given in table 3.6.

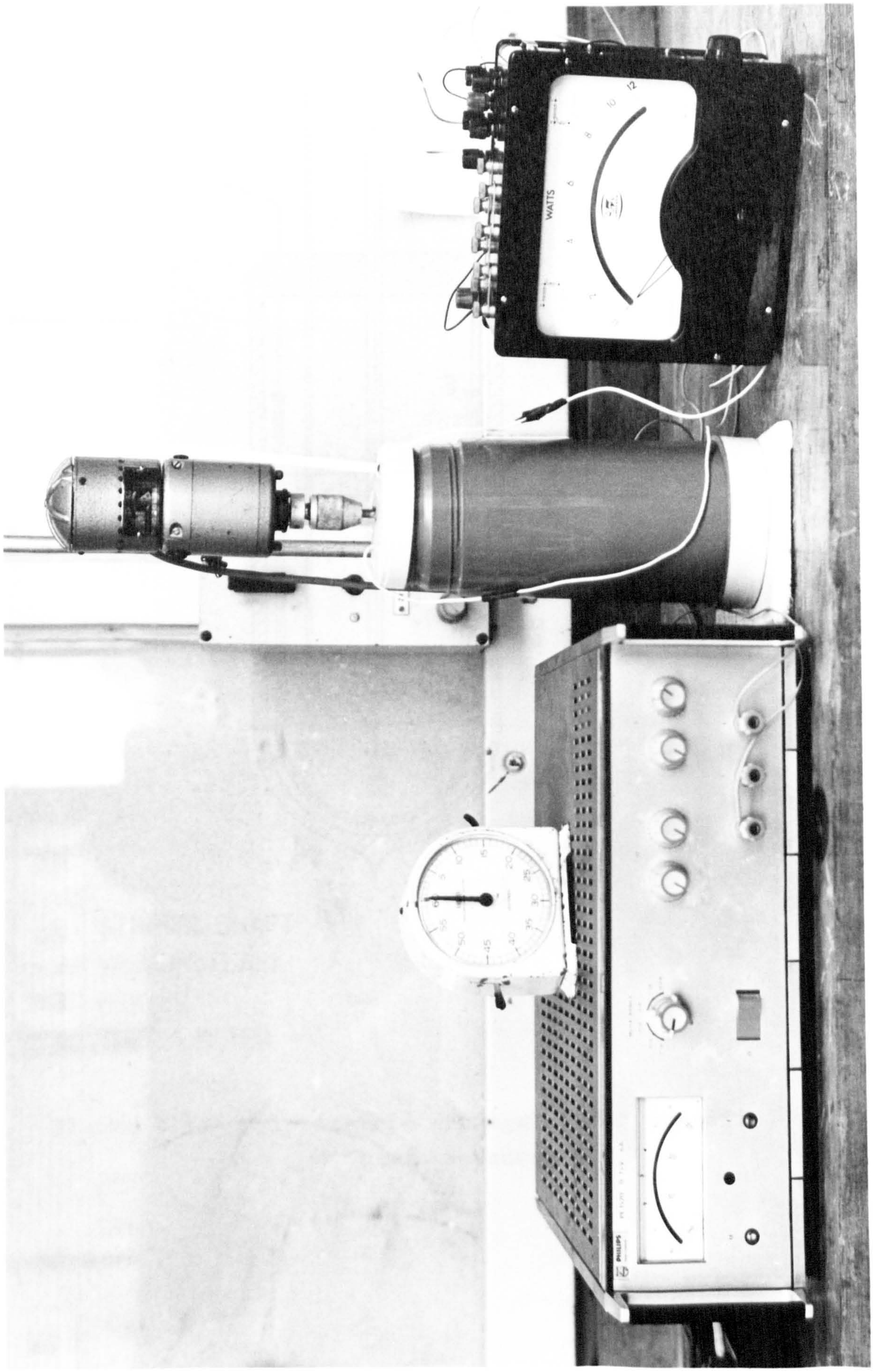

PLATE 3.4

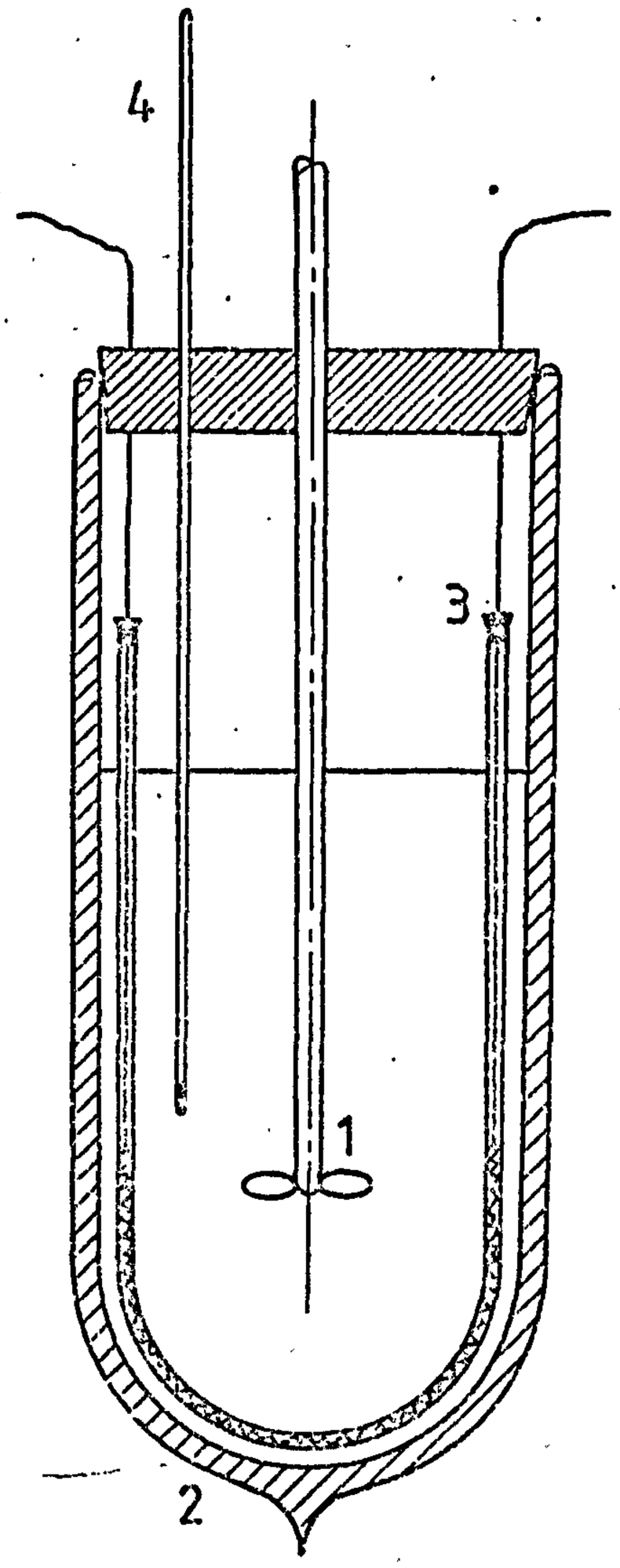

1. STIRRER SHAFT
2. VACUUM FLASK
3. HEATER
4. THERMOMETER

Figure 3.13 Calorimetric arrangment for specific heat measurements

Specific gravity at 15°C	0.930 gm/cm³
Viscosity at 38°C	12.5 CS
Viscosity at 100°C	3.2 CS
Boiling point	224 °C

Table 3.5

Properties of turbine oil No.3

Temperature °C	Specific heat kJ/kg °C
0	1.756
50	1.844
100	1.935
150	2.022

Table 3.6

Specific heat of turbine oil No. 3

The flask was cleaned, dried and weighted to within 0.01 gm and about 600 ml of the oil were poured in, then it was reweighted and the oil mass was determined. The cover, with the heater, stirrer shaft,and the thermometer were attached. The heater power was regulated in order that the rate of temperature increase is controlled. The measurement commenced by switching on the power and at the same time the stop watch was operated. Corresponding temperature and time readings were taken, whilst the wattmeter showed the power. Slight corrections to the power setting were necessary with temperature change as the resistance of the wire also changed. This was done manually by the fine adjustment on the power supply.

After a total temperature change of about 10 ^{o}C was reached, the power was switched off but the reading of temperature and time was continued during cooling. When a temperature drop of about 2-3 ^{o}C was obtained the heating was again switched on, thus new readings were taken. This process of heating and cooling was repeated over a temperature range up to 90 ^{o}C at 10 ^{o}C intervals. The calorimeter was left to cool down and new tests started next day. The same procedure was used to measure c_{ps} of the solutions knowing the heat equivalent of the calorimeter instead of the specific heat of the oil.

3.2.4 Results

Using the data for the specific heat of turbine oil No.3 given in table 3.5 it was possible to determine the heat equivalent of the calorimeter over a temperature range from 50 to 100 ^{o}C. The experimental results were smoothened using the least square principle giving the straight line

$$C = 248.2 + 1.518\ t \quad J/^{o}C \qquad (3.3)$$

where

t is temperature in ^{o}C and

C is heat equivalent J/^{o}C of the calorimeter

This equation correlates the result with a maximum error of 4.3%.

The specific heat of three different concentrations of the solution (40.3%, 31.1% and 24.9%) were measured and the results are given in table 3.7. Using the same principle (least square) these data were correlated by the equation

$$C_p = A + B\,t \quad kJ/kg\ ^oC \tag{3.4}$$

where

$t = {}^oC$

$A = 0.652 + 2.139x - 2.077x^2$

$B = -0.000205 + 0.00928x \mp 0.0101x^2$

x = methanol ratio by weight

Equation 3.4 correlates the specific heat of solutions with an average error of 2% over a concentration range of 24.9% to 40.3% methanol by weight.

3.2.5 Accuracy of Results

In these measurements the only considerable error is that arising in temperature and power readings as error in weight and time are too small to be considered. Temperatures were measured to within 0.1 ^oC, such error representing 1% at the heating temperature difference and about 7% in the cooling temperature difference. The rate of temperature increase was typically ten times the rate of temperature drift due to heat dissipation, accordingly 0.1 ^oC would probably account for only 1% in the specific heat measurements.

The wattmeter used in these measurements had watt scale divisions, but the power was so stable that only 0.2 watt would be a possible error. This value accounts for 0.5% error in the power measurements (40 watts on average).

Although an error of 4.3% is expected in calculation of C from equation 3.3., this error accounts only for about 1% in the specific heat results as the thermalmass of the calorimeter (C) was about one fifth of the sample thermal mass (mC_{ps}).

Concentration % MeOH	Temp ^{o}C	Specific heat kJ/kg ^{o}C
	51.3	1.27
	60.6	1.30
	69.9	1.30
	51.1	1.28
40.3	62.5	1.31
	71.7	1.30
	52.5	1.27
	62.3	1.30
	67.1	1.30
	40.0	1.19
	57.1	1.23
	80.6	1.26
	40.3	1.18
31.1	64.6	1.22
	79.8	1.24
	40.0	1.16
	57.1	1.25
	80.6	1.24
	48.1	1.11
	60.0	1.14
	80.0	1.17
24.9	45.1	1.14
	58.4	1.14
	81.7	1.19

Table 3.7

Specific heat of MeOH/LiBr-$ZnBr_2$ solutions

The average scater of experimental points when correlated by least square was 2%. The specific heat of two of the samples (40.3% and 24.9%) was checked using a differential scanning calorimeter (DSC) at Cambridge University. The results of the first sample 40.3% agreed well with the results obtained from the vacuum flask calorimeter. Results were 4% higher over the temperature range from 50 ^{o}C to 70 ^{o}C. Knowing that the DSC results for water was 2% higher in this test, one would expect a difference of only 2% between results of both measurements. However, the specific heat of the second sample 24.9% given by DSC at 45 ^{o}C was only 2% higher than the corresponding result of the vacuum flask calorimeter, but surprisingly enough, the specific heat decreased over a temperature range from 40 to 90 ^{o}C by about 7%. Crystals which may have been formed in the pan of that sample in the period between preparation and measurement may be the reason, or unperfect sealing of the pan may cause such a result.

The results of the specific heat in this work were compared with previous measurements in References 24 and 30. The specific heat for concentrations 40% and 50% methanol by weight were calculated at temperatures from 20 to 80 from equation 3.4 and compared with data published by Uemura (Ref 30). The difference was as high as 10% at 20 ^{o}C but the average difference at higher temperatures was only 3%. Realising that the smoothed data of both investigations are within about 2.5% error from experimental, the results are considered in good agreement. The only available data in the concentration range measured in this investigation is the specific heat of 30.7% methanol by weight measured by Olama (Ref 24) using DSC. The specific heat of 30.7% concentraction at 80 ^{o}C was found to be 1.27 kJ/kg ^{o}C in Olama's work while that of 31.1% in this work is 1.25 kJ/kg ^{o}C, although one would have expected higher value. A difference of about 3% less than Olama's result is seen.

It is believed that the results of specific heat of solutions given in this work reasonably agree with published results even when they are extrapolated.

CHAPTER 4

PHYSICAL AND THERMOPHYSICAL PROPERTIES OF THE SOLUTIONS

4.1 Thermal conductivity

Most of the processes taking place in a heat pump cycle are accompanied by either heat or heat and mass transfer. The efficiency of the cycle depends on the efficiency of each process. Heat transfer calculations play an important part in the design of the heat pump components. Thermal conductivity is one of the basic properties required for these calculations.

Sherwood (Ref 54) pointed out that there is no adequate theory that will predict accurately the thermal conductivity of liquids. However, he listed eight methods for such predictions. The literature is very poor in the data which enable the use of these methods in predicting thermal conductivity of liquid salt solutions.

He also mentioned that thermal conductivity of most liquids decrease with increasing temperature, but some liquids like water, some polyhydric compounds, and certain allotropic forms of sulphur have been reported to show increase in thermal conductivity with temperature over limited temperature ranges.

No theoretical predictions were made in this work and thermal conductivity of Methanol/2LiBr - $ZnBr_2$ solutions was measured experimentally.

4.1.1 Theory of the measurements

Thermal conductivity measurements using steady state methods demand careful experimentation to minimize corrections for heat losses and to prevent the on-set of turbulent convective motion in the fluid. Furthermore the establishment of a steady state in an apparatus of considerable mass is a slow process and measurements may be time consuming.

It is therefore natural to explore the possibility of emplpying

transient techniques in which the same information may be obtained while the fluid system is subjected, for a short interval of time to the influence of a transient temperature field.

For several years the transient hot wire method has been utilized for the measurements of thermal conductivity in solids. It was first discussed in details by Vos (Ref 55), but his study only applied to solids. In 1962 the same method was used by Horrocks et al (Ref 56) to measure thermal conductivity of liquid polyphenyl. The various sources of error were studied and corrections were applied.

Later on, more reliable experimental aspects were studied by Wakeham et al (Ref 57, 58, 59, 60, & 61) and application of this method was used for determination of thermal conductivity of liquids and gases, utilizing shorter time intervals for measurements and very thin hot wires in an automatic, high-precision Wheatstone bridge.

The theoretical principle of this method arises when solving the heat conduction equation using certain boundary conditions representing the continuous generation of heat uniformly along an infinite line source in an infinite body. As long as the heat transmission mechanism is only pure conduction, the time-dependent temperature in the body around the line source during heating is a direct function of the thermal conductivity of the body.

The conduction equation in Cylindrical coordinate (r, ϑ , Z) is:

$$\frac{\partial t}{\partial \tau} = \frac{k}{C_p \rho}\left(\frac{\partial^2 t}{\partial r^2} + \frac{1}{r}\frac{\partial t}{\partial r} + \frac{1}{r^2}\frac{\partial^2 t}{\partial \theta^2} + \frac{\partial^2 t}{\partial Z^2}\right) \qquad (4.1)$$

Where

t	Temp.
τ	Time
k	Thermal conductivity
C_p	Specific heat of medium
ρ	density of medium.

Assuming uniform generation of heat along the line and homogenous medium around it, r, τ will be the only variables and equation 4.1 becomes:

$$\frac{\partial t}{\partial \tau} = \frac{k}{\rho C_p}\left(\frac{\partial^2 t}{\partial r^2} + \frac{1}{r}\frac{\partial t}{\partial r}\right) \tag{4.2}$$

In the apparatus described below, the development of temperature is observed in an electrically-heated wire immersed axially in a liquid contained in a cylindrical cell which is initially in thermal equilibrium. The cell in the first approximation simulates the system represented by equation (4.2) subjected to the initial condition of thermal equilibrium so that

$$\text{for } \tau \leqslant 0 \quad \Delta t(r, \tau) = 0 \text{ for all } r$$

together with the following boundary conditions:

(a) Infinite circular cylinder so that at $r = \infty$
for all $\tau \geqslant 0$ $\lim_{r\to\infty} \Delta t(r, \tau) = 0$.

(b) Internal generation of heat uniformaly at a rate of Qkwatt/unit length of very thin wire so that temperature discontinuity at the contact surface of the wire and the medium is neglected and also at $r = 0$, $\tau \geqslant o$

$$Q = \lim_{r\to o} (2\pi r)k \frac{\partial t}{\partial r}.$$

Carslaw & Jaeger (Ref 62) gives the solution of equation (4.2) utilizing the above conditions as:

$$t(r, \tau) = \frac{-Q}{4\pi k} \; Ei\left(\frac{-r^2}{4D\tau}\right) \tag{4.3}$$

where

D is the heat diffusivity of the medium

Ei is the exponential integral function.

$t(r, \tau)$ is referred to the initial temperature of the body.

For the small values of the argument $\frac{r^2}{4D\tau}$, i.e. relatively large intervals of time, the temperature at a fixed radial distance can be obtained with adequate accuracy from the first two terms of the series expansion of the exponential integral (Ref 63)

$$Ei\left(\frac{-r^2}{4D\tau}\right) = \left\{\ln \frac{r^2}{4D\tau} + 0.5772 + - - - -\right\} \qquad (4.4)$$

The difference between the expansion of Ei(-x) and the tabulated values of the function in (Ref 64) was found to be $\leqslant 0.72\%$ for $\frac{r^2}{4D\tau} \leqslant 0.02$.

From the measurements of temperatures at a certain radial distance r_o at two different time intervals τ_1, τ_2 one obtains:

$$t_2 - t_1 = \frac{Q}{4\pi k} \ln \frac{\tau_2}{\tau_1} \qquad (4.5)$$

As r_o has been eliminated from this equation, there can be no objection to measuring the temperature on the axis of the system by determining the change in electric resistance of a very thin heated wire. This choice favours the applicability of equation 4.5 for even short intervals of time, which eliminates the effect of the on-set of convection, thus,

$$k = \frac{Q}{4\pi} \frac{\Delta \ln \tau}{\Delta t} \qquad (4.6)$$

A plot of temperature change against the logarithm of time (Fig. 4.1) results in a straight line, the gradient being proporticnal to the thermal conductivity.

4.1.2 The equipment

The objective of the cell design is to fulfil the theoretical assumptions used in the mathematical handling of the theory. A probe was formed of a 0.025 mm diameter platinum wire of known temperature coefficient (α value) and of length 70 to 100 mm. The wire was soldered at one end to a light steel spring and PTFE coated copper connecting wire. To minimize its resistance the connecting wire was used in duplicate and to protect the hot wire from breakage and keep the spring in vertical position, the connecting wire was wound in a spring shape

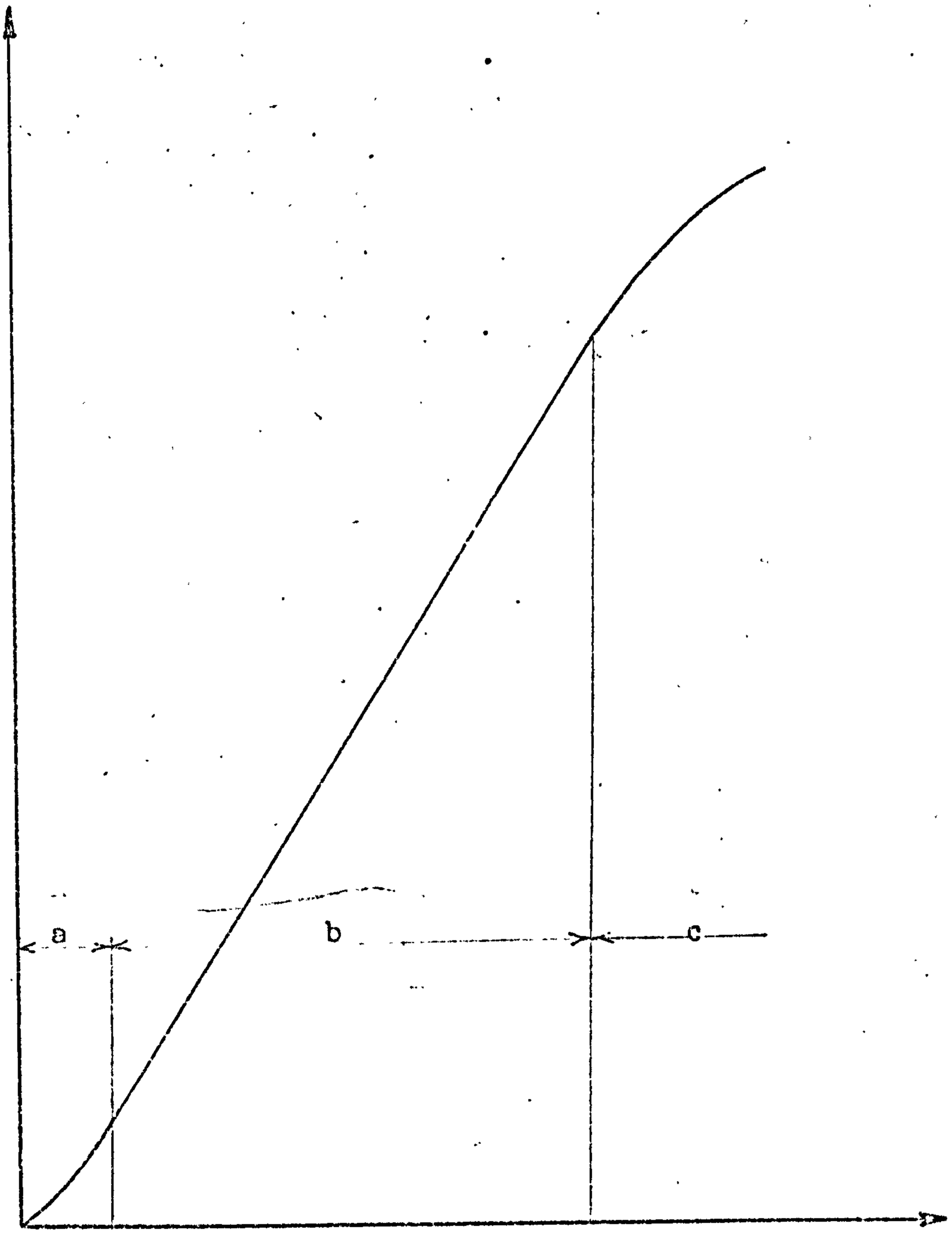

a EFFECT OF FINITE RADUIS OF THE WIRE
b LINEAR ZONE
c EFFECT OF ON-SET OF CONVECTION

Figure 4.1 Typical temperature-time dependance of the hot wire

as shown in plate 4.1 and Fig. 4.2. The steel spring was hooked in a plastic screw by which the spring tension is applied to the wire to keep it stretched during heating. The tension was adjusted so that the spring deflection was at least ten times the expected expansion in the wire length. The plastic screw was attached to a formed piece of tufnol through which a glass tube of 7 mm diameter passes, and its height was kept by a small rubber stopper. The other end of the hot wire was soldered to a copper connecting wire passed through the glass tube. The two soldering points were sealed by silicone rubber to prevent galvanic action.

The cell (Fig. 4.3) and (Plate 4.2) was formed of one litre clear glass dewar vacuum flask containing the solution and providing the infinite body. The probe was attached to a rubber stopper which carried an electric oil immersion heater. Solution temperature was measured by a calibrated electronic thermometer, the thermocouple of which was immersed in a glass tube filled with oil, sealed at the bottom and isolated on top. A rotaflow glass vacuum valve was used to evacuate the cell and charge the solution.

To establish thermal equilibrium in the cell, two copper containers of an old adiabatic calorimeter (Fig. 4.3) were used as an isolated oil bath with an air gap between them, isolated at the top by fiber glass to reduce the effect of free convection around the oil bath. A thermostirer was used to heat the bath and control the temperature. By this arrangement it was possible to keep the temperature fluctuation less than $\pm$ 0.1^{o}C at temperature range below 100^{o}C and less than $\pm$ 0.2^{o}C at higher range. A tufnol base disc with three steel rods each of 1 cm diameter and 40 cm length was used as a stand for the cell in the oil bath.

A DC wheatstone bridge, of which the wire formed a branch, was constructed using three incrementlly adjusted resistance boxes and a 15 volt stabilized power source supplied the bridge. A digital voltmeter was used to measure the input voltage to the bridge and also to measure resistance when a known current was flowing. A storage-osilloscope was used as an indicator when balancing the bridge initially and to trace the time dependant voltage change across the platinum wire during the measurement. A diagram of the

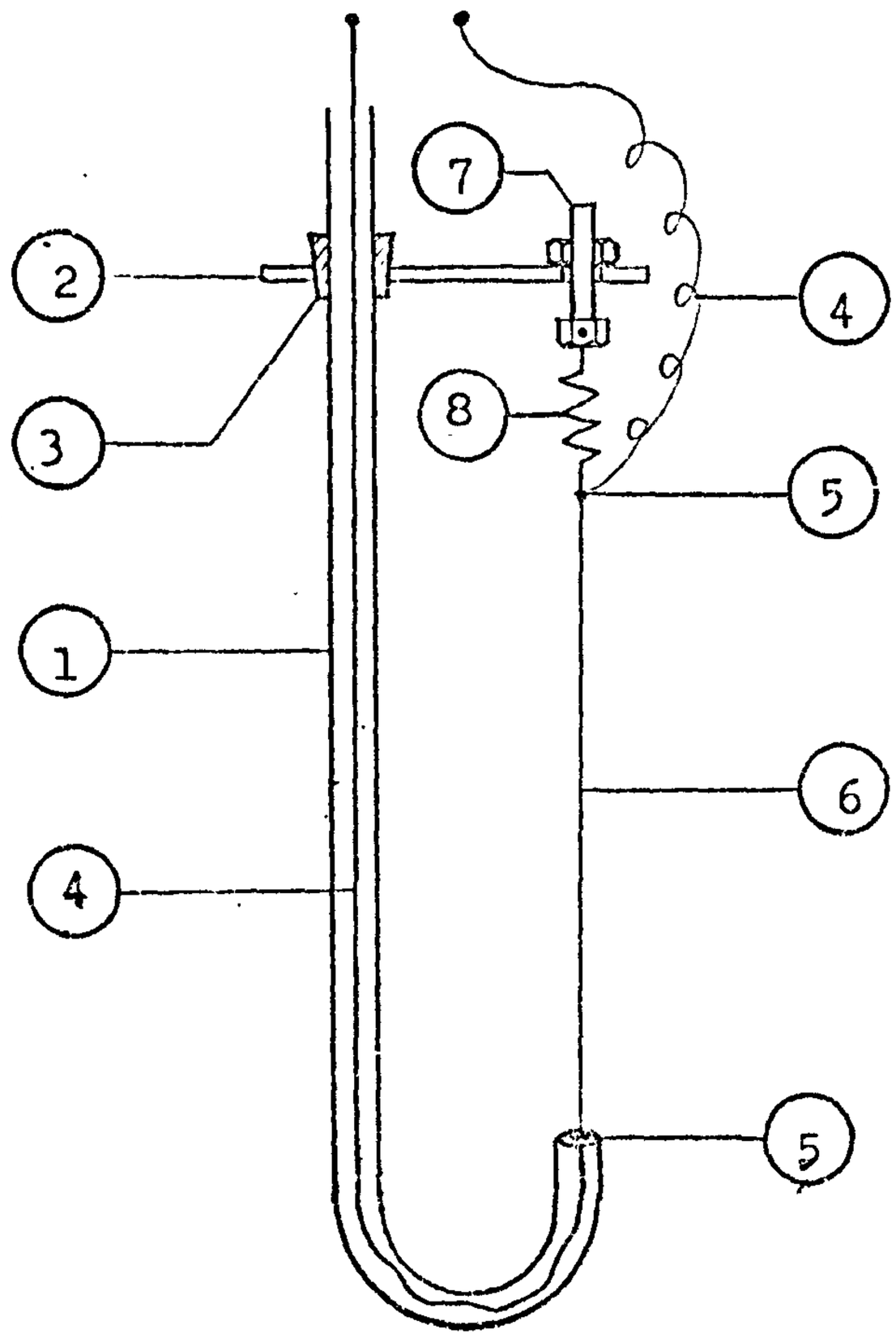

1 GLASS TUBE
2 TUFNOL PIECE
3 RUBBER STOPPER
4 CONNECTING WIRE
5 WIRE ENDS
6 Pt WIRE
7 PLASTIC SCREW
8 LIGHT STEEL SPRING

Figure 4.2 The probe

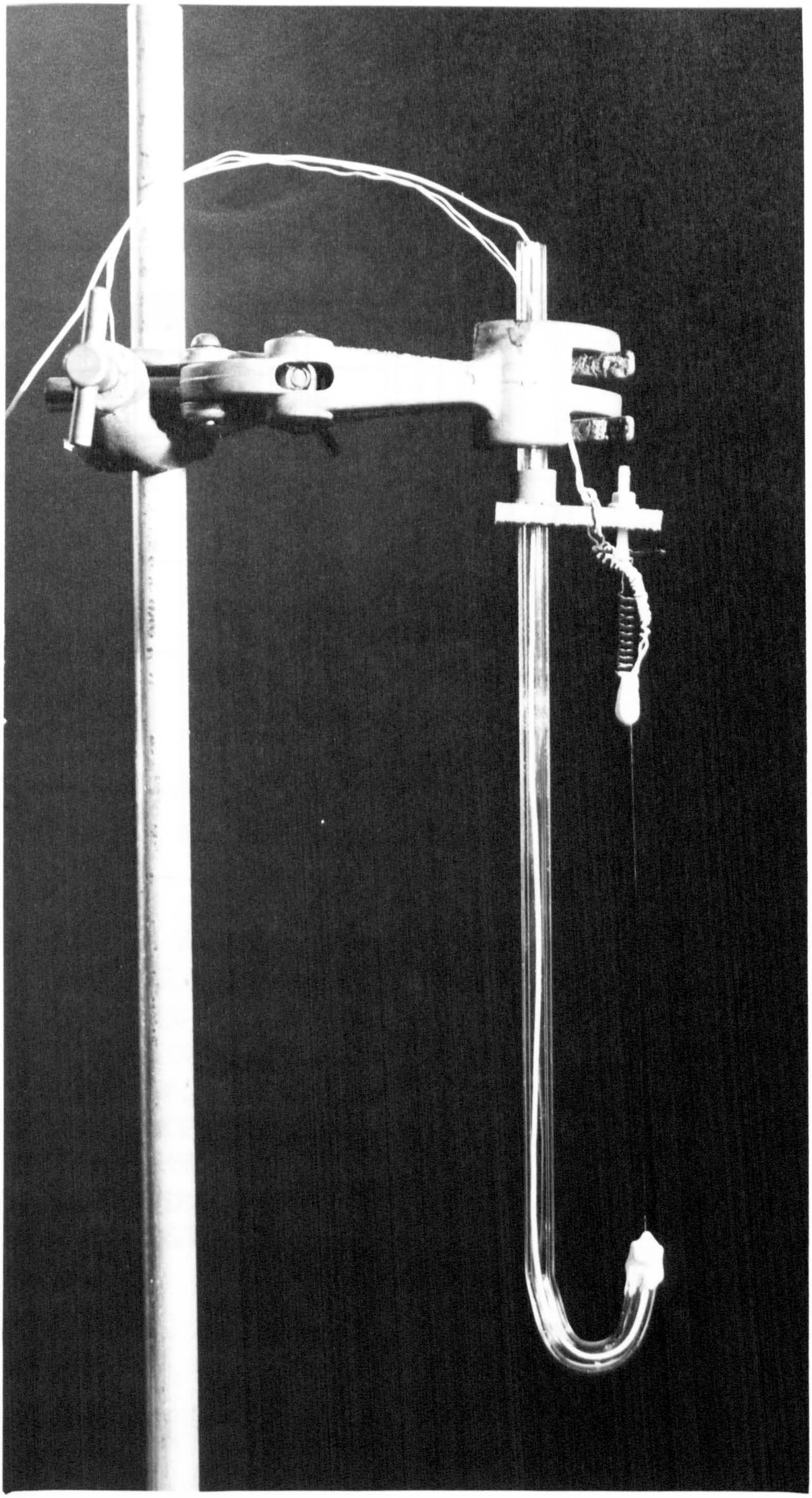

PLATE 4.1

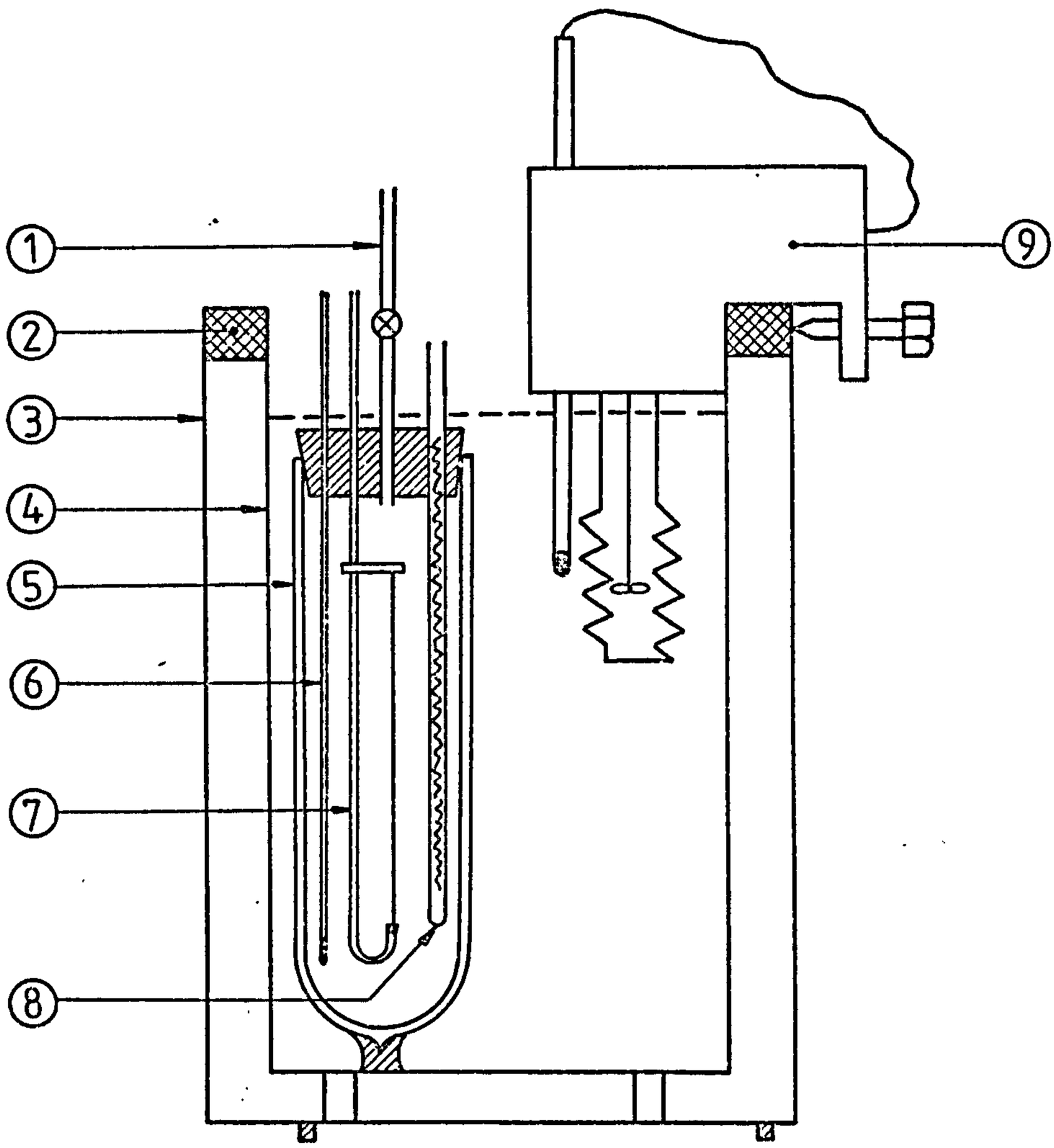

1. VACUUM VALVE
2. FIBRE GLASS
3. OUTER COPPER CYLINDER
4. INNER COPPER CYLINDER
5. DEWAR FLASK
6. THERMOCOUPLE WELL
7. THE PROBE
8. IMMERSION HEATER
9. THERMOSTIRRER

Figure 4.3 The thermal conductivity cell

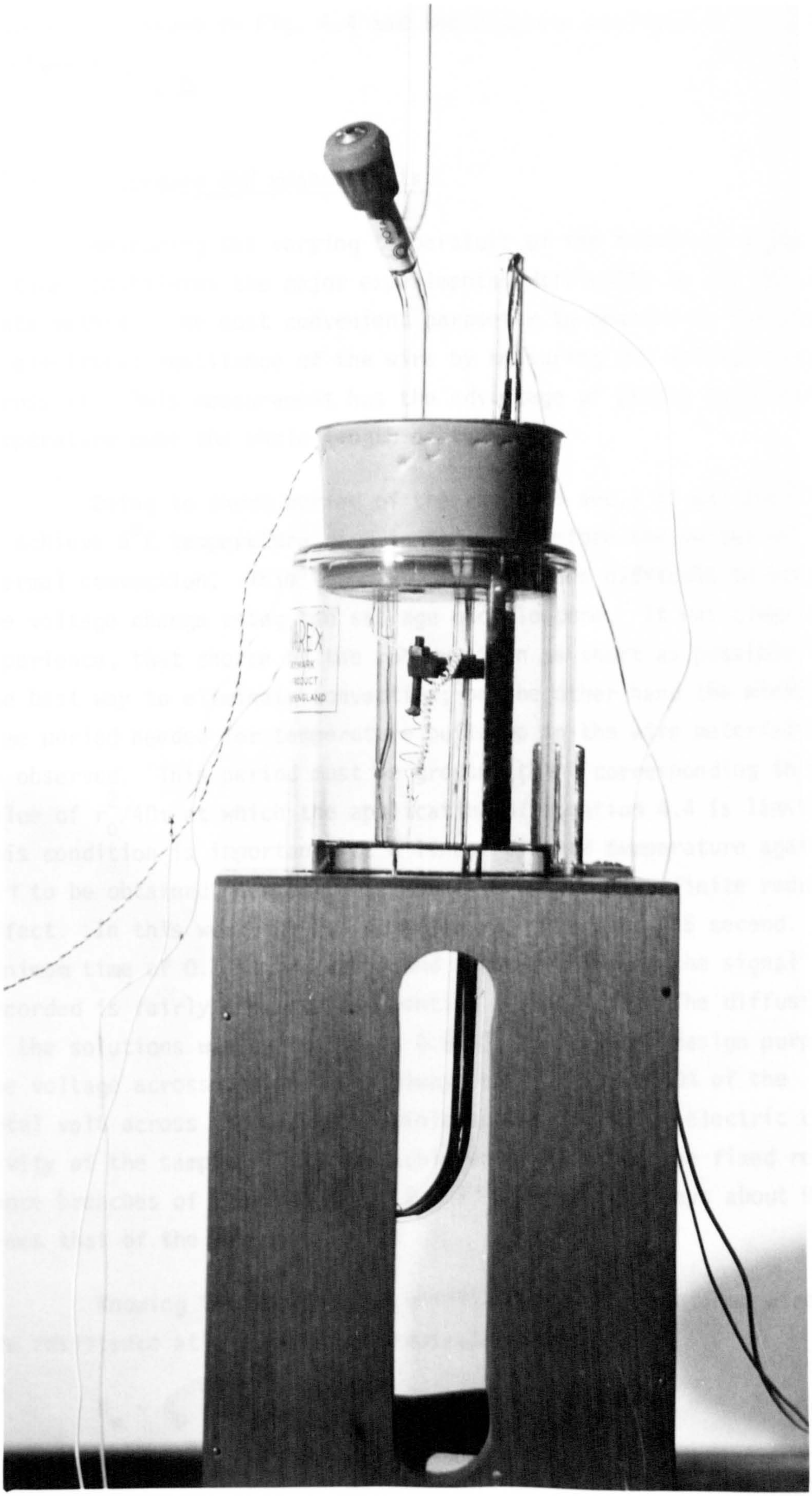

PLATE 4.2

equipment is shown in Fig. 4.4 and the complete arrangement is shown in Plate 4.3.

4.1.3 Procedure and measurements

Measuring the varying temperature of the heater as a function of time constitutes the major experimental difficulty in the non-steady state method. The most convenient parameter to measure is the change in electrical resistance of the wire by measuring the voltage change across it. This measurement has the advantage of giving an average temperature over the whole length of the wire.

Owing to short period of the run (0.5 sec.) it was possible to achieve $6^{o}C$ temperature rise in the wire before the on-set of thermal convection. This technique made it less difficult to measure the voltage change using the storage oscilloscope. It was clear from experience, that choice of the run duration as short as possible is the best way to eliminate convection; on the other hand the minimum time period needed for temperature build up in the wire material should be observed. This period must be greater than τ corresponding to the value of $r_o^2/4D\tau$ at which the application of equation 4.4 is limited. This condition is important for a linear plot of temperature against $\ln\tau$ to be obtained, hence the elimination of the wire finite raduis effect. In this work the run duration was chosen as 0.5 second. Minimum time of 0.1 second was found satisfactory and the signal recorded is fairly accurate exponential (Plate 4.4). The diffusivity of the solutions was estimated as 0.9_x10^{-7} m^2/sec for design purposes. The voltage across the wire was always kept at about 10% of the total volt across the bridge to minimize the effect of electric conductivity of the sample. This was achieved by altering the fixed resistance branches of the bridge R_1, R_2 (Fig.4.4)to be always about 9 times that of the wire.

Knowing the temperature coefficient of the platinum wire,(α) its resistance at a particular temperature is:

$$R_w = R_o + \alpha R_o t$$

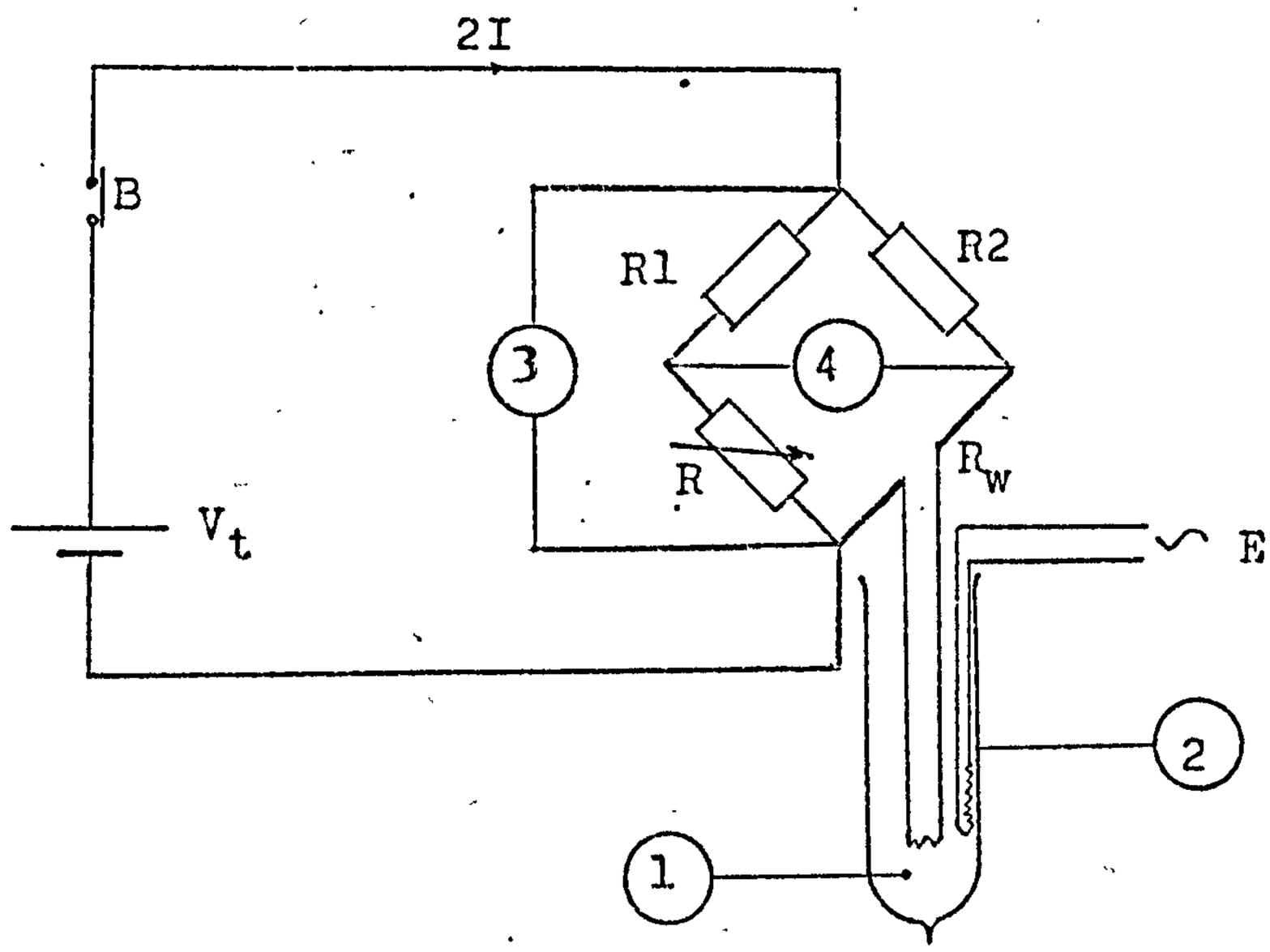

R1,R2 FIXED EQUAL RESISTANCES
R ADJUSTABLE RESISTANCE BOX
R_W Pt WIRE RESISTANCE
V_t VOLTAGE ACROSS THE BRIDGE
B SWITCH
E IMMERSION HEATER
1 ELECTRONIC THERMOMETER
2 CONDUCTIVITY CELL
3 DVM
4 STORAGE OSCILLOSCOPE

Figure 4.4 The equipment for thermal conductivity measurements

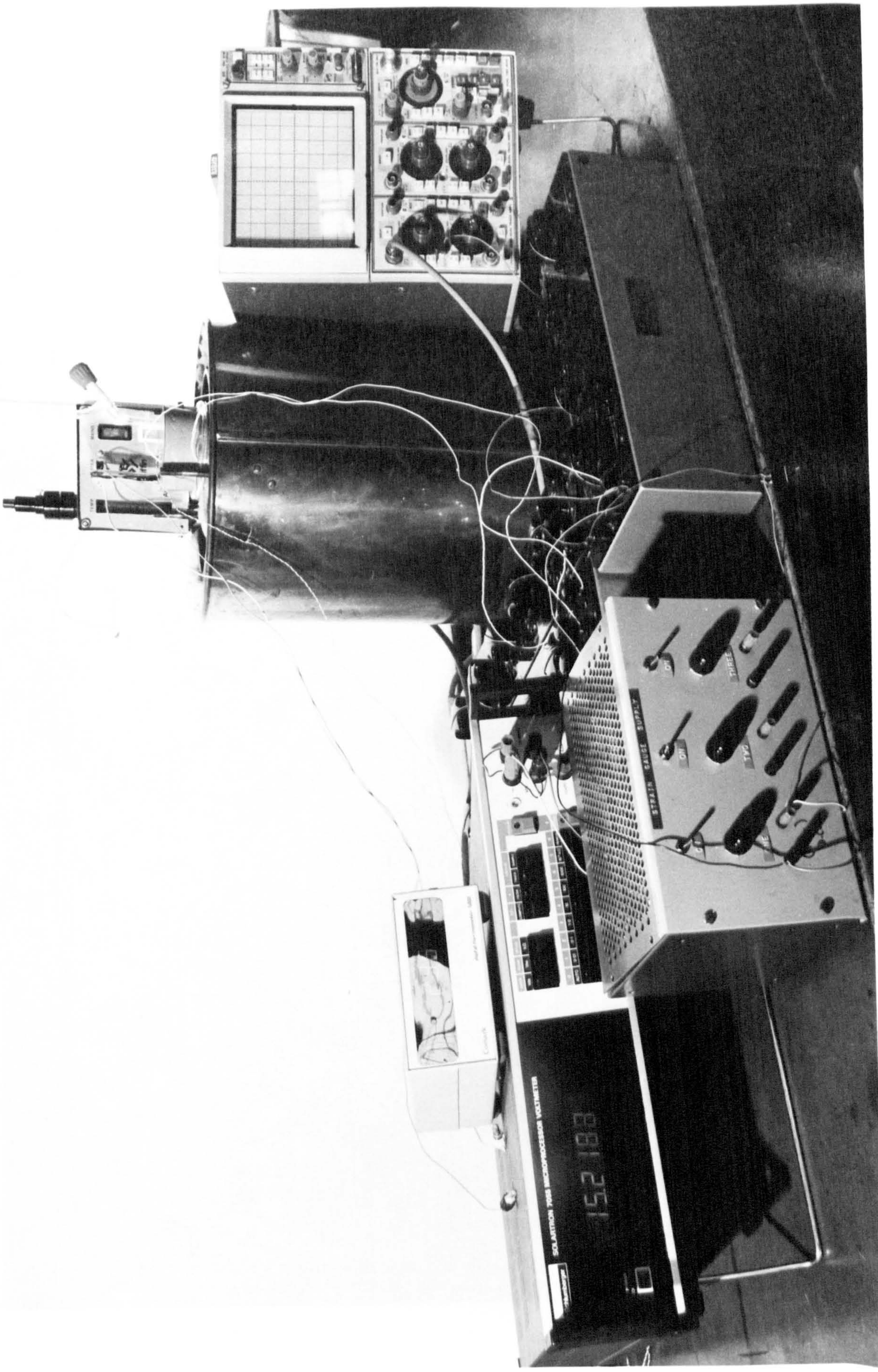
STRAIN GAUGE SUPPLY
ON
TWO
THREE
SOLARTRON 7081 MULTIMETER

PLATE 4.3

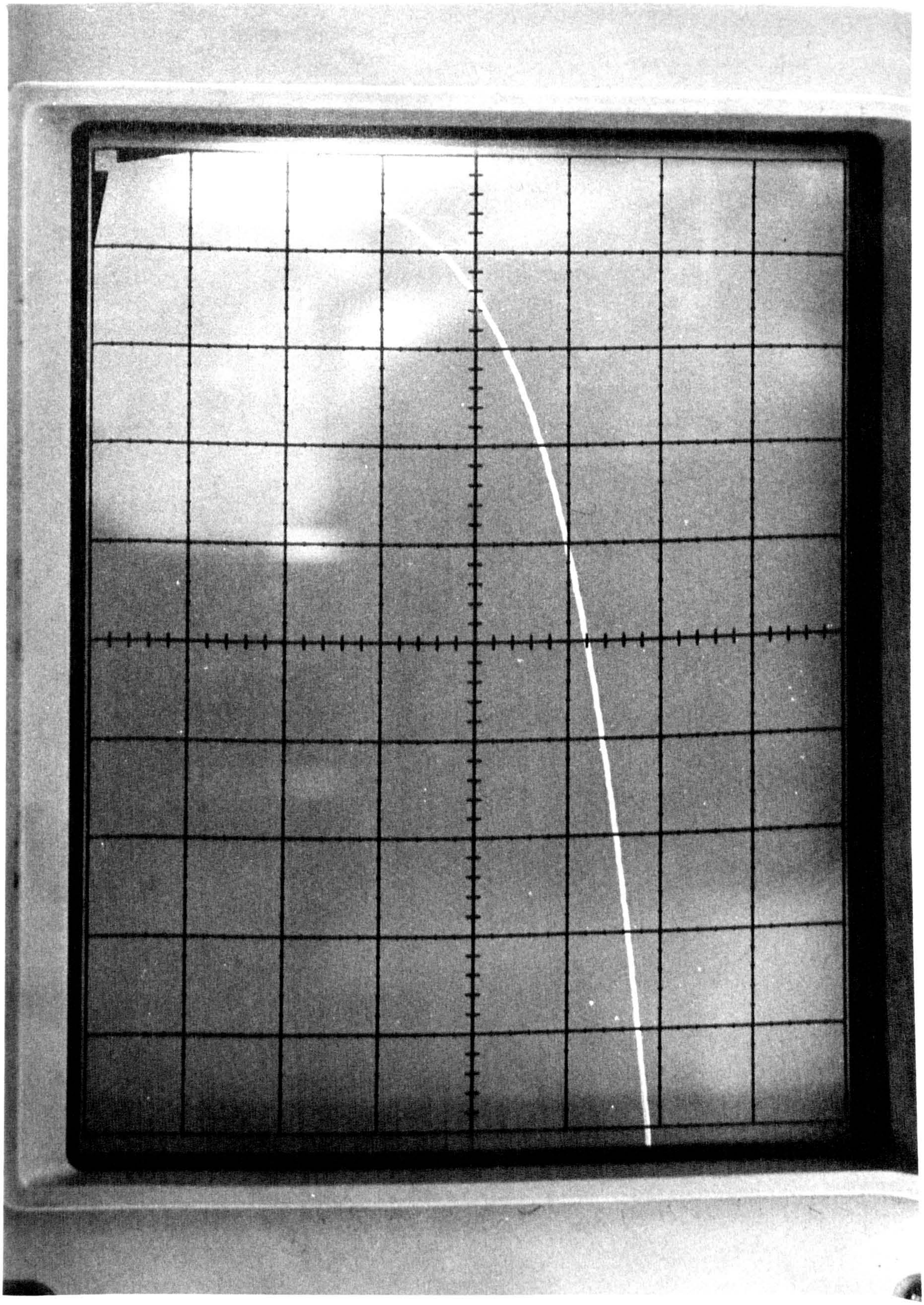

PLATE 4.4

where

R_o resistance at 0^oC

α temp coefficient

t wire temp ^oC

Assuming that at a time $\Delta\tau$, the change in wire temperature is Δt corresponding to a change of ΔR_W in the wire resistance,

then $\Delta R_W = R_o \alpha \Delta t$

and $$\frac{\Delta R_W}{R_W} = \frac{\alpha \Delta t}{1+\alpha t}$$

from which $$\Delta t = \frac{1+\alpha t}{\alpha} \frac{\Delta R_W}{R_W}$$

substituting in equation 4.6 gives

$$k = \frac{Q}{4\pi} \frac{\alpha}{1+\alpha t} \frac{\Delta \ln \tau}{\frac{\Delta R_W}{R_W}} \qquad (4.7)$$

From the circuit shown in Fig.4.4

$$I = \frac{V_t}{R_t} \qquad \text{where } R_t = R_1 + R = R_2 + R_W$$

but V_t is constant during the run

then $$\Delta I = \frac{-V_t \Delta R_t}{R_t^2}$$

and $$\frac{\Delta I}{I} = \frac{-\Delta R_t}{R_t}$$

but $\Delta R_t = \Delta R_W$ and $R_t = \frac{R_t}{R_W} : R_W$

so $$\frac{\Delta I}{I} = -\frac{\Delta R_W}{R_W} \cdot \frac{R_W}{R_t} \qquad (4.8)$$

the voltage across the wire is:

$$V_W = IR_W$$

$$\Delta V_w = I \Delta R_w + R_w \Delta I$$

So $$\frac{\Delta V_w}{V_w} = \frac{\Delta R_w}{R_w} + \frac{\Delta I}{I}$$

substituting from 4.8

then $$\frac{\Delta V_w}{V_w} = \frac{\Delta R_w}{R_w} - \frac{\Delta R_w}{R_w} \cdot \frac{R_w}{R_t}$$

$$= \frac{\Delta R_w}{R_w} (1 - \frac{R_w}{R_t})$$

rewriting it gives

$$\frac{\Delta R_w}{R_w} = \frac{\Delta V_w}{V_w} \cdot \frac{1}{1 - \frac{R_w}{R_t}}$$

substituting in 4.7 yields

$$k = \frac{\alpha}{1 + \alpha t} V_w (1 - \frac{R_w}{R_t}) \frac{Q}{4\pi} \frac{\Delta \ln \tau}{\Delta V_w} \qquad (4.9)$$

values of t, R_w, V_t, R_t and $\frac{\Delta \ln \tau}{\Delta V_w}$ were measured experimentally.

The temperature coefficient of the platinum wire, supplied by the manufacturer (Johnson, Matthey) was 0.0038 and was assumed constant over the temperature range employed.

Procedure

Because the flask was sealed in order to avoid the ingress of atmospheric moisture, it was first evacuated prior to charging with about 600 ml of the solution. The cell was then placed in the oil bath. The temperature was set up by controlling the oil bath temperature and heating the sample in the cell using the immersion heater to a temperature close to that of the bath. The cell was left for about one hour to get thermal equilibrium and temperature drift was recorded with time. A maximum drift of $1^{o}C$ per hour was accepted.

At the desired temperature, the bridge was initially balanced to within 0.1 Ω, using the oscilloscope. After an interval of 3 minutes, 5 runs were carried out with a time interval of about 2 minutes in between them. The set of readings thus occupied about 15 minutes.

The changes in the wire voltage at 0.1, 0.25 and 0.45 seconds into run were noted. A least square straight line was fitted to the results and from its slope the thermal conductivity was calculated knowing the values of R_w, V_t, R_t, and t obtained by seperate measurement.

4.1.4 Accuracy of Results

The thermal conductivity of 4 solutions of different concentration were measured over a temperature range of 17 - 123^{o}C. Solutions were prepared from BDH supplied methanol and salts of typical specifications mentioned in section 3.1. Samples were always sealed, to prevent the absorption of atmospheric moisture. The results are shown in table 4.1. A typical data sheet of readings and sample of calculations are given in Appendix (C).

The main sources of error were considered to be:

(a) The wire length, a millimeter scale was used to measure the wire, and a maximum error of not more than 0.5 mm was expected which would correspond to an error of less than 1%.

(b) The accuracy of the storage oscilloscope, the time base is accurate to within 3% and the readings were chosen to be on the graticule; hence no physical interpolation was necessary. The accuracy of the ordinate when using maximum sensitivity of 1 mV/div is 2%. The oscilloscope graticule was 0.2 mV per subdivision. An error of less than 0.05 mV would be expected when reading the change of the voltage across the platinum wire (V_w), which represents a 3% error in the slope $\Delta \ln \tau / \Delta V_w$. It is believed that the oscilloscope was the main source of error in the measurements.

(c) Temperature drift during the measurement.

A maximum temperature drift of 1^{o}C per hour was accepted. As

% MeOH	Temp. ^{o}C	k watt/m ^{o}C
25.3	17.1	0.188
	40.8	0.190
	69.7	0.190
	99.7	0.198
	123.3	0.192
31.0	27.3	0.194
	51.8	0.197
	84.8	0.197
	120.6	0.192
37.4	22.7	0.201
	51.2	0.199
	80.9	0.201
	111.3	0.195
45.1	30.0	0.202
	58.2	0.207
	84.5	0.200

Table 4.1

Thermal conductivity of
MeOH/LiBr-$ZnBr_2$ solutions

the run duration is 0.5 sec., this drift represents 1.4×10^{-4} ^{o}C in the wire temperature which is very small compared to $6^{o}C$ temperature rise due to heating. The maximum temperature drift during a complete reading was $0.25^{o}C$ representing only an error of 0.025% in the thermal conductivity.

(d) Initial unbalance in the bridge. It was possible to balance the bridge within 0.1 Ω, which represents 0.6% of the wire resistance.

(e) The effect of solution conductivity; Different adhesives were used to seal the end points of the platinum wire, (araldite, silver paint, Cylolos paints, nitric rubber and Silicone rubber), Silicone rubber proved the only successful method of sealing. The power dissipation along the wire due to the electric conductivity of the solutions was determined by measuring the wire resistance in air and in each sample. The DVM driven by 10 mV was used for that and it indicated that this effect could be neglected.

End corrections were not applied as it is believed that these were small as compared with the other errors.

To check the overall accuracy of the apparatus, the thermal conductivity of water was measured at room temperature and yielded an error of 1.2% when compared with the results of (Ref 65). The thermal conductivity of toluene, an ideal fluid for conductivity cells calibration, (Ref 63), was measured at three different temperatures. Results were compared with smoothed data of Ziebland (Ref 66) and the error was found to be a maximum of 3%.

The thermal conductivity of aqueous potassium iodide (of high electrical conductivity) was measured at two different concentrations, 20% and 40%. The results were compared with those given in Ref 67, when the error was found to be 0.2% to 1.5%.

The results and comparisons are given in Appendix (C).

All runs were repeated five times at each temperature. At room temperature the readings were rather more consistent than at higher temperatures. The maximum scatter from the mean value in all cases was around 3%.

4.2 Viscosity and Relative Density

It will be appreciated that one or more heat exchangers will be required in the absorption cycle to transfer heat to and from the absorbing solution. One heat exchanger is necessary to recover heat from solutions returning from the generator to the absorber and another must be used to extract heat from the solutions after the absorption process in an adiabatic absorber. Owing to the fact that these heat exchangers are of considerable capacity relative to the capacity of the heat pump cycle itself (Fig. 2.1 page 19) properties affecting the heat transfer process are very necessary. In this respect viscosity is one of the most important properties necessary for the system design.

Although Aker (Ref 28) pointed out that the combination 2LiBr-$ZnBr_2$ - methanol, of all other investigated combinations, has the lowest viscosity, no actual values were reported. The data published by Uemura (Ref 30) do not include the concentration range which may be employed in the proposed heat pump cycle. Accordingly, it was necessary to carry out viscosity measurements to confirm Uemura's results and extend the range of data to be useful in the heat pump design.

4.2.1. Equipment

The SETA viscometer 8354-phase I was used in the measurements of the viscosity of the solutions. The principle of the measurements (Fig.4.5) is the time necessary for a given quantity of fluid to flow through a capilliary tube under a given head. The viscometer consists mainly of a cylinderical - glass - oil bath in which up to six viscometer tubes are mounted semi-permanently. A stirrer/heater assembly is mounted on the top plate of the oil bath which temperature can be set up to within 0.03 ^{o}C. The temperature is sensed by means of immersed thermosistors and is possible to control within 0.01 ^{o}C over the range from ambiant to 110 ^{o}C.

1 VISCOMETER TUBE
2 UPPER TIMING MARK
3 LOWER TIMING MARK

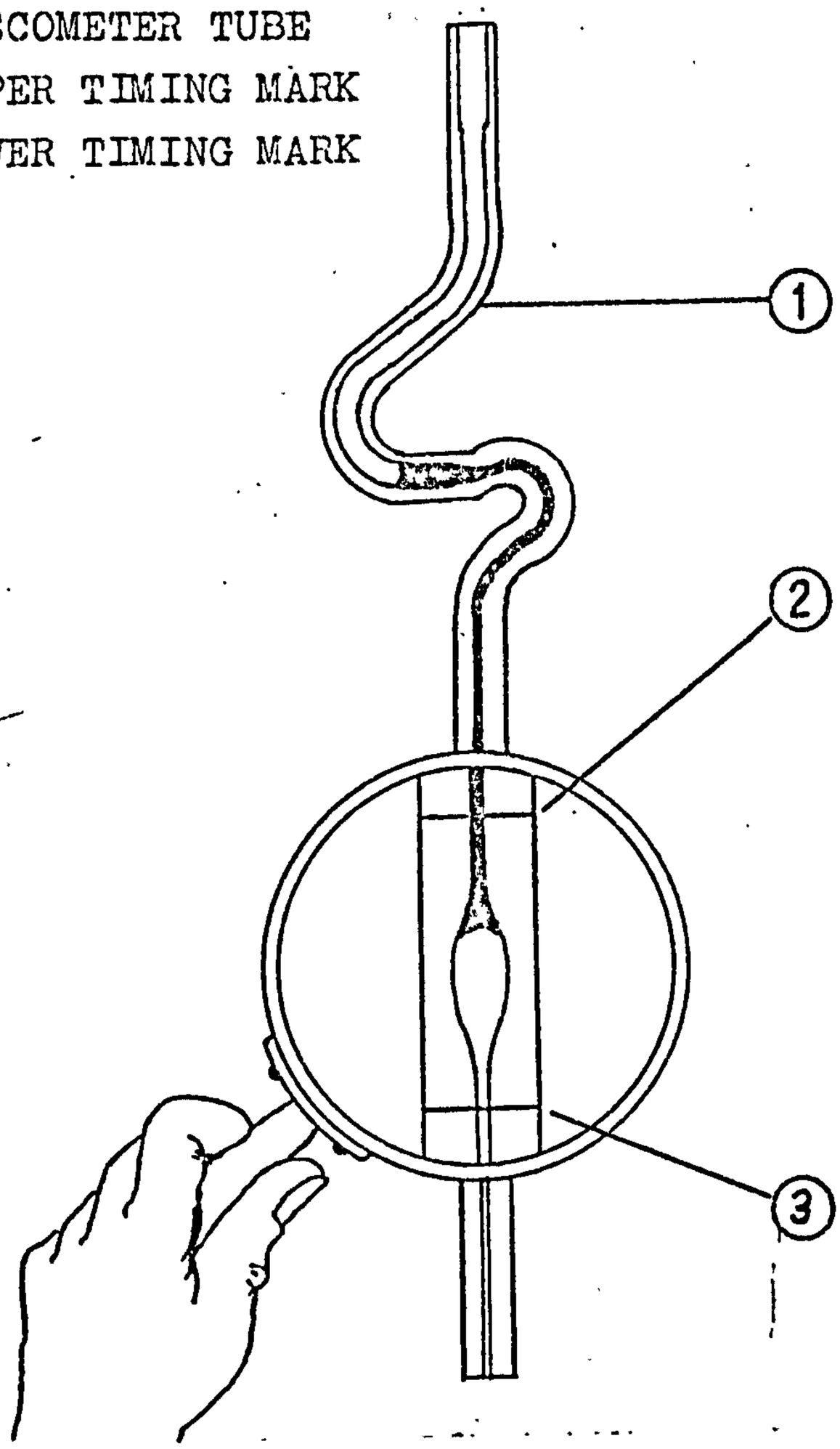

Figure 4.5 The viscometer tube

The bath temperature was measured by means of mercury in glass thermometer to within 0.1 ^{o}C. The compartment below the bath houses a glass manifold trap for the collection of discarded samples and cleaning fluids. The viscometer tubes are individually calibrated and constants are given for each and specified for certain range of viscosity. A vacuum pump is connected to the glass manifold trap to help in cleaning the tubes by sucking the residue of sample and cleaning fluid.

Time was measured to within 0.1 sec. by means of an electronic timer integrated in the apparatus.

4.2.2. Procedure of Measurements

Samples to be tested were prepared and kept under vacuum in flasks sealed with rubber stoppers. The apparatus was thoroughly cleaned (as prescribed by the Manufacturer) by passing toluene solvent through the tubes, followed by petroleum spirit of appropriate boiling range. The bath temperature was adjusted using the coarse and fine controls provided on the instrument, and tempeatures of 40, 55, 70, 85 and 100 $^{o}C \pm 0.1$ were employed. To save time a residual heater was used to boost the heating of the bath oil up to a temperature of 2 ^{o}C lower than required temperature. The viscometer tubes were selected to give a discharge time greater than 80 sec. to achieve a high precision of timing.

A sample of (0.2 to 0.25 ml) of the solution was withdrawn from the flask by means of a syringe and injected in the appropriate tube in a single operation. Pure methanol and distilled water were used to rinse the tube after every sample to prevent the effect of sample residual on the forcoming measurement, methanol was used at temperatures 40, 55 ^{o}C and wáter was used at the high temperatures. Measurements were repeated for each sample five times at one temperature and the arithmetic mean was taken to calculate the viscosity of the sample at that temperature.

4.2.3. Results

The results given by the viscometer represent the kinematic viscosity of the samples and relative density must be known at the same temperature in order to determine the dynamic viscosity. The density of the samples was measured in a clear Dewar flask by means of hydrometers and results are given in table 4.2. The results of the relative density were smoothed by the least square straight line.

$$\rho = 2.55 - 2.366\,x - 0.0068\,t \qquad (4.10)$$

where ρ is density gm/cc
x methanol fraction by weight kg/kg
t temperature ^{o}C

This correlation is applicable to within 1.5% over the temperature range from 20 to 100 ^{o}C and concentration from 25% to 50% methanol by weight. The experimental results of relative density of two of the tested samples (32.8 and 40.1%) were directly used to determine the dynamic viscosity. Smoothed data were employed to determine the viscosity of the third sample (27.3%).

Experimental results for the viscosity are given in table 4.3 and were correlated by means of the Guzman& Andrade equation (Ref 38).

$$\mu = A\, e^{B\left(\frac{10^3}{T}-2\right)} \qquad (4.11)$$

where $A = (2.516 - 5.722x + 3.304x^2)$

$B = (-.5424 + 22.3009x - 38.558x^2)$

μ is viscosity cp

x is methanol weight fraction

T is absolute temperature ^{o}K

% Concentration	Temperature ^{o}C	Density kg/m^3
25.3	44.5	1908
	50.0	1914
	61.0	1903
	72.0	1883
	80.0	1878
	95.0	1870
32.8	35	1718
	50	1705
	61.5	1687
	70.0	1678
	82.0	1661
	90.0	1654
40.1	31.0	1574
	43.0	1550
	52.0	1540
	67.0	1538
	75.0	1526
	80.0	1520
	86.0	1490
50.0	20.0	1348
	25.0	1344
	30.0	1342
	35.0	1339
	45.0	1330
	50.0	1328
	55.0	1314

TABLE 4.2

Relative density of MeOH/2LiBr-$ZnBr_2$ solutions

% Concentration	Temperature ^{o}C	Viscosity cp
27.3	40.0	30.5
	55.0	19.5
	70.0	13.9
	85.0	10.2
	100.0	7.6
32.8	40.0	22.3
	55.0	15.1
	70.0	10.5
	85.0	7.67
	100.0	5.78
40.1	40.0	11.2
	55.0	7.50
	70.0	5.36
	85.0	4.46
	100.0	3.55

TABLE 4.3

Viscosity of MeOH/2LiBr-$ZnBr_2$ solutions

The previous equation correlates the experimental data to within 3%.

The accuracy of the viscosity measurements depends on the accuracy of measurements of the time and temperature as well as the accuracy of the measured relative density. Relative density data obtained in this investigation were compared with the data published by Uemura (Ref 30). Difference fluctuated between 0.5% and 2%. Time was measured to within 0.1 sec. and with a human error of about 0.2 sec., this would account for less than 0.5% error. The accuracy of temperature measurement and fluctuation in this test accounted for a maximum error of less than 0.5%. Thus it is believed that the error expected in the viscosity measurement is less than 3%.

It was not possible to compare the results with Uemura's viscosity data as the concentration range he investigated was different. However, when Uemura's data were extrapolated to calculate the viscosity of a 40.1% methanol solution the results showed a difference of only 2% on average. Figure 4. shows the experimental results obtained in this work and those reported by Uemura.

4.3. Surface Tension

Surface tension is a manifestation of the forces of attraction that hold the molecules together in the liquid (or solid) state; thus, liquid droplets tend to become spheres - the form of least surface area - because of the mutual cohesion of the molecules. Conversely, work must be expended to increase the surface area of a liquid. The most important object in the design of absorbers for absorption heat pumps is to maximise the surface area in as small a volume as possible. For this reason a knowledge of the surface tension of liquid absorbent is important. The dependence of droplet size in liquid dispersion absorbers and the wetted area in packed column absorbers on the liquid surface tension will be shown in Chapter 6.

Practical methods for surface tension measurements were described in the book by Levitt (Ref 68). It can be determined

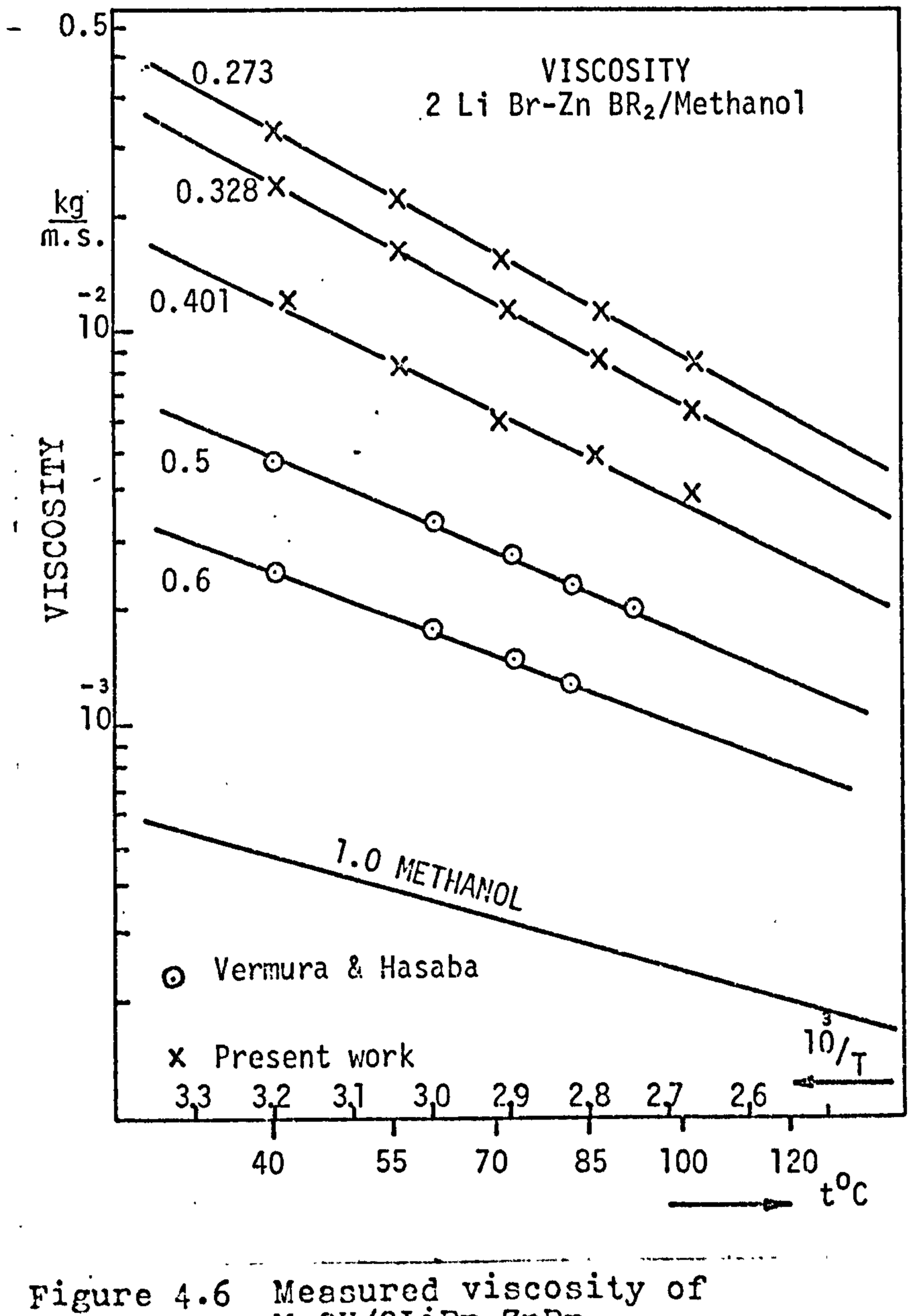

Figure 4.6 Measured viscosity of MeOH/2LiBr-$ZnBr_2$

quickly and with sufficient accuracy by measuring the force required to detach a horizontal ring of platinium wire (radius R) from the surface of the liquid. On the elementary theory, the force P should be given by twice the perimeter of the ring times the surface tension, i.e. $P = 4\pi R\sigma$, σ being the surface tension of the liquid. More precisely, the pull must be multiplied by a correction factor F which varies from 0.75 to 1.1, and depends on the dimensions of the ring.

The apparatus used in these measurements is du Nouy's torsion balance shown in Fig. 4.6. The balance consisted essentially of a horizontal taut wire which degree of torsion can be controlled by an adjustable screw (A) at one end and vernier torsion dial (B) at the other end. The tension in the wire can be controlled by means of an adjustable screw. A beam C, hooked at one end, is fixed rigidly to the wire and at right angles to it. The platform D suspended by the arm E carried the dish with the liquid sample. The height of the platform was adjusted with the effect of two adjustable screws F and G. The platinium wire was hung in beam C as shown in the figure. The balance was zeroed and then calibrated by measuring the surface tension of distilled water at room temperature (20 ^{o}C). Readings were repated five times and the mean, 0.0759 N/m, was compared with data at Ref 68, 0.0727 N/m, giving an apparatus constant of F = 0.96. Following that the surface tension of four concentrations (25.3%, 27.3%, 32.8% and 40.1%) was measured at 20 ^{o}C, the results of which are given in table 4.4. Surface tension of other concentrations at the same temperature may be interpolated and the dependence of surface tension on temperature for a wide range is accurately given by MacLeod relationship namely $\sigma = k\rho^4$ where k is a constant and ρ is the density at that temperature (Ref 68).

Although it was claimed in Ref 69 that results are repeatable within 1.0×10^{-3} N/m, it was found that the repeatability of this test is much better (0.5×10^{-3} N/m). The balance dial reads to within 0.5×10^{-3} N/m and visual interpolation to within 0.2×10^{-3} was possible.

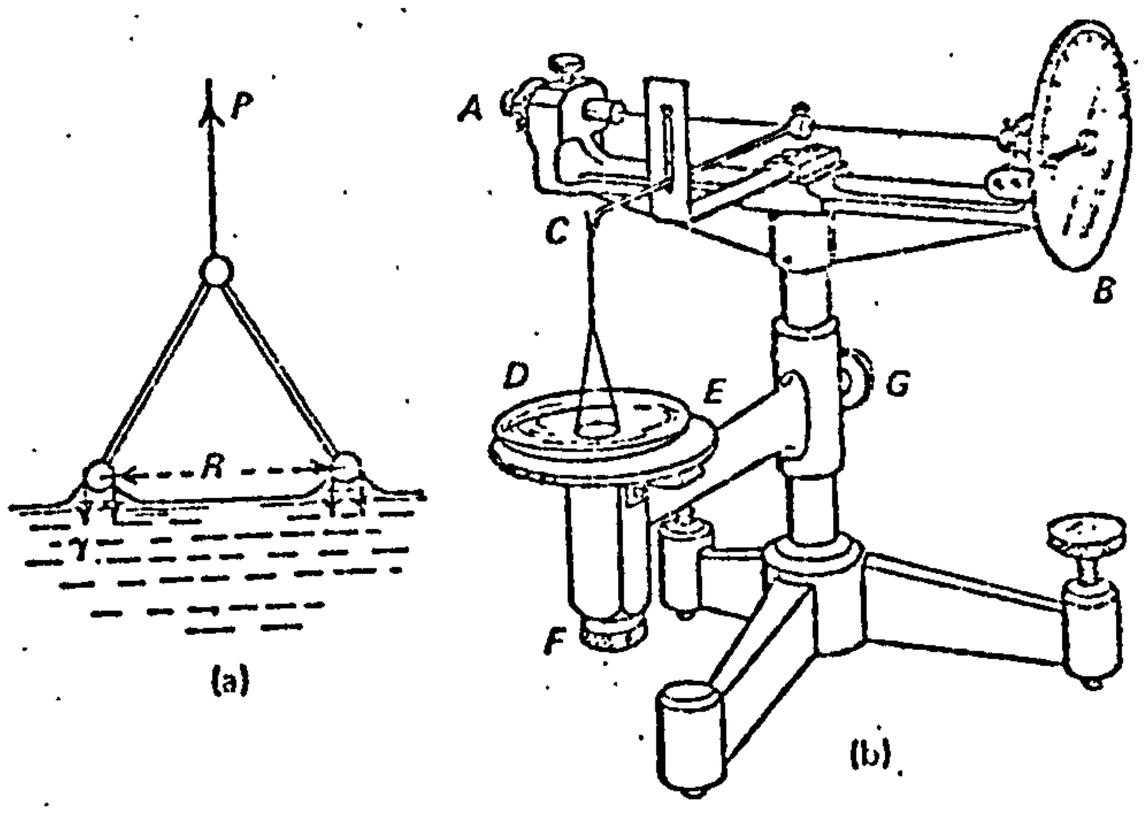

Figure 4.7 The torsion balance

Mass fraction of methanol	0.253	0.273	0.328	0.401
Surface tension N/m	0.0496	0.0491	0.0472	0.0461

Table 4.4.

Surface tension of solutions at 20 ^{o}C

CHAPTER 5

THE ABSORPTION PROCESS

Vapour absorption is an essential process in the operation of thermal heat pump and it is, technologically, perhaps the most "difficult" aspect of the cycle.

5.1 Fundamentals of diffusion and mass transfer

The absorption of a pure gas or vapour in a liquid is controlled by diffusion or convection within the liquid at the gas/liquid interface. The diffusion of solute molecules in a liquid occurs as a result of difference in the chemical potential of the solute in one part of a phase and another. Badger (Ref 70) states that "limited information as to actual values of the chemical potential, usually make it necessary to substitute other driving forces more or less related to the chemical potential". The partial pressure of the solute or its concentration have been used in literature to express the effective drive to the process. In fact there is no fundamental reason why the diffusion process should not be related to any physical property which has appropriate dependence on the percentage of constituents in the solution. Danckwerts (Ref 71) pointed out that, although it is common to speak of driving forces causing the diffusion of molecules in a liquid, these molecules experience no force acting specifically in the direction of a concentration gradient, but rather it is the random thermal motion of the molecules that cause a bulk transport down the concentration gradient.

Although there is no physical driving force in the diffusion process, Jeans (Ref 72) showed, statistically, that it takes place in a manner described by a rate equation. Consequently, the rate of mass transfer is given by the equation:

$$R = - Da\frac{\partial X}{\partial S} \qquad (5.1)$$

where R is rate of transport of solute

X is the appropriate potential form to which diffusion process is related

S is distance

D is mass diffusivity

a interfacial area

The most convenient form of potential is the concentration which will be used in this text.

Equation 5.1 is written for diffusion in one direction only (S). It is strictly applicable, under conditions where effects of convective transport due to density changes are negligible, and where other possible modes of mass transfer are not operative.

For a pure gas or vapour undergoing absorption in quiescent liquid, the surface concentration will at all times correspond to the saturation or (equilibrium) value X*, and the concentration at a long distance below the surface will be the bulk concentration X and will remain unchanged. These two boundary conditions are used to solve the basic diffusion equation in the S direction,

$$D \frac{\partial^2 X}{\partial S^2} = \frac{\partial X}{\partial \tau} \qquad (5.2)$$

for X as function of τ, S. Therefore the rate of gas absorption through the interface at any time τ will be given by:

$$R = -Da\left(\frac{\partial X}{\partial S}\right)_{S=0} \qquad (5.3)$$

In systems where the bulk of the liquid is agitated so that its concentration is uniform at a distance $s = \delta$ from the surface, and if the quantity of absorbed gas is too small to affect the bulk concentration, then the rate of absorption R is controlled by diffusion in the surface film of interface which is supposed to

be quiescent and is given by

$$R = -Da \frac{x^* - x}{\delta} \qquad (5.4)$$

where $\frac{x^* - x}{\delta}$ is concentration gradient.

Thus the absorption process may be regarded as a three stage process:

1. the diffusion of the gas into the liquid surface, a process which has no significant resistance in case of pure gases.

2. the flow of the gas caused by diffusion through a boundary layer close to the surface of interface.

3. the flow of the gas into the bulk of the fluid either by further diffusion in the case of quiescent liquids or by convective motion in agitated liquids.

The whole process may be combined in an equivalent diffusivity or a "film coefficient", and equation 5.4 can be written in a more general form

$$R = k_l a (x^* - x) \qquad (5.5)$$

R is absorption rate

k_l is film coefficient

x^* is equilibrium concentration

x is bulk concentration

Perhaps, it would be useful to mention here that the definition of k_l in equation 5.4 depends on the definition of x. In most cases x is given in kg of solution per cubic meter of solution, when k_l has the dimensions m/sec. In thermally driven heat pumps, it is convenient to use the concentration of refrigerant or absorbent as a weight % ratio to define the quality of the solution. For this reason, x will be expressed in kg of methanol per 100 kg of solution, k_l will then be given in $kg/m^2\%$ sec.

5.2 Experimental determination of film coefficient

Mass transfer coefficients in gas-liquid systems can be determined experimentally, without involving the kinetics of the diffusion process. Various methods and laboratory models have been described in Ref. 71 Chapter 4, 5 and 7 as well as in Ref 72 Chapter 8. However few formulae are available to predict the diffusivity of the system with reasonable accuracy (e.g. 10-20%, Ref 73). This is referred to in Section 6.5. These diffusion coefficients may be used to predict mass transfer coefficients in different types of absorber.

Although the diffusion coefficient of the system under investigation was predicted in Chapter 6, it was not measured. Instead, the mass transfer coefficient in packed column absorber was determined experimentally following the procedure described in Ref 71 (Page 212). The rate of absorption of methanol in its solutions with 2LiBr-$ZnBr_2$ was measured in an apparatus of known interfacial area. The results were employed in the design of an experimental absorber, the performance of which was subsequently determined.

5.2.1 Apparatus

An apparatus based on the stirred cell model introduced by Danckwert & Gillham (Ref 75), was used to determine the film coefficient in the interface of the system. They mentioned that the disadvantage of the model was the sensitivity of the results to the immersion depth of the stirrer blades that agitated the surface of the liquid. The best results were obtained when the stirrer blades were adjusted precisely just to cut the liquid surface. To overcome this difficulty, it was decided to use a floating stirrer, with an additional submerged one to ensure a uniform concentration throughout the bulk of the liquid.

The apparatus shown in Fig. 5.1 was constructed from a 125 ml. gas-wash bottle as the solution cell and a volumetrically graduated glass vessel containing liquid methanol connected by means of a glass stopcock. Both vessels were placed in thermostatically controlled water baths accurate to within $1^{o}C$ and constant to $0.1^{o}C$. The stirrers consisted of a rectangular rod magnet at the bottom and a PTFE tube

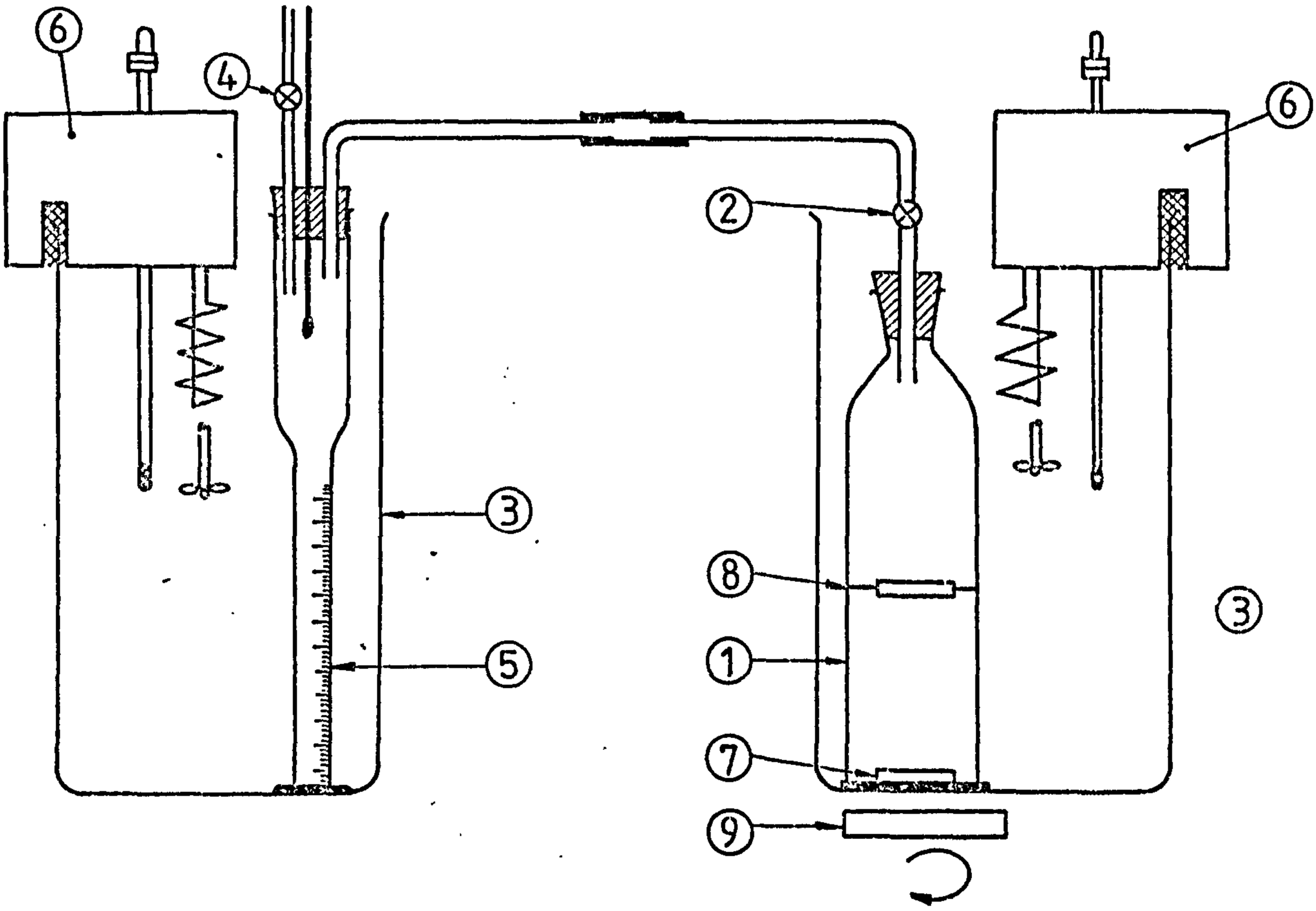

1. SOLUTION CELL
2. VAPOUR CONTROL VALVE
3. WATER BATHS
4. VACUUM VALVE
5. THE METHANOL CELL
6. THERMOSTIRRERS
7. LOWER MAGNETIC STIRRER
8. FLOATING STIRRER
9. ROTATING MAGNETIC FIELD

Figure 5.1 Equipment for the measurement of the mass transfer coefficient

floating on the liquid surface. The drive for the stirrers was provided by a rotating magnetic field under the cell. Coupling of the two stirrers was by means of a thin steel strip of 10 mm wedth fixed in the rod magnet and passing through a slot in the PTFE tube. In this way the floating stirrer was free to move vertically to adopt to the liquid level. The lower stirrer was covered with few layers of PTFE tape to minimise friction with the bottle. The speed of rotation was measured by means of a stroboscope. The temperature of methanol was measured using a mercury in glass thermometer which could be read to 0.1^{o}C.

5.2.2 Procedure

1. The cell was thoroughly cleaned and dried, then evacuated through valve (2). With the two stirrers inside, the cell was weighed to 0.01 gm. While still under vacuum, about 150 gm of the solution sample was fed into the cell.

2. Vessel (5) containing pure liquid methanol was connected to the cell through a rubber hose and with valve (2) closed, was evacuated via valve (4). Methanol was allowed to boil for short time in order to ensure that no air remained.

3. The system was placed in the constant temperature baths and allowed to equilibrate for 30 minutes with the stirrers operating.

4. Valve (2) was opened and the time needed for the transfer of about 2 ml of liquid methanol was recorded (at low stirring rates, 1ml was sufficient).

5. At the end of the run, valve 2 was closed, the cell disconnected, dried thoroughly, and re-weighed.

6. The effect of surface agitation was determined by measuring the rate of absorption at various stirrer speeds while the other were held constant.

7. For each particular concentration difference the experiment was carried out at different stirring speeds with fresh sample every time.

5.2.3 Results

The rate of absorption of pure methanol was measured for six different values of concentration potential. Solution samples of two different concentrations, 40.1% and 29.5%, were used in these experiments. The methanol temperature was kept at about 30°C to reduce heat losses from the vapour along the connecting tube, and the temperature of the solution was varied to obtain different equilibrium concentration for each test.

In studying the effect of agitation rate, it was found that the rate of absorption increased rapidly as stirrer speed was increased upto 4-5 rps. At higher stirrer speeds 5-7 rps. the absorption rate increased more slowly until a certain speed was reached when vortex formation occurred and later splashing of the liquid took place. As a result of the increased and (unknown) liquid area the absorption rate increased rapidly, but the results in this regime were of no significance. Typical results are shown in Fig. 5.2. These results were clearly repeated in tests 1 - 4 (figures 5.3 to 5.6), so that it was not necessary to repeat in tests 5 and 6 (Fig. 5.7, 5.8). Readings corresponding to the highest stirrer speed, before splashing occurred, typically 5 - 6 rev/sec, were selected to represent the rate of absorption in the apparatus.

To calculate equilibrium concentrations higher than 50%, the smoothed data from Ref [29] shown in table 5.1 were employed, otherwise the data in section 3.1 are used. The actual concentration in the cell (X) was calculated as:

$$X = \frac{X_i + X_f}{2}$$

where X_i initial bulk concentration

X_f final bulk concentration.

X_f was calculated knowing the quantity of absorbed methanol observed during the reading within a test. Readings of different tests are shown in tables 5.2 to 5.7 and the selected readings are given in Table 5.8.

Temperature ^{o}C	% MeOH	Pressure mm Hg
20	60	39.88
	70	65.69
	80	79.09
	90	89.69
30	60	67.73
	70	110.1
	80	135.9
	90	151.08
40	60	110.6
	70	177.65
	80	214.8
	90	244.95
50	60	174.4
	70	277.0
	80	335.85
	90	383.6
60	60	266.3
	70	418.9
	80	508.9
	90	582.7
70	60	395.55
	70	616.2
	80	750.2
	90	860.3

Table 5.1

Vapour pressure of MeOH/2LiBr-$ZnBr_2$(Ref.29)

Test No 1

Methanol temperature 34.8 ^{o}C

Solution temperature 60.0 ^{o}C

Initial solution concentration χ = 40.3 %

Equilibrium concentration χ^* = 44.3 %

Reading No	Stirrer speed rps	absorbed Meth roughly ml	Time min sec	Weight of cell + solution before test	Weight of cell + solution after test	Absorbed Meth gms	10^3 R gm/sec
1	2	0.8	15 22	424.19	424.86	0.67	0.727
2	3	0.9	5 10	423.92	424.64	0.72	2.32
3	4	0.9	4 42	423.15	423.90	0.75	2.66
4	5	0.9	4 48	425.54	426.54	0.81	2.81
5	7	1.8	5 41	422.72	424.17	1.45	4.25

Table 5.2

Experimental data of Test No.1 of the stirred cell

Test No 2

Methanol temperature 30.0 °C

Solution temperature 34.9 °C

Initial solution concentration χ = 40.7 %

Equilibrium solution concentration χ^* = 60.3 %

Reading No	Stirrer speed rps	absorbed Meth roughly ml	Time min sec	Weight of cell + solution before test	Weight of cell + solution after test	Absorbed Meth gms	10^3 R gm/sec
1	3	0.7	1 -	419.95	420.51	0.56	9.3
2	4	1.8	1 36	422.78	423.22	1.44	15.0
3	5	2.4	2 -	424.11	425.99	1.88	15.7
4	6	2.4	2 0	424.50	426.37	1.87	15.6
5	7	2.1	1 22	422.63	424.25	1.62	19.76

Table 5.3

Experimental data of Test No.2 of the stirred cell

Test No 3

Methanol temperature 30.0 ^{o}C

Solution temperature 40.4 ^{o}C

Initial solution concentration χ = 40.4 %

Equilibrium concentration χ^* = 50.9 %

Reading No	Stirrer speed rps	absorbed Meth roughly ml	Time min	Time sec	Weight of cell + solution before test	Weight of cell + solution after test	Absorbed Meth gms	10^3 R gm/sec
1	2	0.8	1	16	421.52	422.17	0.65	8.56
2	3	1.2	1	32	423.32	424.28	0.96	10.4
3	4	2.3	2	58	424.44	426.35	1.91	10.7
4	5	2.0	2	33	425.51	427.15	1.64	10.72
5	7.2	2.2	1	15	424.80	426.58	1.78	23.73

Table 5.4

Experimental data of Test No.3 of the stirred cell

Test No 4

Methanol temperature 30.0 °C

Solution temperature 30.0 °C

Initial solution concentration χ = 40.7 %

Equilibrium solution concentration χ^* = 74.2 %

Reading No	Stirrer speed rps	absorbed Meth roughly ml	Time min	Time sec	Weight of cell + solution before test	Weight of cell + solution after test	Absorbed Meth gms	10^3 R gm/sec
1	4	1.7	2	0	422.25	423.63	1.38	11.5
2	5	2.3	1	31	425.33	427.21	1.88	20.7
3	6.1	1.6	1	7	425.47	426.82	1.35	20.1
4	7.2	1.8	1	10	424.21	425.64	1.43	20.4
5	8.5	1.9	–	50	423.50	424.96	1.46	29.2

Table 5.5

Experimental data of Test No.4 of the stirred cell

Test No 5

Methanol temperature 30.1 ^{o}C

Solution temperature 41.7 ^{o}C

Initial solution concentration χ = 30.0 %

Equilibrium concentration χ^* = 49.5 %

Reading No	Stirrer speed rps	absorbed Meth roughly ml	Time min	Time sec	Weight of cell + solution before test	Weight of cell + solution after test	Absorbed Meth gms	10^3 R gm/sec
1	1.6	1.7	7	1	424.32	425.69	1.37	3.25
2	4	1.6	1	58	425.22	426.37	1.25	10.6
3	6	1.7	2	-	424.81	426.14	1.33	11.1

Table 5.6

Experimental data of Test No.5 of the stirred cell

Test No 6

Methanol temperature 30.2 ^{o}C

Solution temperature 58.4 ^{o}C

Initial concentration χ = 30.1 %

Equilibrium concentration χ^{*} = 43.5 %

Reading No	Stirrer speed rps	absorbed Meth roughly ml	Time min	Time sec	Weight of cell + solution before test	Weight of cell + solution after test	Absorbed Meth gms	10^{3} R gm/sec
1	1	0.6	4	2	427.53	428.04	0.51	2.1
2	3.8	1.0	1	32	424.40	425.22	0.82	8.9
3	5	2.4	3	32	424.62	426.50	1.88	8.9

Table 5.7

Experimental data of Test No.6 of the stirred cell

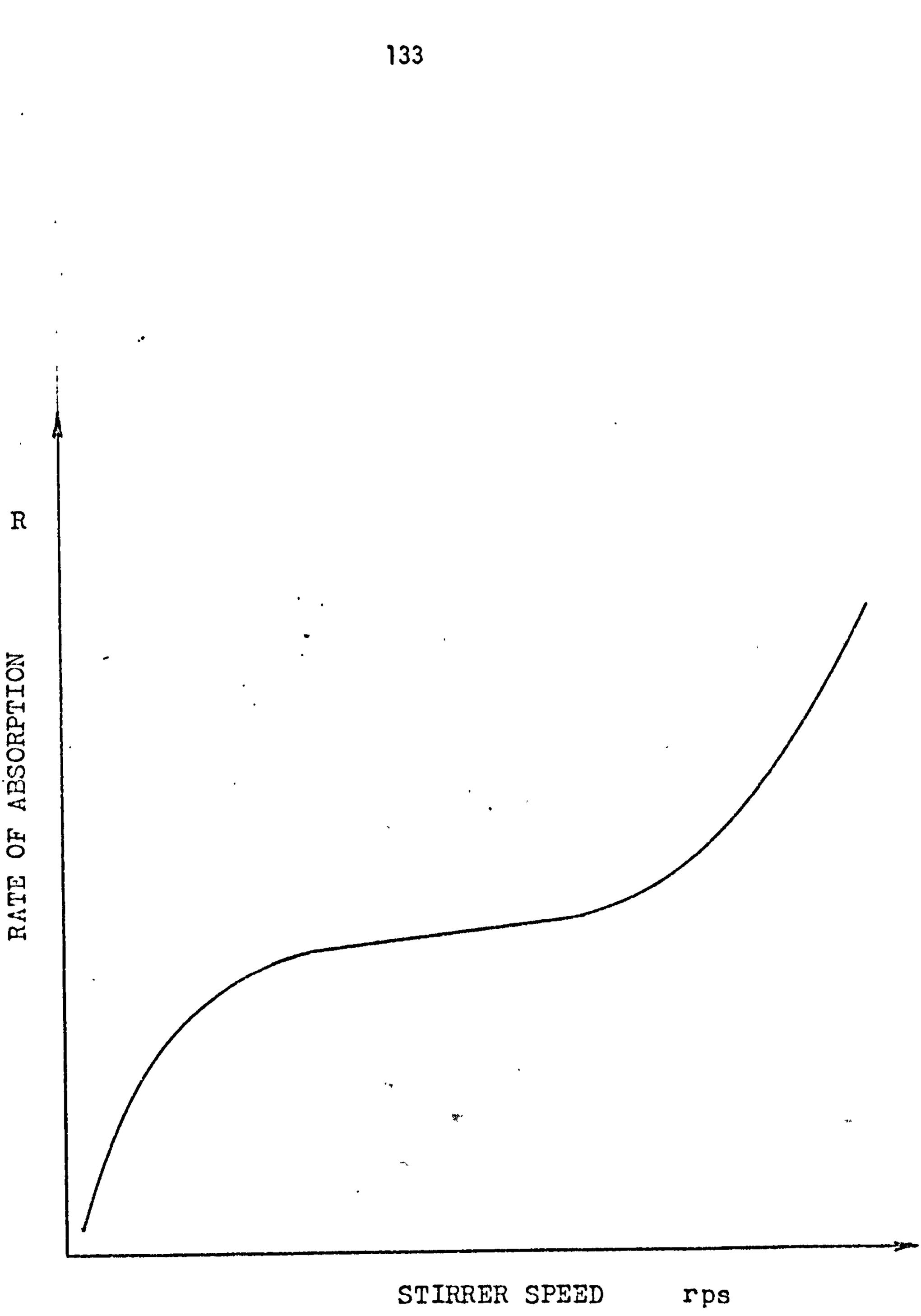

Figure 5.2 Typical performance of the stirred cell absorption model

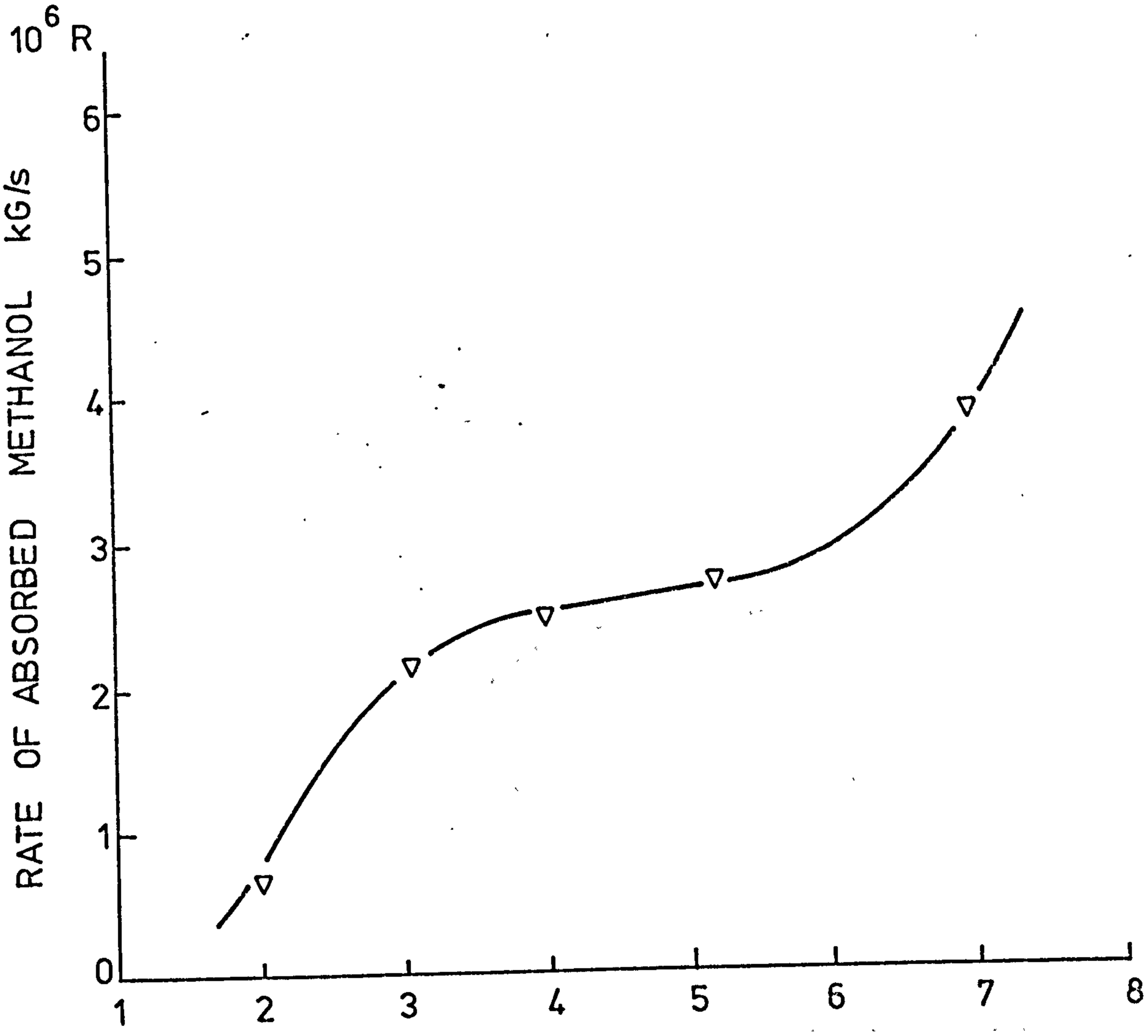

Figure 5.3 Rate of absorption in reation to agitation rate in test No.1

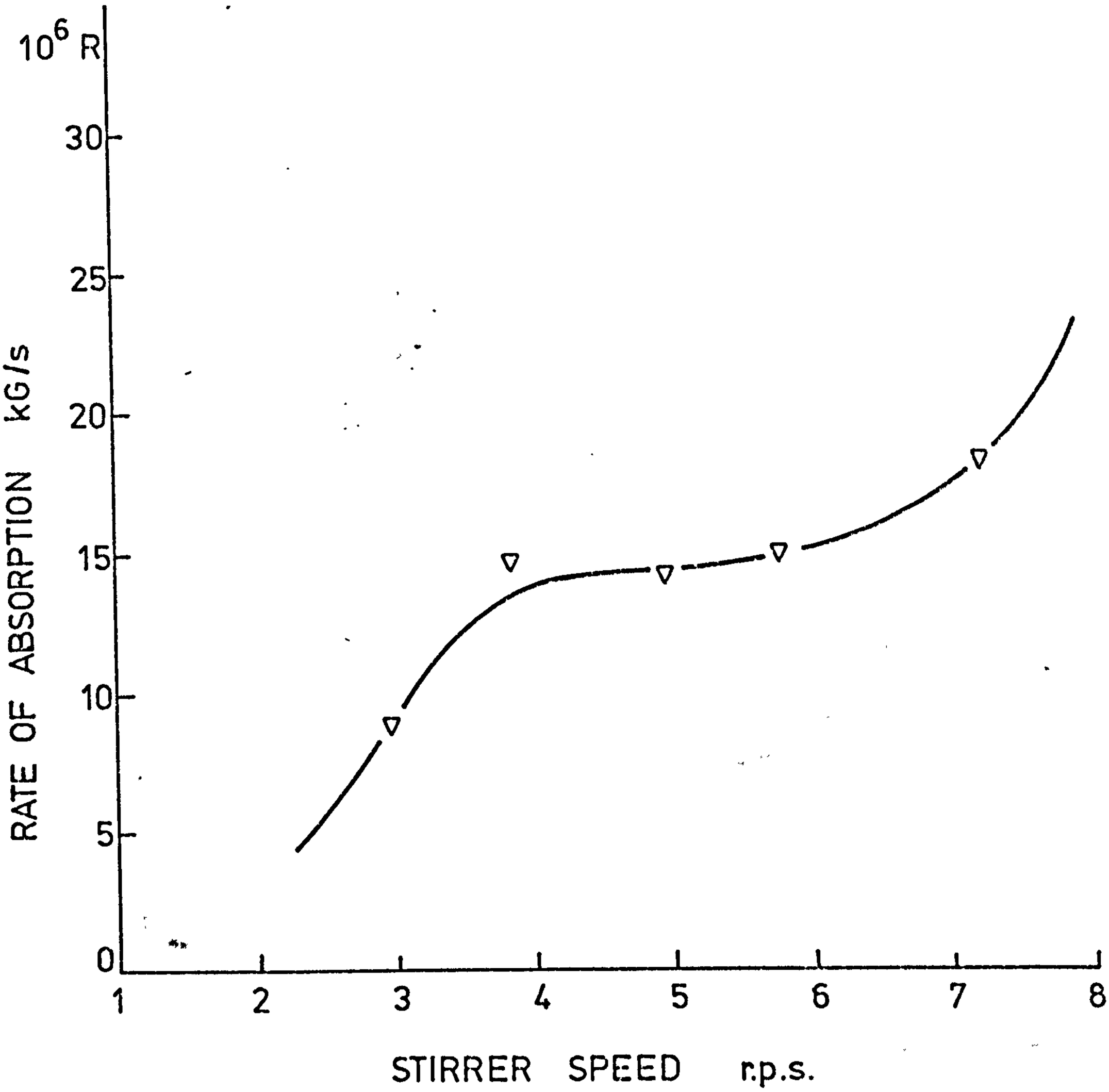

Figure 5.4 Rate of absorption in relation to agitation rate in test No. 2

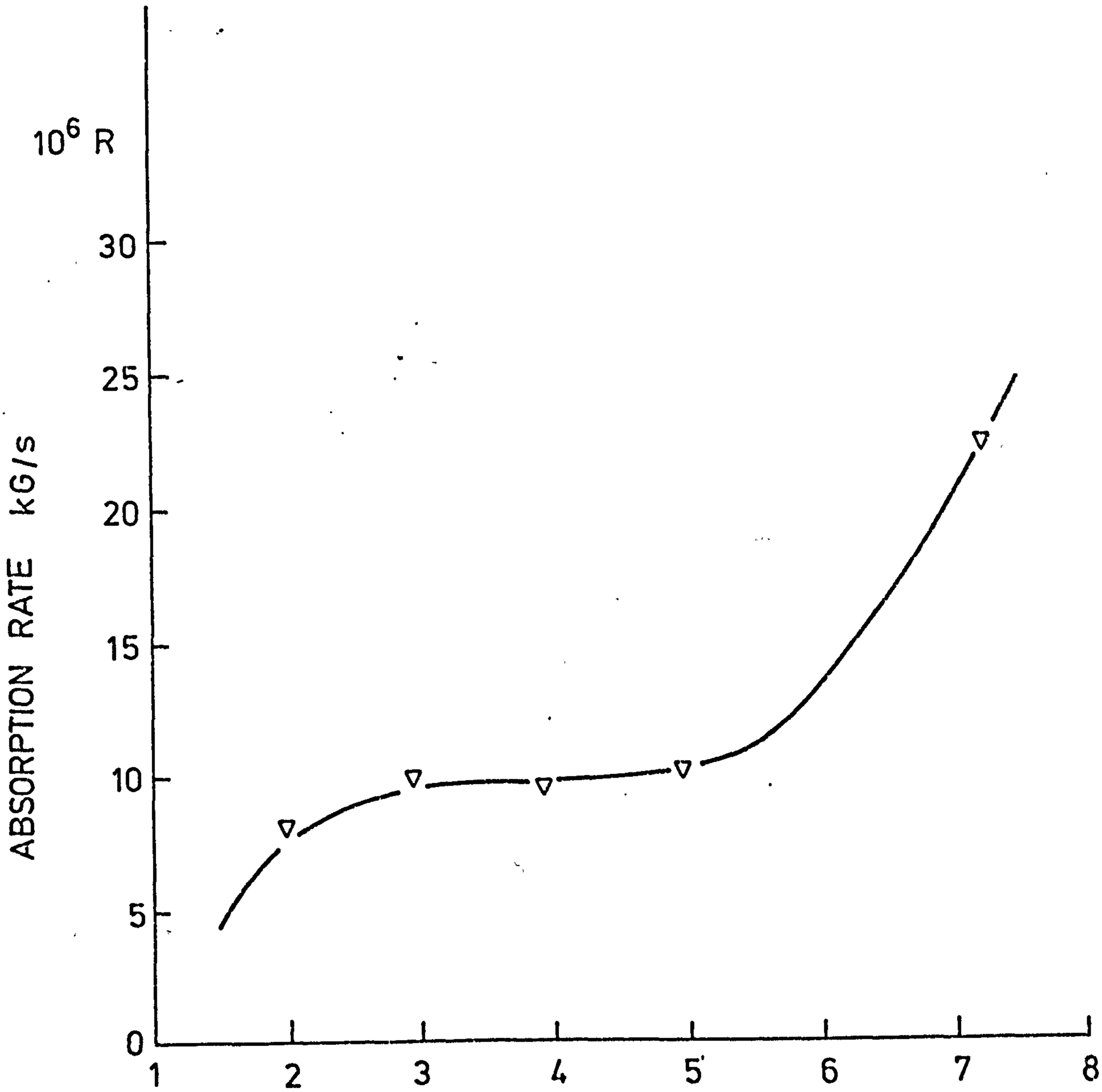

Figure 5.5 Rate of absorption in relation to agitation rate in test No. 3

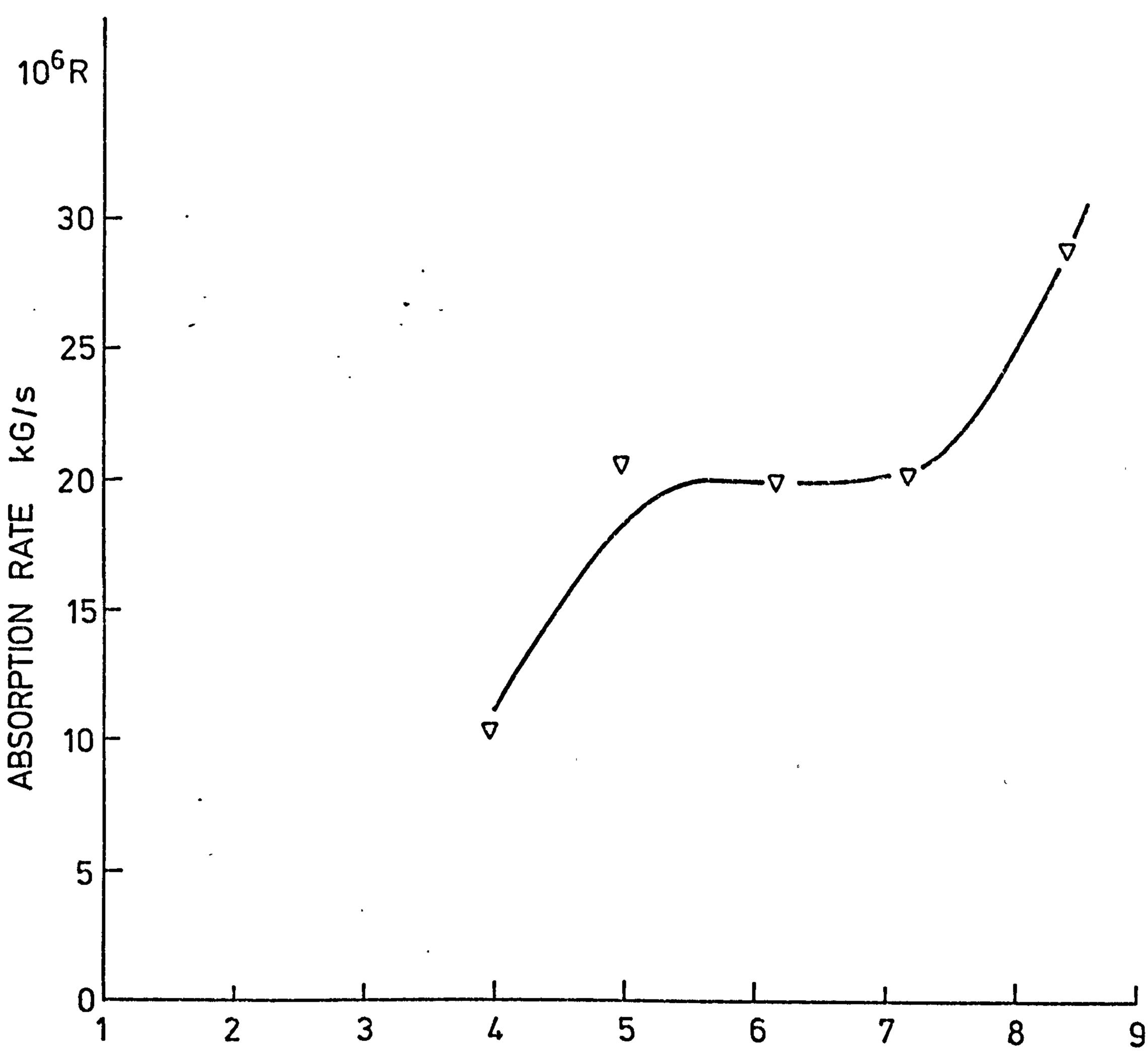

Figure 5.6 Rate of absorption in relation to agitation rate in test No. 4

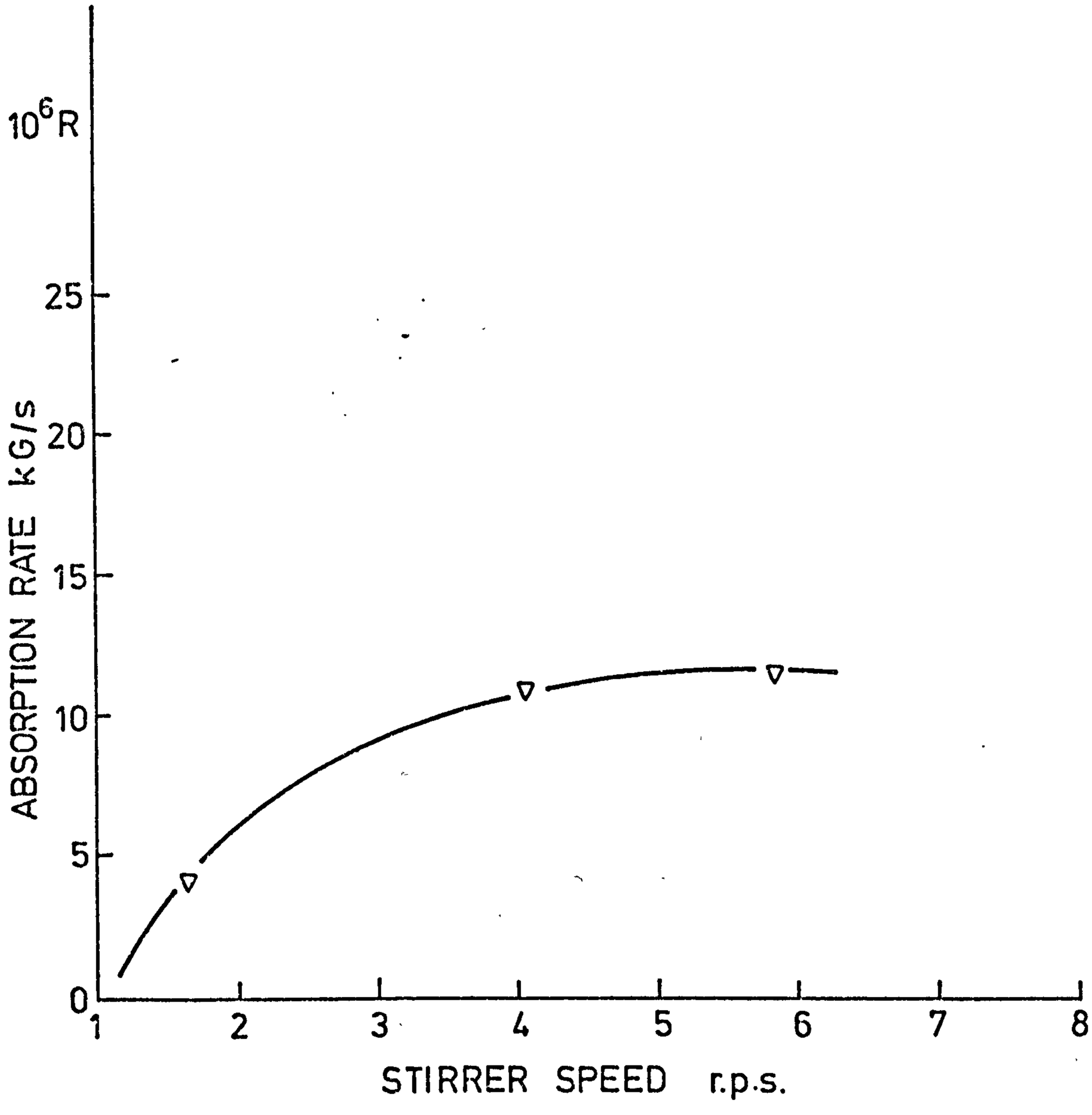

Figure 5.7 Rate of absorption in relation to agitation rate in test No. 5

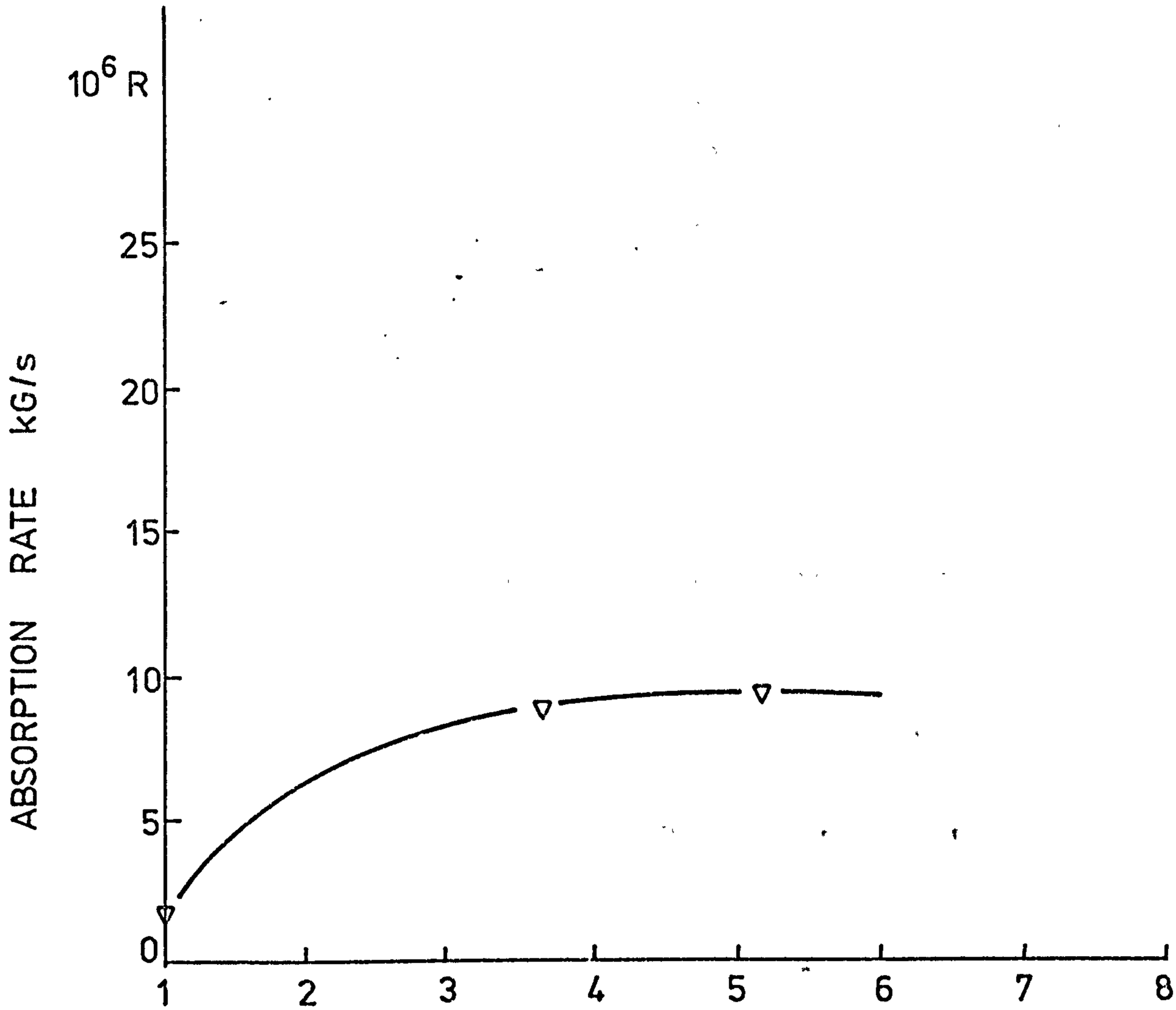

Figure 5.8 Rate of absorption in relation to agitation rate in test No. 6

Test No	Reading No	ss rps	10^6 R kg/sec	X*	X	X* - X
1	4	5	2.81	44.3	40.3	4
2	4	6	15.6	60.3	40.7	19.6
3	4	5	10.72	50.9	40.4	10.5
4	3	6.1	20.1	74.2	40.7	33.5
5	3	6	11.1	49.5	30.0	19.5
6	3	5	8.9	43.5	30.1	13.4

Table 5.8 Selected reading of absorption in the stirred cell.

The rate of absorption kg/sec versus concentration potential $(X^* - X) = \Delta X$ is shown in Fig. 5.9. A least square straight line was determined as given by

$$10^6 \quad R = 1.212 + 0.611 \quad \Delta X \qquad \text{kg/sec.}$$

The slope of which represents the value of $k_1 a$ $(0.611\ 10^{-6}$ kg%sec). The area of interface is equal to the cross-sectional area of the bottle less that of the floating stirrer, i.e. 16.3 cm^2, whence

$$k_1 = \frac{0.611}{0.00163} \quad 10^{-6} \quad = 3.74 \quad 10^{-4} \quad kg/m^2\%sec.$$

5.2.4 Accuracy of measurements

The sources of error were divided into two groups:

(a) errors affecting the rate of absorption (weight and time)

(b) errors affecting the concentrations (temperature and pressure).

When measuring the rate of absorption of methanol, a sensitive balance weighting to 0.01 gm was used. The minimum absorbed quantity of methanol was 0.81 in test (1) consequently an error of not more than 1.2% may be expected. A stop watch of negligible error was used, however, an error of 1 second was assumed due to delay in closing valve (2), Fig. 5.1. This error represents only a maximum value of 1%. The error in absorption rate determination is believed to be less than 2%.

The main uncertainty in the film coefficient measurements lies in the determination of concentration difference (ΔX). This parameter is affected by the pressure drop in the vapour flow of methanol, the temperature difference between the solution sample and its water bath, accuracy of vapour pressure correlations, error in temperature measurements and concentration change during the charge of the sample and during the test.

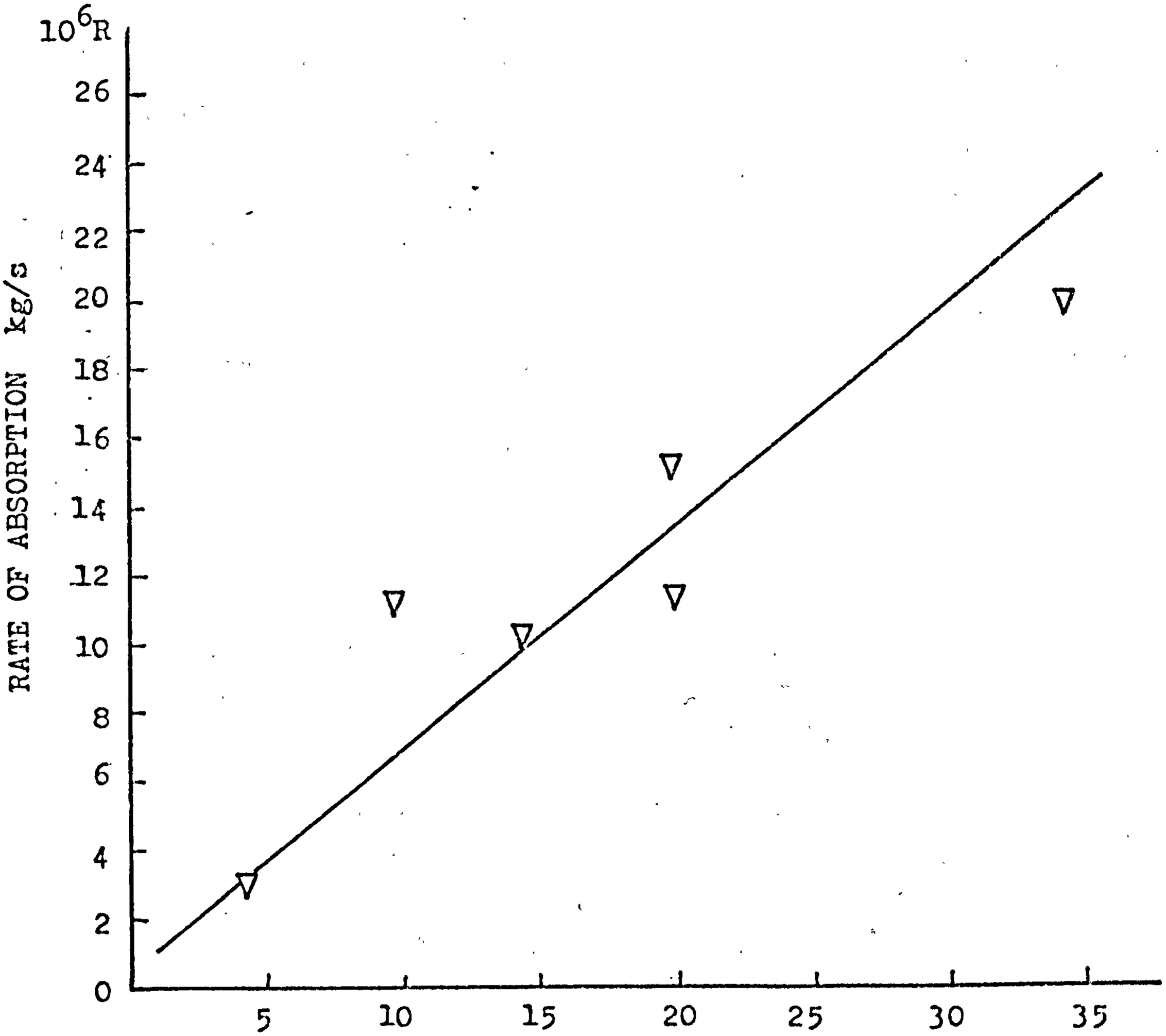

Figure 5.9 Rate of absorption relative to conc^{n} diff. in the stirred cell

The pressure of saturated methanol corresponding to its temperature was determined from the equation $\log P = 7.87863 - \frac{1473.11}{t + 230}$ where t is temperature (Ref 76), with an average error of 3%. The error in Umura's smoothed data (table 5.1) used to calculate X* is average 0.65%, and the total error in pressure calculation is 3.7%. However, when calculating concentration from this equation this error gives only 0.5% absolute error in the concentration range (50 - 75)% methanol by weight. Such error represents an average of 2.5% in concentration difference in tests 2, 3 and 4.

Equilibrium concentrations in tests 1, 5, 6 are determined from diagram in Fig.3.11 page 76 with typical error of 0.5% which represents an average inaccuracy of 4.2% relative to concentration difference in these tests. Error in temperature measurements is of negligible effect.

Concentration change: On average a 150 gm of sample was used, with 1.9 gm being the maximum quantity of methanol absorbed during a test. The concentration change is typically 1% and the average working concentration was calculated as shown above. The maximum error as a result of this occurs in test (1), but is less than 2.5%.

The concentration change due to evaporation of methanol following the charge of the sample in the cell was calculated and found to be less than 0.07% making a relative error of 1.75% as to the lowest concentration difference ($\Delta X = 4$ in test 1). The maximum error in determination of concentration difference is likely to be less than 5%.

Correction of X* due to solution temperature change as a result of the absorption process was applied to each individual test and the error from this is believed to be much less than other factors. The pressure drop in the connecting tube was checked and found to be negligibly small.

The cross-sectional area of the bottle was measured with an expected inaccuracy of less than 1.5% by measuring the height of a known volume of distilled water in the bottle.

From these considerations the maximum error in determining k_1 is estimated to be less than 7%.

CHAPTER 6

PERFORMANCE OF THE EXPERIMENTAL PACKED COLUMN ABSORBER

After a short review of types of absorbers suitable for heat pump applications, the packed column type was used for the experimental investigation of the absorption process. Design calculations of the absorber were carried out based on the results of the last chapter. An absorption device was constructed and the absorber was tested at different working conditions. The mass-transfer coefficient was obtained from the measurements, and was correlated to deduce the diffusion coefficient of the system (Methanol/2LiBr - $ZnBr_2$) at a concentration of 24.5% methanol by weight.

6.1 Absorbers for heat pump applications

Most of the previous work was concentrating in study of absorbers for refrigeration machines, (Ref 77, 78, 79 & 80). Although the principle of operation is the same, one should be aware of the fact that the performance of identical absorbers may differ with heat pumps because of the different temperature range and also lower refrigerant concentrations. Practical absorbers were reviewed in order to find the most suitable type for heat pump working conditions.

6.1.1 Liquid dispersion absorbers

Liquid despersion to creat extended surface area of interface can be done by spraychampers or rotating disc atomizers. Spray champers are widely used in absorption machines, simply because they produce an enormous surface area of droplets which enhance the absorption process. However, they have their own problems in the pumping and spraying of viscous absorbents. Attaining high spray density per unit volume is also another problem if a high surface area per unit volume is to be observed. A more serious one is the blockage of nozzles caused by crystallization in shut-down periods. This particular problem forced Olama (Ref 24) to replace his spray champer with a dripping tray absorber. This, however, does not necessarily eliminate the use of spray champers with methanol solutions, and appropriate designs of this type

of absorber may be possible. The possibility of heat exchange simultaneously with mass transfer in spray champers is limited, but if high absorbent circulation rates can be tolerated the temperature increase due to the absorption process will be minimised.

As the absorber in this investigation is designed to work in the proximity of the crystalization line (X = 24.5%) in an intermitently working system at different temperatures the spray champers were excluded least nozzle blockage should occur.

Spinning disc atomizers are attractive in that their power requirements are modest and the droplet size is independent of the liquid viscosity (Ref 81). However they tend to produce a two dimensional sheet of droplets, making for large linear dimensions in the absorber. There is also the problem of transmitting a drive to the rotating disc which has to operate in a low pressure environment.

6.1.2 Gas dispersion absorbers

Gas dispersions in liquid absorbent can be produced with the aid of impellers, as in turbogas absorbers, or by perforated-plate gas dispersers, as in sieve-plate trays (bubble absorbers). A good review of both types may be found in Perry and Chilton (Ref 38, chapter18).

In the bubble absorber, Fig. (6.1), the gas is bubbled into the absorbing solution and the bubbles ascend through a finite depth providing a useful agitation of the liquid and enabling the removal of heat to be effected via the cooling coil so that isothermal conditions can be achieved.

For moderate bubbling rates the bubble diameter d_b is related to the orifice diameter d_o by the expression.

$$d_b = 2_x(3\ do\ \sigma\ /4\ \rho\ g)^{\frac{1}{3}} \qquad (6.1)$$

where σ and ρ are the liquid surface tension and density respectively.

If the bubble formation rate exceeds the rise rate then coalescence of the bubbles may take place which reduces the surface area of exposed solution. This critical rate may be easily calculated

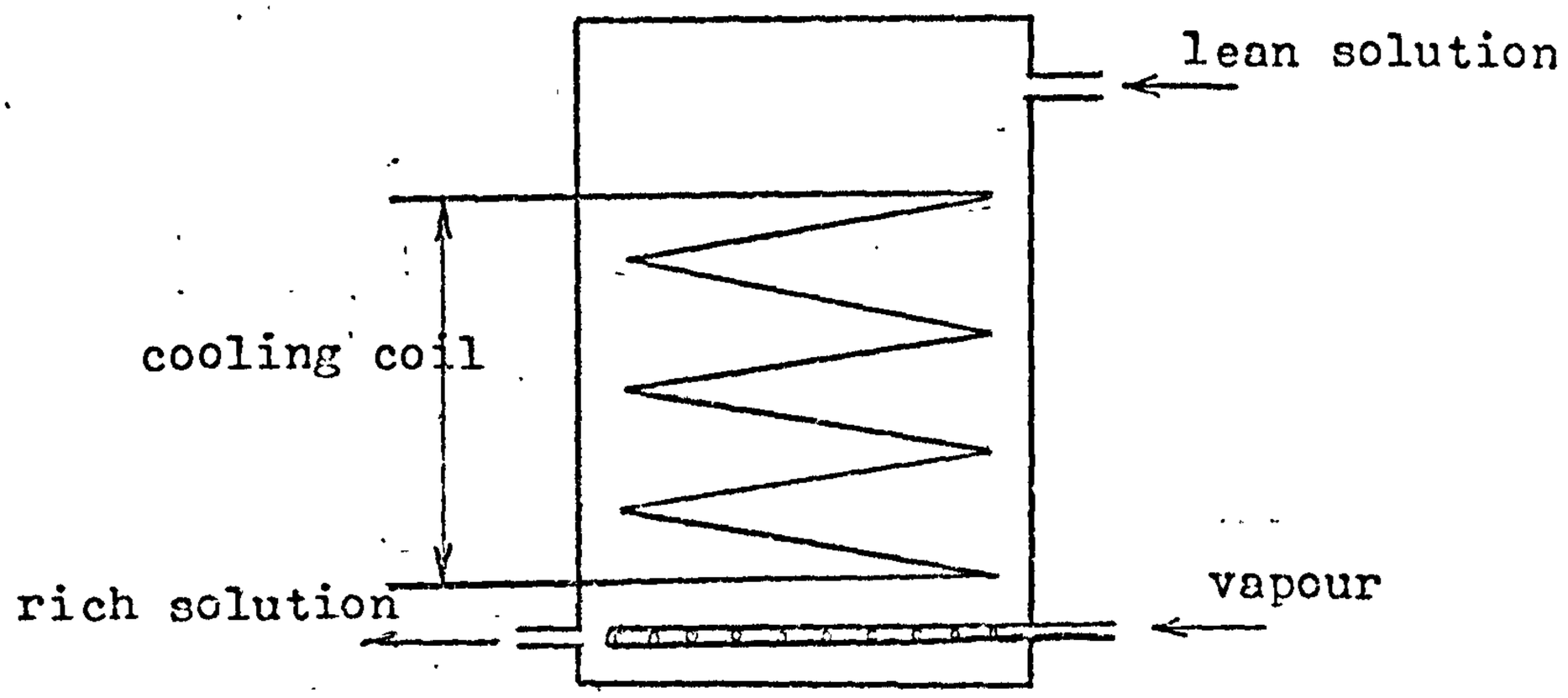

Figure 6.1 The bubble absorber

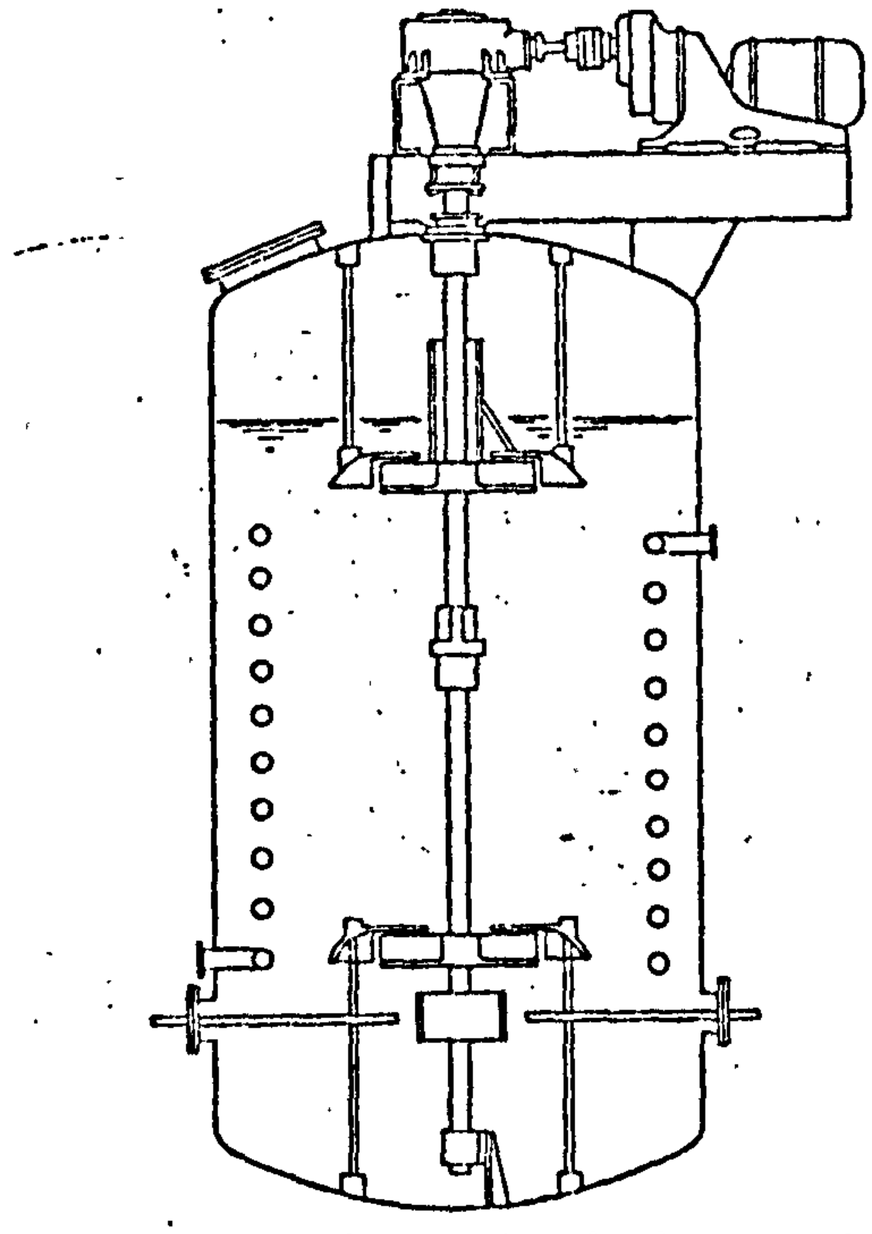

FIG. 18-125. Turbo-gas-absorber with combined pressure and self-induction impellers in hydrogenation vessel. The upper impeller is the gas entrainer. (*Turbo-Mixer Division, General American Transportation Corp.*)

Figure 6.2 The turbo-gas-absorber

from standard relationships for the bubble rise velocity. If a bubbling rate greater than the critical is called for, and mechanical devices can be indulged in them the Turbogas Absorbers, Fig. (6.2), can provide a solution. An open or semi-open impeller breaks up the gas stream which is directed downwards against a target into fine bubbles, and if guide vanes are provided the bubbles may be directed downwards against grovitational force. Thus increasing their residence time. The function of the target is an important one, for if the vapour is directed at the center of the impeller, very large bubbles tend to be formed.

Calenderbank (Ref 82) and Lightfoot (Ref 83) gave a good study of that type of absorbers.

In general, bubble absorbers are restricted to systems where the pressure is moderate or high. At low pressure the sheer volume of vapour that must be handled leads to absorbers of impracticable size and furthermore the hydrostatic head imposed on the vapour by the liquid severely attenuates the temperature difference that is possible between the evaporator and the absorber. However, because bubble absorbers can provide a high rate of both heat and mass transfer, they were examined experimentally. The apparatus is shown in Fig. 6.3 and consists of a glass orifice in hot solution vessel surrounded by a thermally controlled glycerol bath. By means of a small syringe, liquid methanol was injected into the orifice through a segment of rubber hose which seals the glass tube. The rate of bubbling was controlled by the rate of injection of liquid methanol. It was possible to obtain photographs tracing methanol bubbles as they rose through the solution. Plate 6.1 shows a typical behaviour of the bubbles. Such photographs were possible only at a solution temperatures not less than $2.5^{o}C$ below solution boiling point, which gives about 0.6% concentration difference. If this difference was exceeded, the bubbles were absorbed extremely quickly, and tracing them was very difficult. Because the error in equilibrium properties correlations (Section 3.1) is large relative to 0.6% concentration difference, it was not possible to calculate the mass transfer coefficient. However, it was so high that the bubble absorber might well reward further investigation. In spite of the fact that the pressure difference between the evaporator and the absorber in heat pumps is small, bubble absorbers with a low liquid level, e.g. 10 - 20 mm might be considered.

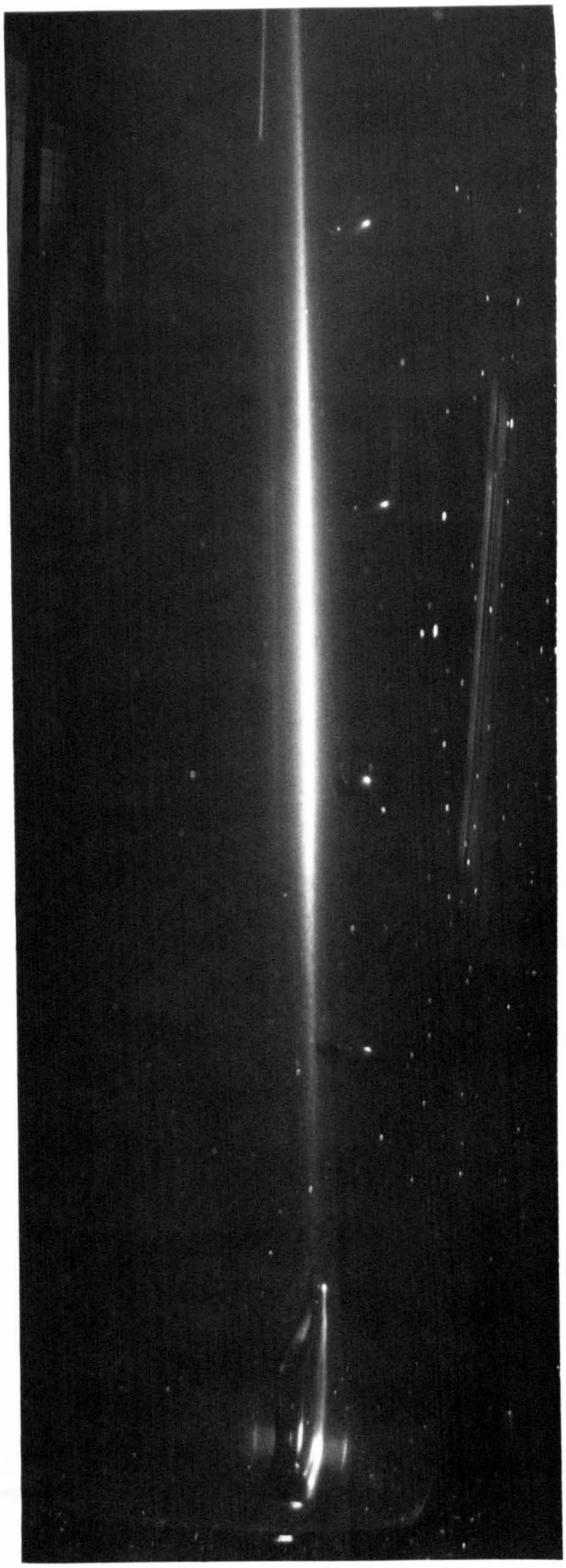

a

Solution is just boiling, no change in bubble size

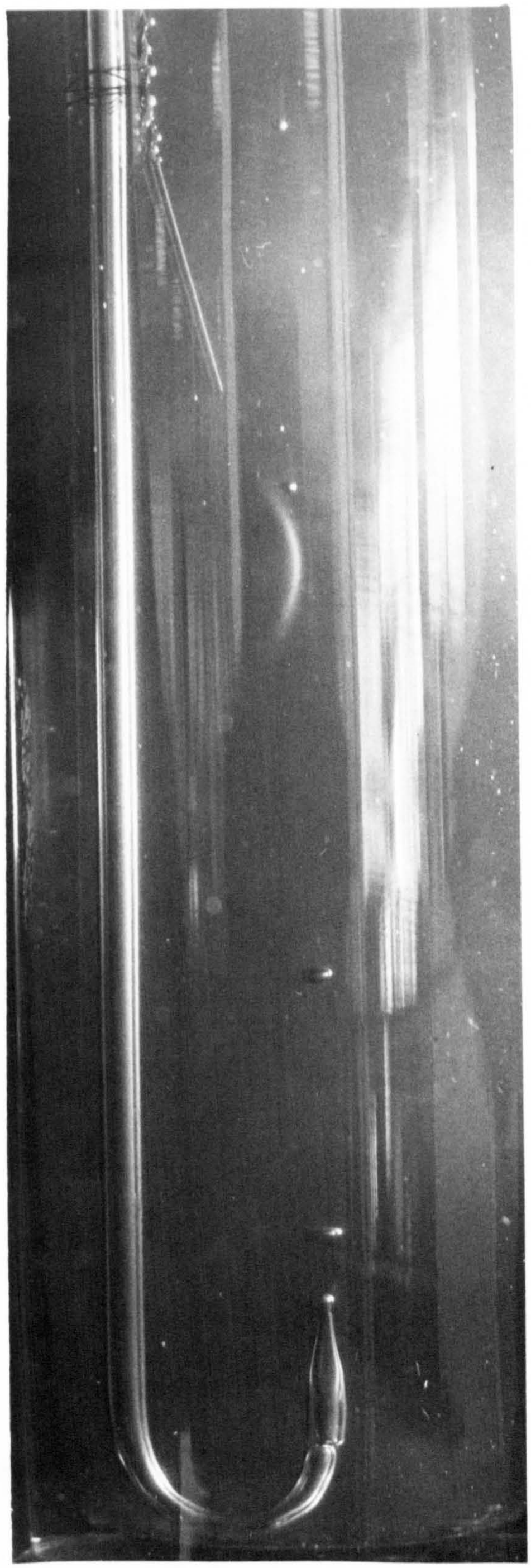

b

Solution temperature is 2.5 ^{o}C lower than boiling temperature, bubbles change the size

PLATE 6.1

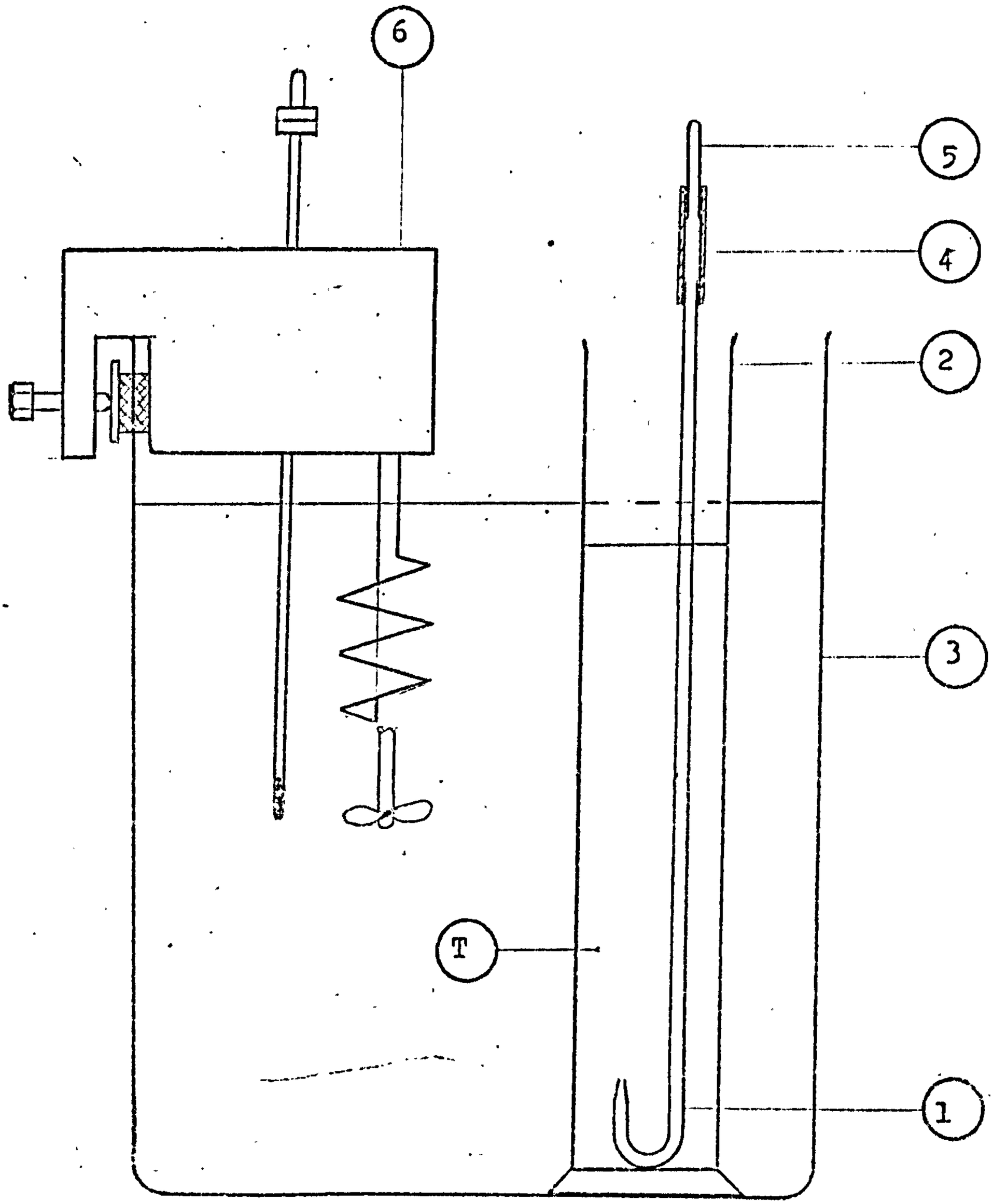

T THERMOCOUPLE

1	GLASS TUBE	2	SOLUTION CONTAINER
3	GLYCEROL BATH	4	RUBBER HOSE
5	SEALED END GLASS TUBE	6	THERMOSTIRRER

Figure 6.3 Test apparatus for bubble absorption

6.1.3 Film absorbers

The most commonly employed arrangement of this type is the falling film or dribble absorber (Fig. 6.4), which consists of a series of heat transfer surface over which the absorbent trickles. The surface may be continuous, i.e., plate like or intermittent as shown in the illustrations. However, whatever form it takes it is vital that the liquid layer is frequently mixed in order to bring fresh solution to the absorbing surface. Such absorbers operate isothermally with heat being transferred through the (normally) laminar layer of liquid into the heat absorbing surface. The capacity of such absorbers may be limited by heat transfer considerations within the liquid film, for the thickness of liquid layer δ_o falling down a plate like surface (not to be confused with the absorbing film thickness) is given by (eq. 329 Ref 84)

$$\delta_o = (3 \mu L/\rho^2 \ell g)^{\frac{1}{3}} \qquad (6.2)$$

where μ, ρ are viscosity and relative density of liquid

L is superficial mass flow rate.

ℓ is plate length normal to flow direction.

and the Nusselt number, $\frac{h\delta_o}{k}$ is numerically equal to about 4. However, if the flow is not fully developed, as may frequently be the case if the height of the element is not very great, considerably greater Nusselt numbers may be encountered (Ref 85).

Olama (Ref 24) obtained better performance of his refrigerator when spray champer was replaced by dripping tray absorber. It is believed that the reason is better heat exchange than before. Idema (Ref 14) used the same type in a low temperature domestic heat pump using the same combination (Methanol/2LiBr - $ZnBr_2$). A mass transfer coefficient of 7×10^{-6} m/sec was claimed and a comparison with coefficient in packed column is made later in this chapter.

6.1.4 Packed column absorbers

Although packed columns are used in the industrial process

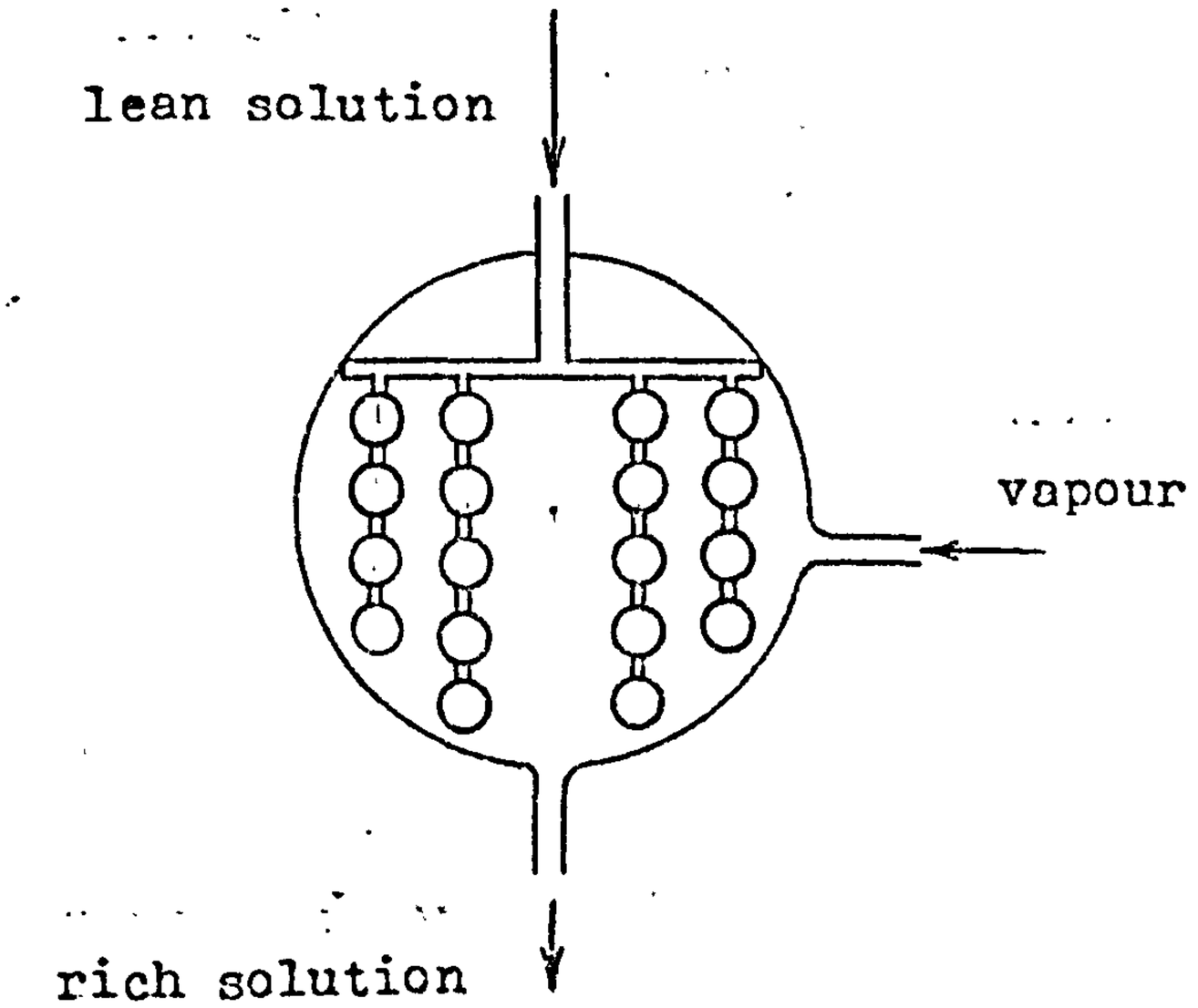

Figure 6.4 The dribble absorber

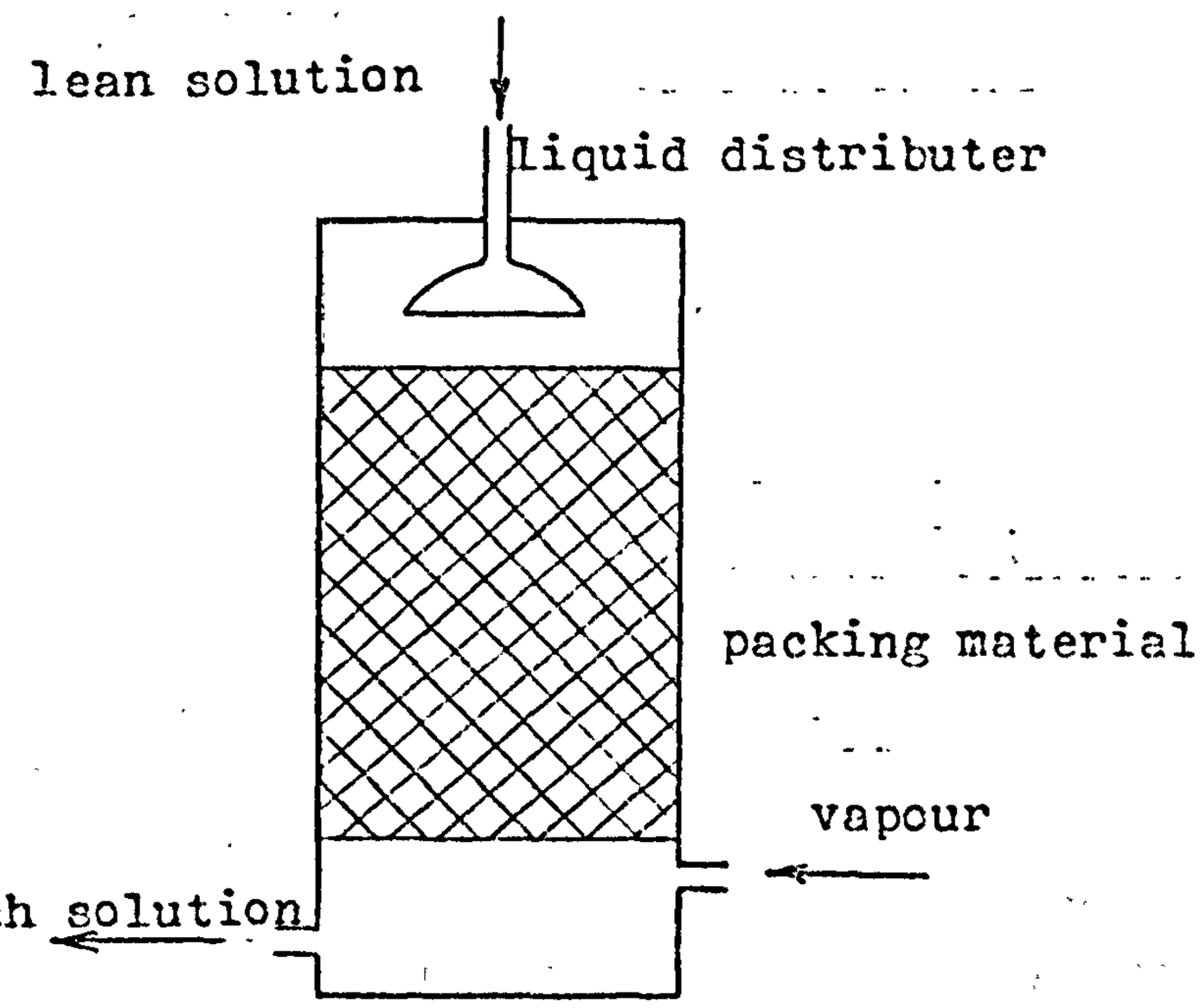

Figure 6.5 The packed bed

(gas absorption, drying and liquid extraction) no absorption machine with packed column was traced. A wide range of packings are available of which the most common and of well known characteristics are Raschig rings. They are obtainable in glass or ceramics which are of high chemical resistance.

The packed bed fig. (6.5) is an adiabatic system, and although packed towers are capable of providing both a large surface area per unit volume and a rapid renewal of the liquid film, they suffer the severe disadvantage that the concentration potential decreases as the absorbent temperature rises. They also require a seperate heat exchanger and pump to return the cooled solution to the column. Whilst the temperature increase can be minimised by employing a high liquid circulation rate, the tower design provides a limitation in this respect in that liquid flooding may occur. Data on permissible rates for a variety of packings have been reviewed in Ref (38). It must not be forgotten that whilst packed beds or towers are simple in concept, there are problems in maintaining a uniform distribution of the liquid, and redistributors are required at regular intervals. Although the illustrations suggests that the gas and solution should be in counter flow, when dealing with a single vapour component there is little virtue in adopting such a flow arrangements.

Because of the well established characteristics of packed columns, it was decided to use such an absorber to investigate the absorption of methanol vapour in the solution of mixed bromides in methanol.

6.2 The experimental absorber

- Design

For design purposes, the mass transfer coefficient in packed column absorber was assumed equal to that of the stirred cell (chapter 5). Based on that assumption the design of 1 kwatt absorber can now proceed. The absorbent is a solution of 24.5% methanol by weight while concentration difference and concentration change of 9% and 2% respectively were taken for calculations. The required rate of gas absorption was

Notations as to Fig. 6.6

1. Lean solution tank
2. Pressure differential tube
3. Refrigeration unit condenser
4. Refrigeration unit compressor
5. Refrigeration unit evaporator
6. Anti-freeze tank
7. Circulation pump
8. Anti-freeze flow meter
9. The evaporator
10. Vacuum stop cock
11. Liquid methanol flask
12. The packed column absorber
13. Vacuum sop cock
14. Solution flow meter
15. Rich solution tank
16. Vacuum stop cock
17. Vacuum magnetic valve
18. Vacuum pump
19. Vacuum stop cock
20. Distiller flask
21. Condenser cooling coil
22. Distiller condenser
23. Vacuum stop cock

TH Thermocouples

determined knowing the output power, latent heat of vaporization of methanol and the heat of dilution of the working concentrations (chapters 2 and 3). The solution mass flow rate was determined so as to achieve a nominal concentration change of 2%. The critical cross-sectional area of the column was determined to avoid flooding through 10 mm glass Raschig rings (Ref 70, page 426). Accordingly a column diameter of 100 mm was chosen, providing a ratio of column to packing diameter of 10, recommended in Ref(86) is 8:1 in order to avoid wall effects. The height of the column was calculated assuming a 30% wetting efficiency.

A boiling pool type evaporator was designed to match the absorber. The heating element was a copper coil with an anti-freeze fluid circulating within. Initially, a fluid of 10% methanol water was used, but it was replaced later with 40% ethylene Glycol mixture to achieve a lower evaporation temperature. The properties of both fluids are given in Ref 38 chapters 3 and 12. Design calculations of the absorber and the evaporator are given in Appendix (D).

- Test rig description

To avoid the engineering difficulties arising with the control of a continuous cycle, a laboratory absorption device built from QVF glass-ware was designed to work intermittently. The test rig shown in Fig. 6.6 and plates 6.2 and 6.3 consists mainly of, low pressure side (absorber and evaporator), high pressure side (distiller), two collection tanks and antifreeze circulation system.

An upper collection tank was used to store lean solutions before introduced into the absorber. The tank was electrically heated and thermally insulated to achieve the solution inlet temperature. The outlet of the tank was connected through a calibrated liquid flow meter and a vacuum stop cock to the absorber inlet. The flowmeter was calibrated using solution of 24.5% concentration at $50^{o}C$. A calibration chart is given in Fig. (6.7) and corrections were necessary to account for the change of liquid density and viscosity for different temperatures See Appendix (E). The absorber shown in Fig. 6.8 was built of QVF glass tube section (1) of length 300 mm and 100 mm diameter packed with 10 mm glass Raschig rings(2) to 180 mm height, supported by a glass packing support (3), the packing was carried by a stainless steel stand (4).

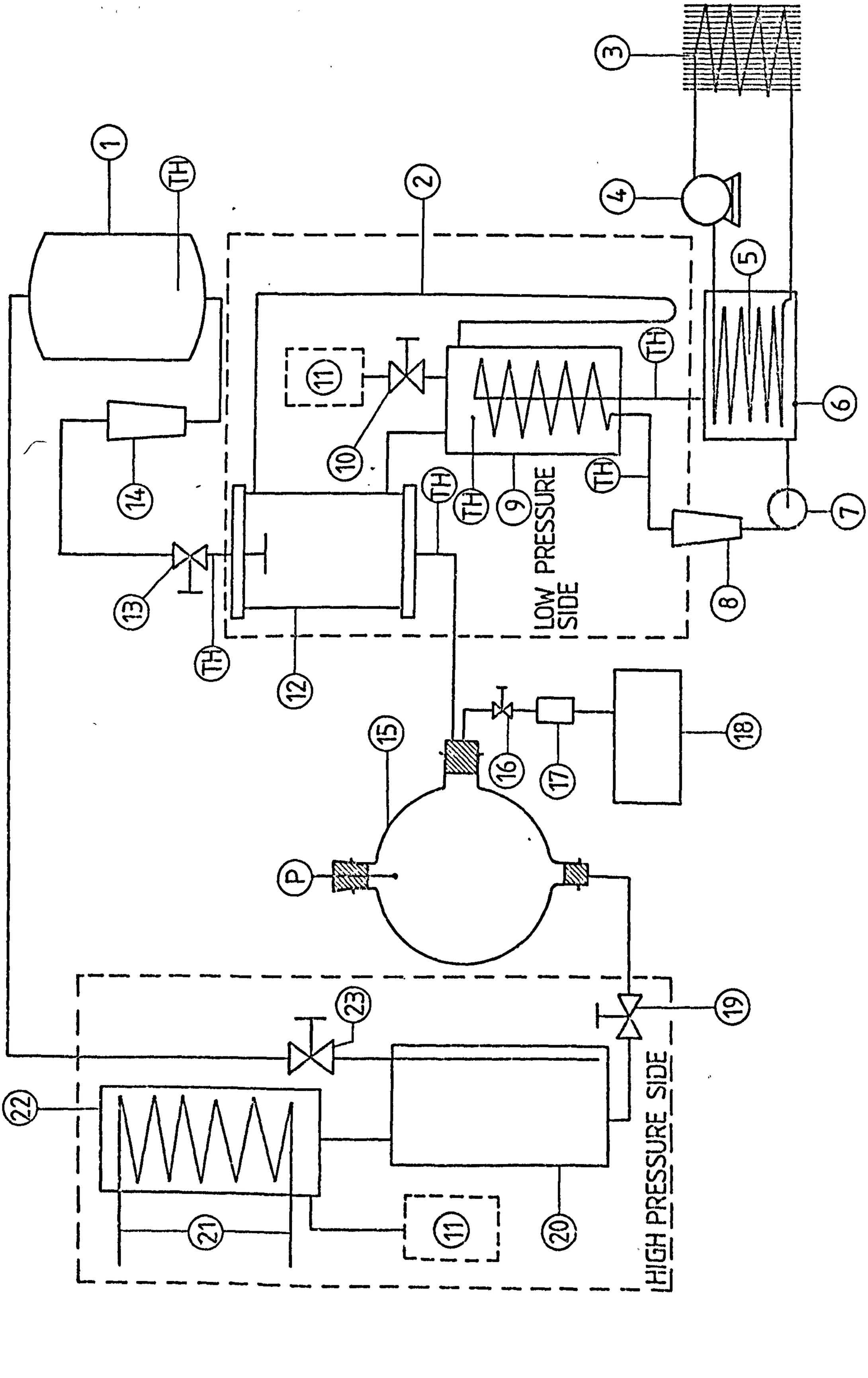

Figure 6.6 Schematic diagram of the test rig

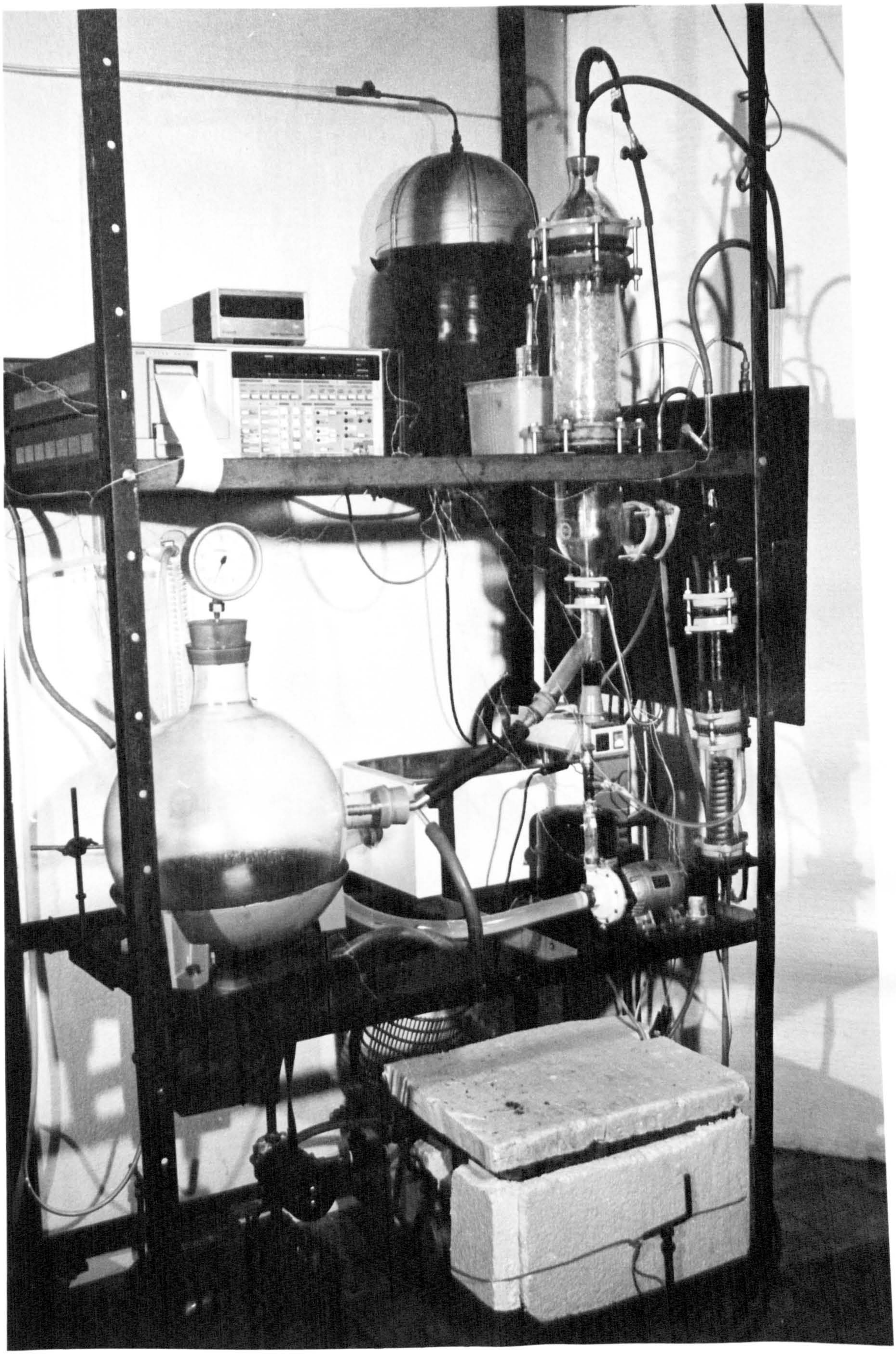

PLATE 6.2

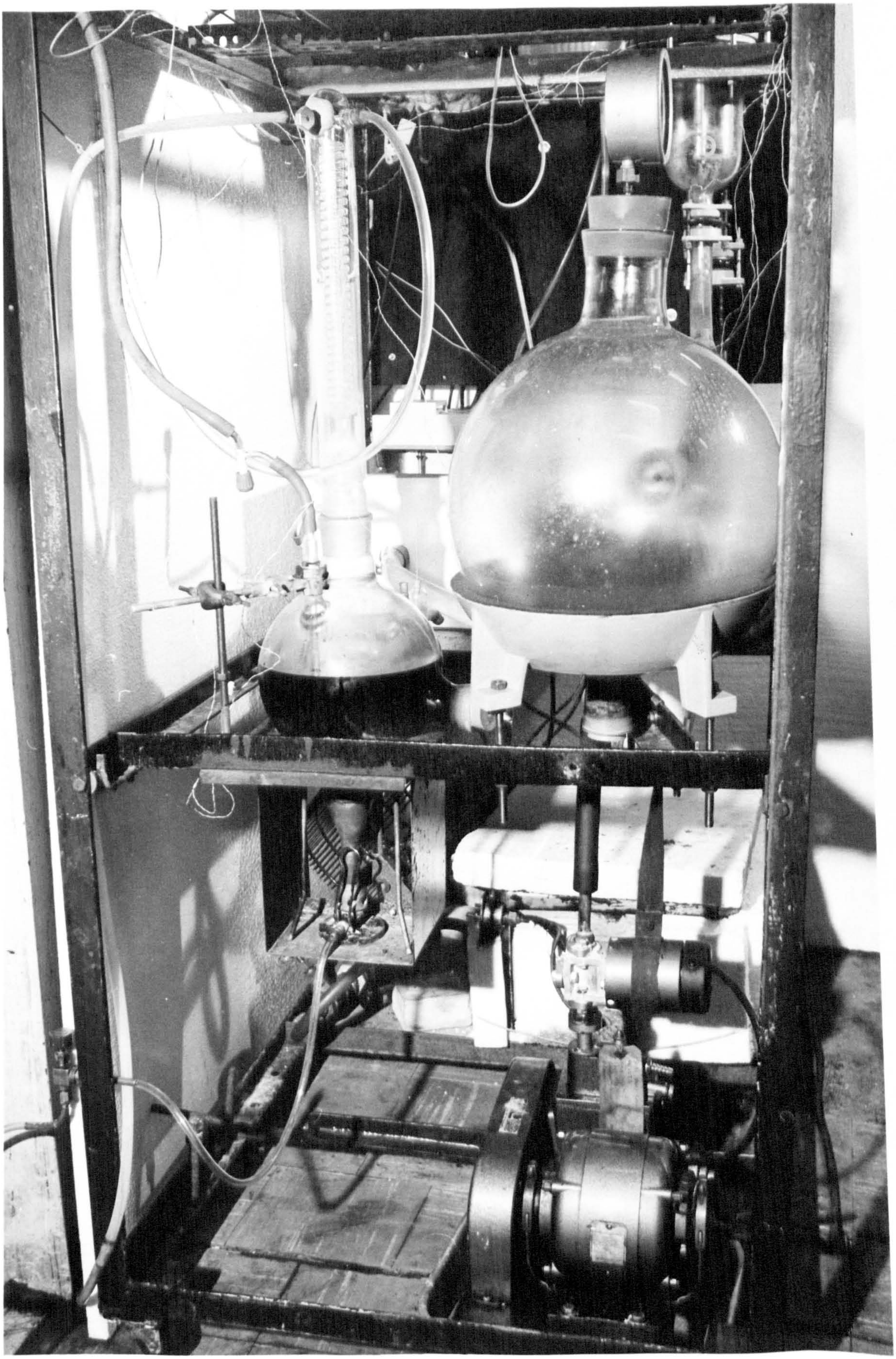

PLATE 6.3

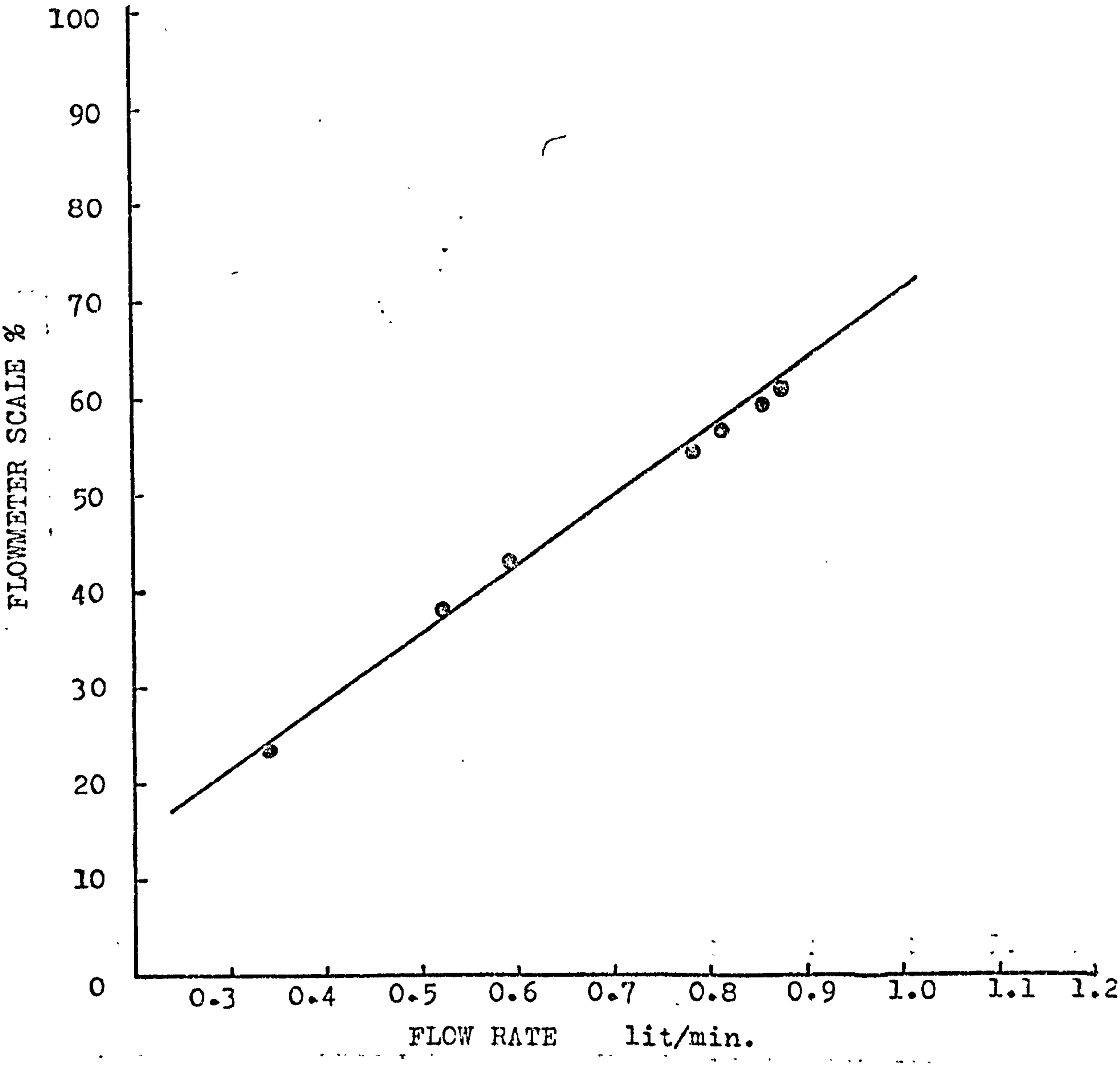

Figure 6.7 Calibration chart for solution flowmeter

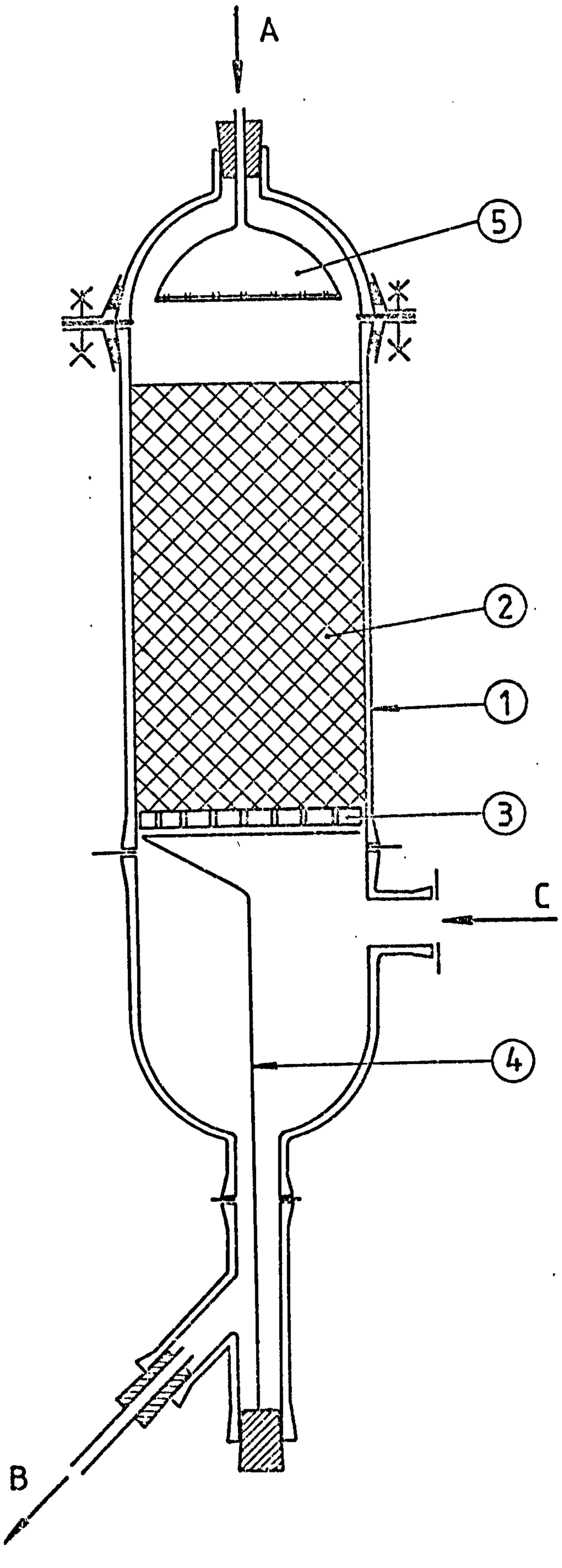

Figure 6.8 The absorber

A sieve plate liquid distributor (5) was used to lead the lean solution to the top of the tower. The absorber outlet was connected to the spherical glass vessel (15) Fig. (6.6) to collect rich solutions.

The evaporator fig. (6.9) was constructed of 2 QVF glass tube sections (1, 2) each of 50 mm diameter and 200 mm length attached to 90^{o} bent (3) of the same diameter with a pore through which a glass vaccum valve was employed to charge the liquid methanol. The copper coil (4) of 40 mm pitch diameter and 14 turns made of ¼" o.d. tube was braced in a steel square plate (5) of 70 mm side and 5 mm thickness tightened to the lower end of the evaporator with the aid of coupling flange. Three circular baffles (6) were used to damp vigorous boiling of methanol and prevent wet vapour from reaching the absorber at the top of the evaporator. Both the evaporator and the absorber were thermally insulated by means of fibre glass and foam rubber. A pressure differential glass U tube was connected between them to measure the actual pressure drop in the absorber. Solutions were boiled in a common water distiller (Fig. 6.10) of 8 liters per hour capacity to generate methanol and provide lean solutions. The distillation flask was heated by means of a butane burner and a water-cooled condenser condensed the pure methanol which was collected in a flask for return to the evaporator.

All connections were made vacuum tight and the tube sections were clamped together using couplings sealed with rubber gaskets. All other connections were by means of rubber hoses on glass, copper or stainless steel tubes. The system proved vacuum tight within the requirements and an absolute pressure of 1 torrwas held for at least 5 hours.

A refrigeration unit was used to cool the 25 litres of the anti-freeze to the selected temperature prior to a run. A centifugal 200 watt water pump circulated the antifreeze in the evaporator copper coil, via a flow meter.

Five copper constantan thermocouples were connected to a FLUK data Loger to measure the temperature of the two streams of solution and antifreeze both in inlet and outlet as well as pure methanol evaporation temperature. Other, steady state, temperatures were measured by

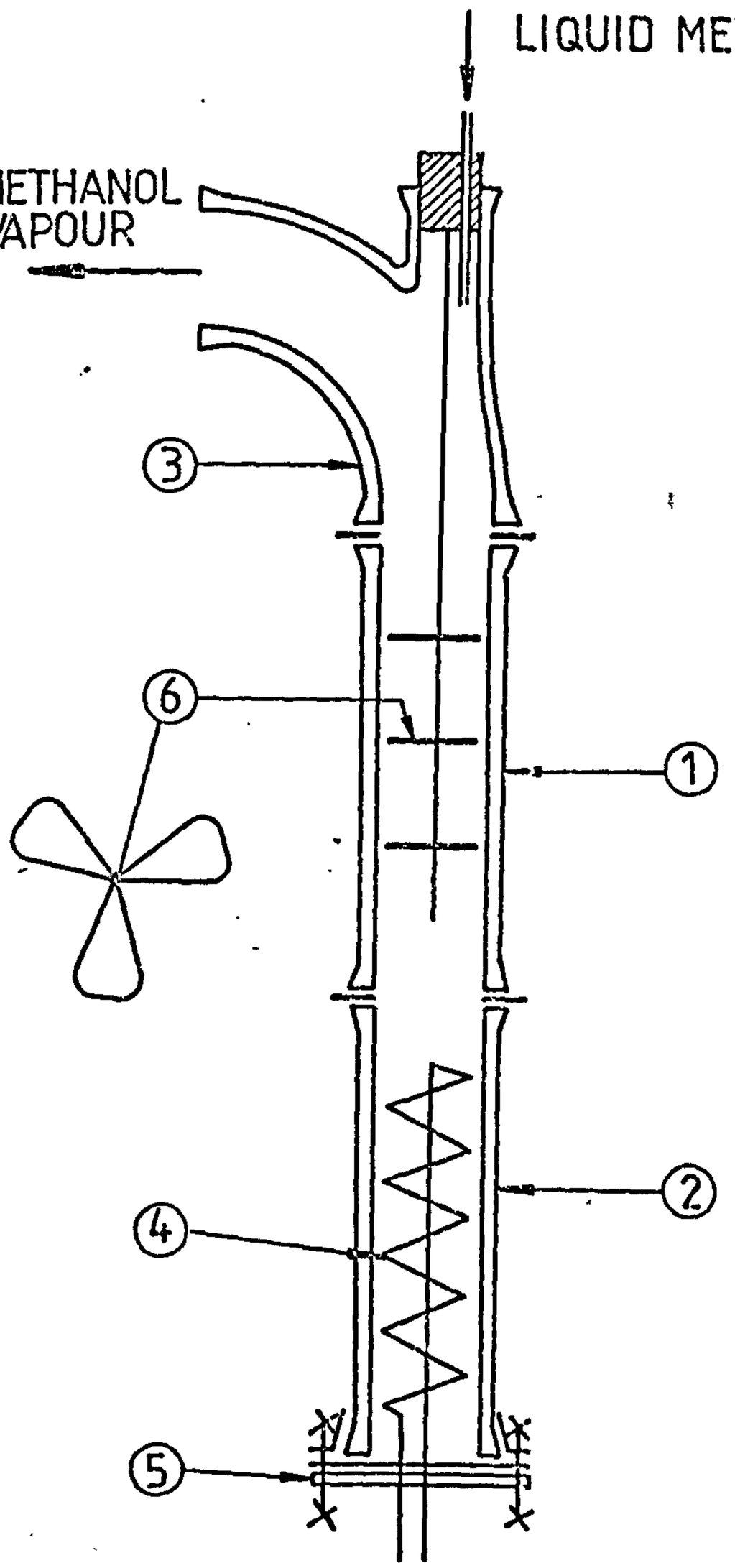

Figure 6.9 The evaporator

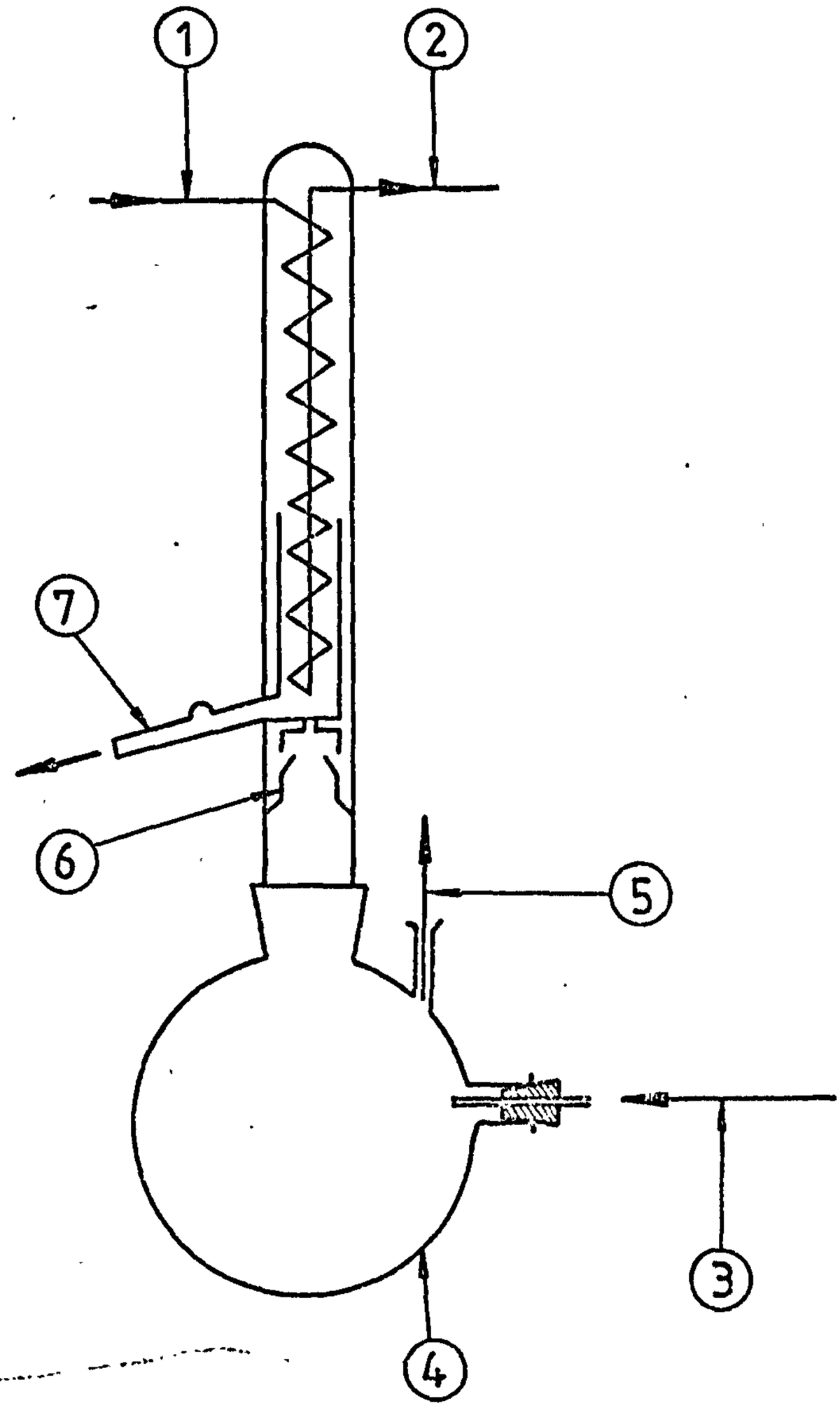

1. COOLING WATER INPUT
2. COOLING WATER OUTPUT
3. RICH SOLUTION
4. FLASK
5. WEAK SOLUTION
6. CONDENSER
7. CONDENSATE METHANOL

Figure 6.10 The distiller

means of thermocouples with an electronic indicator unit. Thermocouples in Fig.(6.6) are indicated by TH.

The absolute pressure in the system during evacuation and inspection was measured by means of a vacuum gauge which read to 1 torr and was connected to the top of the spherical glass collection tank.

6.3 Running the device

To prepare the solutions, the salts were mixed in the distillation flask (20) Fig. (6.6) and dried under vacuum in an oven, following which a solution of about 30% concentration was prepared by the same procedure described in section 3.1. Immediately after preparation, the solutions were boiled in the flask which was connected to the condenser (22) to collect condensate methanol in flask (11). When boiling temperature reached 180^{o}C the burner was removed, and the condenser outlet was connected to silica jel air dryer. Solutions were left to cool to 80 - 90^{o}C before they were driven into the evacuated upper collection tank (1) via valve (23). The outlet of collection tank (15) was connected to the distillation flask. With valves, 10, 13 and 19 closed, the lower pressure side was completely seperated from the rest of the device then it was evacuated via valve (16) and tested.

Several passes of the solutions down the absorber were carried out with dry evaporator (9) in order to thoroughly wet the packings. Then further tests were carried out at different solution temperature with the evaporator still dry to ascertain the heat losses to the surroundings from the absorber (12) at different solution temperatures at a given flow rate.

While the system is evacuated, liquid methanol was charged into the evaporator through valve (10) after the pressure reached 1 torr. The vacuum pump was left on for about five minutes to ensure the absence of air in the system.

The anti-freeze temperature in tank (6) was adjusted to about 10^{o}C lower than the required evaporation temperature, and the temperature of the solutions in tank (1) was also adjusted to the required value. About 10 minutes before the run the anti-freeze was circulated

in the evaporator coil in order to pull down the methanol bulk temperature. Then the system was ready for test. The data logger was set to record five temperature readings every 15 seconds. Valve (13) was opened to enter lean solutions to the absorber and start the absorption process. The valve was also used to control the liquid mass flow rate. The evaporator temperature then started to fall until a steady reading, indicated by the data logger, was reached. The readings then were recorded for at least 4 minutes. The pressure in the absorber and the solution flow rate as well as anti-freeze flow rate were also measured. The above was repeated at different evaporation and absorption temperatures, and nine successful tests were carried out.

6.4 Measurements and results

The performance of the low pressure side of the device was determined by measuring the heat input to the evaporator and heat output of the absorber. The evaporator heat input (Q_E) is equal to the sensible heat lost by the anti-freeze while circulating in the copper coil. This heat was determined by measuring the anti-freeze inlet and outlet temperatures, and its mass flow rate. Corrections to the flowmeter readings were applied as a result of the difference in the density and viscosity of solutions from the properties of the calibrating fluid (water). The rate of evaporated methanol (g_E) was calculated as the ratio of (Q_E) to the latent heat of vaporization of pure methanol at the same temperature. In the steady state where temperature in the evaporator (T_E) is constant, it was assumed that the rate of absorption is equal to the rate of evaporated methanol, however, a fluctuation of $\pm 1^{o}C$ in T_E was accepted.

The heat output of the absorber (Q_A) was determined by measuring the sensible heat gained by the solutions due to absorption plus the heat losses to the surroundings. The heat loss was determined knowing the temperature change of solutions running across a dry absorber, results are shown in Fig. (6.11). The heat ratio $\varepsilon = \frac{Q_A}{Q_E}$ was then calculated. The results are shown in table (6.1) while an example of readings and procedure of calculation is given in Appendix (E).

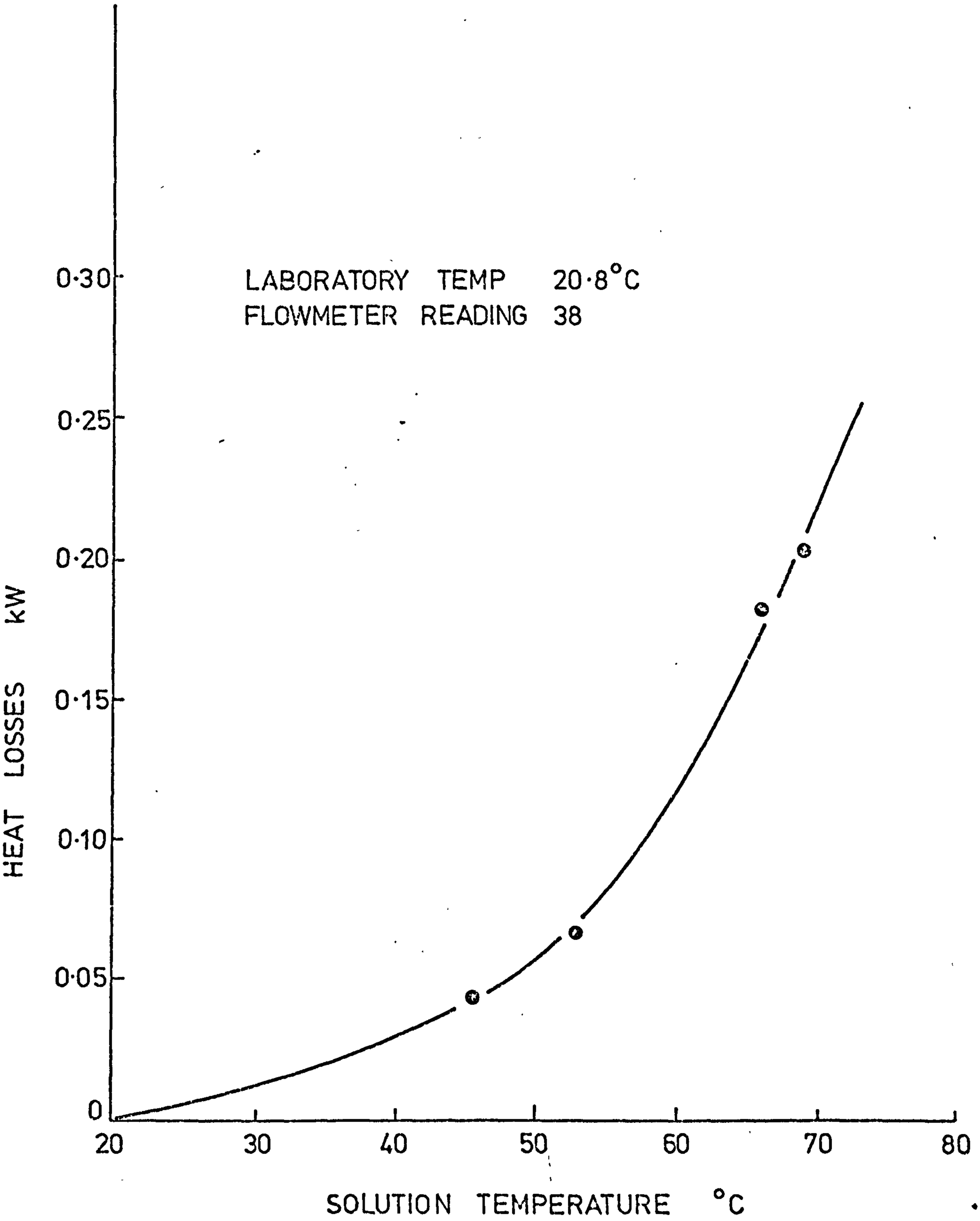

Figure 6.11 Heat losses from the absorber

Test No.	Mean Solution Temperature T_A °C	Mean Evaporation Temperature T_E °C	Evaporator Input Power Q_E kw	Rate of Absorption $10^3 g_E$ kg/sec	Absorber Heat Output Q_A kw	Heat Ratio $\varepsilon = Q_A / Q_E$	Rate of absorption per unit packed volume $10^3 R'$ kg/sec $m^3 = (k_\rho p_a)\Delta x$	Log mean concentration difference		Rate of absorption per unit area $g_{ES} = R/a_e$ kg/m²s
								%	kg/m³	
1	60.1	-2.0	0.287	0.24	0.443	1.54	167.95	8.8	95.7	1.333
2	69.0	-3.9	0.249	0.208	0.434	1.74	145.56	5.2	60.4	1.198
3	58.3	-6.6	0.223	0.186	0.324	1.45	130.16	7.2	81.6	1.071
4	51.8	-7.1	0.289	0.24	0.402	1.39	167.95	8.4	92.2	1.435
5	61.2	-10.3	0.209	0.174	0.33	1.58	121.76	4.9	57.4	1.002
6	68.4	-10.4	0.155	0.129	0.221	1.43	90.27	3.2	39.3	0.734
7	73.2	-8.2	0.111	0.093	0.176	1.59	65.08	2.8	34.9	0.467
8	65.6	-12.1	0.151	0.126	0.239	1.58	88.173	3.92	47.7	0.676
9	48.9	-11.5	0.313	0.261	0.387	1.24	186.14	9.6	105.6	1.724

TABLE 6.1

Data of the absorption test in packed column

6.4.1 Interfacial area

The interfacial area of certain packings is not only a characteristics of the packing, but it is also dependent on the properties of the liquids employed and the working conditions (Liquid and gas flow rates). An extensive study of the dependence of the interfacial area a_e on working conditions for some packings was given by Shulman et al (Ref 87). The interfacial area was calculated by splitting the volumetric gas phase mass transfer coefficient $k_G a$ using published data on the absorption of ammonia by water. The main conclusion was that a_e is fairly independent of gas rate.

Yoshida et al (Ref 88), by comparison of the Reynolds numbers in bead and packed columns corresponding to equal volumetric liquid mass transfer coefficients $k_l a$ in both, were able to find the effective interficial area in packed column for several packings. Their results roughly agree with those of Shulman. However, they are believed to be more reliable as the method is backed by a theoretical approach and directly applied to liquid mass transfer coefficient including methanol as a solvent.

Unfortunately the references mentioned above did not give a general correlation for the effective interfacial area. Their results given on diagrams, had to be extrapolated for 10 mm Raschig rings.The effective interfacial area found from these diagrams for 10 mm Raschig rings is an average of 8% of total area.

A useful review of the experimental work in this field has been made by Onda et al (Ref 89) who gave a correlation for the wetted area of packings taking into account the hydrodynamics of the system, the surface energy of the packings, and the properties of the liquid absorbent:

$$\frac{a_w}{a_t} = 1 - \exp\left(-1.45 \left(\frac{\sigma_c}{\sigma}\right)^{0.75} R_e^{0.1} F_r^{-0.05} W_e^{0.2}\right) \qquad (6.3)$$

where a_t is dry area of packing 450 m^2/m^3 for 10 mm Raschig rings.

a_w is wetted area of packings m^2/m^3.

σ is surface tension of the liquid absorbents.

σ_c is packing surface energy = 0.73 N/m for glass (Ref 38) page 18 - 35.

R_e Reynolds number $\frac{L}{a_t \mu}$

F_r Froude number $(\frac{L}{\rho})^2 \frac{a_t}{g}$

W_e Weber number $\frac{L^2}{\rho a_t \sigma}$

It was claimed that this equation correlates well the data available for gas absorption in water and some organic solvents. This, in addition to being dimensionless, made it acceptable for application. The wetted area was calculated for each test and results are shown in table (6.2). The liquid properties were taken from chapters 3 and 4. A correction coefficient $\zeta = 0.85$ was applied to the calculated area due to observed maldistribution at the top of the absorber.

The wetted area calculated from this equation is assumed by Onda to be equal to the interfacial area and an error of 20% was expected. Onda et al (Ref 90) stressed this assumption and added that it is not only convenient for estimation of the area but also reasonable for mass transfer calculations.

While the effective interfacial area found from Ref 87 and Ref 88 is only 8% of the total dry area of the packings, the interfacial area calculated from equation (6.3) is 28% of the total dry area. Such a difference should have no significant effect in further application of the mass transfer coefficient for design of packed column. The reason is clearly given by Yosida et al (Ref 91) that the choice of the basis on which the value of the k_L and accordingly the effective interfacial area in a packed column are determined is arbitrary, provided that the value of k_1 in the reference apparatus (the experimental packed column) vary with gas or liquid rates just the same way as in the under design packed column.

$\sigma_c = 0.073\ {}^{N}/_{m}$ $\quad y = 1.45\ (\frac{\sigma c}{\sigma})^{0.75} Re^{0.1} Fr^{-0.05} We^{0.2}$

$a_t = 450\ {}^{m^2}/_{m^3}$ $\quad \zeta = 0.85$

$A_s = 7.85\ 10^{-3} m^2$

Measured or calculated Parameter \ Test number	1	2	3	4	5
Mean solution temperature T_A ^oC	60.1	62	58.3	51.8	61.2
Solution flow meter reading %	40	30	38	45	36
Solution flow rate g_s kg/sec	0.0219	.0189	.0206	.0198	.0226
Superficial liquid flow rate $L = \frac{g_s}{A_s}$ $kg/_{m^2}sec$	2.79	2.41	2.55	2.53	2.5
Liquid viscosity $\mu\ \frac{kg}{m\ sec}$	0.022	0.018	0.023	0.027	0.021
Liquid density $\rho\ \frac{kg}{m^3}$	1900	1895	1906	1913	1897
Liquid surface tension $\sigma\ {}^{N}/_{m}$	0.0488	0.0481	0.0490	0.0495	0.0485
Reynolds number $Re = \frac{L}{a_t \mu}$	0.282	0.306	0.250	0.211	0.258
Froude number $Fr = (\frac{L}{\rho})^2 \frac{a_t}{g} \times 10^5$	9.9	7.4	8.2	8.03	7.8
Weber number $We = \frac{L^2}{\rho a_t \sigma} \times 10^4$	1.87	1.42	1.55	1.50	1.51
$(\frac{\sigma_c}{\sigma})^{0.75}$	1.106	1.111	1.105	1.102	1.108
$1 - e^{-y}$	0.33	0.32	0.32	0.31	0.32
$\frac{a_w}{a_t} = \zeta\ (1 - e^{-y})$	0.28	0.27	0.27	0.26	0.27
$a_w = a_e\ {}^{m^2}/_{m^3}$	126	121.5	121.5	117	121.5

Table 6.2

Readings and results of the absorption test in the packed column absorber

Measured or calculated Parameter \ Test number	6	7	8	9
Mean solution temperature T_A ^oC	63.4	73.2	65.6	48.9
Solution flow meter reading %	35	40	32	60
Solution flow rate g_s kg/sec	0.0226	0.0275	0.0227	0.0318
Superficial liquid flow rate $L = \frac{g_s}{A_s}$ $kg/_m{}^2sec$	2.88	3.5	2.88	4.6
Liquid viscosity μ $\frac{kg}{m\ sec}$	.0167	.016	.020	.0285
Liquid density ρ $\frac{kg}{m^3}$	1889	1880	1890	1920
Liquid surface tension σ $N/_m$	.0477	.0476	.0483	.0496
Reynolds number $R_e = \frac{L}{a_t \mu}$	0.383	0.486	0.32	0.317
Froude number $F_r = (\frac{L}{\rho})^2 {a_t}/_g$ 5 10	10.7	15.9	10.7	20.5
Weber number $W_e = \frac{L^2}{\rho a_t}\sigma$ 4 10	2.05	3.04	2.02	3.8
$(\frac{\sigma c}{\sigma})^{0.75}$	1.112	1.113	1.109	1.101
$1 - e^{-y}$	0.33	0.37	0.34	0.28
$\frac{a_w}{a_t} = \zeta(1 - e^{-y})$	.28	.31	0.29	.24
a_e $m^2/_{m^3}$	126	139.5	130.5	108

cont. Table 6.2

6.4.2 Mass transfer coefficient k_1

The rate of absorbed methanol per unit volume of packing is given by $$R = \frac{g_E}{W} = k_1 a_e \Delta X \text{ kg/m}^3\text{sec} \quad (6.4)$$

where k_1 is mass transfer coefficient

a_e is interfacial area per unit volume of packing m^2/m^3.

W Packing volume in the absorber m^3

ΔX log mean concentration difference.

g_E rate of vapour absorption kg/sec.

$$\Delta X = \frac{\Delta X_i - \Delta X_o}{\text{In} \frac{\Delta X_i}{\Delta Y_o}}$$

and ΔX_i is $(X_i^* - X_i)$, ΔX_o is $(X_o^* - X_o)$

X_i is concentration of lean solution entering the absorber.

X_o is concentration of rich solution leaving the absorber.

X_i^*, X^*_o are equilibrium concentrations at absorber input and output conditions respectively taking the increase in surface temperature into consideration.

Concentrations were always expressed in weight ratio, but in order to be able to determine the diffusion coefficient, the calculations were also carried out using volumetric concentrations C kg methanol/m^3 of solution. In the first case k_1 is given in $kg/m^2\%$ sec. and in m/sec in the second.

From table (6.1) values of R were divided by corresponding values of a_e table (6.2), and the result g_{ES} kg/m^2sec was plotted against ΔX in Fig. (6.12) and Fig. (6.13). The least square lines were determined.

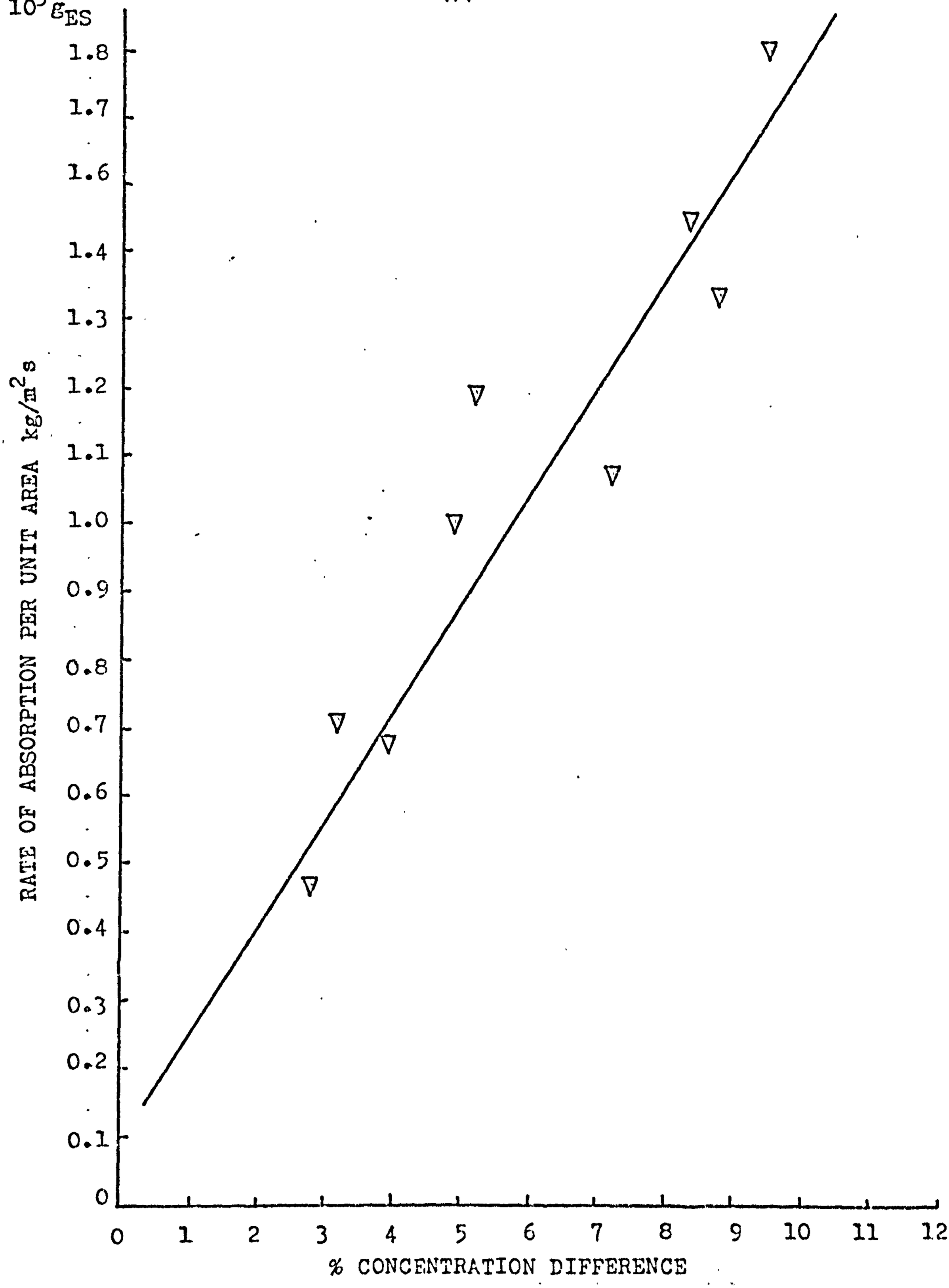

Figure 6.12 Rate of absorption in packed column

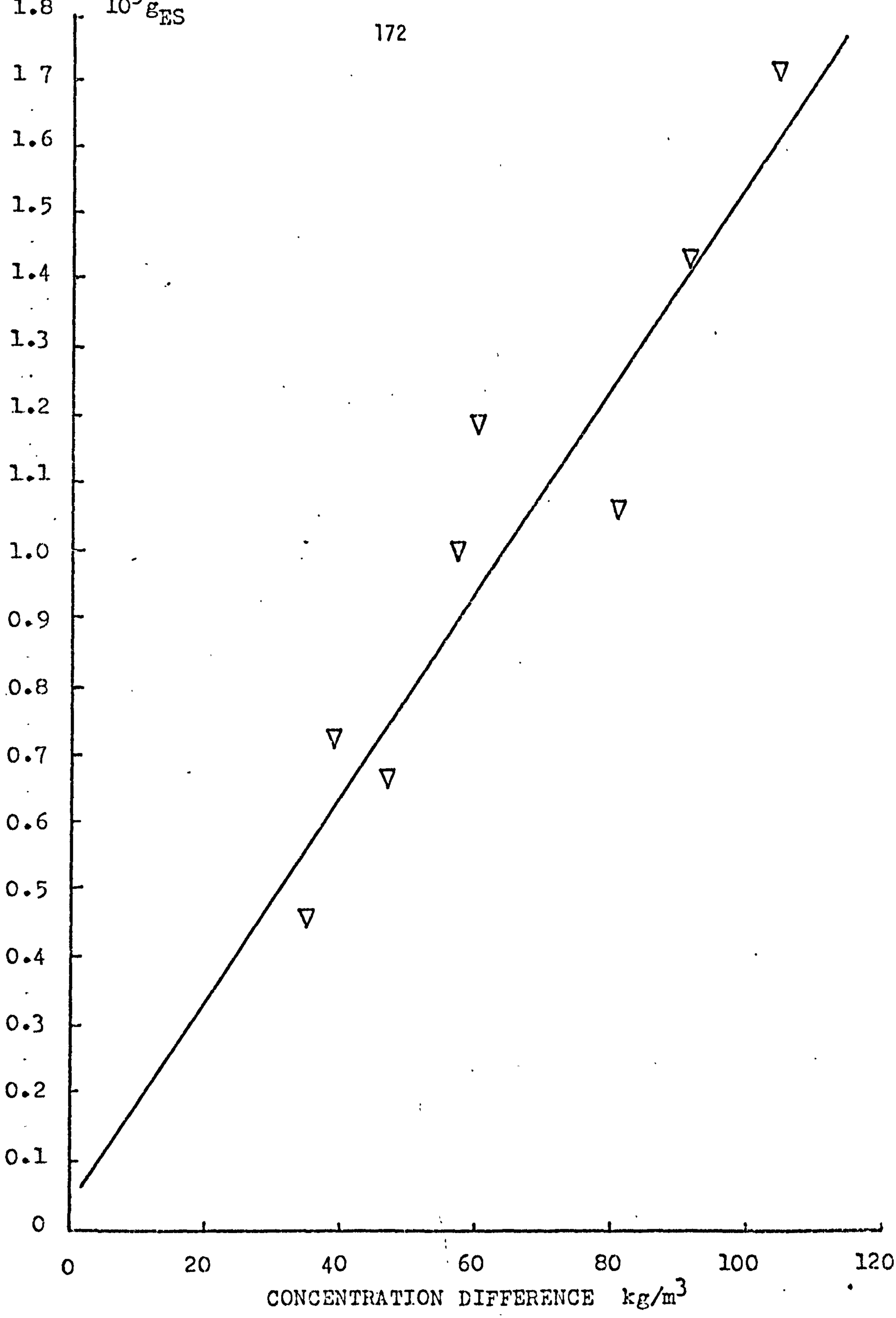

Figure 6.13 Rate of absorption in packed column

$$10^3 \quad g_{ES} = 0.1081 + 0.1584\ \Delta X \qquad \text{fig. (6.12)}$$

$$10^3 \quad g_{ES} = 0.04728 + 0.01491\ \Delta C \qquad \text{fig. (6.13)}$$

The slope of these lines, 1.58 10^{-4} kg/m^2sec% and 14.9 10^{-6} m/sec, represent the mass transfer coefficient (k_1) in the absorber when methanol concentration is expressed in weight percent and in weight per unit volume of solution respectively. And when equation (6.3) is used to find the interfacial area a_e, the value of (k_1 a_e) in the second case which is necessary for the determination of diffusion coefficient is calculated by correlating R directly against ΔX, giving the least square straight line

$$10^3 \quad R = 13.51 + 1.67 \quad \Delta X$$

the slope of which is $k_1 a_e = 1.67 \quad 10^{-3} \quad Sec^{-1}$.

6.4.3 Heat ratio

The heat heat ratio $\varepsilon = \frac{Q_A}{Q_E}$ is a measure of the heat of vaporisation of methanol from solutions relative to latent heat of vaporisation of pure methanol. As the working concentration was always the same, 24.5%, and the pressure was altered only slightly the values of ε so determined had an arithmetic mean of 1.5 and a standard deviation of $\pm$ 0.14. However, if the two extreme values of ε, 1.74 and 1.24 in tests 2 and 9 respectively (Table 6.1), are excluded, this deviation becomes only $\pm$ 0.08. The reason whey these values may be excluded is that the extreme scatter they show is believed to be caused by the difference in the liquid flow rate in tests 2 and 9 shown by solution flowmeter readings 30% and 60% (Table 6.2) as compared with the flowmeter reading in the losses test which was always 38%.

In test number 2 the flow rate is lower causing lower real losses than were accounted for, and accordingly ε is relatively very high. On the other hand it is believed that the opposite took place

in test number 9 and ε is relatively very low. As for the rest of the tests the flow rate is closer to the flow rate at the losses test and their results are more precise. The heats of vaporisation H and H' (Chapter 2) are described in Appendix A at a pressure similar to the pressure employed in the test and were found to be 1193 and 1781 kJ/kg respectively. Thus $\varepsilon = \frac{H'}{H}$ is 1.49 which agrees well with the experimental result.

6.5 Diffusivity coefficient

Although the mass transfer coefficient is determined for packed column absorber in this work, the use of these results will be extremely limited as the coefficient k_1 will be different for absorbers which vary both in dimensions and type of packing. Moreover when other types of absorbers are designed, the results would be of little help, unless the diffusion coefficient of methanol in the solutions can be deduced from them.

A brief study of the different theories and equations for estimation of diffusion coefficient in Gas-liquid binary systems shows that Wilke and Chang empirical equation is the best, (Refs [74], [92] and [93]) with an average error of 12% from experimental results.

Their relationship is:

$$D = 7.4\ 10^{-8}\ \frac{T\ (X\ M)^{\frac{1}{2}}}{\mu\ V^{0.6}}\ \ cm^2/sec \qquad (6.5)$$

where T absolute temperature
μ solvent viscosity
V molecular volume of solute
X association factor of solvent
M molecular weight of solvent.

To apply this formula, a solution of 25% methanol concentration by weight was taken as the solvent at $50^{o}C$ and methanol as the solute.

As the solvent is based on methanol, X is taken 1.9 from Ref 91.

$\mu = 27.3$ CP

$T = 323\ ^{o}K$

$V = 40.6$ Calculated for methanol using Perry, (Ref 38) page 3,329 cc/gmole.

The molecular weight of the solvent was calculated as the total weight of respective number of molecules divided by that number.

$$N_{MeOH} = \frac{(2 \times 86.85 + 225.1)}{3 \times 32} = 4.15 \text{ Moles per 3 Moles of salt mixture}$$

$x = .25$

Weight of 7.15 moles = 132.8 + 225.1 + 173.7

= 531.6

$$M' = \frac{531.6}{7.15} = 74.3$$

$$D = 7.4\ 10^{-8}\ \frac{1.9^{0.5} \times 74.3^{0.5} \times 323}{27.3 \times 40.6^{0.6}}\ cm^2/sec$$

$$= 1.13\ 10^{-10}\ m^2/sec.$$

The Higbie penetration model of absorption (Ref 94) has been the base forafew correlations of mass transfer coefficient in a packed column. They are given as relations of k_1 and $\sqrt{D}$, utilizing both fluid properties and packing characteristics.

Sherwood and Halloway (Ref 95, 96), after review of an extensive collection of experimental data on gas absorption in packed column, introduced a useful relationship.

$$\frac{k_1\ a_e}{D} = \alpha \left(\frac{L}{\mu}\right)^{1-n} \left(\frac{\mu}{\rho D}\right)^{0.5} \qquad (6.6)$$

where a_e is effective interfacial area ft^2/ft^3

D is diffusion coefficient $ft^2/hour$

L is superficial liquid flow rate lb/ft^2 hour.

μ is viscosity $\frac{lb}{ft.hour}$

ρ is liquid density lb/ft^3

The constants α, n are given for different types of packings Ref 71, page 217, which for the existing packing are 550 and 0.46 respectively. Imperial units had to be used in order that equation (6.6) would hold, moreover the value of $k_l a$ is substituted in the equation to eliminate the effect of error in calculation of the interficial area.

$$\text{so} \quad k_l a = 550\left(\frac{L}{\mu}\right)^{0.54}\left(\frac{\mu}{\rho}\right)^{0.5}\sqrt{D} \qquad (6.7)$$

$$k_l a = 16.7^{-4}\ s^{-1} = 6.012\ hour^{-1}$$

$$L = 2.9\ kg/m^2 sec = \frac{2.9 \times 2.205}{(3.28)^2} \times 3600$$

$$= 2139.7\ lb/ft^2 hour$$

$$\rho = 1917\ kg/m^3 = \frac{1917 \times 2.205}{(3.28)^3}$$

$$= 119.8\ lb/ft^3$$

$$\mu = .0273\ kg/m\ sec = \frac{.0273 \times 2.205 \times 3600}{3.28}$$

$$= 65.34\ \frac{lb}{ft\ hour.}$$

$$\text{so} \quad 6.012 = 550\left(\frac{2139.7}{65.66}\right)^{0.54}\left(\frac{65.66}{119.8}\right)^{0.5}\sqrt{D}$$

$$= 550(6.593)(0.7403)\sqrt{D}$$

$$\sqrt{D} = 2.273\ \ 10^{-3}$$

$$D = 5.17\ \ 10^{-6}\ ft^2/hour$$

$$= \frac{4.97\ \ 10^{-6}}{3.28^2 \times 3600} = 1.33\ \ 10^{-10}\ m^2/sec$$

The liquid mass transfer correlation given by Shulman (Ref 87) for a packed column is:

$$\frac{k_l d_p}{D} = 25.1 \left(\frac{d_p L}{\mu}\right)^{.45} \left(\frac{\mu}{\rho D}\right)^{0.5} \qquad (6.8)$$

where $a_e = 0.8 \quad a_t = 0.8 \times 450 = 36 \quad m^2/m^3$

$k_l = k_l a/a_e = 46.39 \quad 10^{-6} \quad m/sec$

d_p = is the diameter of a sphere possessing an equivalent surface area to the dry area of a piece of packing.

$d_p = 0.014$ m

$L = 2.9 \quad kg/m^2 Sec$

$\mu = 0.023 \quad kg/ms = Nsec/m^2$

$\rho = 1917 \quad kg/m^3$

$$\frac{46.39 \quad 10^{-6} \times .014}{\sqrt{D}} = 25.1 \left(\frac{.014 \times 2.9}{.023}\right)^{.45} \left(\frac{.0230}{1917}\right)^{.5}$$

$$= 25.1 \quad (1.291)(3.464) \quad 10^{-3}$$

$$\sqrt{D} = \frac{46.39 \times 10^{-6} \times 0.014}{25.1 \times 1.291 \times 3.464}$$

$$= 5.79 \quad 10^{-6}$$

$$D = 0.335 \quad 10^{-10} \quad m^2/sec.$$

Davidson Ref (97) used statistical models of random packing to predict the performance of packed towers. The calculations were referred to conditions very similar to those of the present work.

- The packing was wetted by liquid running down freely under gravity, and
- the spaces between the packings are filled with stagnant gas which has a negligible effect upon the motion of liquid.

The second of his three models, which assumes that packings are random surfaces of different anagles but of equal length in the direction of flow (d), is more acceptable for the application to Racshig rings, (especially) small ones.

$$\frac{L}{k_l a \rho d} = 0.244 \frac{S_c^{\frac{1}{2}} R_e^{2/3}}{G_r^{1/6}} \qquad (6.9)$$

where S_c is Scmidt Number = ν/D

R_e is Reynolds number $\frac{2\pi L}{a\mu}$

G_r is modified Grashoff number $\frac{gd^3}{\nu^2}$

d is packing diameter.

V is kinematic viscosity.

k_l, a, L, D, μ and ρ are the same as for equation (6.6, 6.8).

Owing to the deviation of the model from experimental results at low Reynolds numbers, which Davidson clearly showed in his report, it was necessary to apply a conection coefficient to the equation constant. This factor was found to be 2.3 calculated as the ratio of the estimated result (a) fig. (6.13) given by equation (6.9) to the experimental result (b) corresponding to the same Reynolds value R_e = 5.4 which is the average value of Reynolds number in this test.

The equation is dimensionless and hence any consistent units may be used.

$$\frac{L}{\rho k_l a d} = 0.244 \times 2.3 \frac{S_c^{\frac{1}{2}} R_e^{2/3}}{G_r^{1/6}} \qquad (6.10)$$

ρ = 1917 kg/m^2

$k_l a$ = 16.7 10^{-4} Sec^{-1}

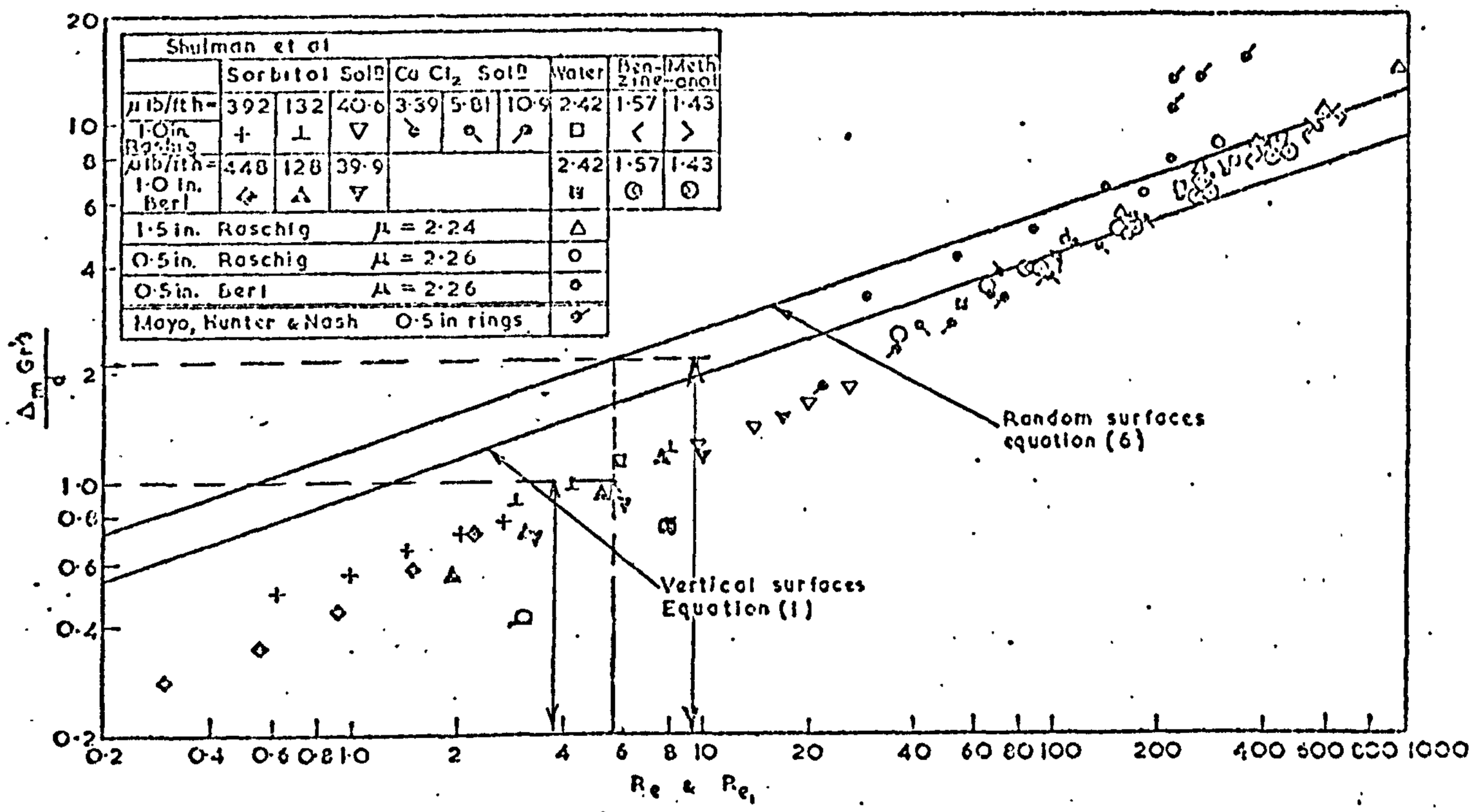

The mean film thickness Δ_m as a function of the film Reynolds number Re. The experimental points were plotted by using the wetted area a_w to calculate Δ_m and Re

Figure 6.14 Davidson equations and the experimental results. (reproduced from Ref 97)

$d = .01$ m

$\mu = 0.0273$ $\frac{Nsec}{m^2}$

$g = 9.8$ m/sec^2

$\nu = 1.42$ 10^{-5} m^2/s

$a = 123.5$ m^2/m^3

$$R_e = \frac{2\pi L}{\mu a} = 5.4$$

$$G_r = \frac{gd^3}{\nu^2} = \frac{9.8\ (.01)^3}{(1.42\ \ 10^{-5})^2} = 48601$$

$$\frac{2.9 \quad 10^4}{16.7 \times 1917 \times .01} = \frac{.244 \times 2.3 \times .00377 \times 3.08}{\sqrt{D} \times 6.041}$$

$$\sqrt{D} = \frac{16.7 \times 1917 \times .01 \times .244 \times 2.3 \times .00377 \times 3.08}{2.9 \quad 10^4 \times 6.041}$$

$= 1.19 \quad 10^{-5}$

$= 1.42 \quad 10^{-10} \quad m^2/sec$

Onda's equation Ref (89, 90) correlated a wide range of experimental results and was claimed to be dimensionally consistent:

$$k_l\left(\frac{\rho}{\mu g}\right)^{1/3} = .0051 \left(\frac{L}{a_w \mu}\right)^{2/3} \left(\frac{\mu}{\rho D}\right)^{0.5} (a_t d_p)^{0.4} \qquad (6.11)$$

Where a_t is total dry area of packing bed m^2/m^3 all other notiations are the same as for previous equations.

$k_l = 14.9 \quad 10^{-6} \quad m/sec$

$d_p = .014 \quad m$

$\rho = 1917 \quad kg/m^3$

$\mu = 0.0273 \quad N\ sec/m^2$

$g = 35316$ $m/hour^2$

$L = 2.9$ kg/m^2sec

$a_w = 123.5$ m^2/m^3

$a_t = 450$ m^2/m^3

$$14.9\ 10^{-6} \times \left(\frac{1917}{.0273 \times 9.8 \times 3600}\right)^{1/3} = .0051\left(\frac{2.9}{123.5 \times .0273}\right)^{3/3}\left(\frac{.0273}{1917}\right)^{-0.5} \times$$

$$(450 \times .014)^{0.4}\ \sqrt{D}$$

$$18.7\ 10^{-6} = .0051 \times 0.904 \times (264.99)\ (2.088)\ \sqrt{D}$$

$$\sqrt{D} = 7.34\ 10^{-6}$$

$$D = 0.54\ 10^{-10}\ m^2/sec$$

The result of diffusion coefficient calculated by the Sherwood empirical equation (6.6) agrees well with that of the corrected Davidson equation (6.10), but they are 15% and 20% different from the predicted value by Wilk and Chang equation respectively. Such deviation is still acceptable.

Although Sherwood's equation is dimensional, it is believed to be reliable as it correlates an extensive data of experimental results. In addition (k_1a) is used as a product, which eliminates the effect of inaccuracy in the calculations of the interficial area.

Bearing in mind that the experimental data correlated by Sherwood's equation include identical packing to this used in the test, and that the maximum error is less than 10%, with Sherwood's claim that the equation agrees well with the experimental results, one would estimate the error as probably less than 10%.

The unique merit of Davidson equation is that it is derived only from theoretical assumptions which fit the working conditions in the existing test. However, it has the drawback of deviation from the

experiments both at very high and very low Reynolds numbers. The use of a_w in the calculation of R_e increases the error specially for small packing where effective area is considerably different from wetted area. Such error is minimized by the correction factor mentioned above and the result is affected by the average scatter of experimental results taken to calculate that factor and the included error of these results.

Although Onda's equation is claimed dimensionally consistent (Ref 38) and correlates a wide range of experimental result, it was recommended that it should not be used for correlating Raschig rings smaller than 15 mm diameter. This recommendation seems strange because such range of packings were included in the correlated data. Owing to the fact that the result of D obtained by this equation is about half those of the other two and the result predicted by Wilk and Chang's equation, the recommendation was accepted and the result was excluded.

Although Shulman, Ref 87 , used experimental results for his correlations, the range of packings covered by these correlations is not wide enough to include 10 mm Raschig rings. Shulman's correlation of liquid mass transfer coefficient against liquid flow rates showed more deviation from experimental results for smaller packings and lower flow rates. Because the liquid flow rate in this work is low and packings are small, it is believed that the actual effective interficial area in the experimental column is much smaller than 8% determined from Shulman's results. This perhaps is why equation (6.8) gives lower value of diffusion coefficient.

It is concluded that the experimental result of (k_1a) of this work can be used in design of packed column absorbers for heat pumps utilizing the system (Methanol-mixed bromides) and that the value of D agreed at by equation (6.5, 6.6, 6.10) may be used for design calculations of different types of absorber employing the same system.

6.6 Accuracy of the results

The source of error in k_1 is of the same nature as in the determination of the mass transfer coefficient in the stirred cell described in chapter 5. The major contribution to the error in k_1

lies in the calculation of a_e using equation (6.3) which accounts for ±20%. But additional error of 5% in the determination of concentration difference and about 7% error in the determination of the rate of absorbed methanol vapour (this error is due to ±0.1°C inaccuracy in the antifreeze temperature measurements and 2.5% error in the antifreeze rate of flow) were observed. From the above considerations the estimated error in k_1 is believed to be less than 22%. On the other hand, the error in the diffusion coefficient is expected to be less. Excluding the 20% error in equation 6.3, but considering a probable error of 7% in $(k_1 a_e)$, which may produce 9% error in D, in addition to 5% average deviation of different correlations from experiments, this derives an average error of 14%.

It was not possible to compare the value of D as no other data were found in literature, but comparison with Idema's result showed that k_1 is about twice the mass transfer coefficient in his falling film absorber. Although both the packed column and the falling film absorbers belong to the same absorption model (Higbie penetration model), it is thought that the mixing is more effective in the packings and a ratio of 2 between mass transfer coefficients looks reasonable.

CHAPTER 7

CONCLUSION

The absorption heat pump is capable of providing signficant energy saving in the field of space heating. If a working coefficient of performance of 1.5 is achieved the energy saving will approach 33%. Should low temperature systems become commonplace (e.g. under-floor heating) then an even higher COP than this should be possible.

The absorption heat pump cycle shows more attractive performance for heating than the vapour compression cycle in that the COP is only weakly dependent on the temperature lift.

The computer program using estimated properties was capable of providing preliminary information as to the performance of the heat pump cycle. Once the measured properties became available, the same program, enabled the study of the effect of working conditions and some design parameters on the performance of such a cycle to be made.

The program was of considerable help in the economic study by evaluating the size, and hence the cost, of the various components. From such information an optimum economic design can be reached.

An enormous number of combinations are listed in the literature and although some current researches are in progress more engineering investigations to explore new combinations should be encouraged.

Attention of the future workers should be drawn to the fact that awaiting the determination of property data is probably the most significant factor in slowing down the development of thermal heat pumps. The methods used in this investigation are reasonably

simple and the results are sufficiently accurate for engineering applications. The specific heat measurements carried out by a simple calorimeter differs only by about 2% from those results measured by a much more sophisticated calorimeter (DSC). Thermal conductivity, again, was measured to within a reasonable accuracy by simple equipment, and had a higher accuracy been required the apparatus would have been very much more complicated.

Although it was not possible in this investigation to construct a continuous cycle in order to measure the overall performance, the data collected within the different stages of the work made it possible to design the low pressure of the cycle. Testing that side assured the high performance of the cycle and its capability to pump heat up over a high temperature gradient (84 ^{o}C).

It is believed that the systematic design of a thermal heat pump cycle utilising methanol/2LiBr-$ZnBr_2$ is now possible. The mass transfer coefficient measured in a packed column can be utilised for the design of such an absorber and the diffusivity coefficient may be used to design any other type of absorber.

Further investigations on the design of a real heat pump machine using methanol are recommended provided that the chemical stability of such a combination over a working temperature range of (150-200) ^{o}C is assured. The cycle control and solution pumping should present no insuperable problems.

With nearly three years of laboratory work with methanol and its solutions revealing no safety problems, it is believed that applications in domestic heating field are now possible.

REFERENCES

1. Thevenot, R. — A History of refrigeration throughout the world, International Institute of Refrigeration, Paris 1979

2. Hal Williams — Mechanical Refrigeration 5th edition PITMAN, London 1946

3. Haldane, T.G.N. — J. of Institute of Elect. Engineers, 1930, 68, 666

4. James E.Woods, John E. Janssen and G.L. Reynolds — International Journal of Energy Conversion and Management. Vol.20, No.4, 1980 pp 264

5. J.Ward Macarthur, Dean W.Finncarlson and Kanhh Ngyen — International Journal of Energy Conversion and Management. Vol.20, No.3, 1980 pp 161

6. Energy Trends (a statistical bulletin — Department of Energy, London, U.K. October 1980

7. National Economic Development Office — "Energy Conservation in the U.K. Achievements, Aims and Options"

8. Howatt, C.T. — Study finds absorption less costly than heat pump. Air Cond.Htg. & VTG 59 May 1962, 97 - 98

9. Merrick, R.H. et al — Design, evaluation and recommendation effort relating to the modification of a residential 3 ton absorption cycle cooling unit for operation with solar energy. N74 - 28536 (NASA-CR-120277), 1973

10. Williams, D.A., Tiedermann, J.B. — Heat pump powered by natural thermal gradients intersocity energy conversion Eng.Conf. Paper No. 749041, Aug., 1974.

11. Best, R. — 1977, Proc. 1st Intl. Conf. on Solar Building Technology, 2, R.I.B.A., London

12. G.Gallagher-Daggitt, R.Hopes and J.Brown — Investigation of a Thermochemical Heat Pump Energy Storage Scheme based on the sulphoric acid-water system. Rutherford Laboratory, Chilton, Oxford, U.K. Report No. 79-041 1979

13. Qasrawi, A.M.S. — Lucas, U.K. Condensed version of final Report LRN 050, October 1980, submitted to the EEC

14. P.Iedema — Refrigeration and Air Conditioning Section, Department of Mechanical Engineering, University of Technology, Mekel Weg 2, Delft, Holland. (Personal communications)

15. Oelert, G., Kohnke, H.J.; Janben, H. — Offenlegungsschrift 2803118. Battelle Institute C.V., 6000 Frankfurt, W.Germany, (by personal communication with the authors)

16. L.Muller — Local Report HP40/78/287 and Local Note HP42/78/15. Electricite De France, Department v Optiminsation Et Automatisation Des Processus, Chatou, France

17. M.H.Hour, R.Bugarel — Entropie, No. 91, 16, 1980 pp 28-37 France

18. Malewski, W. — Heat pump system according to the absorption principle for performance feed into district heating systems (Demonstration plant of "District Heating System Saar") Warmepumpen Technologie Band II, Antried Für Warmepumpen Vulcan-Verlag, Essen, 1979

19. Hainsworth, W.R. — Refrigerants and absorbants, P I Refrig.Eng. Vol. 43, No.2, 1944, pp97-100

20. Hainsworth, W.R. — Refrigerants and absorbants, P II Refrig.Eng. Vol. 48, 1944, pp 201-5

21. Ralph M.Buffington — Qualitative Requirements for Absorbent-Refrigerant Combinations. Refrig.Eng. Vol.57, 1949, pp 343-5, 384-8

22. ASRE Data Book — Basic volume, 6th edition, chapter 3, ASRE, Menasha, Wisconsin, 1949

23. Xavier Jacob, L.F.Albright and W.H. Tucker — Factors affecting the coefficient of performance for absorption air conditioning systems. ASHRAE Semiannual Meeting, Chicargo, Illionois, January 27-30, 1969 Paper No. 2098

24. M.A. Olama — Evaluation of some methanol-salt solutions for absorption refrigeration. Ph.D.Thesis, Department of Mechanical Engineering, King's College, London University, London, 1980

25. F.K.Dockhus, R.H.Krueger & W.F.Rush — Corrosion Ihibition in Lithium Bromide Absorption Refrigeration Systems ASHRAE J. December 1962, pp 67-73

26. R.H.Krueger, K.F.Dockus & W.F.Rush — Lithium Chromate, Corrosion Inhibitor for Lithium Bromide Absorption Refrigeration Systems. ASHRAE J., Feb.1964, pp 40-44

27. R.H. Krueger — Corrosion Inhibitor for Absorption Refrigeration Systems, United States Patent No. 4,019,992. Apr.26, 1977

28. J.E.Aker, R.G. Squires, L.F. Albright — An Evaluation of Alcohol-Salt Mixtures as Absorption Refrigeration Solutions. ASHRAE J., Vol.7, No.5 (1956), pp 90

29. T.Uemura — The vapour pressure of methanol absorbant systems. The Refrigeration (Japan), Vol.47 pp 532

30. T.Uemura & S.Hasaba — Studies on Methanol-Lithium Bromide-Zinc Bromide Absorption Refrigerating Machine. Refrigeration (Japan), Vol.44, No.502, Aug.1969, pp 4-14

31. E.R.Grosman and V.Ya Zhuravlenka — A specific enthalpy versus concentration diagram for methanol and lithium bromide solutions for absorption refrigeration design. Kompressorne I. Kholodil'nol Mashinostroenic (USSR), Vol.3, p 28, 1969

32. E.R.Grosman and A.Tkachuk — The heat capacity and heat of mixing of solutions of methanol and lithium bromide Voprosy Teknicheskoi Teplofiziki (USSR) Vol. 2, 1969

33. G.Grosman and V. Ya Zhuravlenka — The use of methanol and lithium bromide solutions for absorption refrigeration and heat pumps. Teplofizika I. Teplotcknika (USS), Vol. 16, (1970)

34. A.Alloush — Modifications to an experimental absorption refrigerator. M.Sc. Thesis, King's College, London University, October 1979.

35. M.Renz & F.Steimle — Thermodynamic Properties of the binary system methanol-lithium bromide. Internation J. of Refrig. Vol. 4, No. 2, March 1981

36. I.E.Smith & S. El-Shamarka — Absorption heat pumps for space heating. Proceedings of the I.E.E. Third International Conference on "Future Energy Concepts", London, January 1981, pp 232-37

37. K.Stephan, Stuttgart — Working substances for absorption heat pumps and transformers. Published volume on heat pump course. NATO Advanced Study Institute, Espinho, Portugal, Sept. 1980.

38. Perry and Chilton — Chemical Engineer's Handbood 5th Edition, McGraw-Hill, New York 1973

39. D.Cubiccotti and H.Eding — Heat contents of molten zinc chloride and bromide and the molecular constants of gases. Standord Research Institute. J. of Chem. Phys. Vol.40, 15 Feb 1964, pp 978-982

40. E.F.Fioch, D.C. Ginnings, and W.B.Holton — Calorimetric determinations of thermal proprties of methyle alcohol, ethyl alcohol and benzene. Journal of Research. National Bureau of Standards Vol.6, 1931, pp 881-900

41. R.Best — M.Sc. Thesis, School of Mechanical Engineering, Cranfield Institute of Technology, England 1978.

42. Forsythe, William Elmer — Smithsonian Physical Tables 9th edition, pp 166, Smithsonian Institution, Washington, 1954

43. J.M.Smith — Chem.Eng. Proj. 44, 521 (1948)

44. K.P.Tyagi and V.Shankar — Effect of operating variables on COP for certain absorbent-refrigerant mixtures ASHRAE Journal, May 1976, pp 35-38

45. W.F.Stoecker and L.D. Reed — Effect of operating temperature on the coefficient of performance of AQUA-AMMONIA refrigerating system. Paper No. 2183, ASHRAE Semiannual Meeting in Philadelphia, Pennsylvania. January 24-28, 1971

46. A.Alloush — Department of Mechanical Engineering, King's College, London University (Personal communications)

47. E.R.Grosman and V. Ya Zhuravlenka — Investigation for an absorption refrigeration machine operating on a solution of methanol and lithium bromide, Kholodil naya Technika (USSR). Vol.45, 1968, pp 4-6

48. W.Pennington — How to find accurate vapour pressure of LiBr-water solutions. Refrig.Eng. Vol.63, 5, May 1955, pp 57-61

49. J.E.Aker — An evaluation of methanol salt solutions M.Sc.Thesis, School of Chemical Engineering, Purdue University, Indianna, U.S.A. 1964

50. L.F.Albright, T.C. Doody, P.C. Buclez and C.R. Pluche — Solubility of refrigerants 11,21 and 22 in organic solvents containing an oxygen atom. ASHRAE Trans. Vol. 66, 1960 pp 423-433

51. R.P.Benedict — "Fundamentals of temperature, Pressure and flow measurements". J.Wiley & Son, New York, 1969, pp 84-87

52. Esso Research Centre — Esso Product data sheet, Report No. LMR/7008

53. H.M.Spiers — Technical Data of fuel. The British National Committee, London WC2, 1961

54. Reid & Sherwood — Properties of gases and liquids. McGraw-Hill New York 1958, pp 245

55. Vos, H.B. — "Measurements of thermal conductivity by non-steady state method'. Applied Science Res. (Section A), Vol.5 1955, pp 425-438

56. Horrocks, J.K. and McLaughlin E. — Proc. R. Soc., A.273, pp 259-274 (1963)

57. G.P. Anderson, J.J. de Groot, J.Kestin and W.A. Wakeham — Automatic operation of a high-precision wheatstone bridge, Jouranl of Physics E., Vol.7, 1974 U.K.

58. C.A.Nieto De Castro, W.A. Wakeham and J.C.G. Calado — Thermal conductivity measurements of N-Heptane along the saturation line by transient hot wire technique. Rev.Port. Quim 17, 78 (1975), Inst. Superior Tecnico, Lisbon Portugal

59. V.V.Mirkovich — Thermal conductivity 15 (1978), Plenum Publishing Corporation, page 235-243

60. J.J. de Groot, J.Kestin, H. Sookiazian and W.A.Wakeham — The thermal conducitivity of four monatomic gases as a funtion of density near room temperature. Physica 92A (1978), page 117-144, North Holland Publishing Company

61. W.A.Wakeham — Fluid thermal conductivity measurements by the transient hot-wire technique. Symposium on transport properties of fluids and fluid mixtures, their measurement, estimation, correlation and use. 10-11 April 1979. National Engineering Lab., Glasgow U.K.

62. Carslaw, H.S. and Jaeger, J.C. — "Conduction of heat in solids", 2nd edition, Clarendon Press, Oxford. 1959, page 261

63. Tye, R.P. — "Thermal conductivity", Vol.2, page 127-144 Academic Press Inc., London, 1969

64. Beyer, W.H. — C.R.C. Handbook of Mathematical Sciences Page 549, C.R.C. Press Inc., U.S.A., 1975

65. Raznjevic — Handbook of thermodynamic tables and charts. Page 95, Hemisphere Publishing Corporation, U.S.A., 1976

66. Ziebland, H. — "The thermal conductivity of toluene". Explosives Research & Development Establishment. Report No. 12/R/61. (1961) U.K.

67. International Critical Tables — Vol. 1 Page 229, National Research Council U.S.A., McGraw-Hill

68. B.P. Levitt — "Findlay's practical physical chemistry" 9th edition, Longman Group Limited, London 1973

69. I.P. Standard Method for testing petroleum and its products the Institute of Petroleum U.K.

70. Badger and Banchero — Introduction to Chemical Engineering, McGraw-Hill, New York, 1955, pp 367

71. Danckwerts P.V. — Gas liquid reactions. McGraw-Hill, London 1970, pp 6

72. Jeans, J. — An introduction to the kinetic theory of gases, Cambridge University Press, Cambridge, 1948, pp 219

73. Astarita, G. — Mass transfer with chemical reaction, Elsevier Publishing Company, The Netherlands 1967

74. Musa, R.Kamal and L.N. Canjar — Binary liquid diffusion coefficients, A.I. Ch.E. Journal, Vol.8, No.3, July 1962 pp 329-34

75.	Danckwerts, P.V. and A.J.Gillham	Trans. Instn. Chem. Engrs., Vol.44, 1966, pp T42-T54
76.	Timmermans, J.	"Physico-chemical constants of pure organic compounds", 1950, pp305
77.	W.S.Norman and B.K. Solomon	The effect of ammonia absorption on the wetted area of a packed tower. Trans. Instn. Chem. Engrs., Vol.37, 1959 pp 237-243
78.	G.G.Haselden and S.A. Malaty	Heat and mass transfer accompanying the absorption of ammonia in water. Trans. Instn. Chem. Engr.s, Vol.37, 1959, pp 137-146
79.	Sharanjit S. and R.H. Perry	Absorption of ammonia by acetic acid solutions. A.I.Ch.E. Journal, Vol.8, No.3, July 1962, pp 389-393
80.	S.W.Briggs	Concurrent, crosscurrent and counter-current absorption in ammonia-water absorption refrigeration. Paper presented at the ASHRAE Semiannual Meeting, Philadelphia, U.S.A. January 24-28 1971
81.	Smith, I.E.	Heat pump absorbers. Published volume on heat pump course, NATO Advanced Study Instn., Espinho, Portugal, Sept. 1980
82.	P.H. Calderbank	Mass transfer coefficients in gas liquid contacting with and without mechanical agitation. Trans.Instn.Chem.Engrs. Vol.37, 1959, pp 173-181
83.	E.N. Lightfoot	Gas absorption with simultaneous irreversible first-order reaction. A.I.Ch.E. Journal, Vol.8, No.5, November 1962, pp 710-712
84.	Sherwood, T.K. and Pigford, R.L.	Absorption and extraction, McGraw-Hill New York 1952
85.	Knudsen & Katz	Fluid dynamics and heat transfer, McGraw-Hill/Kagakusha 1958
86.	K.E.Porter and J.J.Templeman	Liquid flow in packed columns (Part III wall flow). Trans.Instn.Chem.Engrs. Vol.46, 1968, pp (T86-T94)

87. H.L.Shulman, C.F. Ullrich, A.Z. Proulx and J.O.Zimmerman — Performance of packed column (Part II), Wetted and effective interfacial areas, gas and liquid phase mass transfer rates. A.I.Ch.E. Journal, Vol.1, No.2, 1955, pp 253-258

88. Fumitake Yoshida and Tetsushi Kayanagi — Liquid phase mass transfer rates and effective interfacial area in packed absorption columns. Industrial and Engineering Chemistry, Vol.50, No.3, March 1958, pp 365-374

89. K.Onda, H.Takeuchi and Y.Okumoto — Mass transfer coefficients between gas and liquid phases in packed columns. Journal of Chemical Engineering of Japan Vol. 1, No.1, 1968, pp 56-62

90. K.Onda, E.Sada and H.Takeuchi — Gas absorption with chemical reaction in packed column. Journal of Chemical Engineering in Japan, Vol.1, No.1 1968, pp 62-66

91. F.Yoshida and T.Kayanagi — Mass transfer and effective interfacial areas in packed columns. A.I.Ch.E.Journal Vol.8, No.3, July 1962, pp 309-316

92. M.Kamal and L.N.Canjar — Diffusion coefficient, Chemical Engineering Progress. Vol.62, No.1 Jan. 1966, pp 82-86

93. K.A.Reddy and L.K.Doraiswamy — Estimating liquid diffusivity.industrial & Engineering Chemistry Fundamentals. Vol.6, No.1, Feb.1967, pp 77-79

94. Higbie, R. — Trans.Am. Instn. of Chem. Eng., 31, 365, (1935)

95. T.K.Sherwood and F.A.Holloway — Performance of packed towers - liquid film DATA for several packings. Trans. of Amer. Instn. Chem.Engrs. Vol.36, Part I, 1940, pp 39-69

96. T.K.Sherwood and F.A.Holloway — Ibid pp 181-182

97. J.F.Davidson — The hold-up and liquid film coefficient of packed towers, Part II, statistical models of the random packings. Trans.Instn.Chem. Engrs. Vol.37, 1959, pp 131-136

APPENDIX A

Measured properties employed in the actual cycle analysis

(1) Specific heat of the solution equation 3.4 which reads

$$C_{ps} = 0.652 + 2.139x - 2.077\ x^2 +$$
$$(-0.000205 + 0.00928x - 0.0101x^2)\ t\ kJ/kg\ ^oC$$

was used to determine the specific heat of the solution when the temperature and concentration were known.

(2) The following equilibrium temperatures were determined from the vapour pressure measurements Fig.3.11 for pure methanol and the indicated concentrations at equal pressures

TEMPERATURES

Pressure mm/Hg	Methanol	25%		26.2%		30.1%		35.6%	
	T^oK	T^oK	Ratio	T^oK	Ratio	T^oK	Ratio	T^oK	Ratio
300	316.7	419.0	0.756	411.7	0.769	391.4	0.809	380.3	0.833
400	373.1	426.4	0.758	419.0	0.771	393.3	0.811	387.3	0.834
500	328.3	432.3	0.759	424.8	0.772	403.8	0.813	393.0	0.835
600	332.6	437.2	0.761	429.6	0.774	408.5	0.814	397.0	0.837
700	336.4	441.5	0.762	433.9	0.775	412.5	0.815	401.8	0.837
800	339.7	445.2	0.763	437.6	0.776	416.0	0.816	405.4	0.838
900	342.7	448.6	0.764	441.0	0.777	419.2	0.817	408.6	0.839
1000	345.4	451.6	0.765	444.0	0.778	422.0	0.818	411.5	0.839

As shown in the above table the ratio of equal pressure temperatures was calculated over useful temperature and pressure ranges suitable for heat pump calculations.

The data were correlated with the equation

$$x = 1.336 \frac{T_C}{T_G} - 0.773$$

to be used at generator temperature to determine the lean mixture concentration when T_C and T_G were known.

The estimated relation equation 2.1 was employed to calculate the equilibrium concentration at the absorber conditions.

Enthalpy of vaporisation

Temp ^{o}C	Methanol	Concentration x = 25%	Concentration x = 26.2%	Concentration x = 30.1%	Concentration x=35.6%
10	1193	1940	1879	1766	1601
20	1173	1905	1847	1735	1573
30	1152	1871	1813	1705	1546
40	1131	1837	1777	1673	1518
50	1111	1805	1749	1644	1491
60	1096	1781	1726	1622	1471
70	1070	1741	1688	1589	1438
80	1050	1710	1658	1558	1413
90	1026	1674	1623	1525	1383
100	1002	1645	1592	1491	1352
110	977.1	1599	1555	1459	1221
120	950.5	1559	1512	1421	1288
130	920.3	1515	1468	1380	1251
138	878.0	1451	1407	1322	1198
149	853.0	1417	1375	1292	1171
160	798.7	1340	1299	1221	1107
188	672.0	1168	1132	1064	965
199	605.0	1078	1046	983.3	982

$$H = A + Bx + Cx^2$$

$$A = 2202.6 + 9.24\ T - 0.0218\ T^2$$

$$B = -(4417.8 + 15.53\ T - 0.0392\ T^2)$$

$$C = 3570.0 + 10.81\ T - 0.0294\ T^2 \text{ kJ/kg}$$

APPENDIX B

Specifications of used substances

BDH Methanol (Analar)

Minimum assay	99.5% CH_3 O H by GLC
Distilation range	not less than 95% distils between 64.5 & 65.5°C
Refractive index	$n_D^{20^0}$ 1.328 to 1.330

Maximum limits of impurities

Water	0.1%	Copper Cu	0.00005%
Acidity	0.02 ml N %	Iron (Fc)	0.0001%
Alkalinity	0.01 ml N %	Lead P_b	0.00005%
Non Volatile matter	0.001 %	Aldehydes and Ketones	0.005%

Zinc bromide Zn Br_2

Minimum assay (ex Zn) 98%

Reaction (2% aqueous solution) PH 6 to 7

Maximum limits of impurities

Sulphate (SO_4)	0.02%
Iron (Fe)	0.001%

Lithium bromide Li Br

Minimum assay 98%

Maximum limits of imputities

Chloride cl	0.05%	Iron (Fe)	0.002%
Heavy metals (Pb)	0.002%	Sulphate (SO_4)	0.02%

Vapour pressure test

Evacuated loading cell	297.65 gm
Evacuated cell + dry Li Br	426.52 gm
Evacuated cell + dry Z_n B_{r_2}	592.85 gm
Weight of lithium bromide	128.87 gm
Weitht of dry zinc bromide	166.33 gm

Ratio of number of moles of Li Br to Z_n Br_2

$$= \frac{128.87 \times 225.19}{86.85 \times 166.33} = 2.009 : 1$$

Loading cell + prepared solution = 697.85

Methanol weight = 697.83 - 592.85 = 104.98 gms

Weight of solution = 697.83 - 297.65 = 400.18 gms

$$\text{Concentration} = \frac{104.98}{400.18} = 26.2\%$$

Readings of the previous test

DVM reading	Temperature ^{o}C	P mm Hg barometric	P mm Hg manometer	P result mm Hg	Vapour pressure of butyl phthlate	P mm Hg Final result	P m bar
4.221	68.3	751.2	- 741.5	9.95(Mcleod)	-	9.95	13.09
6.842	107.6	751.5	- 672.0	79.5	-	79.5	104.62
9.365	144.0	750.5	- 376.5	374.0	0.9	273.1	490.98
10.506	160.0	750.0	- 69.5	680.5	2.3	678.2	892.49
12.048	181.3	750.0	+ 665.0	1415.0	4.5	1410.5	1844.32

APPENDIX C

Readings and results of thermal conductivity test

Subsistance x = 0.253 Wire length 77mm

Bath temperature 17.1°C α value 0.0038

Circuit measurements

V_t = 15.216 Volt R = 16.3 Ω

R_t = 241.3 Ω R_W = 16.1 Ω

Temperature history of the sample:

Room temperature

Sample temperature = 17.1°C

Readings

mV sec	1	2	3	4	5
01	3.24	3.22	3.0	3.2	3.16
0.25	4.34	4.3	4.1	4.27	4.22
0.45	5.04	5.0	4.8	4.98	4.92

Correlation of Inτ versus V_W

$$In\tau = A + BV_W$$

	1	2	3	4	5
Vw	3.24	3.22	3.20	3.16	3.0
Inτ	2.3025	2.3025	2.3025	2.3025	2.3025
Vw	4.34	4.3	4.27	4.22	4.1
Inτ	1.3863	1.3863	1.3863	1.3863	1.38629
Vw	5.04	5.0	4.98	4.92	4.8.
Inτ	0.7985	0.7985	0.7985	0.7985	0.7985
B	-0.83536	-0.845279	-0.84589	-0.85538	-0.83536
A	5.0099	5.023427	5.00626	5.00287	4.8094
C	-0.99999	-0.99999	-0.99995	-0.99996	-0.99999

Correlation coefficient C = 0.9999

$$\left(\frac{\Delta \text{In}\tau}{\Delta V_w}\right)_{av} = B = 0.843\ 10^{3}\ (\text{mV})^{-1} \qquad I = \frac{V_t}{R_t} = 63\ \text{mA}$$

$$V_w = 1.0153\ \text{V} \qquad Q = V_w I\ 1000/77 = 0.83\ \text{watt/m}$$

$$k = \frac{\alpha}{1+\alpha t}\ V_w \left(1 - \frac{R_w}{R_t}\right) \frac{Q}{4\pi} \frac{\Delta \text{In}\tau}{\Delta V_w}\ 10^{3}$$

$$= 0.003568 \times (1.0153) \times 0.933 \times \frac{0.83}{4\pi} \times .843\ 10^{3}$$

$$= 0.188\ \text{watt/m}\ ^{o}\text{C}$$

Thermal conductivity of distilled water at room temperature:

temp ^{o}C	k in this work	k from Ref(65)	% error
20 ^{o}C	0.605	0.598	+ 1.2%

Thermal conductivity of toluene:

temp ^{o}C	k watt/m ^{o}C	k watt/m ^{o}C (Ref.66)	% error
18.1	0.136	0.136	± 0%
27.5	0.137	0.133	+ 3%
55.8	0.128	0.125	+ 2.4%

Thermal conductivity of KI at 32 ^{o}C:

concen.	k watt/m ^{o}C	k watt/m ^{o}C (Ref.67)	% error
20	0.528	0.527	+ 0.2%
40	0.479	0.472	+1.5%

APPENDIX D

Design calculations of the absorber

1 k watt packed column absorber

Design Parameters

Output power	$N = 1$ k watt
Packings 10 mm Raschig rings	$a_t = 450\ m^2/m^3$
Lean solution concentration	$X_i = 0.25$ kg/kg
Rich solution concentration	$X_o = 0.27$ kg/kg
Equilibrium solution concentration	$X^* = 0.35$ kg/kg
Liquid film coefficient	$k_1 = 3.74\ 10^{-4}$ kg/m^{2}sec%
Working temperature	$t = 50\ ^oC$
Mean solution density	$\rho_s = 1878\ kg/m^3 = 117.4\ \frac{lb}{ft^3}$
Saturated methanol vapour density	$\rho_g = 5.65\ 10^{-2} kg/m^3 = 0.35\ 10^{-2}\ \frac{lb}{ft^3}$
Liquid viscosity	$\mu = 25\ C_p$
Assumed column efficiency	$\eta = 30\%$

Rate of absorption of methanol $g_E = \frac{N}{1.5H}$

where H is latent heat of pure methanol = 1128 kJ/kg

$$g_E = \frac{1}{1.5 \times 1128} = 5.3\ 10^{-4}\ \text{kg/sec}$$

$$\text{Solution flow rate } g_s = g_E \frac{1 - X_o}{X_o - X_i} = 5.9\ 10^{-4} \frac{0.73}{} = 21.5\ 10^{-3}\ \text{kg/sec}$$

Calculation of critical cross-sectional area for flooding conditions with reference to Page 426 (Ref 70)

$$\frac{G_{LF}}{G_{GF}}\left(\frac{\rho_G}{\rho_L}\right)^{0.5} = \frac{9_s}{9_E}\left(\frac{\rho_G}{\rho_g}\right)^{0.5} = \frac{21.5\ 10^{-3}}{5.9\ 10^{-4}} \cdot \left(\frac{5.6\ 10^{-2}}{1878}\right)^{0.5}$$

$$= 0.199$$

Thus the function $\left(\frac{G^*_{GF}}{3600}\right)^2 \left(\frac{a_\nu}{F^3}\right) \left(\frac{\mu^{0.2}}{\rho_G \rho_L\ 9}\right) = 0.1$

where $\left(\frac{a_\nu}{F^3}\right) =$ 450 for 10 Raschig rings

$$\left(\frac{G^*_{GF}}{3600}\right)^2 = \frac{0.1 \times (.00353) \times 117.35 \times 32.2}{450 \times 60.5^{0.2}}$$

$$= 0.00153$$

$$G^*_{GF} = 3600 \sqrt{.\ 00153} \quad \frac{lb}{ft^2\ hour}$$

$$= 0.039 \quad \frac{lb}{ft^2\ sec}$$

$$G^*_{GE} = 0.19 \quad \frac{kg}{m^2\ sec}$$

Critical cross-sectional area $A^* = \frac{9_E}{G^*_{GF}} \cdot 5.9\ 10^{-4} = 29\ 10^{-4}\ m^2$

The column diameter was chosen as 0.1 m

Then $A = \frac{\Pi D^2}{4} = \frac{\Pi \times 10^{-2}}{4} = 7.85\ 10^{-3}\ m^2$

$\frac{A}{A^*} = \frac{7.85\ 10^{-3}}{2.9\ 10^{-3}} =$ 2.7, so the working conditions are far enough from the flooding point.

Height of the column h: from equation (6.2)

$$g_E = (k_l a_e)\ W\ \Delta X$$

assuming $\frac{a_e}{a} = \eta = 0.3$

then $g_E = k_l \eta a W \Delta x$

$5.9\ 10^{-4} = 3.74\ 10^{-4} \cdot 0.3 \cdot 450 \cdot W \cdot 9$

$W = 1.298\ 10^{-3}\ m^3$

but $A = 7.85\ 10^{-3}\ m^2$

then $h = \frac{W}{A} = 0.165$ m

the height of h was taken 180 mm.

Design calculations of the evaporator

It was assumed that the heat transfer coefficient is controlled by the flow of water inside the copper coil, and that the boiling liquid layer outside the coil has no thermal resistance.

Design Parameters

Evaporator power	$N = 1$ k watt
Evaporation temperature	$T_E = 0\ ^oC$
Heating fluid water	$\rho = 1000$ kg/m^3
	$C_p = 4.186$ kJ/kg ^oK
	$\mu = 1.52\ 10^{-3}$ N sec/m^2

$k = 0.555$ W/mK

Temperature difference $\Delta T = 5\ ^{o}C$

The increase in water temperature $\Delta t = 3\ ^{o}C$

Tube internal diameter $d = 6$ mm

Calculations

water mass flow rate $\dot{m} = \frac{N}{C_p \Delta t} = \frac{1}{4.186 \times 3}$

$= 0.0796$ kg/sec

velocity of water in the coil $V = \frac{\dot{m}}{\rho \pi d^2/4} = \frac{0.0796}{1000 \times \frac{\pi}{4}(.006)^2}$

$V = 2.8$ m/sec

$R_e = \frac{\rho V d}{\mu} = \frac{1000 \times 2.8 \times .006}{1.52\ 10^{-3}}$

$= 11200$

$P_r = \frac{C_p \mu}{k} = \frac{4.186 \times 1.52\ 10^{-3}}{.555\ 10^{-3}} = 11.5$

$Nu = 0.023\ R_e^{0.8}\ P_r^{1/3}$

$= 0.023\ (11200)^{0.8}\ (11.5)^{1/3}$

$= 0.023 \cdot 1735.3 \cdot 2.257$

$\frac{\alpha d}{k} = 90.1$

$$\alpha = \frac{90.1}{d} k = \frac{90.1}{.006} k = 15016.7\ k$$

$$= 8.33\ k\ \text{watt/m}^2\ ^{o}K$$

$$N' = A\alpha\Delta T = A\ (8.33)\ 5 = 1$$

$$A = 0.024\ m^2$$

$$\ell = \frac{A}{\eta d} = 1.27\ m$$

To allow for the assumption of infinite coefficient of heat transfer outside the coil, and to account for change of operational conditions, the coil was made of 14 turns of 40 mm pitch diameter giving ℓ = 1.75 m.

Pressure drop ΔP at the evaporator :

$$\Delta P = 4\ f\ \frac{L}{D}\ \rho_g V^2/_2$$

where f Fannin coefficient
L tube section length 400 mm
D tube section diameter 50 mm
ρ_g vapour density 5.65 10^{-2} kg/m^3
V vapour velocity

Volume flow rate of methanol vapour $V_E = \frac{9_E}{\rho_g} = \frac{5.6\ 10^{-4}}{5.65\ 10^{-2}}$

$$= 0.0099\ m^3/sec$$

$$V' = \frac{V_E}{\pi D^2/_4} = \frac{.0099}{\frac{\pi}{4}(.05)^2} = 5.04\ m/sec$$

$$Re_g = \frac{\rho_g D V'}{\mu_g}$$

$$\mu_g = 8.7\ 10^{-6}\ \frac{N\ sec}{m^2} \quad \text{(Ref 29) Page 301}$$

$$R_{e_g} = \frac{5.65\ 10^{-2}\ x\ .05\ x\ 5.04}{8.7\ 10^{-6}} = 1636.6$$

from (Ref 38) Page 5 - 22 $f = 0.012$

$$\text{then} \quad \Delta P = 4 \times .012 \times \frac{0.4}{0.05} \times \frac{5.65\ 10^{-2} \times (5.04)^2}{2}$$

$$= 0.276\ N/_{m^2} = 2.06\ 10^{-3}\ mm\ kg$$

APPENDIX E

Readings and results of absorption in packed column

Test No.5

Anti-freeze (Ethylene Glycol - water 40%)

Anti-freeze flowmeter reading V_E = 38

Soltuion flowmeter reading V_s = 36

Temperature readings

Reading No.	1	2	3	4	5	6	7	8
Solution input temp. T_{is}	56.3	55.7	55.6	57.2	58.0	55.2	53.4	51.3
Solution output temp. T_{os}	65.2	65.2	66.7	65.4	65.2	66.7	66.1	67.8
Evaporation temp. T_E	-11.3	-11.4	-11.0	11.6	-11.5	-11.2	-10.0	-9.3
Anti-freeze inlet temp. T_{iE}	-2.3	-2.1	-2.2	-2.2	-2.1	-2.1	-1.9	-2.3
Anti-freeze output temp. T_{oE}	-4.6	-4.3	-4.4	-3.7	-4.7	-4.4	-4.4	-4.6

Reading No.	9	10	11	12	13	14	15	16
T_{is}	51.6	54.9	56.2	57.1	57.2	57.1	57.7	57.9
T_{os}	67.6	67.7	68.4	67.9	67.6	66.9	66.5	65.1
T_E	-8.7	-8.7	-9.2	-10.1	-9.6	-10.0	-10.5	-10.7
T_{iE}	-2.2	-2.3	-2.1	-2.2	-2.2	-2.2	-2.2	-2.2
ToE	-4.2	-3.8	-4.2	-4.0	-2.8	-4.8	-3.8	-2.5

Mean temperature readings:-

T_{iE} = -2.2 ^{o}C

T_{oE} = -4.1 ^{o}C

T_E = -10.3 ^{o}C

ΔT_E = -1.9 ^{o}C

T_{is} = 55.8 ^{o}C

T_{os} = 66.6 ^{o}C

T_A = 61.2 ^{o}C

ΔT_s = 10.8 ^{o}C

The anti-freeze flowmeter reading of 100% of the scale is corresponding to 5 lit. of water/min, so the actual anti-freeze flow rate $V_{Ea} = \frac{V_E}{20\rho_a}$

where ρ_a is the relative density of the anti-freeze

$$V_{Ea} = \frac{38}{20 \times 1.03} = 1.84 \text{ litre/minute}$$

$$Q_E = \frac{V_{Ea} \times \rho_a \times C_p \times \Delta T_E}{60} = \frac{1.84 \times 1.06 \times 3.39 \times 1.9}{60}$$

$$= 0.209$$

$$\text{and } 9_E = \frac{Q_E}{H} = \frac{0.209}{1.2} = 0.174 \text{ gm/sec}$$

The solutioh flowrate V_{so} = 0.59 lit/m corresponding to scale reading of 36, chart fig.6.13, then referring to FISCHER & PORTER catalogue No. 10A1021 "Basic rotameter principles", Page 7, the actual solution flowrate is given by

$$V_{sa} = V_{so} K_{\mu s} \sqrt{\frac{\rho_{so}}{\rho_s}}$$

where $K_{\mu s}$ is the viscosity correction number, ρ_{so} is the solution relative density at the calibration temperature 50°C, and ρ_s is the density at the solution temperature T_{is},

$$K_{\mu s} = \frac{K_s}{K_{so}}$$

$$K_{so} = 3.3$$

$$N_s = \frac{\mu}{6.123} = \frac{25.5}{6.123} = 4.16$$

$$K_s = 3.45$$

$$K_{\mu s} = \frac{3.45}{3.3} = 1.045$$

$$V_{sa} = 0.59 \times 1.045 \times \sqrt{\frac{1.917}{1.9}}$$

$$= 0.62 \text{ litre per min.}$$

$$Q_s = \frac{V_{sa} \times \delta_s \times C_{ps} \Delta T_s}{60} = \frac{0.62 \times 1.9 \times 0.92 \times 10.8}{60}$$

$$= 0.195 \text{ kwatt}$$

From Fig.6.11 the losses corresponding to $T_s = 61.2$ is 0.135 kwatt

$$Q_A = 0.195 + 0.135 = 0.330 \text{ kwatt}$$

The heat ratio $\varepsilon = \frac{Q_A}{Q_E} = \frac{0.33}{.209}$

$$= 1.58$$

$$g_s = \frac{V_{sa} \times \rho_s}{60} = 19.6 \text{ gm/sec}$$

so $$X_o = \frac{X_i (g_s) + g_E}{g_s + g_E} = \frac{0.245 (19.6) + 0.174}{19.6 + .174}$$

$$= 0.252$$

$$\Delta X_i = 32.3 - 24.5 = 7.8$$

$$\Delta X_o = 28 - 25.2 = 2.8$$

$$\Delta X = \frac{5}{\text{In } \frac{7.8}{2.8}} = 4.9\%$$

APPENDIX F

```
C
C HEAT BALANCE OF ABSORBTION HEAT PUMP
C LIBR-ZNBR2-METHANOL
      DO10 L =263,283,10
      TE=FLOAT(L)
      DO10 J=323,343,10
      TA =FLOAT(J)
      DO10 I=353,473,10
      TG =FLOAT(I)
      T11 =TA+TDEF
      T10 =TG
      TC=TA
      TDEF = 10.0
C
C
C COMPUTE STRONG SOLUTION CONCENTRATION
      X9=1.502  *(TE/TA)-0.87254
      IF(X9.LT.0.243) GO TO 10
C
C COMPUT WEAK SOLUTION CONCENTRATION
      X10 =1.336*(TC/TG)-0.773
      IF(X10.GT.X9) GO TO 10
      IF(X10.LT.0.243) GO TO 10
      DEFX=X9-X10
C
C CIRCULATION FACTOR
      W=(1.0-X10)/(X9-X10)
      X9A=(1.0-X9)
      X10A=1.0-X10
C
C COMPUTE MEAN TEM OF WEAK SOLUTION
      TMWS=(TC+T11)/2.0
C
C COMPUTE XMEAN IN GENERATOR
      XMSG=(X9+X10)/2.0
      XMSGA=1.0-XMSG
C
C COMPUTE OF STRONG SOLUTION CP AT TMWS
        CP1=0.652+2.139*X9-2.077*X9**2+(0.00928*X9-0.000205
     1 -0.0101*X9**2)*(TMWS-273.0)
C COMPUTE CP OF WEAK SOLUTION AT TMWS
        CP2=0.652+2.139*X10-2.077*X10**2+(0.00928*X10-0.000205
     1   -0.0101*X10**2)*(TMWS-273.0)
C COMPUTE T9


      T9=((W-1.0)*CP2*(TG-T11)+W*CP1*TA)/(W*CP1)
C COMPUTE SATURATION TEMP OF STRONG SOLUTION AT CONDENSER PRESS
      T9E=TC**2/TE
C COMPUTE HEAT OF VAPORIZATION AT PC
        A=2202.6+9.24*TMSG-0.0218*TMSG**2
        B=-(4417.8+15.53*TMSG-0.0392*TMSG**2)
        C=3570.0+10.81*TMSG-0.0294*TMSG**2
        HSPC=(A+B*XMSG+C*XMSG**2)/4.186
      QEX=(W-1)*CP2*(TG-T11)
```

```
C          COMPUTE MEAN TEMPERATURE IN GENERATOR
      TMSG=(TG+T9)/2.0

C COMPUTE SPECIFIC HEAT OF VAPOR AT TMSG

      CVTMSG=                809E-3)*TMSG-(3.5976E-6)*TMSG**2)/32.04

C COMPUTE HEAT TO REF VAPOR
      HRV=CVTMSG*(TG-T9E)

C COMPUTE SPECIFIC HEAT AT TMSG

         CPM=(0.662+2.139*XMSG-2.077*XMSG**2+(0.00928*XMSG-0.000205
     1 -0.0101*XMSG**2)*(TMSG-273.0))/4.186
COMPUTE HEAT TO SOLUTION IN GENERATOR
      QG =W*CPM*(TG-T9)+HSPC+HRV
C
C
C COMPUYE QE CONSEDERING FREE COOLER
      TPCL =(TC+TE+20.0)/2.0
      TPCV =(TC+TE-15.0)/2.0
      CVPC=(5.84+(16.809E-3)*TPCV-(3.5976E-6)*TPCV**2)/32.04
      CLPC=0.568+0.000085*(TPCL-273.0)+0.0000285*(TPCL-273.0)**2
      TPC=TC-(TC-TE-15.0)*CVPC/CLPC
C COMPUTE HEAT OF VAPORIZATIONAT TE
      HVTE=262.79*((513.0-TE)/175.3)**0.38
C COMPUTE MEAN TEMP OF THROTTLE VALVE
      TMTH=(TE+TC )/2.0
C COMPUTE MEAN SPESIFICHEAT OF LIQ REF
      HCLR=0.568+0.000085*(TMTH-273.0)+0.0000285*(TMTH-273.0)**2
C MASS OF REF VAPORIZED AT THE THROTTLE VALVE
      Y=HCLR*(TPC-TE)/HVTE
      QE=(1.0-Y)*HVTE
      ES =(QG/TG+QE/TE)/(QG+QE)*TC
C CALCULATION OF COP OF REFREGIRATION
      COPR=QE/QG
C
C CALCULATION OF COP OF HEAT PUMP
      COPH=1.0+COPR
      WRITE(2,110)
  110 FORMAT (1H     ,4H  TG,5X,4H  TC,5X,4H  TE,5X,4HTDEF,5X,4H  T9
     1,5X,4H T9E,/)
      WRITE(2,120)TG,TC,TE,TDEF,T9,T9E
  120 FORMAT(1H     ,6F8.3,/)
      WRITE(2,130)
  130 FORMAT(1H     ,4H  X9,5X,4H X10,5X,4H   W,5X,4H  QG,5X,4H  QE,/)
      WRITE(2,140)X9,X10,W,QG,QE
  140 FORMAT(1H     ,5F9.3,/)
      WRITE (2,150)



  150 FORMAT(1H     ,4H CP1,5X,4H CP2,5X,4HDEFX,5X,4HCOPH,5X,4H  ES,/)
      WRITE (2,160)CP1,CP2,DEFX,COPH,ES
  160 FORMAT (1H     ,5F7.3,/)
      WRITE(2,170)
  170 FORMAT (1H     ,4HQEX ,5X,5HCPM  ,/)
        WRITE(2,180)QEX,CPM
  180 FORMAT(1H     ,2F14.3,///)
   10 CONTINUE
        END
```

TG TC TE TDEF T9 T9E

363.000 293.000 273.000 75.000 290.409 314.465

X9 X10 W QG QE

0.527 0.305 3.135 421.706 286.241

CP1 CP2 DEFX COPH ES

1.895 1.442 0.222 1.679 0.915

TG TC TE TDEF T9 T9E

368.000 293.000 273.000 75.000 293.000 314.465

X9 X10 W QG QE

0.527 0.291 3.003 424.363 286.241

CP1 CP2 DEFX COPH ES

1.914 1.416 0.236 1.575 0.908

TG TC TE TDEF T9 T9E

373.000 293.000 273.000 75.000 295.351 314.465

X9 X10 W QG QE

0.527 0.276 2.889 427.410 286.241

CP1 CP2 DEFX COPH ES

1.933 1.390 0.250 1.670 0.901